Linear Control Theory to Introduce Periodic Parameters for a Marine Ecosystem Model

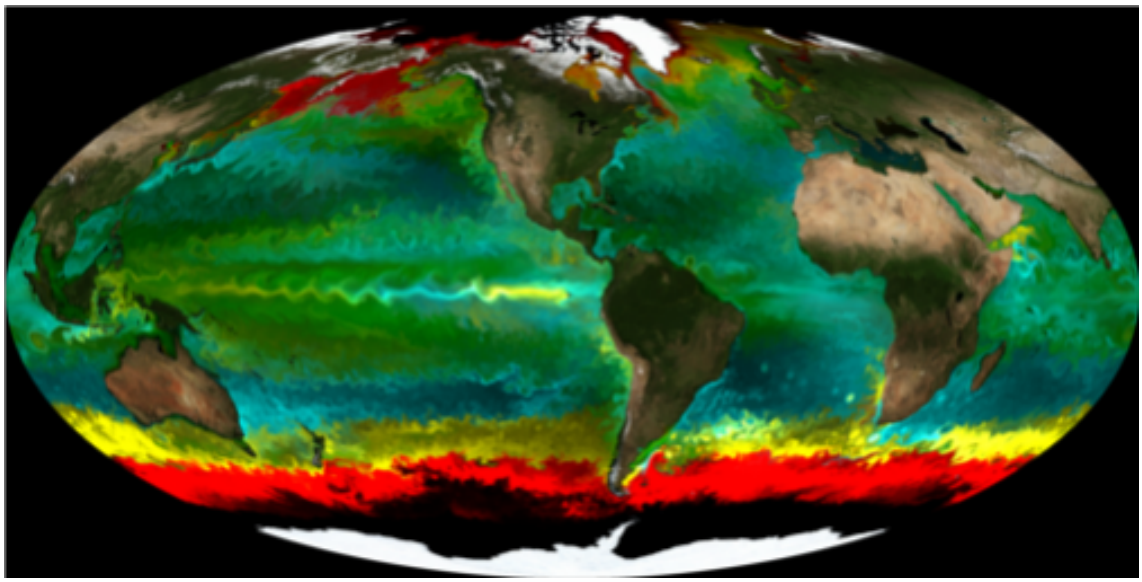

Dissertation

zur Erlangung des akademischen Grades
Doktor der Naturwissenschaften
(Dr. rer. nat)

der Technischen Fakultät
der Christian-Albrechts-Universität zu Kiel

Dipl.-Math. Mustapha El Jarbi

Kiel

2014

Referent:	Prof. Dr. Thomas Slawig
1. Koreferent:	Prof. Dr. Thomas Meurer
2. Koreferent:	Prof. Dr. Andreas Oschlies.
Tag der mündlichen Prüfung:	04. 12. 2014

gez. Prof. Dr.-Ing. Eckhard Quandt, Dekan

To my family and friends

Zusammenfassung

Globale biogeochemische Ozeanmodelle sind von großer Bedeutung für die Beurteilung, welche Rolle der Ozean im globalen Kohlenstoffkreislauf spielt, und für die Einschätzung des Einflusses des Klimawandels auf das marine Ökosystem. Der Ozean erfüllt die Funktion einer riesigen Senke für Kohlenstoffdioxid und nimmt etwa ein Drittel des anthropogenen CO_2 auf. Diese Besonderheit spielt eine zentrale Rolle in der aktuellen Klimadiskussion. Die CO_2-Aufnahme des Meeres wird von biogeochemischen Prozessen beinflusst, die durch parametrisierte Modelle so gut wie möglich wiedergespiegelt werden sollen. Die Bewertung dieser Modelle führt zu einer Zustandsschätzung und einer Sensitivitätsanalyse der Modellparameter. Hierfür werden die verfügbaren Messdaten jener Größen benutzt, die in den biogeochemischen Modellen betrachtet werden. Für gewöhnlich sind die biogeochemischen Modelle ihrerseits an Ozeanzirkulationsmodelle gekoppelt.

Diese Arbeit umfasst die Untersuchung und Anwendung von Methoden der Kontrolltheorie und Optimierung unter Verwendung der diskreten linear-quadratischen optimalen Kontrolle, sowohl für den geschlossenen Regelkreis als auch für den offenen Regelkreis, und die Kalman-Filter Methode. Das Hauptziel der Arbeit ist die Erforschung der Möglichkeiten dieser vorgeschlagenen Methoden im Hinblick auf die Verbesserung eines Klimamodells, nämlich eines eindimensionalen nicht-linearen marinen Ökosystemmodells vom NPZD-Typ (N steht für gelösten anorganischen Stickstoff, P steht für Phytoplankton, Z steht für Zooplankton, D steht für Detritus). Dieses Ökosystemmodell, das von Oschlies und Garçon entwickelt wurde, simuliert die Verteilung von Stickstoff, Phytoplankton, Zooplankton und Detritus in einer Wassersäule und stützt sich auf Daten zur Ozeanzirkulation. Die vorgeschlagenen Methoden dienen dazu, jährlich periodische Modellparameter in einer linearisierten Version des Modells einzuführen.

Zunächst verwenden wir die diskrete linear-quadratische optimale Kontrolle mit geschlossenem Regelkreis (LQOC). Es wird gezeigt, dass mit der dadurch erhaltenen Version des Modells eine signifikante Verringerung des Modell-Daten-Misfits im Vergleich zum Originalmodell mit optimierten konstanten Modellparametern erzielt werden kann. Die gefundene jährliche Variabilität der optimierten Parameter liefert Hinweise zur Verbesserung des nichtlinearen Originalmodells. Die erhaltenen optimalen periodischen Parameter werden auch für Validierungs- und Vorhersage-Experimente mit der nichtlinearen Originalversion des Modells verwendet. Diese Experimente deuten darauf hin, dass die

von uns vorgeschlagene Methode für das betrachtete marine Ökosystemmodell sehr geeignet ist. Als Zweites werden wir dann die gefundenen periodischen Parameter in einer Zustandsschätzung unter Verwendung des Kalman-Filters benutzen. Ein Vergleich mit Ergebnissen, die nach dem Ansatz der Kalman-Filter-Zustandsschätzung für konstante Parameter erzielt werden, wird durchgeführt. Wir zeigen, dass die Kalman-Filter-Methode mit periodischen Parametern deutlich plausiblere Lösungen liefert als mit konstanten Parametern. Zum Dritten verwende ich die diskrete linear-quadratische optimale Kontrolle mit offenem Regelkreis (DOLOC), um die Auswirkungen der Linearisierung um die Zustandsgrößen auf den Fehler zwischen Modelloutput und Messdaten zu untersuchen. Dazu setzte ich die erhaltenen periodischen Parameter in das ursprüngliche nicht-lineare NPZD-Modell ein.
Die vorgeschlagenen Methoden, insbesondere der Ansatz der geschlossenen Regelkreis linear-quadratischen optimalen Kontrolle, dienen als erster Schritt für ein Werkzeug zur Verbesserung von marinen Ökosystemmodellen. Die Untersuchung weiterer Verbesserungen der vorgestellten Algorithmen sowie weiterer vielversprechender Ansätze im Rahmen der linear-quadratischen optimalen Kontrolle werden als sehr wertvoll eingeschätzt.

Abstract

Global ocean biogeochemical models are of great importance for the assessment of the role of the ocean in the global carbon cycle and for the estimation of the impact of the climate change on marine ecosystems. The ocean acts as a major sink of carbon dioxide and takes up about one third of anthropogenic CO_2. This characteristic plays a central role with respect to the climate discussion. The CO_2-uptake of the ocean refers to biogeochemical processes which are simulated by corresponding parameterized models. The evaluation of these models leads to a sensitivity analysis of the model parameters and a model state estimation using associated measurement data. Usually, the biogeochemical models are coupled to ocean circulation models.

This work comprises an investigation and application of control theory and optimization methodologies using discrete linear quadratic optimal control with both closed loop and open loop and the Kalman filter method. The fundamental aim of this work is to explore the potentialities of those proposed methods regarding an enhancement of a one-dimensional non-linear marine ecosystem model of NPZD (N for dissolved inorganic nitrogen, P for phytoplankton, Z for zooplankton and D for detritus) type. This ecosystem model, developed by Oschlies and Garçon, simulates the distribution of nitrogen, phytoplankton, zooplankton and detritus in a water column and is driven by ocean circulation data. The proposed methods are used to introduce annually periodic model parameters in a linearized version of the model.

Firstly, I use the closed loop discrete linear quadratic optimal control (LQOC). It will be shown that the obtained version of the model gives a significant reduction of the model-data misfit, compared to the misfit obtained for the original model with optimized constant parameters. The found inner-annual variability of the optimized parameters provides hints for an improvement of the original model. The obtained optimal periodic parameters are also used in validation and prediction experiments with the original non-linear version of the model. The experiments indicate that the considered method is very suitable for the considered marine ecosystem models. Secondly, I use the obtained periodic parameters in a state estimation applying the Kalman filter method. A comparison with results obtained by using optimized constant parameters in the Kalman filter state estimation approach is performed. We show that the Kalman filter method provides a very reasonable solution with periodic parameters compared to that with constant parameters. Thirdly, I use the open loop discrete linear quadratic optimal control (DOLOC) to investigate the impact of the linearization scheme about the state variables on the model-data-fit by using these periodic parameters in the original non-linear NPZD model.

The proposed methodologies, particularly the closed loop discrete linear quadratic optimal control approach, serve as initial steps towards a tool for an efficient enhancement of marine ecosystem models. The investigation of further improvements of the presented algorithms as well as other promising approaches in the framework of linear quadratic optimal control optimization are considered to be highly valuable.

Acknowledgements

First of all, I want to say thank you to my supervisor Prof. Dr. Thomas Slawig for his encouragement and enduring support during the last years. I want to thank Thomas for all the inspiring discussions and for sharing his profound knowledge with me during the last years. He also supported me with various decisions throughout the whole process. Thomas always took the time for listening and encouraging me. Thomas, thank you for all your support.

The position in Thomas' working group, I partially owe to Prof. Dr. Andreas Oschlies from the GEOMAR in Kiel. I would like to thank him that he decided to be the co-supervisor and suggested to be one of my reviewers of my thesis. Thank you, Andreas, for the great collaboration and your support during the last years. I am also very happy that Prof. Dr.-Ing. habil. Thomas Meurer from the Faculty of Engineering in Kiel, agreed to be my second reviewer.

Moreover, I want to thank all my colleagues in the working group for all the valuable discussions. Thank you that I could bombard you with all my questions during the last years. Thanks for all your great support.

I am particularly indebted to my wife Dr. Christiane El Jarbi, Dr. Volkmar Sauerland and Dr. Mourad El Ouali, who spent various hours in proof-reading my thesis. Without their precious comments, many parts of this work would probably still be up to the confusions of my head. Thank you for your support.

I also would like to thank all my friends for encouraging me during the last years and for patiently bearing all the frustrations about my work in the past.

Finally, I want to say thank you to my wife Christiane and my parents for all their support during the last years. Without all their help, writing this thesis would clearly not have been possible.

List of Abbreviations

$[N]$	the discrete interval $\{1, \ldots, N\} \subset \mathbb{N}$
$\mathbb{N}$	the set of natural numbers
$\mathbb{R}_{\geq 0}$	the set of positive real numbers
LQOC	Closed Loop Discrete Linear Quadratic Optimal Control
DOLOC	Open Loop Discrete Linear Quadratic Optimal Control
DRE	Difference Riccati Equation
LTV	Linear Time-Varying
EKF	Extended Kalman Filter
$E[\mathbf{x}]$	Expected Value of random variable $\mathbf{x}$
$Var[\mathbf{x}]$	Variance of of random variable $\mathbf{x}$
$Cov(\mathbf{x}, \mathbf{y})$	Covariance of of random variable $\mathbf{x}$ and $\mathbf{y}$
$\mathcal{N}(\mu, \sigma^2)$	Normal Distribution with Expected Value μ and Variance σ^2

Contents

List of Figures

1 Preface

The topic of this thesis is the investigation of parameter optimization and state estimation in a marine ecosystem model using Discrete Linear Quadratic Optimal Control with both Closed Loop (LQOC) and Open Loop (DOLOC), as well as the Extended Kalman Filter (EKF).
More precisely, we deal with the application of these three methodologies on a biogeochemical ocean model. This so called NPZD model simulates the circulation of nitrogen in a vertical water column. It supposes nitrogen to occur in four different states in the ocean, dissolved in water as inorganic nitrogen (N), within phytoplankton (P), within zooplankton (Z) and detritus (D), i.e., dead organic particles. The parameters that have to be optimized belong to functions describing the change of nitrogen state and vertical nitrogen fluctuation within partial differential equations.
The aim of closed loop discrete linear quadratic optimal control (LQOC) is to minimize a given quadratic cost function subject to a linear or non-linear system with time dependent parameters. As a cost function a least squares system-error w.r.t. given data can be used. Thus the method is applicable to parameter optimization or model calibration problems. The main objective of the application of the LQOC method to the NPZD model is to obtain a model that is applicable for arbitrary time intervals. We allow the parameters to vary temporally over the year while remaining periodic over all years of the considered time interval. The LQOC method used here does not require a prescribed periodic parameterization, but will rather automatically generate an optimal periodic function for each parameter. Moreover, it allows to balance the aims of good model-data fit and parameter periodicity by introducing weighting matrices.
We want to apply the LQOC method as follows:

- We give a brief description of the temporal and spatial discretization of the NPZD model.
- Since the NPZD model is nonlinear, we perform a linearization about reference trajectories of model variables and model parameters, which can be based on available measurement data and parameter guesses.
- Then, we apply the LQOC method to the linearized NPZD model.

- Next, we present the results of the parameter optimization runs performed with the LQOC method. We examine both, the obtained fit of the linearized model output to the measurement data and the annual periodicity of the obtained parameters.

- To verify this approach, the periodic parameters obtained by the LQOC method will be used in a validation and prediction experiment using the nonlinear NPZD model.

A open loop discrete linear quadratic optimal control (DOLOC), also called a non-feedback controller, is a type of controller that computes its input (control, parameter vector) to a system using only the current state and its model of the system. A characteristic of the open loop controller is that it does not use feedback to determine if its output has achieved the desired goal of the input (control). This means that the system does not observe the output of the process that it is controlling. Consequently, a true open loop system can not correct any errors that might occur. The main objective of the application of the DOLOC method on the NPZD model is first to obtain periodic parameters and then to investigate the impact of the linearization scheme about the state variables on the model-data-fit by using these periodic parameters in the original non-linear NPZD model.
We want to apply the DOLOC method as follows:

- First we perform a linearization of the NPZD model about a reference trajectory of model parameters, which will be based on parameter guesses.

- Then, we perform two linearization schemes of the NPZD model about a reference trajectory of model variables which will be based on available measurement data and on synthetic data, respectively.

- Next, we apply the DOLOC method to both linearization schemes. This yields two periodic parameter sequences.

- To verify our approach, we introduce a validation experiment employing the two optimized periodic parameter sequences in the original non-linear NPZD model.

The aim of the Extended Kalman Filter (EKF) is to estimate the state of a dynamical system from a sequence of incomplete or noisy measurements. The measurements need not to be of the state variables themselves, but must be related to the state variables through a linearizable functional relationship. The EKF is a solution to the linear quadratic Gaussian problem, which is the problem of estimating the instantaneous state of a linear dynamical system which is perturbed by Gaussian white noise by using measurements of quantities that are linearly related to the state, but are corrupted by white

noise. The EKF is an optimal filter in the mean square sense. It is one of the greatest innovations in statical estimation theory and it is widely used in a variety of applications. We want to apply the EKF method as follows:

- First, we perform the EKF approach on the NPZD model, in which we employ the optimized periodic parameters that have been obtained with the LQOC method.
- Then, we perform the EKF approach on the NPZD model again. But this time we employ the optimized constant parameters that have been obtained with a sequential quadratic programming (SQP) method (see, Rückelt et al. (2010)).
- Next, in order to compare the quality of the estimated state variables of both approaches, we present their model-data-fit.
- Moreover, we investigate the impact of the choice of the model and measurement noise covariance matrices on the state assimilation for both approaches.

The outline of the thesis is as follows:

- Chapter 2 starts with some knowledge of CO_2 uptake of the ocean, the ocean carbon pumps. We give an overview of climate models, and modeling of marine ecosystems.
- In chapter 3, we introduce basic elements of linear control theory, especially the closed loop linear quadratic optimal control (LQOC), and the Extended Kalman Filter (EKF).
- In chapter 4, we investigate the finite-time stability of the linearized version of the NPZD model.
- In chapter 5 we give a detailed summary of our papers - $A.1$ to $A.4$. We also discuss the application of the here used methodologies on the NPZD model.

2 Carbon Pump in the Ocean and the Climate Change

Climate change is a long lasting change of weather conditions, where long means periods of decades up to periods of millions of years. Climate change can concern both, the average weather conditions and the frequency of extreme meteorological events. (see Arias et al. (2013)). Climate change is driven by oceanic processes such as oceanic circulation as well as by the heat transport between atmosphere and ocean (see, e.g., Kusky (2009)). One driver assigned to climate change is the increase of atmospheric carbon dioxide (CO_2) over the last century. Since the ocean plays an important role in the global carbon cycle and thus in the evolution of atmospheric CO_2, it is necessary to understand the interactions between atmosphere and ocean, particularly the CO_2-uptake of the ocean, to assess further changes.

2.1 CO_2-Uptake of the Ocean

Over the last millions of years, the concentrations of carbon dioxide (CO_2) in the atmosphere varied continuously between 180 and 280 pm. Within the last 100 years, however, the atmospheric CO_2 increased up to 367 ppm and the average temperature of the climate system, which includes the atmosphere and the oceans, increased by about 0.8^oC (IPCC (2007)). Since CO_2 is a greenhouse gas and the solubility of CO_2 in the ocean decreases with increasing temperature, the positive correlation between the increase of atmospheric CO_2 and the temperature is relatively easy to understand. It is however unclear, in general, whether an increase of temperature causes an increase of the atmospheric CO_2 concentration. Further, which trends do we have to expect in the near and remote future?

Nowadays, it is clear that a drastic reduction of anthropogenic emissions of greenhouse gases is of primary importance to limit global warming. However, according to the prevailing scientific understanding, it is unlikely that a steep reduction in global greenhouse gas emissions can be achieved. Therefore, in the last several years, investigations have been conducted to artificially remove greenhouse gases from the atmosphere or to reflect incoming solar radiation back to space.

The ocean exchanges large amounts of CO_2 with the atmosphere. This includes the natural cycling of CO_2 as well as the uptake of CO_2 from fossil fuel burning and other human activities. The ocean exchanges this CO_2 by a complex combination of physical, chemical, and biological processes. The processes driving this exchange are vulnerable to the effects of climate change and contribute to important climate feedbacks.
The oceanic net uptake of carbon dioxide is essentially driven by its transport from the ocean surface to the deep sea. Important in this context is the fact that any carbon (whether CO_2 or organic carbon) reaching the deep water remains for several centuries in the deep ocean. The different transport mechanisms that transfer carbon from the ocean surface to the deep are summarized under the term "oceanic carbon pumps"

Oceanic Carbon Pumps

Three processes summarily called the carbon pumps transfer carbon between the surface and the deep ocean: The solubility pump moves inorganic dissolved carbonate to the depth. The biological pump transports organic particulate carbon downwards. The carbonate counter pump describes the formation and sedimentation of carbonate tests, whereby CO_2 is released into the surface ocean. The carbon pumps are presented diagrammatically in Figure 2.1, which shows that carbon and other bio-limiting nutrients, are continuously cycled from the surface waters to the deep waters and back again.

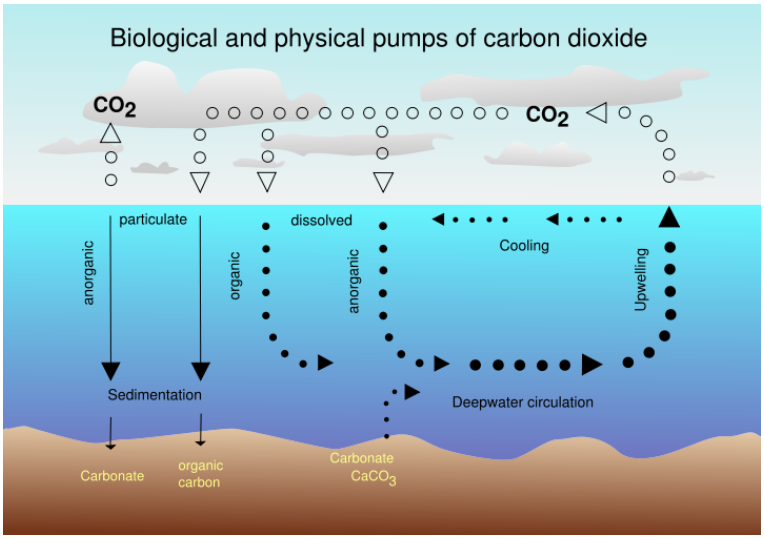

Figure 2.1: *Gas exchange of O_2 and CO_2, (Grobe (2006))*[1]

.

[1]Image Courtesy of Hannes Grobe, Alfred Wegener Institute for Polar and Marine Research, Bremerhaven, Germany (Grobe (2006)), From Wikipedia, the free encyclopedia `http://www.en.wikipedia.org`

The first mechanism is the so-called solubility pump. It is based on the fact that the solubility of CO_2 in the ocean is dependent on the temperature. In the solubility pump, CO_2 is transferred from air to sea by gas exchange as dissolved inorganic carbon (DIC, defined as CO_2 plus bicarbonate and carbonate ions) as sea water is undersaturated with CO_2 compared to the atmosphere. The CO_2 is subsequently distributed by mixing and ocean currents. The process is more efficient at higher latitudes as the uptake of CO_2 as DIC increases at lower temperatures since the solubility of CO_2 increases in cold water. For example in the Greenland Sea, CO_2 sinks rapidly to the deep ocean taking much higher concentrations of DIC with it (see,Archer et al. (2000); Raven and Falkowski (1999)). In such regions of deep water formation, carbon is delivered at high concentrations to the deep ocean where the deep circulation carries it around the world and keeps it out of contact with the atmosphere for up to 500 years. In consequence, there is a steep vertical gradient in the concentration of DIC and it has been estimated that about 25% to 50% of this gradient may be contributed by the solubility pump (see,Archer et al. (2000); Raven and Falkowski (1999)). If the natural carbon cycle in the ocean would be reduced or ceased to operate and the stored carbon were re-equilibrated with the atmosphere, current concentrations would increase substantially (see, Archer et al. (2000); Raven and Falkowski (1999)).

The second mechanism is the so-called biological pump. It involves a series of processes through which CO_2 fixed as organic matter by photosynthesis and transferred to the interior of the ocean resulting in a temporary or permanent storage of carbon (see, Ducklow et al. (2001); Eppley and Peterson (1979). Photosynthesizing microalgae (phytoplankton) can only live in the upper water layers, since they are dependent on light for generating energy via photosynthesis. Those organisms use dissolved nitrogen, dissolved phosphates in water, and carbon dioxide to produce organic material. Many species of phytoplankton form mineral constructions made of silica or calcium carbonate. The organic and mineral material sinks down while it is gradually disintegrated by the activity of bacteria so that only a small percentage is deposited in sediments. Those processes of absorption in the ocean surface and remineralization in deep water layers of the ocean leads to a reduction of the concentration of many chemical substances in the surface water with simultaneous enrichment in the deep water (see, Archer et al. (2000); Raven and Falkowski (1999)). The whole process of the removal of carbon and nutrients from the surface and its release into the depth is referred to as the biological pump. In order to predict future CO_2 concentrations in the atmosphere, it is necessary to understand the way the biological pump varies both geographically and temporally and the effects of changes in temperature, ocean circulation and ocean chemistry on the pump (e.g. acidification due to increased CO_2) (see, Archer et al. (2000); Raven and Falkowski (1999))

According to model calculations, the biological pump tends to ensure that the reduction of the CO_2 uptake by the solubility pump will be weakened. If the biological pump should effectively exploit anthropogenic CO_2, however, its efficiency should be increased, e.g. by higher nutrient concentration, this can be achieved by a further increase in the use of nitrogen fertilizer in agriculture, which is than flushed into the sea by rivers. Independently of the pump, it must also be noted that the dissolution of CO_2 in the ocean water will not always be as effective as it is now. The reason is that the oceans' CO_2 uptake rate decreases with increasing degree of its CO_2 saturation. The ability to absorb CO_2 is not unlimited. The ocean would become more acidic due to a higher amount of CO_2, which has a negative impact on the organisms living in it (see, Archer et al. (2000); Raven and Falkowski (1999); Sarmiento and Gruber (2004)).

The third mechanism is the so-called carbonate counter pump. This pump cannot be considered a pump in the proper sense of the word since it, in contrast to both preceding pumps, doesn't change the content of CO_2 in the atmosphere. It is therefore known as "counter pump". Its mode of operation, being the result of rather complicated ocean chemistry, is hard to describe. Generally, a reaction of carbonate with carbon dioxide to form hydrogen carbonate is considered responsible for it. The more carbonate there is, the more CO_2 gets lost in reaction. Thus, both compounds act in opposing directions as far as their concentration is concerned. Usually, the proportion of these carbonate compounds remains the same; thus, the reaction described above is an exception of this principle and therefore marks a difference in contrast to other acids in water (see, Archer et al. (2000); Bathmann and Passow (2010); Raven and Falkowski (1999); Riebesell et al. (2007); Sarmiento and Gruber (2004)).

The carbonate counter pump works due to some animals (like crustaceans) building up lime shells consisting of calcium carbonate. After their death they sink down into the deep, thus removing the compound carbonate from the upper layers. Consequently, the content of CO_2 increases there. An alternate and better explanation can be seen in the fact that also calcium ions get lost together with the carbonate, thus influencing the ionic balance (the offsetting of positively charged particles with negatively charged ones). The calcium carbonate falling down is electrically neutral; however, the balance of the buffer system doesn't only depend on the (hydrogen) carbonate ions and protons, but also on some other positively charged ions electrically balancing out the negative DIC components (see, Bathmann and Passow (2010); Riebesell et al. (2007)).

The carbonate pump may work in opposing direction to the other two, but since it only disposes of approximately one tenth of the power of the organic and solubility pump, it isn't of the same importance in transferring CO_2 from the upper layer into the deep (see, Bathmann and Passow (2010); Riebesell et al. (2007)).

2.2 Climate Models

Climate models are a simplified representation of reality and therefore include several uncertainties. Complex climate models, which are used today to reproduce past and present climate conditions, rely on high complex computational frameworks and require extensive calculations. Those models reflect the respective subsystems of the climate system (i.e. the atmosphere, the ocean, ice and snow, the vegetation, and the soil) or individual components of those subsystems in separated models that are linked to each other (see, e.g., McGuffie and Henderson-Sellers (2005); Stoer and Bulirsch (2002)). Climate models have several purposes. They are used to understand present climate and what factors create a particular climate in any one region. They are used to project climatic conditions into the future. Climate models are a tool to find out what natural processes or human activities may affect a region's environment in the future (see, e.g.,McGuffie and Henderson-Sellers (2005); Prieß (2012); Storch et al. (1999)). Climate models offer the possibility to investigate the influencing factors of the climate system isolated from each other. Therefore, they help to understand the climatological process. Additionally, it is possible to filter out the anthropogenic influence. Those models help to take a look into the climatic future because it is possible to calculate future changes under certain scenarios. The changes over time of the values at one place are expressed by differential equations and this results in complex systems of equations.

The biogeochemical processes in the subsystems and the connection between the respective systems are described as precisely as possible, atmosphere and ocean are assumed to be the most important components in the climate system. Climate models reflecting those processes for the whole planet are called global circulation models (GCMs) as well as atmospheric global circulation model (AGCM) or oceanic global circulation model (OGCM) (see, e.g., McGuffie and Henderson-Sellers (2005)). A climate model is often formulated as a coupled system of non-linear, partial differential, and algebraic equations. The underlying equations are typically too complex for analytical solutions, and thus, only an approximate solution of the model equations will be seeked by a suitable computer implementation which is referred to as a model simulation or numerical model (see, e.g., McGuffie and Henderson-Sellers (2005); Prieß (2012); Storch et al. (1999)).

To construct a specific model it is necessary to first understand the processes to be simulated along with its external driving mechanisms and internal interactions. Within this process, the parameterization is the main source of uncertainty of those models because the implemented parameters, which are derived from individual measurements, are not necessarily representative for all regions and seasons (see, e.g., McGuffie and Henderson-Sellers (2005); Prieß (2012); Storch et al. (1999)). As a consequence, very different parameterizations are used and the respective simulation results have then to

be compared. To evaluate the quality of a model, it always has to be examined to what extent its most important characteristics are dependent of the parameters (see, e.g., McGuffie and Henderson-Sellers (2005); Stoer and Bulirsch (2002)). Another difficulty is to find 'initial data' for such models. Usually, measurements are used, but the quality of such measurements is often debatable. Once a model is constructed, the time and storage requirements for its computational calculation highly depend on the complexity of the models underlying system of equations. Frequently, models have to be run over several months and need a lot of computational storage

The significance of the climate models can then be evaluated by their validity which is done by simulating the present and past climate. Nowadays, climate simulation is standard tool used in various application areas, such as the simulation of the dynamic evolutions of marine ecosystems which are of primary importance for understanding and simulating the oceanic uptake of carbon dioxide as well as for projections of the oceanic ecosystem's dynamics and their responses to climate change.

Therefore, to take into account the entire range of possible developments of the climate, several climate simulations are needed. Nowadays, climate simulations are a standard tools used in various application areas, such as the simulation of the dynamic evolutions of marine ecosystems which are of primary importance for understanding and simulating the oceanic uptake of carbon dioxide as well as for projections of the oceanic ecosystem's dynamics and their responses to climate change.

2.3 Modeling of Marine Ecosystems

The change in the marine ecosystems caused by global climate change can already be observed and encompasses the entire spectrum of physical (water temperature, salinity, vertical stratification, turbulence), chemical (gas solubility, PH values, nutrients), and biological factors like the food web. In order to understand and to quantitatively describe marine ecosystems, an integration of physics, chemistry, and biology is required. In general, the theoretical investigation of marine ecosystems is done by coupled models, which integrate physical, chemical and biological interactions. Marine ecosystem models are formulated as time-dependent systems of equations, which describe the interaction between their components. There are currently numerous different approaches for the modeling of marine ecosystem. According to the considered spatial dimension one can distinguish between zero-dimensional, one-dimensional and three-dimensional models. In so called box models, the physical processes are largely simplified while the resolution of biogeochemical processes can be very complex. Such models are easy to run and many of them serve as workbenches for model development. The next step is one-dimensional ecosystem models, which allow a detailed description of the important control of biolog-

ical processes. Such models may be useful for systems of weak horizontal advection (see, Fennel and Neumann (2004)).

Ecosystem models can be characterized roughly by their complexity, i.e., by the number of state variables and the degree of process resolution. The resolution of processes can be scaled up or down by aggregation of variables into a few integrated ones or by increasing the number of variables, respectively. It has to be pointed out that models with numerous state variables are not automatically better than those with only a few variables. The higher the number of variables, the larger the requirement of process understanding and quantification (see, Fennel and Neumann (2004)).

The marine ecosystem is an especially complicated object both due to the large number of interacting species and due to the complex properties of the marine environment (e.g., turbulence). The dynamics of a marine ecosystem is affected by the fact that the temporal and spatial scales of the underlying physical and biological processes often appear to be of the same order. The interaction between physics and biology in the sea occurs in a very complicated way. Turbulence is one of the most important factors affecting the dynamics of marine ecosystems, e.g., bringing up the nutrients necessary for the spring bloom of phytoplankton. The rates of phytoplankton grazing and zooplankton mortality also strongly depend on the intensity of turbulent mixing. Clearly, the development of suitably complex ecosystem models, reliable parametrizations therein as well as an assessment of their quality are an indispensable part of current research (see, Evans and Garçon (1997)).

One model that will be applied in the context of the current CO_2 research for the simulation of the marine ecosystem, a so called NPZD-model, is described and examined in this work.

3 Mathematical Preliminaries

3.1 Basis of Control Theory

This section presents the basics of discrete linear quadratic optimal control. The aim of this method is to influence the state of a system to obtain an optimal state related to a cost function by using controls. Figure 3.1 shows a so called open loop discrete linear quadratic optimal control, where $\mathbf{u} = (\mathbf{u}_1, \mathbf{u}_2, \ldots, \mathbf{u}_{N-1})$ represents the input (control) and $\mathbf{x} = (\mathbf{x}_1, \mathbf{x}_2, \ldots, \mathbf{x}_N)$ the state of the system. The output $\mathbf{y} = (\mathbf{y}_1, \mathbf{y}_2, \ldots, \mathbf{y}_N)$ of the system depends on the input $\mathbf{u}$ and the state $\mathbf{x}$. An open loop system is a type of continuous control system in which the output has no influence or effect on the input.

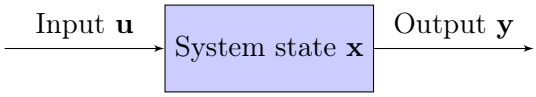

Figure 3.1: *Open loop system*

A Closed-loop Control System, also known as a feedback control system is a control system which uses the concept of an open loop system as its forward path but has one or more feedback loops or paths between its output and its input. The reference to "feedback" means that some portion of the output is returned "back" to the input to form part of the system's excitation, this is shown in Figure 3.2.

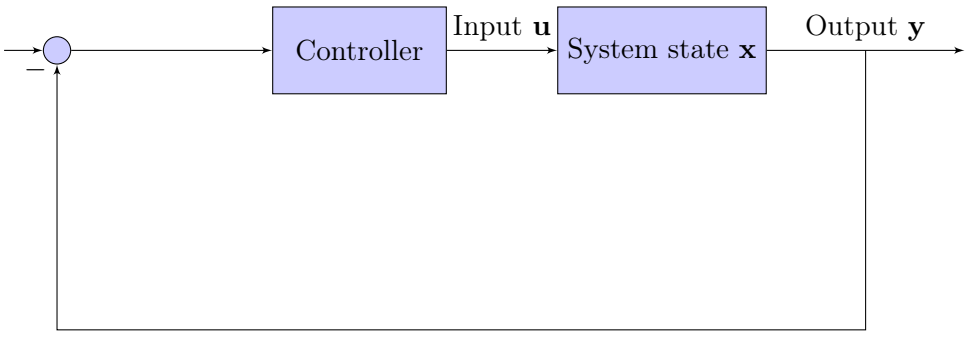

Figure 3.2: *Closed loop system*

3.1.1 Closed Loop Discrete Linear Quadratic Optimal Control

In this subsection we give an overview about the theory of closed loop discrete linear quadratic optimal control method. For more details we refer to Anderson and Moore (1971); Athans and Falb (1966); Casti (1987); Friedland (1986); Geering (2003); Knobloch and Kwakernaak (1985); Kosmol (2010); Locatelli (2001); Lunze (1997); Sima (1996); Sontag (1998); Zabczyk (1992). The basic representation for a discrete linear system is given by the linear discrete-time state equation:

$$\begin{aligned} \mathbf{x}_{k+1} &= \mathbf{A}_k \mathbf{x}_k + \mathbf{B}_k \mathbf{u}_k, \quad \forall\, k \in [N-1] := \{1, 2, \ldots, N-1\}, \\ \mathbf{x}_1 &= \mathbf{x}_1^*, \qquad \text{the given initial value,} \end{aligned} \tag{3.1}$$

and the linear discrete-time output equation

$$\mathbf{y}_k = \mathbf{C}_k \mathbf{x}_k, \qquad \forall\, k \in [N-1], \tag{3.2}$$

where in every time step k

- $\mathbf{x}_k = \mathbf{x}(t_k) \in \mathbb{R}^n$ is called the state vector,
- $\mathbf{u}_k = \mathbf{u}(t_k) \in \mathbb{R}^p$ is the control vector,
- $\mathbf{y}_k = \mathbf{y}(t_k) \in \mathbb{R}^m$ is the output vector,
- the matrices $\mathbf{A}_k \in \mathbb{R}^{n \times n}$, $\mathbf{B}_k \in \mathbb{R}^{n \times p}$, and $\mathbf{C}_k \in \mathbb{R}^{m \times n}$ are called the system matrix, the input matrix and the output matrix respectively.

We will use the notations

- $\mathbf{x} := (\mathbf{x}_k)_{k \in [N]}$,
- $\mathbf{u} := (\mathbf{u}_k)_{k \in [N-1]}$,
- $\mathbf{y} := (\mathbf{y}_k)_{k \in [N]}$,

for the whole discrete trajectories of state, control and output vector, respectively.
We wish to find the optimal control sequence $(\mathbf{u}_k)_{k \in [N-1]}$ that minimizes the cost function

$$\mathcal{J}(\mathbf{u}) = \frac{1}{2} \mathbf{x}_N^\top \mathbf{Q}_N \mathbf{x}_N + \frac{1}{2} \sum_{k=1}^{N-1} \left(\mathbf{x}_k^\top \mathbf{Q}_k \mathbf{x}_k + \mathbf{u}_k^\top \mathbf{R}_k \mathbf{u}_k \right), \tag{3.3}$$

- $\mathbf{Q}_k$ is a positive semidefinite diagonal weighting matrix assigned to the state vector for every model time step $k \in [N]$,

- $\mathbf{R}_k$ is a positive definite diagonal weighting matrix assigned to the control vector for every model time step $k \in [N-1]$,
- If the outputs are to be weighted in the cost function, then the weighting matrix for the state vector can be replaced by $\mathbf{C}_k^\top \mathbf{Q}_k \mathbf{C}_k$.

Theorem 1. *If the $\mathbf{Q}_k, k \in [N]$, are positive semi-definite and the $\mathbf{R}_k, k \in [N-1]$, are positive definite, then there exists a unique solution of the closed loop discrete linear quadratic optimal control method (3.1), (3.3). The optimal control is given by the* feedback law

$$\begin{aligned} \mathbf{u}_k &= \mathbf{G}_k \mathbf{x}_k, \quad \forall\, k \in [N-1], \\ \mathbf{G}_k &:= -(\mathbf{R}_k + \mathbf{B}_k^\top \mathbf{P}_{k+1} \mathbf{B}_k)^{-1} \mathbf{B}_k^\top \mathbf{P}_{k+1} \mathbf{A}_k \qquad \forall\, k \in [N-1], \\ \mathbf{x}_{k+1} &= (\mathbf{A}_k + \mathbf{B}_k \mathbf{G}_k)\mathbf{x}_k \qquad \forall\, k \in [N-1], \end{aligned}$$

where $(\mathbf{P}_k)_{k\in[N]}$ is the unique symmetric solution of the Discrete Riccati Equation.

$$\begin{aligned} \mathbf{P}_{N-k} = \mathbf{Q}_{N-k} + \mathbf{A}_{N-k}^\top \mathbf{P}_{N-k+1} \mathbf{A}_{N-k} \\ -\mathbf{A}_{N-k}^\top \mathbf{P}_{N-k+1} \mathbf{B}_{N-k} (\mathbf{R}_{N-k} + \mathbf{B}_{N-k}^\top \mathbf{P}_{N-k+1} \mathbf{B}_{N-k})^{-1} \mathbf{B}_{N-k}^\top \mathbf{P}_{N-k+1} \mathbf{A}_{N-k}, \\ \forall\, k \in [N-1], \end{aligned} \tag{3.4}$$

with final value boundary condition

$$\mathbf{P}_N = \mathbf{Q}_N.$$

Furthermore, the minimum value of the cost function, $\mathcal{J}$, is given by

$$\mathcal{J}^* = \frac{1}{2} \mathbf{x}_1^\top \mathbf{P}_1 \mathbf{x}_1,$$

where $\mathbf{P}_1$ is found by the Riccati equation (3.4). The goal of closed loop discrete linear quadratic optimal control method is to keep $\mathbf{x} = (\mathbf{x}_k)_{k\in[N]}$ close to $\mathbf{0}$, especially, at the final time step N, using control vector $\mathbf{u} = (\mathbf{u}_k)_{k\in[N-1]}$.

Proof. In order to solve the closed loop discrete linear quadratic optimal control problem, we introduce a set of auxiliary parameters $\boldsymbol{\lambda}_k$ called Lagrange multiplier, we turn the constrained optimization problem into a unconstrained problem. The new cost function is

$$\bar{\mathcal{J}}(\mathbf{u}) = \frac{1}{2} \mathbf{x}_N^\top \mathbf{Q}_N \mathbf{x}_N + \sum_{k=1}^{N-1} \left[\frac{1}{2} \left(\mathbf{x}_k^\top \mathbf{Q}_k \mathbf{x}_k + \mathbf{u}_k^\top \mathbf{R}_k \mathbf{u}_k \right) + \boldsymbol{\lambda}_{k+1}^\top \left(\mathbf{A}_k \mathbf{x}_k + \mathbf{B}_k \mathbf{u}_k - \mathbf{x}_{k+1} \right) \right].$$

Another notational advice is to make the above expression a bit shorter by introducing a new variable called Hamiltonian function

$$\mathcal{H}_k(\mathbf{x}_k, \mathbf{u}_k, \boldsymbol{\lambda}_{k+1}) = \frac{1}{2}\left(\mathbf{x}_k^\top \mathbf{Q}_k \mathbf{x}_k + \mathbf{u}_k^\top \mathbf{R}_k \mathbf{u}_k\right) + \boldsymbol{\lambda}_{k+1}^\top \left(\mathbf{A}_k \mathbf{x}_k + \mathbf{B}_k \mathbf{u}_k\right). \quad (3.5)$$

this gives

$$\bar{\mathcal{J}}(\mathbf{u}) = \frac{1}{2}\mathbf{x}_N^\top \mathbf{Q}_N \mathbf{x}_N + \sum_{k=1}^{N-1}\left[\mathcal{H}_k(\mathbf{x}_k, \mathbf{u}_k, \boldsymbol{\lambda}_{k+1}) - \boldsymbol{\lambda}_{k+1}^\top \mathbf{x}_{k+1}\right].$$

The optimal control sequence $(\mathbf{u})_{k\in[N-1]}$ that minimizes the cost function (3.3) is obtained by solving simultaneously the following equations:

$$\begin{aligned}
\mathbf{x}_{k+1} &= \frac{\partial \mathcal{H}_k}{\partial \boldsymbol{\lambda}_{k+1}} = \mathbf{A}_k \mathbf{x}_k + \mathbf{B}_k \mathbf{u}_k, && (3.6)\\
\boldsymbol{\lambda}_k &= \frac{\partial \mathcal{H}_k}{\partial \mathbf{x}_k} = \mathbf{Q}_k \mathbf{x}_k + \mathbf{A}_k^\top \boldsymbol{\lambda}_{k+1}, && (3.7)\\
0 &= \frac{\partial \mathcal{H}_k}{\partial \mathbf{u}_k} = \mathbf{R}_k \mathbf{u}_k + \mathbf{B}_k^\top \boldsymbol{\lambda}_{k+1}, && (3.8)\\
\boldsymbol{\lambda}_N &= \frac{\partial (\frac{1}{2}\mathbf{x}_N^\top \mathbf{Q}_N \mathbf{x}_N)}{\partial \mathbf{x}_N} = \mathbf{Q}_N \mathbf{x}_N, && (3.9)\\
\mathbf{x}_1 &= \mathbf{x}_1^* \quad \text{the given initial value.} && (3.10)
\end{aligned}$$

The first equation (3.6) can be recognized as the original state equation. The second equation (3.7) is called a co-state equation and the variable $\boldsymbol{\lambda}_k$ is called a co-state variable. The third equation (3.8) is called an equation of stationarity. The last two equations (3.9) and (3.10) represent boundary conditions.
The equation (3.8) can be used to extract the optimal control:

$$\mathbf{u}_k = -\mathbf{R}_k^{-1}\mathbf{B}_k^\top \boldsymbol{\lambda}_{k+1}, \quad \forall\, k \in [N-1], \quad (3.11)$$

where the positive definiteness of $\mathbf{R}_k$ ensures its invertibility. Using the obtained optimal control (3.11) in (3.6), we get

$$\mathbf{x}_{k+1} = \mathbf{A}_k \mathbf{x}_k - \mathbf{B}_k \mathbf{R}_k^{-1}\mathbf{B}_k^\top \boldsymbol{\lambda}_{k+1}, \quad \forall\, k \in [N-1]. \quad (3.12)$$

In order to obtain closed loop optimal control, we need to express the co-state variable $\boldsymbol{\lambda}_{k+1}$ in the optimal control (3.11) in term of the state variable $\mathbf{x}_k$. The final condition (3.9) yields

$$\boldsymbol{\lambda}_k := \mathbf{P}_k \mathbf{x}_k, \quad \forall\, k \in [N], \quad (3.13)$$

where $\mathbf{P}_k$ is yet to be determined. This linear transformation is called the Riccati transformation and is of fundamental importance in the solution of the closed loop discrete linear quadratic optimal control problem.
Using the transformation (3.13) in the state and co-state equations (3.6) and (3.7), we have

$$\mathbf{P}_{N-k}\mathbf{x}_{N-k} = \mathbf{Q}_{N-k}\mathbf{x}_{N-k} + \mathbf{A}_{N-k}^{\top}\mathbf{P}_{N-k+1}\mathbf{x}_{N-k+1}, \quad \forall\, k \in [N-1], \quad (3.14)$$

and

$$\mathbf{x}_{k+1} = \mathbf{A}_k\mathbf{x}_k - \mathbf{B}_k\mathbf{R}_k^{-1}\mathbf{B}_k^{\top}\mathbf{P}_{k+1}\mathbf{x}_{k+1}, \quad \forall\, k \in [N-1]. \quad (3.15)$$

Solving for $(\mathbf{x}_{k+1})$ yields

$$\mathbf{x}_{k+1} = \left(\mathbf{I}_n + \mathbf{B}_k\mathbf{R}_k^{-1}\mathbf{B}_k^{\top}\mathbf{P}_{k+1}\right)^{-1}\mathbf{A}_k\mathbf{x}_k, \quad (3.16)$$

substituting (3.16) into (3.14) gives for each $k \in [N-1]$

$$\left(-\mathbf{P}_{N-k} + \mathbf{Q}_{N-k} + \mathbf{A}_{N-k}^{\top}\mathbf{P}_{N-k+1}\left(I_n + \mathbf{B}_{N-k}\mathbf{R}_{N-k}^{-1}\mathbf{B}_{N-k}^{\top}\mathbf{P}_{N-k+1}\right)^{-1}\mathbf{A}_{N-k}\right)\mathbf{x}_{N-k+1} = 0. \quad (3.17)$$

Since equation (3.17) must hold for any $\mathbf{x}_k$, we get the following equation in matrices $\mathbf{P}_k$

$$\mathbf{P}_{N-k} = \mathbf{Q}_{N-k} + \mathbf{A}_{N-k}^{\top}\mathbf{P}_{N-k+1}\left(I_n + \mathbf{B}_{N-k}\mathbf{R}_{N-k}^{-1}\mathbf{B}_{N-k}^{\top}\mathbf{P}_{N-k+1}\right)^{-1}\mathbf{A}_{N-k}, \quad (3.18)$$

This equation is called the matrix Riccati equation named after Count Riccati (Riccati (1724)). The final condition to solve the Riccati equation (3.18) is obtained from (3.13) as

$$\boldsymbol{\lambda}_N = \mathbf{Q}_N\mathbf{x}_N = \mathbf{P}_N\mathbf{x}_N, \quad (3.19)$$

which gives

$$\mathbf{P}_N = \mathbf{Q}_N. \quad (3.20)$$

In equation (3.18), we start with (3.20) and iteratively determine $\mathbf{P}_k$ from $\mathbf{P}_{k+1}$, $k = N-1, \ldots, 1$. Since $\mathbf{Q}_k$ is assumed to be positive semidefinite for all $k \in [N]$, we can show that the Riccati matrix $\mathbf{P}_k$ is positive semidefinite for all $k \in [N]$.

We use the matrix inversion lemma:

$$(A+BCD)^{-1} = A^{-1} - A^{-1}B(DA^{-1}B + C^{-1})^{-1}DA^{-1}, \tag{3.21}$$

where A, B, C, and D all denote matrices of the correct size. Specifically, A is $n \times n$, B is $n \times m$, C is $m \times m$ and D is $m \times n$ (Hager (1989)).
The equation (3.18) can be rewritten as

$$\begin{aligned}\mathbf{P}_{N-k} = \mathbf{Q}_{N-k} + \mathbf{A}_{N-k}^{\top}\mathbf{P}_{N-k+1}\mathbf{A}_{N-k} \\ + \mathbf{A}_{N-k}^{\top}\mathbf{P}_{k+1}\mathbf{B}_{N-k}\left(\mathbf{R}_{N-k} + \mathbf{B}_{N-k}^{\top}\mathbf{P}_{N-k+1}\mathbf{B}_{N-k}\right)^{-1}\mathbf{B}_{N-k}^{\top}\mathbf{P}_{N-k+1}\mathbf{A}_{N-k}, \\ \mathbf{P}_N = \mathbf{Q}_N.\end{aligned}$$

Now to obtain the closed loop optimal control, we eliminate $\boldsymbol{\lambda}_{k+1}$ from (3.11) and (3.13), substitute the state equation and get

$$\mathbf{u}_k \;=\; -\mathbf{R}_k^{-1}\mathbf{B}_k^{\top}\mathbf{P}_{k+1}\left(\mathbf{A}_k\mathbf{x}_k + \mathbf{B}_k\mathbf{u}_k\right).$$

Given that $\mathbf{R}_k$ is positive definite and $\mathbf{P}_{k+1}$ positive semi-definite, then $\left(\mathbf{R}_k + \mathbf{B}_k^{\top}\mathbf{P}_{k+1}\mathbf{B}_k\right)$ is positive definite (thus invertible). Solving this equation for $\mathbf{u}_k$ gives

$$\mathbf{u}_k \;=\; -\left(\mathbf{R}_k + \mathbf{B}_k^{\top}\mathbf{P}_{k+1}\mathbf{B}_k\right)^{-1}\mathbf{B}_k^{\top}\mathbf{P}_{k+1}\mathbf{A}_k\mathbf{x}_k, \quad \forall\, k \in [N-1]. \tag{3.22}$$

This equation is the desired version for the closed loop optimal control in terms of the state. We may write the closed loop optimal control equation in a simplified form as

$$\mathbf{u}_k \;=\; \mathbf{G}_k\mathbf{x}_k, \quad \forall\, k \in [N-1], \tag{3.23}$$

where

$$\mathbf{G}_k \;=\; -\left(\mathbf{R}_k + \mathbf{B}_k^{\top}\mathbf{P}_{k+1}\mathbf{B}_k\right)^{-1}\mathbf{B}_k^{\top}\mathbf{P}_{k+1}\mathbf{A}_k, \quad \forall\, k \in [N-1]. \tag{3.24}$$

This is the required relation for the optimal feedback control law and the matrix $\mathbf{G}_k$ is called the "Kalman gain".
The optimal state $(\mathbf{x}_k)_{k\in[N]}$ is obtained by substituting the optimal control $(\mathbf{u}_k)_{k\in[N-1]}$ given by (3.23) in the original state equation (3.1) as

$$\mathbf{x}_{k+1} \;=\; \left(\mathbf{A}_k + \mathbf{B}_k\mathbf{G}_k\right)\mathbf{x}_k, \quad \forall\, k \in [N-1]. \tag{3.25}$$

□

Remark 1. *The discreet time Riccati equation (3.18) may be formulated as*

$$\begin{aligned}\mathbf{P}_{N-k} &= (\mathbf{A}_{N-k} + \mathbf{B}_{N-k}\mathbf{G}_{N-k})^\top \mathbf{P}_{N-k+1}(\mathbf{A}_{N-k} + \mathbf{B}_{N-k}\mathbf{G}_{N-k}) \\ &\quad + \mathbf{G}_{N-k}^\top \mathbf{P}_{N-k+1}\mathbf{G}_{N-k} + \mathbf{Q}_{N-k}, \qquad \forall\, k \in [N-1], \\ \mathbf{P}_N &= \mathbf{Q}_N.\end{aligned} \tag{3.26}$$

This formulation of the discrete time Riccati equation is known in the literature as the Josephs stable version of the Riccati equation. This Riccati equation consists only of symmetric terms and can be used in order to find the stationary solution to the closed loop discrete linear quadratic optimal control problem, i.e. the problem with infinite horizon $N \to \infty$.

Table 3.1 show a summary of closed loop discrete linear quadratic optimal control method.

Table 3.1: ***Summary of closed loop discrete linear quadratic optimal control.***

(a) Given the state and output equations $\mathbf{x}_{k+1} = \mathbf{A}_k\mathbf{x}_k + \mathbf{B}_k\mathbf{u}_k, \quad \forall k \in [N-1],$ $\mathbf{y}_k = \mathbf{C}_k\mathbf{x}_k, \quad \forall k \in [N-1],$ and the cost function as $\mathcal{J}(\mathbf{u}) = \frac{1}{2}\mathbf{x}_N^\top \mathbf{Q}_N \mathbf{x}_N + \frac{1}{2}\sum_{k=1}^{N-1}\left(\mathbf{x}_k^\top \mathbf{Q}_k \mathbf{x}_k + \mathbf{u}_k^\top \mathbf{R}_k \mathbf{u}_k\right),$ and the boundary conditions $\mathbf{x}_1 = \mathbf{x}^1, \qquad \mathbf{x}_N$ is free.
(b) Solve the matrix Riccati equation $\mathbf{P}_{N-k} = \mathbf{Q}_{N-k} + \mathbf{A}_{N-k}^\top \mathbf{P}_{N-k+1}\mathbf{A}_{N-k}$ $+\ \mathbf{A}_{N-k}^\top \mathbf{P}_{k+1}\mathbf{B}_{N-k}\left(\mathbf{R}_{N-k} + \mathbf{B}_{N-k}^\top \mathbf{P}_{N-k+1}\mathbf{B}_{N-k}\right)^{-1}\mathbf{B}_{N-k}^\top \mathbf{P}_{N-k+1}\mathbf{A}_{N-k},$ with final condition $\mathbf{P}_N = \mathbf{Q}_N$
(c) Solve the optimal state $\mathbf{x} = (\mathbf{x}_k)_{k\in[N]}$ from $\mathbf{x}_{k+1} = (\mathbf{A}_k + \mathbf{B}_k\mathbf{G}_k)\,\mathbf{x}_k,$ with initial condition $\mathbf{x}_1 = \mathbf{x}_1^*$, where $\mathbf{G}_k = -\left(\mathbf{R}_k + \mathbf{B}_k^\top \mathbf{P}_{k+1}\mathbf{B}_k\right)^{-1}\mathbf{B}_k^\top \mathbf{P}_{k+1}\mathbf{A}_k.$
(d) Solve the optimal control $\mathbf{u} = (\mathbf{u}_k)_{k\in[N-1]}$ from $\mathbf{u}_k = \mathbf{G}_k\mathbf{x}_k,$ where $\mathbf{G}_k$ is the Kalman gain.

3.1.2 Nonlinear Quadratic Optimal Control

Consider the following class of discrete-time nonlinear system

$$\mathbf{x}_{k+1} = \mathbf{f}(\mathbf{x}_k, \mathbf{u}_k), \quad \forall k \in [N-1], \text{state equation}, \tag{3.27a}$$

$$\mathbf{x}_1 = \mathbf{x}_1^*, \qquad \text{the given initial value}, \tag{3.27b}$$

$$\mathbf{y}_k = \mathbf{g}(\mathbf{x}_k), \quad \forall k \in [N-1], \quad \text{output equation}. \tag{3.27c}$$

Where $\mathbf{x}_k \in \mathbb{R}^n$, $\mathbf{y}_k \in \mathbb{R}^m$, $k \in [N]$, $\mathbf{u}_k \in \mathbb{R}^p$, $k \in [N-1]$, $\mathbf{f}\colon \mathbb{R}^{n\times p} \to \mathbb{R}^n$, and $\mathbf{g}\colon \mathbb{R}^n \to \mathbb{R}^m$. We assume the following conditions:

- for each $k \in [N-1]$, $\mathbf{f}$ is continuously differentiable with respect to each component of $\mathbf{x}_k$ and $\mathbf{u}_k$.

- for each $k \in [N-1]$, $\mathbf{g}$ is continuously differentiable with respect to each component of $\mathbf{x}_k$.

In order to apply the control method discussed in the first part of this chapter, we musst rewrite (3.27a) and (3.27c) in the form (3.1) and (3.2). To do this, we need to linearize equations (3.27a)and (3.27c), we use a time-varing reference trajectories $(\mathbf{x}_k^{(ref)})_{k\in[N]}$, $(\mathbf{u}_k^{(ref)})_{k\in[N-1]}$, and $(\mathbf{y}_k^{(ref)})_{k\in[N]}$ for the linearization, which results in a time-varing matrices $(\mathbf{A}_k)_{k\in[N-1]}$,$(\mathbf{B}_k)_{k\in[N-1]}$, and $(\mathbf{C}_k)_{k\in[N]}$, and consequently in an linear discrete-time equations (3.1) and (3.2).

Given a particular reference (or desired) state trajectory $(\mathbf{x}_k^{(ref)})_{k\in[N]}$, control trajectory $(\mathbf{u}_k^{(ref)})_{k\in[N-1]}$, and output trajectory $(\mathbf{y}_k^{(ref)})_{k\in[N]}$, which satisfy the equations (3.27a) and (3.27c), i.e., $\mathbf{x}_{k+1}^{(ref)} = \mathbf{f}(\mathbf{x}_k^{(ref)}, \mathbf{u}_k^{(ref)})$ and $\mathbf{y}_k^{(ref)} = \mathbf{g}(\mathbf{x}_k^{(ref)})$. We develop an approximation by truncating the Taylor series expansion of $\mathbf{f}$ about $\mathbf{x}_k^{(ref)}$ and $\mathbf{u}_k^{(ref)}$ and $\mathbf{g}$ about $\mathbf{x}_k^{(ref)}$ after the first-order terms.
For small deviations $(\tilde{\mathbf{x}}_k, \tilde{\mathbf{u}}_k, \tilde{\mathbf{y}}_k)$ to the solution curve, the following notation are given as

$$\mathbf{x}_k = \mathbf{x}_k^{(ref)} + \tilde{\mathbf{x}}_k, \quad \forall\, k \in [N], \tag{3.28}$$

$$\mathbf{u}_k = \mathbf{u}_k^{(ref)} + \tilde{\mathbf{u}}_k, \quad \forall\, k \in [N-1], \tag{3.29}$$

$$\mathbf{y}_k = \mathbf{y}_k^{(ref)} + \tilde{\mathbf{y}}_k, \quad \forall\, k \in [N]. \tag{3.30}$$

The equations (3.27a) and (3.27c) can be written in the form

$$\begin{aligned}
\mathbf{x}_{k+1}^{(ref)} + \tilde{\mathbf{x}}_{k+1} &= \mathbf{f}(\mathbf{x}_k^{(ref)} + \tilde{\mathbf{x}}_k, \mathbf{u}_k^{(ref)} + \tilde{\mathbf{u}}_k), && (3.31)\\
&\simeq \mathbf{f}(\mathbf{x}_k^{(ref)}, \mathbf{u}_k^{(ref)}) + \mathcal{D}_x\mathbf{f}(\mathbf{x}_k^{(ref)}, \mathbf{u}_k^{(ref)})(\mathbf{x}_k - \mathbf{x}_k^{(ref)})\\
&+ \mathcal{D}_u\mathbf{f}(\mathbf{x}_k^{(ref)}, \mathbf{u}_k^{(ref)})(\mathbf{u}_k - \mathbf{u}_k^{(ref)}), && (3.32)\\
\mathbf{y}_k^{(ref)} + \tilde{\mathbf{y}}_k &= \mathbf{g}(\mathbf{x}_k^{(ref)} + \tilde{\mathbf{x}}_k), && (3.33)\\
&\simeq \mathbf{g}(\mathbf{x}_k^{(ref)}) + \mathcal{D}_x\mathbf{g}(\mathbf{x}_k^{(ref)})(\mathbf{x}_k - \mathbf{x}_k^{(ref)}),
\end{aligned}$$

The linearized state and output equations are given as:

$$\tilde{\mathbf{x}}_{k+1} = \mathbf{A}_k\tilde{\mathbf{x}}_k + \mathbf{B}_k\tilde{\mathbf{u}}_k, \quad \forall\, k \in [N-1], \tag{3.34a}$$

$$\tilde{\mathbf{x}}_1 = \mathbf{x}_1 - \mathbf{x}_1^{(ref)}, \tag{3.34b}$$

$$\tilde{\mathbf{y}}_{k+1} = \mathbf{C}_k\tilde{\mathbf{x}}_k, \quad \forall\, k \in [N-1], \tag{3.34c}$$

where $\mathbf{A}_k = \mathcal{D}_x\mathbf{f}(\mathbf{x}_k^{(ref)}, \mathbf{u}_k^{(ref)}), \mathbf{B}_k = \mathcal{D}_u\mathbf{f}(\mathbf{x}_k^{(ref)}, \mathbf{u}_k^{(ref)})$ and $\mathbf{C}_k = \mathcal{D}_x\mathbf{g}(\mathbf{x}_k^{(ref)})$. $\mathcal{D}_x$ denotes the Jacobian of $\mathbf{f}$ with respect to x, $\mathcal{D}_u$ denotes the Jacobian of $\mathbf{g}$ with respect to u, and the Jacobians are evaluated at $\mathbf{x}_k^{(ref)}$ and $\mathbf{u}_k^{(ref)}$. We note, that if we linearize (3.27a) and (3.27c) about an operating point $(\bar{\mathbf{x}}, \bar{\mathbf{u}})$, i.e., $\bar{\mathbf{x}} = \mathbf{f}(\bar{\mathbf{x}}, \bar{\mathbf{u}})$ with $\bar{\mathbf{y}} = \mathbf{g}(\bar{\mathbf{x}})$, then the obtained matrices A, B and C have to be constant and the linearized state and output equations are given as:

$$\tilde{\mathbf{x}}_{k+1} = \mathbf{A}\tilde{\mathbf{x}}_k + \mathbf{B}\tilde{\mathbf{u}}_k, \quad \forall\, k \in [N-1], \tag{3.35a}$$

$$\tilde{\mathbf{x}}_1 = \mathbf{x}_1 - \bar{\mathbf{x}}, \tag{3.35b}$$

$$\tilde{\mathbf{y}}_{k+1} = \mathbf{C}\tilde{\mathbf{x}}_k, \quad \forall\, k \in [N-1], \tag{3.35c}$$

where

$$\begin{aligned}
\tilde{\mathbf{x}}_k &= \mathbf{x}_k - \bar{\mathbf{x}}, & \mathbf{A} &= \mathcal{D}_x\mathbf{f}(\bar{\mathbf{x}}, \bar{\mathbf{u}}),\\
\tilde{\mathbf{u}}_k &= \mathbf{u}_k - \bar{\mathbf{u}}, & \mathbf{B} &= \mathcal{D}_u\mathbf{f}(\bar{\mathbf{x}}, \bar{\mathbf{u}}),\\
\tilde{\mathbf{y}}_k &= \mathbf{y}_k - \bar{\mathbf{y}}, & \mathbf{C} &= \mathcal{D}_x\mathbf{g}(\bar{\mathbf{x}}).
\end{aligned}$$

The optimization problem is defined as follows

$$\min_{\tilde{\mathbf{u}}} \mathcal{J}(\tilde{\mathbf{u}}), \quad \text{where} \qquad \mathcal{J}(\tilde{\mathbf{u}}) = \frac{1}{2}\tilde{\mathbf{x}}_N^\top\mathbf{Q}_N\tilde{\mathbf{x}}_N + \frac{1}{2}\sum_{k=1}^{N-1}\left(\tilde{\mathbf{x}}_k^\top\mathbf{Q}_k\tilde{\mathbf{x}}_k + \tilde{\mathbf{u}}_k^\top\mathbf{R}_k\tilde{\mathbf{u}}_k\right)$$

subject to

$$\begin{aligned}\tilde{\mathbf{x}}_{k+1} &= \mathbf{A}\tilde{\mathbf{x}}_k + \mathbf{B}\tilde{\mathbf{u}}_k, \quad \forall\, k \in [N-1],\\ \tilde{\mathbf{x}}_1 &= \mathbf{x}_1 - \bar{\mathbf{x}}.\end{aligned}$$

If the outputs are to be weighted in the cost function, then the weighting matrix for the state vector can be replaced by $\mathbf{C}_k^\top \mathbf{Q}_k \mathbf{C}_k$.

3.1.3 Selection of the weighting matrices $(\mathbf{Q}_k)_{k\in[N]}$, $(\mathbf{R}_k)_{k\in[N-1]}$

The quality of the control design using linear quadratic optimal control method depends on the choice of the weighting matrices $\mathbf{Q}_k$ and $\mathbf{R}_k$. Normally, this requires some kinds of trial and error

- If there is a specific output $\mathbf{y}_k = \mathbf{C}_k\mathbf{x}_k, k \in [N]$ that needs to be kept small, choose $\mathbf{Q}_k = \mathbf{C}_k^\top \mathbf{C}_k, k \in [N]$.
- Obtain acceptable bounds:

  $$\begin{aligned} |x_i| &\leqslant x_{i,max}, & |u_j| &\leqslant u_{j,max},\\ i &= 1,\ldots,n, & j &= 1,\ldots,p\end{aligned}$$

  then choose $\mathbf{Q}_k$ and $\mathbf{R}_k$ to be inversely proportional to $x_{i,max}$ and $u_{j,max}$, respectively.
- If $\mathbf{R}_k = diag\,[r_1, r_2, \ldots, r_p]$ and $|\mathbf{u}_{j,k}|$ is to large after simulation, then increase r_j.

In general good results will be obtained when the matrix $\mathbf{Q}_k$ is selected to be relatively large in the ratio of $\mathbf{R}_k$.

3.2 State Estimation with Kalman Filter

This section presents the basics of the discrete Kalman filter. It was developed by Rudolf E. Kalman (see Kalman (1960)). Essentially, the Kalman filter is a set of mathematical equations that allows an efficient estimation of the state of a process by minimizing the mean of the squared error. The filter is very powerful in several aspects: It supports estimations of past, present, and even future state, even if the precise nature of the modeled systems is unknown (see, e.g., Welch and Bishop (2004)). In this section we introduce the discrete Kalman filter together with some necessary basic statistical definitions and the extended Kalman filter for nonlinear problems (see, e.g., Athans (1996); Balakrishnan (1987); Catlin (2011); Grewal and Andrews (2001); Gibbs (2011); Gillijns et al. (2006);

Sorenson (1960)).
The Kalman filter addresses the general problem of estimating the state $\mathbf{x} = (\mathbf{x}_k)_{k\in[N]}$ of a discrete-time controlled process that is governed by the linear discrete-time state equation

$$\begin{aligned} \mathbf{x}_{k+1} &= \mathbf{A}_k\mathbf{x}_k + \mathbf{B}_k\mathbf{u}_k + \mathbf{q}_k, \quad \forall\, k \in [N-1], \\ \mathbf{x}_1 &\quad \text{the given initial state,} \end{aligned} \tag{3.36}$$

and the linear discrete-time measurement equation

$$\mathbf{y}_k \quad = \mathbf{C}_k\mathbf{x}_k + \mathbf{b}_k, \quad \forall\, k \in [N-1],. \tag{3.37}$$

where in every time step k

- $\mathbf{q}_k = \mathbf{q}(t_k) \in \mathbb{R}^n$ is the unknown model error,
- $\mathbf{b}_k = \mathbf{b}(t_k) \in \mathbb{R}^m$ is the measurement error,

Here, the evolutions of the state $\mathbf{x}$ and the measurement $\mathbf{y}$ are subject to some noise processes $\mathbf{q}$ and $\mathbf{b}$, respectively. These two noise are white, zero-mean, and correlated. Let $\mathbf{Q}_k$ and $\mathbf{R}_k$ be their covariance matrices, respectively. Then the noise characteristics are given as follows:

$$\begin{aligned} \mathbf{q}_k &\simeq \mathcal{N}(0, \mathbf{Q}_k), \\ \mathbf{b}_k &\simeq \mathcal{N}(0, \mathbf{R}_k), \\ E[\mathbf{q}_k\mathbf{q}_j^\top] &= \begin{cases} \mathbf{Q}_k & \text{if } k = j, \\ 0 & \text{otherwise,} \end{cases} \\ E[\mathbf{b}_k\mathbf{b}_j^\top] &= \begin{cases} \mathbf{R}_k & \text{if } k = j, \\ 0 & \text{otherwise,} \end{cases} \\ E[\mathbf{q}_k\mathbf{b}_j^\top] &= 0. \end{aligned}$$

The goal is to estimate the state $\mathbf{x} = (\mathbf{x}_k)_{k\in[N]}$ based on the known system equations (3.36) and (3.37). In the following we give the statistical definitions which form a base for the filter presented here.

Expected Value

Let $\mathbf{x} = (\mathbf{x}_k)_{k\in[N]}, \mathbf{x}_k \in \mathbb{R}^n$ be discrete random variables, the expected value $E[\mathbf{x}_k]$ can be approximated by

$$E[\mathbf{x}_k] \approx \bar{\mathbf{x}}_k = \frac{1}{n}\sum_{j=1}^{n} x_{k,j}, \tag{3.38}$$

where $\bar{\mathbf{x}}_k$ denotes the sample mean of $\mathbf{x}_k$.

Sample Variance

The sample variance can be approximated as

$$Var[\mathbf{x}_k] \quad = \quad E[(\mathbf{x}_k - E[\mathbf{x}_k])^2] \approx \frac{1}{n-1}\sum_{j=1}^{n}\left(x_{k,j} - \bar{\mathbf{x}}_k\right)^2. \tag{3.39}$$

Sample Covariance

The covariance is derived using the same properties as above and is given by

$$Cov(\mathbf{x}_k, \mathbf{y}_k) \quad \approx \quad \frac{1}{n-1}\sum_{j=1}^{n}\left(x_{k,j} - \bar{\mathbf{x}}_k\right)\left(y_{k,j} - \bar{\mathbf{y}}_k\right). \tag{3.40}$$

Kalman Filter Derivation

The Kalman filter algorithm has two main steps: The Forecast Step using the state equation and the Data Assimilation Step using the measurement equation. Hence the Kalman Filter has a "predictor-corrector" structure. Let $(\mathbf{x}_k^f)_{k\in[N]}$ be a priori state estimate and $(\mathbf{x}_k^a)_{k\in[N]}$ be a posteriori state estimate. We can define a priori and a posteriori estimate errors as

$$\mathbf{e}_k^f = \mathbf{x}_k - \mathbf{x}_k^f, \tag{3.41a}$$

$$\mathbf{e}_k^a = \mathbf{x}_k - \mathbf{x}_k^a, \tag{3.41b}$$

the a priori and a posteriori estimate error covariance are

$$\mathbf{P}_k^f = E[\mathbf{e}_k^f(\mathbf{e}_k^f)^\top], \tag{3.42a}$$

$$\mathbf{P}_k^a = E[\mathbf{e}_k^a(\mathbf{e}_k^a)^\top]. \tag{3.42b}$$

($\mathbf{x}^\top$, ($\mathbf{A}^\top$) denotes the transpose of vector $\mathbf{x}$, (the transpose of matrix $\mathbf{A}$)). The above mentioned two steps can be written as

Model Forecast Step (Prediction)

The prediction is the first step of the Kalman filter. The predicted state or better the a priori state is calculated by neglecting the model error $(\mathbf{q}_k)_{k\in[N]}$ and solving the state equation

$$\begin{aligned} \mathbf{x}_{k+1}^f &= \mathbf{A}_k\mathbf{x}_k^a + \mathbf{B}_k\mathbf{u}_k, \\ \mathbf{x}_1^a &= E[\mathbf{x}_1], \end{aligned} \tag{3.43}$$

The forecast error covariance is given by

$$\begin{aligned} \mathbf{P}_{k+1}^{f} &= \mathbf{A}_k \mathbf{P}_k^a \mathbf{A}_k^\top + \mathbf{Q}_k, \\ \mathbf{P}_1^a &= E[\mathbf{e}_1^a (\mathbf{e}_1^a)^\top]. \end{aligned} \tag{3.44}$$

Data Assimilation Step

The a posteriori state estimate $\mathbf{x}_{k+1}^a$ is computed as a linear combination of an a priori estimate $\mathbf{x}_{k+1}^f$ and a weighted difference between an actual measurement $\mathbf{y}_{k+1}$ and a measurement prediction $\mathbf{C}_{k+1}\mathbf{x}_{k+1}^f$:

$$\mathbf{x}_{k+1}^a = \mathbf{x}_{k+1}^f + \mathbf{G}_{k+1}\left(\mathbf{y}_{k+1} - \mathbf{C}_{k+1}\mathbf{x}_{k+1}^f\right). \tag{3.45}$$

The difference $(\mathbf{y}_{k+1} - \mathbf{C}_{k+1}\mathbf{x}_{k+1}^f)$ in equation (3.45) is called the measurement innovation, or the residual. It reflects the discrepancy between the predicted measurement $\mathbf{C}_{k+1}\mathbf{x}_{k+1}^f$ and the actual measurement $\mathbf{y}_{k+1}$.
The $n \times m$ matrix $\mathbf{G}_k$ in (3.45) is called the Kalman gain matrix which minimizes the a posteriori error covariance:

$$\begin{aligned} \mathbf{P}_k^a &= E[\mathbf{e}_k^a (\mathbf{e}_k^a)^\top] \\ &= E[(\mathbf{x}_k - \mathbf{x}_k^a)(\mathbf{x}_k - \mathbf{x}_k^a)^\top]. \end{aligned}$$

According to equations (3.43) and (3.45), the a posteriori estimate errors is given as

$$\begin{aligned} \mathbf{e}_k^a &= \mathbf{x}_k - \mathbf{x}_k^a, \\ &= \mathbf{A}_{k-1}\mathbf{x}_{k-1} + \mathbf{B}_{k-1}\mathbf{u}_{k-1} + \mathbf{q}_{k-1} - \mathbf{x}_k^f - \mathbf{G}_k\left(\mathbf{y}_k - \mathbf{C}_k\mathbf{x}_k^f\right), \\ &= \mathbf{A}_{k-1}\mathbf{e}_{k-1}^a - \mathbf{G}_k\mathbf{C}_k\mathbf{A}_{k-1}\mathbf{e}_{k-1}^a + (\mathbf{I}_n - \mathbf{G}_k\mathbf{C}_k)\mathbf{q}_{k-1} - \mathbf{G}_k\mathbf{b}_k, \\ &= (\mathbf{I}_n - \mathbf{G}_k\mathbf{C}_k)(\mathbf{A}_{k-1}\mathbf{e}_{k-1}^a + \mathbf{q}_{k-1}) - \mathbf{G}_k\mathbf{b}_k. \end{aligned} \tag{3.46}$$

Then , the a posteriori covariance matrix is:

$$\begin{aligned} \mathbf{P}_k^a &= E[\mathbf{e}_k^a (\mathbf{e}_k^a)^\top], \\ &= E[((\mathbf{I}_n - \mathbf{G}_k\mathbf{C}_k)(\mathbf{A}_{k-1}\mathbf{e}_{k-1}^a + \mathbf{q}_{k-1}) - \mathbf{G}_k\mathbf{b}_k)((\mathbf{I}_n - \mathbf{G}_k\mathbf{C}_k)(\mathbf{A}_{k-1}\mathbf{e}_{k-1}^a + \mathbf{q}_{k-1}) - \mathbf{G}_k\mathbf{b}_k)^\top], \\ &= \mathbf{P}_k^f - \mathbf{G}_k\mathbf{C}_k\mathbf{P}_k^f - \mathbf{P}_k^f\mathbf{G}_k^\top\mathbf{C}_k^\top + \mathbf{G}_k((\mathbf{C}_k\mathbf{P}_k^f\mathbf{C}_k^\top + \mathbf{R}_k)\mathbf{G}_k^\top. \end{aligned} \tag{3.47}$$

The a posteriori covariance matrix holds for any $\mathbf{G}_k$. The goal is now to minimize the mean squared estimation error with respect to the Kalman gain $\mathbf{G}_k$. The cost function

to be minimized can be expected as the trace of the error covariance

$$\mathcal{J} \quad = \quad tr(\mathbf{P}_k^a), \tag{3.48}$$

differentiating with respect to $\mathbf{G}_k$ gives

$$\frac{\partial tr(\mathbf{P}_k^a)}{\partial \mathbf{G}_k} \quad = \quad -2\mathbf{P}_k^f \mathbf{C}_k^\top + 2\mathbf{G}_k(\mathbf{C}_k \mathbf{P}_k^f \mathbf{C}_k^\top + \mathbf{R}_k). \tag{3.49}$$

Setting to zero and re-arranging gives

$$\mathbf{G}_k \quad = \quad \mathbf{P}_k^f \mathbf{C}_k \left(\mathbf{C}_k \mathbf{P}_k^f \mathbf{C}_k^\top + \mathbf{R}_k\right)^{-1}. \tag{3.50}$$

Setting this back into (3.47), then the a posteriori error covariance $\mathbf{P}_{k+1}^a$ is given by

$$\mathbf{P}_{k+1}^a \quad = \quad (\mathbf{I}_n - \mathbf{G}_{k+1}\mathbf{C}_{k+1})\,\mathbf{P}_{k+1}^f, \tag{3.51}$$

Figure 3.3 shows a complete picture of the two steps: The Forecast Step and the Data Assimilation Step. The forecast equations are responsible for projecting forward (in time) the current state and error covariance estimates to obtain the a priori estimates for the next time step. The Data Assimilation equations are responsible for incorporating a new measurement into the a priori estimate to obtain an improved a posteriori estimate.

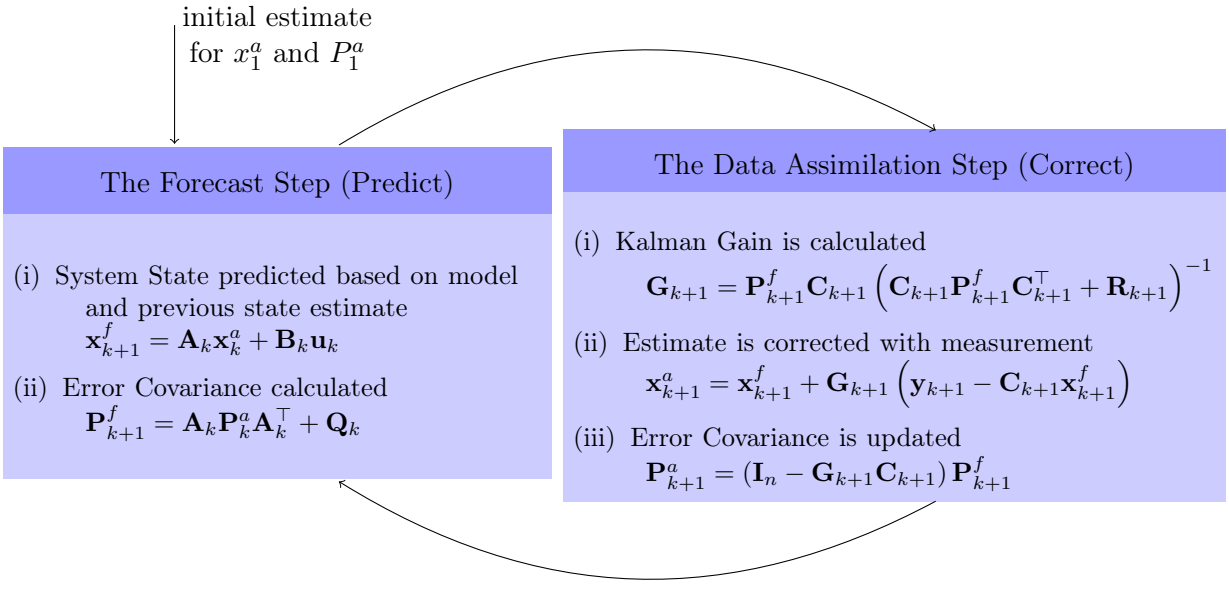

Figure 3.3: *Predictor-Corrector Structure of Kalman Filter with Equations*

The Extended Kalman Filter

Consider the following nonlinear system, consisting of the state equation and the measurement equation with additive noise:

$$\mathbf{x}_{k+1} = \mathbf{f}(\mathbf{x}_k, \mathbf{u}_k) + \mathbf{q}_k, \quad \forall k \in [N-1] \tag{3.52a}$$

$$\mathbf{x}_1 \quad \text{the given initial state,} \tag{3.52b}$$

$$\mathbf{y}_k = \mathbf{g}(\mathbf{x}_k) + \mathbf{b}_k, \quad \forall k \in [N-1]. \tag{3.52c}$$

Where $\mathbf{x}_k \in \mathbb{R}^n$, $\mathbf{y}_k \in \mathbb{R}^m$ $k \in [N]$, $\mathbf{u}_k \in \mathbb{R}^p$, $k \in [N-1]$, $\mathbf{f}\colon \mathbb{R}^{n\times p} \to \mathbb{R}^n$, and $\mathbf{g}\colon \mathbb{R}^n \to \mathbb{R}^m$. We assume the following conditions:

- for each $k \in [N-1]$, $\mathbf{f}$ is continuously differentiable with respect to each component of $\mathbf{x}_k$ and $\mathbf{u}_k$.
- for each $k \in [N-1]$, $\mathbf{g}$ is continuously differentiable with respect to each component of $\mathbf{x}_k$.

The Extended Kalman filter (EKF) gives an approximation of the optimal estimate of the state $(\mathbf{x}_k)_{k\in[N]}$. The non-linearities of the state and measurement equations are approximated by a linearized version of the non-linear system model about the previous state estimate. One iteration of the EKF is composed by the following consecutive steps:

- Consider the last filtered state estimate $\mathbf{x}_k^a$
- Linearize the state equation (3.52a) about $\mathbf{x}_k^a$
- Apply the Forecast Step of the Kalman filter to the linearized state equation just obtained, yielding $\mathbf{x}_{k+1}^f$ and $\mathbf{P}_{k+1}^f$
- Linearize the measurement equation (3.52c) about $\mathbf{x}_{k+1}^f$
- Apply the Data Assimilation Step of the Kalman filter to the linearized measurement equation, yielding $\mathbf{x}_{k+1}^a$, $\mathbf{P}_{k+1}^a$ and $\mathbf{G}_{k+1}$.

Let $\mathbf{A}_k$ and $\mathbf{C}_k$ be the Jacobian matrices of $\mathbf{f}$ and $\mathbf{g}$, denoted by

$$\mathbf{A}_k = \mathcal{D}_x\mathbf{f}(\mathbf{x}_k^a, \mathbf{u}_k), \quad \mathbf{C}_k = \mathcal{D}_x\mathbf{g}(\mathbf{x}_{k+1}^f). \tag{3.53}$$

Figure 3.4 shows a complete picture of the two groups of the EKF: The Forecast Step and The Data Assimilation Step.

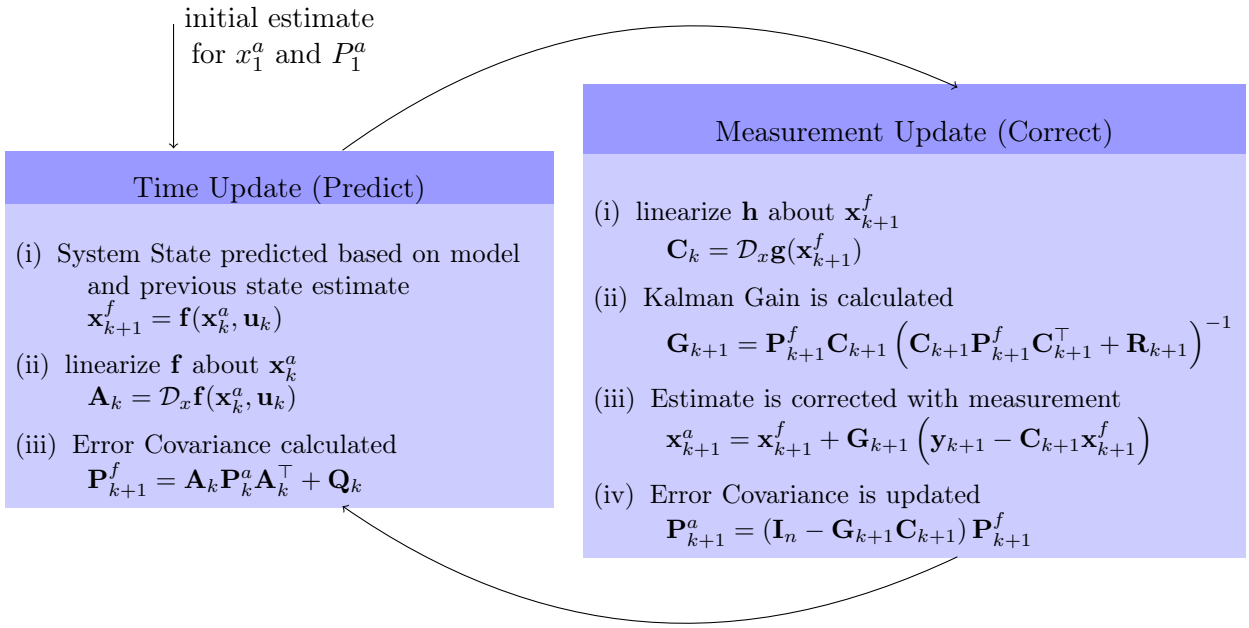

Figure 3.4: *Predictor-Corrector Structure of Extended Kalman Filter with Equations*

4 Numerical Analysis of the Linearized NPZD Model

In this Section, we investigate the finite-time stability over a finite time interval of a linearized version of the one-dimensional NPZD-model. First, we briefly describe the considered NPZD-model in both forms, continuous and discrete. The linearization of the model about a selected reference trajectory will be described, and finally we analyze the finite-time stability.

4.1 NPZD Model

The 1-dimensional marine ecosystem model considered here was developed by Oschlies and Garçon (1999). It simulates the interaction of dissolved inorganic nitrogen (N), phytoplankton (P), zooplankton (Z), and detritus (D). The interactions of the four variables are sketched in Figure 4.1. The arrows in Figure 4.1 indicate the nitrogen fluxes, with symbols indicating those parameters that are associated with the rates for each particular flux. All model parameters are listed in Table 4.1.
In the NPZD model, the concentrations (in mmol N m^{-3}) of dissolved inorganic nitrogen ($x^{(N)}$), phytoplankton ($x^{(P)}$), zooplankton ($x^{(Z)}$), and detritus ($x^{(D)}$), are summarized in the model variables $(x^{(l)})_{l=N,P,Z,D} := \mathbf{x}$. These four variables are functions $x^{(l)}\colon [0,L] \times [0,t_e] \to \mathbb{R}$ of space and time, with L denoting the depth of the water column and t_e the total integration time.
The model is given as follows. For $l = N, P, Z, D$:

$$\left.\begin{array}{l} \frac{\partial x^{(l)}}{\partial t}(z,t) + w^{(l)}\frac{\partial x^{(l)}}{\partial z}(z,t) - \frac{\partial}{\partial z}\left(\nu \frac{\partial x^{(l)}}{\partial z}\right)(z,t) = S^{(l)}(\mathbf{x},\mathbf{u}), \quad z \in]0,L[\,,\ t \in]o,t_e]\,, \\ \text{subject to Neumann boundary conditions :} \\ \frac{\partial x^{(l)}}{\partial z}(0,t) = 0, \quad \frac{\partial x^{(l)}}{\partial z}(L,t) = 0, \quad t \in]0,t_e]\,, \\ \text{and initial condition} \\ x^{(l)}(z,0) = x^{(l)}_{init}(z), \quad z \in]0,L[\,, \end{array}\right\} \tag{4.1}$$

where, z denotes the only (vertical) spatial coordinate. The vector-valued function $\mathbf{x}_{init} = (x^{(l)}_{init})_{l=N,P,Z,D}$ is the given initial value. Neumann boundary conditions at $z = 0$ and $z = L$ express the fact that there is no flux through the surface of the ocean and

through the ocean floor. The term $S^{(l)}$ represents the biogeochemical coupling terms for the four tracers which depend on space and time via light intensity and also on temperature, and on most of the physical and biological parameters summarized in the vector $\mathbf{u} = (u_1, \ldots, u_p)^\top$. For simplicity, their dependence on space, time and given temperature data is omitted in the notation. The circulation data are the turbulent mixing coefficient $\nu = \nu(z,t)$ and the temperature $T = T(z,t)$. The vertical sinking velocity $w^{(l)}$ is a parameter of the biological model that is nonzero only for $x^{(D)}$, i.e. $w^{(N)} = w^{(P)} = w^{(Z)} = 0$, $w^{(D)} = w_s > 0$.

In the one-dimensional model no advection term is used, since a reduction to vertical only would make no sense. The biogeochemical coupling (or source-minus-sink) terms

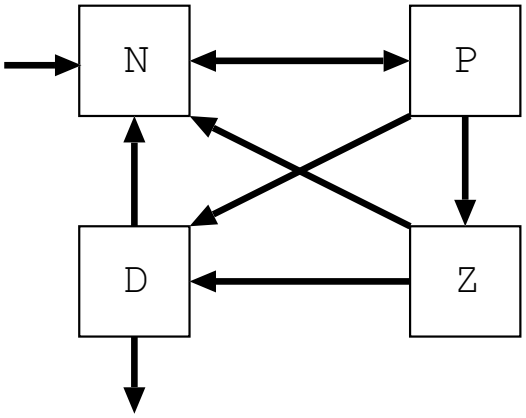

Figure 4.1: *Structure of the ecosystem model. The state variables are dissolved inorganic nitrogen (N), phytoplankton (P), zooplankton (Z) and detritus (D). The arrows indicate the direction of mass flux. (see Schartau and Oschlies (2003a))*

of the four tracers are given as:

$$\left.\begin{aligned} S^{(N)}(\mathbf{x},\mathbf{u}) &= -J(x^{(N)},z,t)x^{(P)} + u_4 x^{(Z)} + u_{10}x^{(D)}, \\ S^{(P)}(\mathbf{x},\mathbf{u}) &= J(x^{(N)},z,t)x^{(P)} - u_8 x^{(P)} - G(u_6,u_7)x^{(Z)}, \\ S^{(Z)}(\mathbf{x},\mathbf{u}) &= u_1 G(u_6,u_7)x^{(Z)} - u_4 x^{(Z)} - u_9 (x^{(Z)})^2, \\ S^{(D)}(\mathbf{x},\mathbf{u}) &= (1-u_1)G(u_6,u_7)x^{(Z)} + u_9(x^{(Z)})^2 + u_8 x^{(P)} - u_{10}x^{(D)}. \end{aligned}\right\} \tag{4.2}$$

Here, $\mathbf{x} = (x^{(N)}, x^{(P)}, x^{(Z)}, x^{(D)})^\top$ denotes the state of the system, and $\mathbf{u} = (u_1, \ldots, u_p)^\top$ with $p = 12$, denotes the vector of the model parameters. J is the daily averaged phytoplankton growth rate as a function of depth z and time t, and is modeled after the

minimum principle of von Liebig (Liebig et al. (1842)) as

$$\begin{aligned} J(x^{(N)}, t, z) &= \min\left(\bar{J}(z,t), V_p \frac{x^{(N)}}{u_{12} + x^{(N)}}\right), \\ V_p &= u_2 (C_{ref})^{cT}, \end{aligned} \tag{4.3}$$

where C_{ref} and c along with the model parameters $(u_1, \ldots, u_p)$ are briefly described in Table 4.1, and where V_p further depends on the water temperature T, which has to be provided by an ocean circulation model. $\bar{J}$ is the light-limited growth rate according to Evans and Parslow (Evans and Parslow (1985)), integrated down to the given depth z (Oschlies and Garçon (1999); Rückelt et al. (2010)). Due to the minimum in the growth rate of phytoplankton in equation (4.3), the model becomes non-differentiable. G is the grazing function and given as

$$G(u_6, u_7) \quad = \quad \frac{u_7 u_6 (x^{(P)})^2}{u_7 + u_6 (x^{(P)})^2}. \tag{4.4}$$

It describes the transfer from phytoplankton to zooplankton and detritus with the parameters u_7 and u_6 again briefly described in Table 4.1.
We point out that the daily averaged phytoplankton growth rate function J for the implementation of the NPZD model will be chosen as follows :

$$J(x^{(N)}, t, z) \quad = \quad V_p \frac{x^{(N)}}{u_{12} + x^{(N)}}. \tag{4.5}$$

It follows that the function J is differentiable and thus the model becomes differentiable.

Discretization of the NPZD Model

Here we give a brief description of the temporal and spatial discretization of the model equations described in (4.1). The vertical grid consists of 32 layers with thickness increasing with depth. The model described by (4.1) is solved using an operator splitting method. Let a time step $\Delta t > 0$ (one hour in the model) be given. At first, in every time step $k \to k+1$, the non-linear coupling terms $\mathbf{S}_k = (S_k^{(N)}, S_k^{(P)}, S_k^{(Z)}, S_k^{(D)})^\top$ (see equation 4.2) are computed.
Now, four explicit Euler steps with step-size $\frac{\Delta t}{4}$ are performed, each of which is described by the operator

$$\mathcal{L}_k(\mathbf{x}_k, \mathbf{u}_k) := \left[\mathbf{x}_k + \frac{\Delta t}{4} \mathbf{S}_k(\mathbf{x}_k, \mathbf{u}_k)\right], \quad \forall k \in [N-1], \tag{4.6}$$

Table 4.1: *Parameters of the ecosystem model. Here* $\mathbf{u}_0 = (u_{i,0})_{i=1,\dots,12}$ *is the vector of parameters which are used for the linearization scheme, they are taken from Oschlies and Garçon (1999).*

$u_{i,0}$	symbol	value	unit($d = 86400s$)	parameter meaning
	C_{ref}	1.066	1	growth coefficient
	c	1	$^\circ C^{-1}$	growth coefficient
	R	6.625	1	molar carbon to nitrogen ratio (Redfield ration)
	k_w	25	m^{-1}	PAR extinction length
$u_{1,0}$	β	0.75	1	assimilation efficiency of zooplankton
$u_{2,0}$	μ_m	0.6	day^{-1}	phytoplankton growth rate parameter
$u_{3,0}$	α	0.025	$\mathrm{m}^2\ \mathrm{W}^{-2}\ \mathrm{d}^{-1}$	initial slop of P-I Curve
$u_{4,0}$	ϕ_m^z	0.03	day^{-1}	zooplankton excretion
$u_{5,0}$	k	1	$(\mathrm{mmol\ m}^{-3})^{-2}\,\mathrm{d}^{-1}$	light attenuation by phytoplankton
$u_{6,0}$	ϵ	1	$(\mathrm{mmol\ m}^{-3})^{-2}\,\mathrm{d}^{-1}$	Pry capture efficiency
$u_{7,0}$	g	2	d^{-1}	maximum grazing rate
$u_{8,0}$	ϕ_m^p	0.03	day^{-1}	specific mortality rate
$u_{9,0}$	ϕ_z^*	0.2	$(\mathrm{mmol\ m}^{-3})^{-1}\ \mathrm{d}^{-1}$	zooplankton quadratic mortality
$u_{10,0}$	γ_m	0.05	day^{-1}	remineralization rate parameter of detritus
$u_{11,0}$	K_N	0.5	$\mathrm{m\,day}^{-1}$	Sinking velocity of detritus
$u_{12,0}$	w_s	5	$\mathrm{mmol\ m}^{-3}$	half-saturation constant for N uptake rate

where $\mathbf{x}_k = (x_k^{(N)}, x_k^{(P)}, x_k^{(Z)}, x_k^{(D)})^\top$ is the state vector of all four tracers and $\mathbf{u}_k$ is the parameter vector. We note that in our considered model, the dimension n of $\mathbf{x}_k$ is determined by the number of tracers (in our case 4) and the number of grid cells in the water column (in our case $m = 32$), which results in $n = 4m$. We give an intermediate iterate:

$$\widetilde{\mathbf{x}}_{k+1} := \mathcal{L}_k \circ \mathcal{L}_k \circ \mathcal{L}_k \circ \mathcal{L}_k(\mathbf{x}_k, \mathbf{u}_k). \tag{4.7}$$

Then, an explicit Euler step with full step size Δt is performed for the sinking term, which is spatially discretized by an upstream schema.

Discretization of the Sinking Term

We solve the PDE system (4.1) for grid points using the finite difference method where we discretize in space z and time t for $0 \le z \le L$ and $0 \le t \le t_e$. We discretize in time with time step Δt and in space with grid distances Δz. For $0 \le k \le N$, let $t_k = k\Delta t$. We will use the following notations (see Figure 4.2):

- z_j denotes the center of the (j)-th layer of depth,
- $dzt_j := z_{j+\frac{1}{2}} - z_{j-\frac{1}{2}}$ denotes the thickness of layer j.
  where $z_{j+\frac{1}{2}}$ denotes the depth at bottom of layer j and $z_{j-\frac{1}{2}}$ denotes the depth at bottom of layer $j-1$

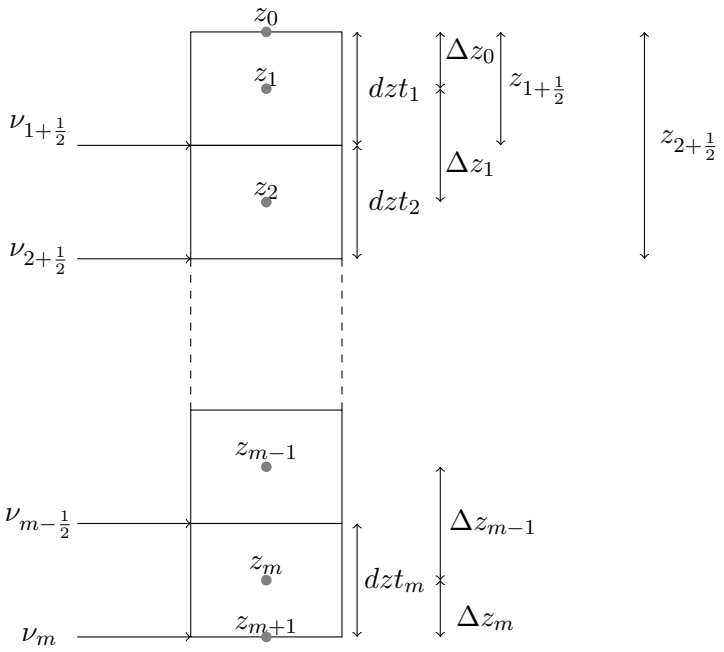

Figure 4.2: *Grid of vertical water column used for the discretization of the continuous model.*

- $\Delta z_j := \begin{cases} \frac{1}{2} dzt_1 & \text{if } j = 0, \\ z_{j+1} - z_j & \text{if } 2 \leqslant j \leqslant m-1, \\ \frac{1}{2} dzt_m & \text{if } j = m, \end{cases}$
  denotes the distance between the centres of the $(j-1)$-th and the (j)-th layer,

- $x_{j,k}^{(l)} := x^{(l)}(z_j, t_k)$ denotes the state variable at time t_k and space z_j for all tracers $l \in N, P, Z, D$,

- $\mathbf{x}_k^{(l)} = (x_{1,k}^{(l)}, x_{2,k}^{(l)}, \ldots, x_{m,k}^{(l)})$,

- $\nu_{j-\frac{1}{2},k} := \nu(z_{j-\frac{1}{2}}, t_k)$ denotes the turbulent mixing coefficient between the j-th and the $(j-1)$-th layer at time t_k,

- $\nu_{j+\frac{1}{2},k} := \nu(z_{j+\frac{1}{2}}, t_k)$ denotes the turbulent mixing coefficient between the j-th and the $(j+1)$-th layer at time t_k,

For simplification of notation we write $\nu_{j,k}^- := \nu_{j-\frac{1}{2},k}$ and $\nu_{j,k}^+ := \nu_{j+\frac{1}{2},k}$.
As mentioned above, the vertical sinking velocity $w^{(l)}$ is nonzero only for $x^{(D)}$.
Let $x_{j,k}^{(D)} := x^{(D)}(z_j, t_k)$. Then the finite difference approximation for the sinking term

(4.1) is given by

$$\begin{aligned} -w_s \frac{\partial x^{(D)}}{\partial z}(z_j, t_k) &\approx -w_s \frac{x^{(D)}_{j,k} - x^{(D)}_{j-1,k}}{z_j - z_{j-1}} \\ &\approx \frac{w_s}{\Delta z_{j-1}} x^{(D)}_{j-1,k} - \frac{w_s}{\Delta z_{j-1}} x^{(D)}_{j,k}, \quad \forall\, j = 2, \ldots, m-1. \end{aligned}$$

The boundary conditions are given as:

$$\begin{aligned} -w_s \frac{\partial x^{(D)}}{\partial z}(z_1, t_k) &\approx -w_s \frac{x^{(D)}_{1,k} - x^{(D)}_{0,k}}{z_1 - z_0} \\ &\approx -\frac{w_s}{\Delta z_0} x^{(D)}_{1,k}, \end{aligned}$$

$$\begin{aligned} -w_s \frac{\partial x^{(D)}}{\partial z}(z_m, t_k) &\approx -w_s \frac{x^{(D)}_{m,k} - x^{(D)}_{m-1,k}}{z_m - z_{m-1}}, \\ &\approx \frac{w_s}{\Delta z_{m-1}} x^{(D)}_{m-1,k}. \end{aligned}$$

since $x^{(D)}_{0,k} = 0$, $x^{(D)}_{m,k} = 0$. With the notation $b_j := \frac{w_s}{\Delta z_{j-1}}$, $j = 1, \ldots, m$, we can write the sinking matrix $H^{\text{sink}} \in \mathbb{R}^{m \times m}$ as follows

$$H^{\text{sink}} := \begin{bmatrix} -b_1 & 0 & \ldots & & & & \\ b_1 & -b_2 & 0 & \ldots & & & \\ & & & & & & \\ 0 & \ddots & \ddots & 0 & \ldots & & \\ 0 & & b_j & -b_j & 0 & \ldots & \\ & & & & & & \\ & \ldots & & \ddots & \ddots & 0 & \ldots \\ 0 & \ldots & 0 & & b_{m-1} & -b_{m-1} & 0 \\ 0 & \ldots & & & & b_m & 0 \end{bmatrix} \tag{4.8}$$

Altogether, for an intermediate state vector $\widehat{x}^{(D)}_{k+1}$ we obtain for the explicit formulation of the sinking:

$$\frac{\widehat{x}^{(D)}_{k+1} - \widetilde{x}^{(D)}_{k+1}}{\Delta t} = H^{\text{sink}} \widetilde{x}^{(D)}_{k+1},$$

where $\widetilde{x}_{k+1}^{(D)}$ is given by the discretization of the non-linear coupling terms $S^{(D)}$. This gives:

$$\widehat{x}_{k+1}^{(D)} \quad := \quad [\mathcal{I}_m + \Delta t H^{\text{sink}}]\widetilde{x}_{k+1}^{(D)}.$$

Let $\widehat{\mathbf{x}}_k = (\widehat{x}_k^{(N)}, \widehat{x}_k^{(P)}, \widehat{x}_k^{(Z)}, \widehat{x}_k^{(D)})^\top$ be the discrete state vector at time t_k. Then the sinking matrix for all tracers N, P, Z, D is summarized in the 4×4 block-diagonal matrix $\widetilde{H}^{\text{sink}} \in \mathbb{R}^{n \times n}$ for $n = 4m$,

$$\widetilde{H}^{\text{sink}} := \begin{bmatrix} 0_{m\times m} & & & \\ & 0_{m\times m} & & \\ & & 0_{m\times m} & \\ & & & H^{\text{sink}} \end{bmatrix} \tag{4.9}$$

Thus, at the end of this step, the intermediate state vector $\widehat{\mathbf{x}}_{k+1}$ is computed as

$$\widehat{\mathbf{x}}_{k+1} := [\mathbf{I}_n + \Delta t \widetilde{H}^{\text{sink}}]\widetilde{\mathbf{x}}_{k+1}. \tag{4.10}$$

Finally, an implicit Euler step for the diffusion operator discretized with second central differences, is applied.

Discretization of the Diffusion Term

The diffusion of the four tracers is considered down to a vertical layer $\bar{m}$, which is temperature dependent and defined as

$$\bar{m} \quad = \quad \max\left\{j,\ T(z_j, t_k) > 0, \forall k \in [N-1]\right\}.$$

Below this layer it is assumed that diffusion is not apparent anymore. For our case, the implemented one-dimensional version of the NPZD model satisfies the condition $T(z_j, t_k) > 0$ for $j = 1, \ldots, m,\ k = 1, \ldots, N-1$ with $m = 32$ and $N = 8760$. The discretization of the diffusion term in equation (4.1) is given as follows:

First, we define variable coefficients

$$\varphi(z_j, t_k) \quad := \quad \nu(z_j, t_k) \cdot \frac{\partial x^{(l)}}{\partial z}(z_j, t_k). \tag{4.11}$$

Then we obtain

$$\begin{aligned}
\frac{\partial\varphi}{\partial z}(z_j,t_k)) &\approx \frac{\varphi_{j+\frac{1}{2},k}-\varphi_{j-\frac{1}{2},k}}{z_{j+\frac{1}{2}}-z_{j-\frac{1}{2}}} \\
&\approx \frac{\nu_{j+\frac{1}{2},k}\frac{x^{(l)}_{j+1,k}-x^{(l)}_{j,k}}{z_{j+1}-z_j}-\nu_{j-\frac{1}{2},k}\frac{x^{(l)}_{j,k}-x^{(l)}_{j-1,k}}{z_{j+1}-z_j}}{z_{j+\frac{1}{2}}-z_{j-\frac{1}{2}}} \\
&\approx \left(\nu^+_{j,k}\frac{x^{(l)}_{j+1,k}-x^{(l)}_{j,k}}{z_{j+1}-z_j}-\nu^-_{j,k}\frac{x^{(l)}_{j,k}-x^{(l)}_{j-1,k}}{z_j-z_{j-1}}\right)/(z_{j+\frac{1}{2}}-z_{j-\frac{1}{2}}) \\
&\approx \left(\nu^+_{j,k}\frac{x^{(l)}_{j+1,k}-x^{(l)}_{j,k}}{\Delta z_j}-\nu^-_{j,k}\frac{x^{(l)}_{j,k}-x^{(l)}_{j-1,k}}{\Delta z_{j-1}}\right)/(dzt_j), \\
&\approx \frac{\nu^-_{j,k}}{\Delta z_{j-1}dzt_j}x^{(l)}_{j-1,k}-\left(\frac{\nu^+_{j,k}}{\Delta z_j dzt_j}+\frac{\nu^-_{j,k}}{\Delta z_{j-1}dzt_j}\right)x^{(l)}_{j,k}+\frac{\nu^+_{j,k}}{\Delta z_j dzt_j}x^{(l)}_{j+1,k}.
\end{aligned}$$

The boundary conditions are given as

$$\frac{\partial x^{(l)}}{\partial z}(z_1,t_k) \approx \frac{x^{(l)}_{1,k}-x^{(l)}_{0,k}}{\Delta z_0} =: b_1, \tag{4.12}$$

$$\frac{\partial x^{(l)}}{\partial z}(z_m,t_k) \approx \frac{x^{(l)}_{m+1,k}-x^{(l)}_{m,k}}{\Delta z_m} =: b_m. \tag{4.13}$$

Substituting the equations (4.12) and (4.13) in equation (4.11) we obtain the following discretization for the boundary layers

$$\begin{aligned}
\frac{\partial\varphi}{\partial z}(z_1,t_k)) &\approx \nu^+_{1,k}\frac{x^{(l)}_{2,k}-x^{(l)}_{1,k}}{\Delta z_1 dzt_1}-\nu^-_{1,k}\frac{x^{(l)}_{1,k}-x^{(l)}_{0,k}}{\Delta z_0 dzt_1}, \\
&\approx -\frac{\nu^+_{1,k}}{\Delta z_1 dzt_1}x^{(l)}_{1,k}+\frac{\nu^+_{1,k}}{\Delta z_1 dzt_1}x^{(l)}_{2,k}-\frac{\nu^-_{1,k}}{dzt_1}b_1, \\
\frac{\partial\varphi}{\partial z}(z_m,t_k)) &\approx \nu^+_{m,k}\frac{x^{(l)}_{m+1,k}-x^{(l)}_{m,k}}{\Delta z_m dzt_m}-\nu^-_{m,k}\frac{x^{(l)}_{m,k}-x^{(l)}_{m-1,k}}{\Delta z_{m-1}dzt_m}, \\
&\approx \frac{\nu^-_{m,k}}{\Delta z_{m-1}dzt_m}x^{(l)}_{m-1,k}-\frac{\nu^-_{m,k}}{\Delta z_{m-1}dzt_m}x^{(l)}_{m,k}+\frac{\nu^+_{m,k}}{dzt_m}b_m.
\end{aligned}$$

With the notations $c_{j,k} := \frac{\nu^-_{j,k}}{\Delta z_{j-1}dzt_j}$, $d_{j,k} := \frac{\nu^+_{j,k}}{\Delta z_j dzt_j}$, $\widetilde{b}^{(l)}_{1,k} := -\frac{\nu^-_{1,k}}{dzt_1}b_1$,$\widetilde{b}^{(l)}_{m,k} := \frac{\nu^+_{m,k}}{dzt_m}b_m$, the time dependent diffusion matrix $H^{\text{diff}}_k \in \mathbb{R}^{m\times m}$ is a tridiagonal matrix and given as

follows

$$H_k^{\text{diff}} = \begin{bmatrix} -d_{1,k} & +d_{1,k} & 0 & \dots & & & \\ c_{2,k} & -(c_{2,k}+d_{2,k}) & d_{2,k} & 0 & \dots & & \\ & \ddots & \ddots & \ddots & 0 & \dots & \\ 0 & \dots & c_{j,k} & -(c_{j,k}+d_{j,k}) & d_{j,k} & 0 & \\ 0 & \dots & \ddots & \ddots & \ddots & 0 & \\ 0 & \dots & 0 & c_{m-1,k} & -(c_{m-1,k}+d_{m-1,k}) & d_{m-1,k} & 0 \\ & & \dots & 0 & & c_{m,k} & -c_{m,k} \end{bmatrix}$$

Altogether we obtain for the implicit formulation of the diffusion:

$$\frac{x_{k+1}^{(l)} - \widehat{x}_{k+1}^{(l)}}{\Delta t} \quad = \quad H_k^{\text{diff}} x_{k+1}^{(l)} + \widetilde{b}_k^{(l)}, \quad \forall l \in \{N, P, Z, D\},$$

where $\widehat{x}_{k+1}^{(l)}$ is given by the discretization of the sinking term. Since the value of $\widetilde{b}_k^l$ is assumed to be equal to zero for all $k \in [N-1]$ (Neumann boundary), we have:

$$[\mathbf{I}_m - \Delta t H_k^{\text{diff}}] x_{k+1}^{(l)} \quad = \quad \widehat{x}_{k+1}^{(l)}, \quad \forall\, l \in \{N, P, Z, D\}.$$

Then the diffusion matrix for all tracers N, P, Z, D is summarized in the 4×4 block-diagonal matrix $\widetilde{H}_k^{\text{diff}} \in \mathbb{R}^{n \times n}$ which only contains the sub-matrices $H_k^{\text{diff}} \in \mathbb{R}^{m \times m}$ on the diagonal.

$$\widetilde{H}_k^{\text{diff}} := \begin{bmatrix} H_k^{\text{diff}} & 0 & 0 & 0 \\ o & H_k^{\text{diff}} & 0 & 0 \\ 0 & 0 & H_k^{\text{diff}} & 0 \\ 0 & 0 & 0 & H_k^{\text{diff}} \end{bmatrix}. \tag{4.14}$$

Now the system is solved directly for $\mathbf{x}_{k+1}$

$$[\mathbf{I}_n - \Delta t \widetilde{H}_k^{\text{diff}}]\, \mathbf{x}_{k+1} =: \widehat{\mathbf{x}}_{k+1}. \tag{4.15}$$

Summarizing, according to equations (4.7), (4.10) and (4.15), the discrete system can be written as

$$\mathbf{x}_{k+1} := [\mathbf{I}_n - \Delta t \widetilde{H}_k^{\text{diff}}]^{-1} [\mathbf{I}_n + \Delta t \widetilde{H}^{\text{sink}}] \mathbf{h}(\mathbf{x}_k, \mathbf{u}_k), \forall\, k \in [N-1], \tag{4.16}$$

where

$$\mathbf{h}(\mathbf{x}_k, \mathbf{u}_k) := \mathcal{L}_k \circ \mathcal{L}_k \circ \mathcal{L}_k \circ \mathcal{L}_k(\mathbf{x}_k, \mathbf{u}_k), \forall\, k \in [N-1]. \tag{4.17}$$

The function $\mathbf{h}$ is nonlinear and represents the discretized source-minus-sink terms. Starting from equations (4.16) and (4.17), the linearization of the model about selected reference trajectories of the state and the control are used. For the reference control, we choose the parameter vector $\mathbf{u}_0 = (u_{1,0}, u_{2,0}, \ldots, u_{12,0})^\top$ (see Table 4.1). The reference state trajectory will be based on the given measurement data

$$\mathbf{x}^{(obs)} = (x^{(N,obs)}, x^{(P,obs)}, x^{(Z,obs)}, x^{(D,obs)})^\top.$$

Since the data for the difference tracers are not given for the same instances of time, we only use those instances where data for all tracers are available. For this purpose we define

- $n^{(l)}$ denotes the number of data for $x^{(l,obs)}, l = N, P, Z, D$.
- $x_i^{(l,obs)}$ denotes the i-th measurement data, $i = 1, \ldots, n^{(l)}$
- $t_i^{(l)}$: denotes the instance of time of $x_i^{(l,obs)}, i = 1, \ldots, n^{(l)}$ (rounded to an integer number)
- I: denotes the set of instances where data for all tracers are available:

$$I := \bigcap_{l \in \{N,P,Z,D\}} \{t_i^{(l)}\}_{i=1,\ldots,n^{(l)}} =: \{t_i\}_{i=1,\ldots,\widetilde{n}},$$

  where $\widetilde{n}$ denotes the number of elements in this intersection.

Now we define the $\widetilde{n}+1$ discrete time intervals between the subsequent instances of time defined above

$$\begin{aligned}
T_i &:= [t_i, t_{i+1}] \bigcap \mathbb{N}, \quad i = 0, 1, \ldots, \widetilde{n}, \\
&:= \{t_i, t_i + 1, t_i + 2, \ldots, t_{i+1} - 1, t_{i+1}\} \\
\widetilde{T}_i &:= [t_i, t_{i+1} - 1] \bigcap \mathbb{N}, \quad i = 0, 1, \ldots, \widetilde{n}, \\
&:= \{t_i, t_i + 1, t_i + 2, \ldots, t_{i+1} - 1\} \\
t_0 &:= 1, \text{and} \quad t_{\widetilde{n}+1} := N.
\end{aligned}$$

Where t_i and $k \in [t_i, t_{i+1}]$, for $i = 0, 1, \ldots, \widetilde{n}$ are in $\mathbb{N}$.
For example, for the first year, $\widetilde{n} = 10$ (the number of measurement data that we have

in the first year)

$$\begin{aligned} T_0 &:= \{1, 2, \ldots, t_1\}, \qquad \text{for i} = 0, \\ T_1 &:= \{t_1, t_1 + 1, t_1 + 2, \ldots, t_2\}, \qquad \text{for i} = 1, \end{aligned} \tag{4.18}$$

The idea is that, one year ($8760h$) will be devided into $\widetilde{n} + 1$ intervals, where we only have number from $\mathbb{N}$. For more accuracy, we have defined the intervals $\widetilde{T}_i, i = 0, 1, \ldots, \widetilde{n}$, this means that the defined k in 4.19 do not go until t_{i+1}, but only up $t_{i+1} - 1$.

On the other hand, the vertical grid layer consists of 32 layer with thickness increasing with depth.

$$z = (z_1, z_2, \ldots, z_m)^\top, \qquad m = 32,$$

since there are not necessary measurement data $(x^{(l,obs)})_{l=N,P,Z,D}$ for every vertical layer $(z_j)_{j=1,\ldots,m}$, we additionally interpolate the data linearly in space to obtain a reference trajectory in every grid point z_j for each measurement data $x^{(l,obs)}$.
For that we use the function interp1 ($Matlab^{®}$ function interp1) for the 1D interpolation between given data points $(z, x^{(l,obs)})$

$$x_j^{(l,obs)} = interp1(z, x^{(l,obs)}, z_j, 'linear'),$$

this function predicts the value of $x^{(l,obs)}$ at a given z_j using linear interpolation between the original data points $(z, x^{(l,obs)})$. The variable z_j represents the point(s) at which the $x_j^{(l,obs)}$ need to be predicted. The output $x_j^{(l,obs)}$ represents the interpolated value at the corresponding point z_j. The string 'linear' represents the interpolation method to will be used.
And at the end we get fully staffed vectors $x_i^{(l,obs)} = \left(x_{1,i}^{(l,obs)}, \ldots, x_{m,i}^{(l,obs)}\right)^\top$, for all $i = 1, \ldots, \widetilde{n}$, and $l = N, P, Z, D$.
Finally, we use the relation between model variables and measurement data described in Section 2.3 in paper 1 (Appendix A.1) to define the reference trajectory $\mathbf{x}_i^{(ref)}$, $i = 0, 1, \ldots, \widetilde{n}$. They are defined as $\mathbf{x}_i^{(ref)} := \mathbf{x}_{i+1}^{(obs)}$, $i = 0, 1, \ldots, \widetilde{n}$ (in our considered NPZD model $\widetilde{n} = 10$). Since we have no reference value $\mathbf{x}^{(ref)}$ at time step $t_{\widetilde{n}+1}$, we use linear interpolation between the data $\mathbf{x}_{\widetilde{n}}^{(obs)}$ and $\breve{\mathbf{x}}^{(obs)}$ (the first measurement in the next year) to generate such value, denoted by $\mathbf{x}_{\widetilde{n}+1}^{(obs)}$. We want to linearize the function $\mathbf{h}$ (4.17) about a constant operating point $(\mathbf{x}_i^{(ref)}, \mathbf{u}_0)$ on every interval T_i, $i = 0, 1, \ldots, \widetilde{n}$. Since the goal of the LQOC applied on each interval T_i, $i = 0, 1, \ldots, \widetilde{n}$ lies in the fact that the controller leads to transfer the state from a known initial state $\mathbf{x}_{t_i}$ to a specified fixed final

state $\mathbf{x}_{t_{i+1}} = \mathbf{x}_i^{(ref)}$ at a specified time t_{i+1}, $i = 0, 1, \ldots, \widetilde{n}$. Thereby, The final states $\mathbf{x}_i^{(ref)}$, $i = 0, 1, \ldots, \widetilde{n}$, represents the operating points of the system on each interval T_i. This means that we obtain on each interval T_i constant matrices $\mathbf{A}_i = \mathcal{D}_x\mathbf{h}(\mathbf{x}_i^{(ref)}, \mathbf{u}_0)$ and $\mathbf{B}_i = \mathcal{D}_u\mathbf{h}(\mathbf{x}_i^{(ref)}, \mathbf{u}_0)$. For this example, they were generated by Algorithmic or Automatic Differentiation (AD), see Griewank (2000). Here we used the software TAF (Transformations of Algorithms in Fortran), see Giering and Kaminski (1998).
The linearized state equation on every interval T_i reads:

$$\begin{aligned} \widetilde{\mathbf{x}}_{k+1} &= \widetilde{\mathbf{A}}_k\widetilde{\mathbf{x}}_k + \widetilde{\mathbf{B}}_k\widetilde{\mathbf{u}}_k \quad \forall k \in \widetilde{T}_i, \\ \widetilde{\mathbf{x}}_{t_i} &\quad \text{the given initial state,} \end{aligned} \tag{4.19}$$

where for all $k \in \widetilde{T}_i$

$$\begin{aligned} \widetilde{\mathbf{A}}_k &= [\mathbf{I}_n - \Delta t\widetilde{H}_k^{\text{diff}}]^{-1}[\mathbf{I}_n + \Delta t\widetilde{H}^{\text{sink}}]\mathbf{A}_i, & \mathbf{A}_i &= \mathcal{D}_x\mathbf{h}(\mathbf{x}_i^{(ref)}, \mathbf{u}_0), \\ \widetilde{\mathbf{B}}_k &= [\mathbf{I}_n - \Delta t\widetilde{H}_k^{\text{diff}}]^{-1}[\mathbf{I}_m + \Delta t\widetilde{H}^{\text{sink}}]\mathbf{B}_i, & \mathbf{B}_i &= \mathcal{D}_u\mathbf{h}(\mathbf{x}_i^{(ref)}, \mathbf{u}_0), \\ \widetilde{\mathbf{x}}_k &= \mathbf{x}_k - \mathbf{x}_i^{(ref)}, & \widetilde{\mathbf{u}}_k &= \mathbf{u}_k - \mathbf{u}_0, \\ \widetilde{\mathbf{x}}_{t_i} &= \mathbf{x}_{t_i} - \mathbf{x}_i^{(ref)}, \quad i = 0, \ldots, \widetilde{n}. \end{aligned}$$

The linearization of a nonlinear state equation of the form (4.17) about a given operating state yields a linear system which, in general, will be time-invariant. But the diffusion matrix is time-varying. Therefore the linearized state equation (4.19) will be time-varying. Since stability is a local property one might expect that the linearization provides sufficient information to determine whether or not the trajectory is stable. Actually, our considered NPZD model is only defined over a finite time interval. Therefore, we investigate finite-time boundedness of the time-varying state equation (4.19) on each finite time interval T_i, $i = 0, \ldots, \widetilde{n}$, and give a sufficient and necessary condition of Finite-Time Stability (FTS). For certain systems, FTS is the only useful definition of stability. In contrast to classical stability concept, FTS enables the examination of the stability of systems which are defined on a finite interval of time, (see., Dorato (2006)). A system (or state equation) is said to be finite-time stable if, given a bound on the initial condition, its state does not exceed a certain threshold during a specified time interval. FTS is a more practical concept, useful to study the behavior of the system within a finite interval. Therefore it is applied whenever it is desired that the state variables do not exceed a given threshold during the time horizon. It is worth noting that the term finite-time stability has also been used to refer to systems that converge to their operating states in a finite time, (see., Amato et al. (2006); Amato and Carbone et al. (2004); Amato and Ariola et al. (2010); Amato and Carbone et al. (2004); Dorato (1996); Su et al. (2013)).

The definition of state stability refers to an uncontrolled system ($\mathbf{u}_0 = 0$) with initial state value $\widetilde{\mathbf{x}}_{t_i} \in \mathbb{R}^n$. We are concerned with the stability of a zero input discrete-time linear state equation

$$\begin{aligned} \widetilde{\mathbf{x}}_{k+1} &= \widetilde{\mathbf{A}}_k \widetilde{\mathbf{x}}_k \quad \forall\, k \in \widetilde{T}_i, \\ \widetilde{\mathbf{x}}_{t_i} &= \mathbf{x}_{t_i} - \mathbf{x}_i^{(ref)} \quad \text{the given initial state.} \end{aligned} \tag{4.20}$$

Definition 1. *The state equation (4.20) is finite-time stable (FTS) with respect to the 5-tuple* $(\alpha, \gamma, t_i, t_{i+1}, \|.\|)$ *, where* $\alpha \leq \gamma$*,* $\|.\|$ *is any norm, if for every trajectory* $\widetilde{\mathbf{x}}_k$*, the condition* $\|\widetilde{\mathbf{x}}_{t_i}\| = \|\mathbf{x}_{t_i} - \mathbf{x}_i^{(ref)}\| \leq \alpha$ *implies* $\|\widetilde{\mathbf{x}}_k\| = \|\mathbf{x}_k - \mathbf{x}_i^{(ref)}\| \leq \gamma$ *for all* $k \in T_i$

We consider three classes of systems described in Figures (4.3), (4.4), (4.5): Systems for which the state trajectories always decrease in the norm (Figure 4.3), systems for which states always increase in the norm (Figure 4.4), and systems whose state trajectories behavior's is mixed (Figure 4.5). If the state trajectory is always decreasing (in the norm) and it starts inside the bound, the FTS is guaranteed. In the case where the trajectory is always increasing during the time interval of interest, it suffices to verify that the state at the last time of the interval does not exceed the bound. In the case of a mixed behavior, it is necessary to verify if the trajectory is bounded at each time step.

Figure 4.3: *Decreasing state trajectory.*

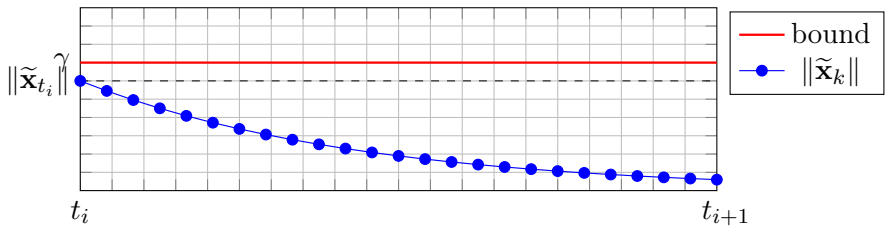

Figure 4.4: *Increasing state trajectory.*

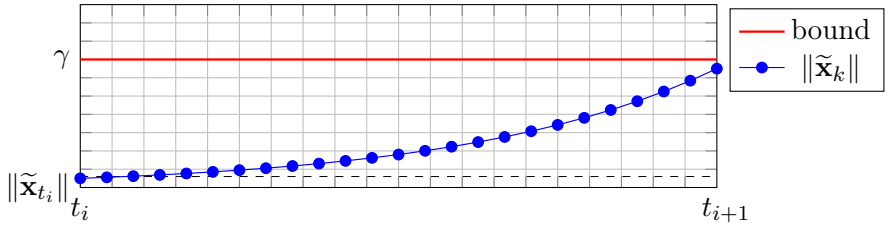

Figure 4.5: *Mixed state trajectory.*

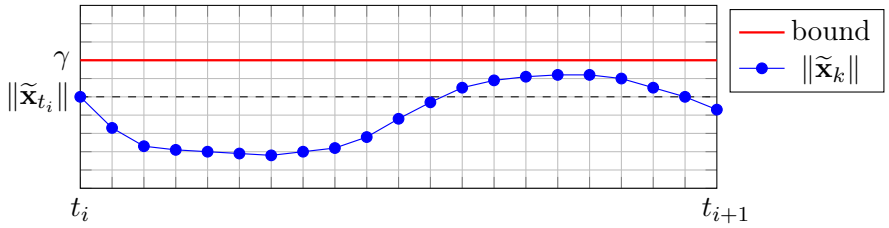

Definition 2. *The state equation (4.20) is said to be contractively stable with respect to the 5-tuple* $(\alpha, \beta, \gamma, t_i, t_{i+1}, \|.\|)$ *where* $\beta < \alpha \leq \gamma$, $\|.\|$ *is any norm, if for every trajectory* $\widetilde{\mathbf{x}}_k$ *with the initial condition* $\|\widetilde{\mathbf{x}}_{t_i}\| \leq \alpha$

1. *the state equation (4.20) is finite-time stable with respect to the set* $(\alpha, \gamma, t_i, t_{i+1}, \|.\|)$,
2. *there exists a* $t_p \in \widetilde{T}_i$ *such that* $\|\widetilde{\mathbf{x}}_k\| \leq \beta$ *for all* $k \in \{t_p, t_p + 1, \ldots, t_{i+1}\}$

Remark 2.

- *It is strongly emphasized that the numbers* $\alpha, \beta, t_i, t_{i+1}$ *and the norm* $\|.\|$ *are almost always specified a priori in a given problem.*
- *Although there is some analogy between the usual classical definition of stability and the above definitions, we point out that a system which is stable in the classical sense may be unstable in the sense of the above definitions, and vice versa.*

Figure 4.6: *Illustration concerning contractive stability.*

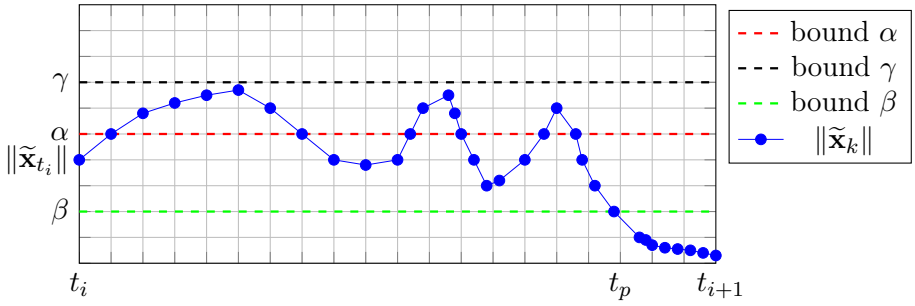

- *Definition 2 are finite-time analogue of asymptotic stability. Since the term "asymptotic" has little meaning in the context of a finite-time interval, the word "contractive" is utilized instead.*

The state transition sequence to state equation (4.20) is given by:

$$\widetilde{\mathbf{x}}_k = \left(\prod_{l=t_i}^{k-1} \widetilde{\mathbf{A}}_l \right) \widetilde{\mathbf{x}}_{t_i}, \text{ where } \widetilde{\mathbf{A}}_l = [\mathbf{I}_n - \Delta t \widetilde{H}_l^{\text{diff}}]^{-1} [\mathbf{I}_n + \Delta t \widetilde{H}^{\text{sink}}] \mathbf{A}_i,$$

Theorem 2. *Let $\widetilde{\mathbf{x}}_k$ be an arbitrary trajectory of (4.20) with $k \in \widetilde{T}_i$. There exists a constant $\gamma > 0$, such that*

$$\|\widetilde{\mathbf{x}}_k\|_\infty \leq \gamma^{k-t_i} \|\widetilde{\mathbf{x}}_{t_i}\|_\infty \quad \forall\, k \in \widetilde{T}_i,$$

where

$$\gamma := \left[(1 + \Delta t b_1) \|\mathbf{A}_i\|_\infty \right].$$

Proof. We have for all $k \in \widetilde{T}_i$

$$\begin{aligned}
\|\widetilde{\mathbf{x}}_k\|_\infty &= \| \left(\prod_{l=t_i}^{k-1} \widetilde{\mathbf{A}}_l \right) \widetilde{\mathbf{x}}_{t_i} \|_\infty, \\
&\leq \left(\prod_{l=t_i}^{k-1} \| [\mathbf{I}_n - \Delta t \widetilde{H}_l^{\text{diff}}]^{-1} \|_\infty \| [\mathbf{I}_n + \Delta t \widetilde{H}^{\text{sink}}] \|_\infty \|\mathbf{A}_i\|_\infty \right) \|\widetilde{\mathbf{x}}_{t_i}\|_\infty \\
&\leq \left(\prod_{l=t_i}^{k-1} \| [\mathbf{I}_n - \Delta t \widetilde{H}_l^{\text{diff}}]^{-1} \|_\infty \right) \left(\| [\mathbf{I}_n + \Delta t \widetilde{H}^{\text{sink}}] \|_\infty \right)^{k-t_i} \left(\|\mathbf{A}_i\|_\infty \right)^{k-t_i} \|\widetilde{\mathbf{x}}_{t_i}\|_\infty.
\end{aligned}$$

It is sufficient to show that

$$\begin{aligned} \|[\mathbf{I}_n - \Delta t \widetilde{H}_l^{\text{diff}}]^{-1}\|_\infty &\leq 1, \quad \forall\, t_i \leq l \leq k-1, \\ \|\mathbf{I}_n + \Delta t \widetilde{H}^{\text{sink}}\|_\infty &\leq 1 + \Delta t b_1, \end{aligned}$$

Proof of $\|[\mathbf{I}_n - \Delta t \widetilde{H}_l^{\text{diff}}]^{-1}\|_\infty \leq 1$.
According to equation (4.14), the matrix $(\mathbf{I}_n - \Delta t \widetilde{H}_l^{\text{diff}})$ contains only the sub-matrix $(\mathbf{I}_m - \Delta t H_l^{\text{diff}})$ on the block-diagonal. The matrix $(\mathbf{I}_m - \Delta t H_l^{\text{diff}})$ is a tridiagonal matrix and their entries satisfy:

$$r_i\left(\mathbf{I}_m - \Delta t H_l^{\text{diff}}\right) = \begin{cases} |\Delta t d_{1,l}| & \text{for } i = 1, \\ |\Delta t (c_{i,l} + d_{i,l})| & \text{for } 2 \leq i \leq m-1, \\ |\Delta t c_{m,l}| & \text{for } i = m, \end{cases} \tag{4.21}$$

$$|a_{ii}| = \begin{cases} |1 + \Delta t d_{1,l}| & \text{for } i = 1, \\ |1 + \Delta t (c_{i,l} + d_{i,l})| & \text{for } 2 \leq i \leq m-1, \\ |1 + \Delta t c_{m,l}| & \text{for } i = m, \end{cases} \tag{4.22}$$

(4.23)

where for a given matrix $\mathbf{A} = (a_{ij})_{1 \leqslant i,j \leqslant m}$, $r_i(A)$ is given as

$$r_i(A) = \sum_{\substack{j=1 \\ j \neq i}}^{m} |a_{ij}|, \text{ deleted } i\text{th row sum.}$$

Since, for our considered NPZD model, we have for all $t_i \leq l \leq k-1$, $k \in \widetilde{T}_i$ and $1 \leq i \leq m$, $c_{i,l} \geq 0$, $d_{i,l} \geq 0$, this implies

$$r_i\left(\mathbf{I}_m - \Delta t H_l^{\text{diff}}\right) < |a_{ii}|, \quad \forall\, 1 \leq i \leq m.$$

Definition 3. *(Quarteroni et al. (2007); Moraca (2007); Li (2008))*
A matrix $\mathbf{A} = (a_{ij})_{1 \leqslant i,j \leqslant m}$ *is called strictly diagonal dominant (SDD) if*

$$\sum_{\substack{j=1 \\ j \neq i}}^{m} |a_{ij}| < |a_{ii}|, \quad \forall\, 1 \leq i \leq m.$$

Theorem 3. *(Moraca (2007); Li (2008); Varah (1975))*

If A is an (SDD) matrix, then

$$\|A^{-1}\|_\infty \leq \frac{1}{\min\limits_{1\leq i\leq m}\left(|a_{ii}| - r_i(A)\right)}, \quad r_i(A) = \sum_{\substack{j=1\\ j\neq i}}^{m} |a_{i,j}|. \tag{4.24}$$

Thereby the matrix $(\mathbf{I}_m - \Delta t H_l^{\text{diff}})$ is strictly diagonal dominant. According to Theorem 3, the following upper bound for the norm of the inverse of the matrix $(\mathbf{I}_m - \Delta t H_l^{\text{diff}})$ is given as

$$\|[\mathbf{I}_m - \Delta t H_l^{\text{diff}}]^{-1}\|_\infty \leq \frac{1}{\min\limits_{1\leq i\leq m}\left(|a_{ii}| - r_i\left(\mathbf{I}_m - \Delta t H_l^{\text{diff}}\right)\right)}.$$

Since

$$\begin{aligned}\min_{1\leq i\leq m}\left(|a_{ii}| - r_i\left(\mathbf{I}_m - \Delta t H_l^{\text{diff}}\right)\right) &= \min_{1\leq i\leq m}\begin{cases}1 & \text{for } i = 1,\\ 1 & \text{for } 2 \leq i \leq m-1,\\ 1 & \text{for } i = m,\end{cases}\\ &= 1,\end{aligned}$$

we obtain

$$\|[\mathbf{I}_m - \Delta t H_l^{\text{diff}}]^{-1}\|_\infty \leq 1, \ \forall\, t_i \leq l \leq k-1,$$

and, thus,

$$\|[\mathbf{I}_n - \Delta t \widetilde{H}_l^{\text{diff}}]^{-1}\|_\infty \leq 1, \ \forall\, t_i \leq l \leq k-1.$$

Proof of $\|\mathbf{I}_n + \Delta t \widetilde{H}^{\text{sink}}\|_\infty \leq 1 + \Delta t b_1$.
According to equation (4.9), the matrix $(\mathbf{I}_n + \Delta t \widetilde{H}^{\text{sink}})$ is a 4×4 block-diagonal and contains the sub-matrix $(\mathbf{I}_m + \Delta t H^{\text{sink}})$ and all other sub-matrices are equal to the zero matrix.

For all $1 \leq i \leq m$, the entries of the matrix $(\mathbf{I}_m + \Delta t H^{\text{sink}})$ satisfy:

$$\sum_{j=1}^{m} |a_{ij}| = |1 + \Delta t b_i|, \quad \textit{where} \quad b_i = \frac{w_s}{h_{i-1}}.$$

Since in the implementation of our model, b_i satisfy $0 \leq \Delta t b_i \leq 1$ and the sequence

$b_1, b_2, \ldots, b_m$ fulfils the condition $b_m \leqslant b_{m-1} \leqslant \ldots \leqslant b_1$, it follows that

$$\begin{aligned} \|\mathbf{I}_m + \Delta t H^{\text{sink}}\|_\infty &= \max_{1\leq i\leq m} \left(\sum_{j=1}^{m} |a_{ij}| \right) \\ &= \max_{1\leq i\leq m} \left(|1 + \Delta t b_i| \right) \\ &= 1 + \Delta t b_1, \end{aligned}$$

and thus,

$$\|\mathbf{I}_n + \Delta \widetilde{H}^{\text{sink}}\|_\infty = 1 + \Delta t b_1.$$

For our NPZD model, the value of b_1 is given as $b_1 = \frac{w_s}{h_0} \approx 0.03$, where $w_s \approx 5m/d$ and $h_0 \approx 5.37m$. □

Concerning the time-varying state equation (4.20) on each finite time interval T_i, $i = 0, \ldots, \widetilde{n}$, we can only give sufficient conditions for the finite-time stability terms.
Let $k \in T_i$, and let $\widetilde{\mathbf{x}}_k$ be an arbitrary trajectory of state equation (4.20) with initial conditions $\|\widetilde{\mathbf{x}}_{t_i}\|_\infty \leq \alpha$. Then we have

$$\begin{aligned} \widetilde{\mathbf{x}}_k = \left(\prod_{l=t_i}^{k-1} \widetilde{\mathbf{A}}_l \right) \widetilde{\mathbf{x}}_{t_i} \text{ which implies } \|\widetilde{\mathbf{x}}_k\|_\infty &= \| \left(\prod_{l=t_i}^{k-1} \widetilde{\mathbf{A}}_l \right) \widetilde{\mathbf{x}}_{t_i} \|_\infty \\ &\leq \prod_{l=t_i}^{k-1} \|\widetilde{\mathbf{A}}_l\|_\infty \|\widetilde{\mathbf{x}}_{t_i}\|_\infty \\ &\leq \alpha \prod_{l=t_i}^{k-1} \left((1 + \Delta t b_1) \|\mathbf{A}_i\|_\infty \right) \\ &\leq \alpha \left((1 + \Delta t b_1) \|\mathbf{A}_i\|_\infty \right)^{k-t_i}. \end{aligned}$$

If $\|\mathbf{A}_i\|_\infty \leq \frac{1}{1+\Delta t b_1}$, then $\|\widetilde{\mathbf{x}}_k\|_\infty \leq \beta = \alpha$. This implies that $(\|\widetilde{\mathbf{x}}_k\|_\infty)_{k\in T_i}$ is always monotonically decreasing and converging to 0. Thus, the state equation (4.20) is finite-time stable over the 5-tuple $(1, 1, t_i, t_{i+1}, \|.\|_\infty)$.

If $\frac{1}{1+\Delta t b_1} \leq \|\mathbf{A}_i\|_\infty \leq 1$, the assertion holds for $\beta = \alpha(1 + \Delta t b_1)$, the state equation (4.20) is finite-time stable over the 5-tuple $(\alpha, \alpha(1+\Delta t b_1), t_i, t_{i+1}, \|.\|)$.

Otherwise, we set $\beta = \alpha \left((1 + \Delta t b_1) \|\mathbf{A}_i\|_\infty \right)^{k-t_i}$.

We note that we actually have a time varying state equation (4.20), but since the norm of the time varying diffusion matrix is smaller as 1, the finite-time stability over each

interval $T_i,\ i = 0, \ldots, \widetilde{n}$ is strongly dependent on the matrices $\mathbf{A}_i$, which are results of the linearization of the function $\mathbf{h}$ (4.17) about a constant operating point $(\mathbf{x}_i^{(ref)}, \mathbf{u}_0)$. For the contractive stability given in Definition 2, we have to ensure the existence of $t_p \in \widetilde{T}_i$ such that $\|\widetilde{\mathbf{x}}_k\|_\infty \leq \beta$ for all $k \in \{t_p, \ldots, t_{i+1}\}$. Let $\widetilde{\mathbf{x}}_k$ be an arbitrary trajectory of state equation (4.20) with initial condition $\|\widetilde{\mathbf{x}}_{t_i}\|_\infty \leq \alpha$ and $\|\widetilde{\mathbf{x}}_k\|_\infty \leq \gamma$ for all $k \in T_i$ (finite-time stable over $(\alpha, \gamma, t_i, t_{i+1}, \|.\|_\infty)$).
Then, there exists a $t_p \in T_i$ with $\|\widetilde{\mathbf{x}}_{t_p}\|_\infty = \min\limits_{k \in \{t_i, \ldots, t_p\}} \|\widetilde{\mathbf{x}}_k\|_\infty$. Therefore, for all $k \in \{t_p, \ldots, t_{i+1}\}$, we have

$$
\begin{aligned}
\widetilde{\mathbf{x}}_k = \left(\prod_{l=t_p}^{k-1} \widetilde{\mathbf{A}}_l\right) \widetilde{\mathbf{x}}_{t_p} \text{ which implies } \|\widetilde{\mathbf{x}}_k\|_\infty &= \| \left(\prod_{l=t_p}^{k-1} \widetilde{\mathbf{A}}_l\right) \widetilde{\mathbf{x}}_{t_p}\|_\infty \\
&\leq \prod_{l=t_p}^{k-1} \|\widetilde{\mathbf{A}}_l\|_\infty \|\widetilde{\mathbf{x}}_{t_p}\|_\infty \\
&\overset{\|\widetilde{\mathbf{x}}_{t_p}\|_\infty \leq \alpha}{\leq} \alpha \prod_{l=t_p}^{k-1} \left((1 + \Delta t b_1)\|\mathbf{A}_i\|_\infty\right) \\
&\leq \alpha \left((1 + \Delta t b_1)\|\mathbf{A}_i\|_\infty\right)^{k-t_p},
\end{aligned}
$$

If $\|\mathbf{A}_i\|_\infty < \frac{1}{1+\Delta t b_1}$, then the assertion holds for $\beta = \alpha \left((1 + \Delta t b_1)\|\mathbf{A}_i\|_\infty\right) < \alpha$.
Now, given the state equation (4.19), we consider the time varying state feedback controller

$$
\widetilde{\mathbf{u}}_k \quad = \quad \mathbf{G}_k \widetilde{\mathbf{x}}_k,\ \forall\ k \in \widetilde{T}_i. \tag{4.25}
$$

Therefore, a sufficient condition which guaranteeing that the state equation (4.19) with the controller (4.25) is stable over a finite-time interval $T_i, i = 0, \ldots, \widetilde{n}$, will be derived. The goal is to find a state feedback controller (4.25) so that the closed loop state equation

$$
\widetilde{\mathbf{x}}_{k+1} \quad = \quad (\widetilde{\mathbf{A}}_k + \widetilde{\mathbf{B}}_k \mathbf{G}_k)\widetilde{\mathbf{x}}_k,\ \forall\ k \in \widetilde{T}_i \tag{4.26}
$$

is finite-time stable with respect to $(\alpha, \beta, \mathbf{R}, t_{i+1})$. First, the above given definition of the finite stability (Definition 1) can also be written as follows

Definition 4. *(Amato and Ariola et al. (2003))*
The state equation (4.20) is said to be finite-time stable with respect to the 4-tuple $(\alpha, \beta, \Gamma, t_{i+1})$, where $\Gamma \in \mathbb{R}^{n \times n}$ is a positive definite matrix, $0 < \alpha \leq \gamma$, if

$$
\widetilde{\mathbf{x}}_{t_i}^\top \Gamma \widetilde{\mathbf{x}}_{t_i} \leq \alpha \quad \textit{implies} \quad \widetilde{\mathbf{x}}_k^\top \Gamma \widetilde{\mathbf{x}}_k \leq \gamma,\ \forall\ k \in T_i. \tag{4.27}
$$

We point out that with the norm $\|\widetilde{\mathbf{x}}\|_\Gamma = \widetilde{\mathbf{x}}^\top \Gamma \widetilde{\mathbf{x}}$, the inequality in Definition 1 holds. We note, given a $n \times n$-matrix Γ, we write $\Gamma > 0$ ($\Gamma \geq 0$) meaning that Γ is positive definite (semidefinite), i.e., that there exists $\alpha > 0$ such that for all $\mathbf{x} \in \mathbb{R}^n$:

$$\mathbf{x}^\top \Gamma \mathbf{x} \geq \alpha \|\mathbf{x}\|^2 \qquad \left(\mathbf{x}^\top \Gamma \mathbf{x} \geq 0\right).$$

Given two matrices Γ_1 and Γ_2, the notation $\Gamma_1 > \Gamma_2$ ($\Gamma_1 \geq \Gamma_2$) means that $\Gamma_1 - \Gamma_2 > 0$ ($\Gamma_1 - \Gamma_2 \geq 0$).

Definition 5. *(Finite-time stability via state feedback)(Amato and Abdallah et al. (2003)) The state equation (4.26) is finite-time stable via state feedback with respect to the set $(\alpha, \gamma, \Gamma, t_{i+1})$ if there exists a sequence of symmetric matrices $(\mathbf{P}_k)_{k \in \widetilde{T}_i}$ and a sequence of symmetric matrices $(\mathbf{G}_k)_{k \in \widetilde{T}_i}$ such that*

$$-\mathbf{P}_{N-k} + (\widetilde{\mathbf{A}}_{N-k} + \widetilde{\mathbf{B}}_{N-k}\mathbf{G}_{N-k})^\top \mathbf{P}_{N-k+1}(\widetilde{\mathbf{A}}_{N-k} + \widetilde{\mathbf{B}}_{N-k}\mathbf{G}_{N-k}) < 0 \quad \forall\, k \in \widetilde{T}_i, \tag{4.28}$$

$$\mathbf{P}_k \geq \Gamma,\ \forall\, k \in \widetilde{T}_i, \tag{4.29}$$

$$\mathbf{P}_1 < \tfrac{\alpha}{\gamma}\Gamma, \tag{4.30}$$

Let $V(\widetilde{\mathbf{x}}_k) = \widetilde{\mathbf{x}}_k^\top \mathbf{P}_k \widetilde{\mathbf{x}}_k$, $k \in T_i$, a quadratic function. Then, we have for all $k \in \widetilde{T}_i$

$$\begin{aligned}
\Delta V(\widetilde{\mathbf{x}}_k) &= V(\widetilde{\mathbf{x}}_{k+1}) - V(\widetilde{\mathbf{x}}_k) \\
&= \widetilde{\mathbf{x}}_{k+1}^\top \mathbf{P}_{k+1} \widetilde{\mathbf{x}}_{k+1} - \widetilde{\mathbf{x}}_k^\top \mathbf{P}_k \widetilde{\mathbf{x}}_k \\
&= \widetilde{\mathbf{x}}_k^\top (\widetilde{\mathbf{A}}_k + \widetilde{\mathbf{B}}_k \mathbf{G}_k)^\top \mathbf{P}_{k+1} (\widetilde{\mathbf{A}}_k + \widetilde{\mathbf{B}}_k \mathbf{G}_k) \widetilde{\mathbf{x}}_k - \widetilde{\mathbf{x}}_k^\top \mathbf{P}_k \widetilde{\mathbf{x}}_k \\
&= \widetilde{\mathbf{x}}_k^\top \{-\mathbf{P}_k + (\widetilde{\mathbf{A}}_k + \widetilde{\mathbf{B}}_k \mathbf{G}_k)^\top \mathbf{P}_{k+1} (\widetilde{\mathbf{A}}_k + \widetilde{\mathbf{B}}_k \mathbf{G}_k)\} \widetilde{\mathbf{x}}_k.
\end{aligned} \tag{4.31}$$

According to Theorem 3.4, there exists a unique solution of the closed loop discrete time linear quadratic optimal control. The optimal control is given by (4.25) and the state feedback equation is given by (4.26). The feedback matrix is given as

$$\mathbf{G}_k := -(\mathbf{R}_k + \widetilde{\mathbf{B}}_k^\top \mathbf{P}_{k+1} \widetilde{\mathbf{B}}_k)^{-1} \widetilde{\mathbf{B}}_k^\top \mathbf{P}_{k+1} \widetilde{\mathbf{A}}_k,\ \forall\, k \in \widetilde{T}_i,$$

where $\mathbf{P}_k$, is the unique symmetric solution of the Discrete Riccati Equation.

$$\begin{aligned}
-\mathbf{P}_{N-k} + (\widetilde{\mathbf{A}}_{N-k} + \widetilde{\mathbf{B}}_{N-k}\mathbf{G}_{N-k})^\top \mathbf{P}_{N-k+1}(\widetilde{\mathbf{A}}_{N-k} + \widetilde{\mathbf{B}}_{N-k}\mathbf{G}_{N-k}) \\
= -\mathbf{G}_{N-k}^\top \mathbf{P}_{N-k+1} \mathbf{G}_{N-k} - \mathbf{Q}_{N-k}
\end{aligned} \tag{4.32}$$

with terminal condition $\mathbf{P}_N = \mathbf{Q}_N \geq \mathbf{I}_n$, $(\mathbf{Q}_k)_{k\in T_i}$, are positive semi-definite and $(\mathbf{R}_k)_{k\in\widetilde{T}_i}$, are positive definite.
Using (4.31) and (4.32), we have

$$\Delta V(\widetilde{\mathbf{x}}_k) \quad = \quad -\widetilde{\mathbf{x}}_k^\top \{\mathbf{G}_{N-k}^\top \mathbf{P}_{N-k+1}\mathbf{G}_{N-k} + \mathbf{Q}_{N-k}\}\widetilde{\mathbf{x}}_k.$$

Thus, the assertion (4.28) hold when the sequence of matrices $(\mathbf{Q}_k)_{k\in T_i}$, are positive definite. We note that the quadratic function V is named by the stability of the infinite time Lyapunov function. moreover the sequence matrices $(\mathbf{p}_k)_{k\in T_i}$ are non-increasing, we have for $\Gamma = \mathbf{I}_n$

$$\mathbf{P}_k \geq \mathbf{P}_N \geq \mathbf{I}_n, \, \forall \, k \in \widetilde{T}_i.$$

The inequality (4.30) yields through the definition 4 of the finite-time stability (see, e.g. Amato et al. (2006); Amato and Carbone et al. (2004); Amato and Ariola et al. (2010)). We can see, that the finite-time stability via state feedback will be guaranteed over each interval $T_i, i = 0, \ldots, \widetilde{n}$ if we choose positive definite weighting matrices $\mathbf{Q}_k$ and $\mathbf{R}_k$, $k \in T_i$, i.e., $\mathbf{Q}_k > 0$ and $\mathbf{R}_k > 0$ for all $k \in \tilde{T}_i$.

5 Study Design and Results

The aim of this work is to examine the application of Discrete Linear Quadratic Optimal Control with both closed loop (LQOC) and open loop (DOLOC) and the Extended Kalman Filter (EKF) to parameter optimization and state estimation. The two proposed methodologies LQOC and EKF were introduced in Chapter 3, DOLOC in Paper 3 (Appendix A.3), and are applied for a nitrogen ecosystem model, namely the NPZD model that has been introduced in Section 4.1.

The considered NPZD model has been previously used for parameter optimization by local, gradient-based algorithms as well as global genetic algorithms (see,e.g., Schartau and Oschlies (2003a); Rückelt et al. (2010); Schartau (2001)). Further, surrogate-based optimization methodologies employing a physics-based low-fidelity model (see Prieß et al. (2011)) have been applied. In all these studies, the quality of the model fit to measurement data has not been optimal and it was difficult to identify the parameters uniquely (see also Ward (2009)). The parameters of the marine ecosystem model (NPZD model) were assumed to be temporally constant. In this chapter we analyze the application of the three above mentioned methodologies. The chapter is organized as follows: As a first case study, we present the application of the LQOC method to the NPZD model (This method is covered in Papers 1 and 4 (Appendix A.1 and Appendix A.4)). Below, we discuss the structure and the main goal of this method. As a second case study, the application of the EKF will be presented (this method is covered in Paper 2 (Appendix A.2)). We investigate two kinds of state estimation to the NPZD model, using optimal periodic parameters, which are obtained in the first case study, and using optimal constant parameters, which have been obtained by using a sequential quadratic programming (SQP) method (see Rückelt et al. (2010)). As a third case study, we present the application of the DOLOC method (this method is covered in Paper 3 (Appendix A.3)). We investigate the impact of the linearization scheme about the state variables, which have been used to linearize the non-linear NPZD model, on the quality of the model-data misfit of the original non-linear NPZD model. The focus of this three studies is on the applicability of the proposed methodologies to the considered models to improve the model-data fit using periodic parameters.

Closed Loop Discrete Linear Quadratic Optimal Control

In this Section, we introduce the application of closed loop discrete linear quadratic optimal control (LQOC). We investigate the applicability of this approach to achieve a good model-data fit and efficient periodic parameters of the NPZD model.
The discretized NPZD model can be summarized as (cf. (4.1), (4.16), (4.17) in Section 4.1):

$$\left.\begin{array}{lcl} \mathbf{x}_{k+1} & = & [\mathbf{I}_n - \Delta t \widetilde{H}_k^{\text{diff}}]^{-1}[\mathbf{I}_n + \Delta t \widetilde{H}^{\text{sink}}]\mathbf{h}(\mathbf{x}_k, \mathbf{u}_k), \forall k \in [M-1], \\ \mathbf{h}(\mathbf{x}_k, \mathbf{u}_k) & := & \mathcal{L}_k \circ \mathcal{L}_k \circ \mathcal{L}_k \circ \mathcal{L}_k(\mathbf{x}_k, \mathbf{u}_k), \forall k \in [M-1]. \\ \mathcal{L}_k & := & \mathbf{x}_k + \frac{\Delta t}{4}\mathbf{S}(\mathbf{x}_k, \mathbf{u}_k), \\ M & := & j_{max} N, \end{array}\right\} \quad (5.1)$$

where j_{max} is the number of all years, and N denotes the number of hours in a year. For each tracer $l \in \{N, P, Z, D\}$ and each year $j \in [j_{max}]$ of the considered time horizon we denote with $n_j^{(l)}$ the number of available measurements and with $t_{j,i}^l$, $i = 1, \ldots, n_j^{(l)}$, the corresponding times, which are measured in integral hours counted from the beginning of the time horizon.
Now, we introduce similar intervals as defined in Section 4.1 for all years $j = 1, \ldots, j_{max}$:

$$I_j := \bigcap_{l \in \{N,P,Z,D\}} \{t_{j,i}^l\}_{i=1,\ldots,n_j^{(l)}} =: \{t_{j,i}\}_{i=1,\ldots,\widetilde{n}_j},$$

where $\widetilde{n}_j$ denotes the number of elements in this intersection. For all $j = 1, \ldots, j_{max}$ and for all $i = 0, \ldots, \widetilde{n}_j$ the $\widetilde{n}_j + 1$ discrete time intervals between the subsequent instances of time $\{t_{j,i}\}$ are given as

- $T_{j,i} := [t_{j,i}, t_{j,i+1}] \bigcap \mathbb{N}$,
- $\widetilde{T}_{j,i} := [t_{j,i}, t_{j,i+1} - 1] \bigcap \mathbb{N}$,
- $t_{1,0} := 1$, and $t_{1,\widetilde{n}_1+1} := N$.
- $t_{j,0} := (j-1)N$, and $t_{j,\widetilde{n}_1+1} := jN, \quad j = 2, \ldots, j_{max}$

We apply the linearization on each time interval $[t_{j,i}, t_{j,i+1}]$ separately. For this purpose, we split the interval into sections of the length Δt (here $\Delta t = 1$h), as shown in Figure 5.1.

Figure 5.1: *Example for an interval on which the linearization is applied.*

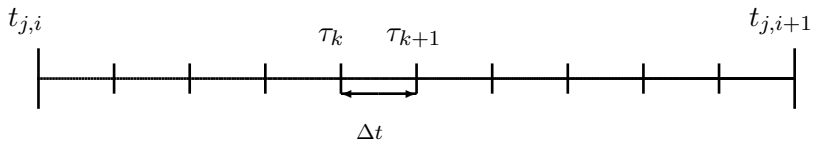

The discrete time steps τ_k in this interval are

$$\begin{aligned} \tau_{t_{j,i}} &= t_{j,i}, \\ \tau_{k+1} &= \tau_k + \Delta t, \quad k = t_{j,i}, t_{j,i}+1, \ldots, t_{j,i+1}. \end{aligned}$$

Next, we try to linearize the nonlinear function $\mathbf{h}$ on every interval $T_{j,i}$, $j = 1, \ldots, j_{max}$, $i = 0, \ldots, \widetilde{n}_j$. The linearization will be done about a given reference trajectory $(\mathbf{x}^{(ref)}, \mathbf{u}^{(ref)})$, which we define below in detail.
We start with the first year ($j = 1$):
Let $i \in \{0, \ldots, \widetilde{n}_1\}$. The goal of applying the LQOC on $T_{1,i}$ is to lead the system from a given initial state $\mathbf{x}_{t_{1,i}}$ to a fixed final state $\mathbf{x}_{t_{1,i+1}} = \mathbf{x}_{i+1}^{(obs)} =: \mathbf{x}_i^{(ref)}$, which together with the given constant control $\mathbf{u}^{(ref)} = \mathbf{u}_0$ is the operating point of the system on $T_{1,i}$. Since we have no reference value $\mathbf{x}^{(ref)}$ at the end of each year, we use linear interpolation between the data $\mathbf{x}_{1,\widetilde{n}_j}^{(obs)}$ and $\mathbf{x}_{2,1}^{(obs)}$ to generate such value, denoted by $\mathbf{x}_{1,\widetilde{n}_1+1}^{(obs)}$ (this will also be applied for $j = 2, \ldots, j_{max}$).
The linearized state equation on $T_{1,i}$ reads:

$$\begin{aligned} \widetilde{\mathbf{x}}_{k+1} &= \widetilde{\mathbf{A}}_k \widetilde{\mathbf{x}}_k + \widetilde{\mathbf{B}}_k \widetilde{\mathbf{u}}_k, \quad \forall\, k \in \widetilde{T}_{1,i}, \\ \widetilde{\mathbf{x}}_{t_{1,i}} &= \mathbf{x}_{t_{1,i}} - \mathbf{x}_i^{(ref)} \quad \text{the given initial state}, \end{aligned} \tag{5.2}$$

where

$$\widetilde{\mathbf{A}}_k := [\mathbf{I}_n - \Delta t \widetilde{H}_k^{\text{diff}}]^{-1} [\mathbf{I}_n + \Delta t \widetilde{H}^{\text{sink}}] \mathbf{A}_i, \qquad \mathbf{A}_i := \mathcal{D}_x \mathbf{h}(\mathbf{x}_i^{(ref)}, \mathbf{u}_0), \tag{5.3}$$

$$\widetilde{\mathbf{B}}_k := [\mathbf{I}_n - \Delta t \widetilde{H}_k^{\text{diff}}]^{-1} [\mathbf{I}_n + \Delta t \widetilde{H}^{\text{sink}}] \mathbf{B}_i, \qquad \mathbf{B}_i := \mathcal{D}_u \mathbf{h}(\mathbf{x}_i^{(ref)}, \mathbf{u}_0), \tag{5.4}$$

$$\widetilde{\mathbf{x}}_k := \mathbf{x}_k - \mathbf{x}_i^{(ref)}, \qquad \widetilde{\mathbf{u}}_k := \mathbf{u}_k - \mathbf{u}_0. \tag{5.5}$$

We note that the matrices $\mathbf{A}_i$ and $\mathbf{B}_i$ are constant on $T_{1,i}$. The optimization problem

on $T_{1,i}$ is defined as

$$\min_{\widetilde{\mathbf{u}}} \mathcal{J}(\widetilde{\mathbf{u}}) \quad \text{where} \quad \mathcal{J}(\widetilde{\mathbf{u}}) = \frac{1}{2} \sum_{k=t_{1,i}}^{t_{1,i+1}-1} \left(\widetilde{\mathbf{x}}_k^\top \mathbf{Q}_i \widetilde{\mathbf{x}}_k + \widetilde{\mathbf{u}}_k^\top \mathbf{R}_i \widetilde{\mathbf{u}}_k \right),$$

subject to (5.2)

where the matrices $\mathbf{Q}_i$ and $\mathbf{R}_i$ are constant on $T_{1,i}$. Since the system is supposed to reach the steady final value which corresponds to the operating point, the first term of (3.3) can be neglected due to $\widetilde{\mathbf{x}}_{t_{1,i+1}} = 0$. The choice of both matrices is given in section 3.6 in paper 1 (Appendix A1).
Now, we consider all further years. Let $j \in \{2, \ldots, j_{max}\}$:
From the second year on, the main goal is to enforce periodicity of the parameters. To obtain annually period parameters, we choose the period $T = N$ (which in our case is one year).
Let $i \in \{0, 1, \ldots, \widetilde{n}_j\}$. The choice of the reference trajectories $(\mathbf{x}^{(ref)}, \mathbf{u}^{(ref)})$ on $T_{j,i}$ is given as

$$\begin{aligned} \mathbf{x}^{(ref)} &:= (\mathbf{x}_{k-T})_{k \in T_{j,i}} \\ \mathbf{u}^{(ref)} &:= (\mathbf{u}_{k-T})_{k \in \widetilde{T}_{j,i}} \end{aligned}$$

The linearized state equation on $T_{j,i}$ reads

$$\begin{aligned} \widetilde{\mathbf{x}}_{k+1} &= \widetilde{\mathbf{A}}_k \widetilde{\mathbf{x}}_k + \widetilde{\mathbf{B}}_k \widetilde{\mathbf{u}}_k, \quad \forall\, k \in \widetilde{T}_{j,i}, \\ \widetilde{\mathbf{x}}_{t_{j,i}} &= \mathbf{x}_{t_{j,i}} - \mathbf{x}^{(ref)}_{t_{j,i}+1} \quad \text{the given initial state,} \end{aligned} \tag{5.6}$$

where

$$\begin{aligned} \widetilde{\mathbf{A}}_k &:= [\mathbf{I}_n - \Delta t \widetilde{H}_k^{\text{diff}}]^{-1} [\mathbf{I}_n + \Delta t \widetilde{H}^{\text{sink}}] \mathbf{A}_k, & \mathbf{A}_k &:= \mathcal{D}_x \mathbf{h}(\mathbf{x}_k^{(ref)}, \mathbf{u}_k^{(ref)}) \\ \widetilde{\mathbf{B}}_k &:= [\mathbf{I}_n - \Delta t \widetilde{H}_k^{\text{diff}}]^{-1} [\mathbf{I}_n + \Delta t \widetilde{H}^{\text{sink}}] \mathbf{B}_k, & \mathbf{B}_k &:= \mathcal{D}_u \mathbf{h}(\mathbf{x}_k^{(ref)}, \mathbf{u}_k^{(ref)}) \\ \widetilde{\mathbf{x}}_k &:= \mathbf{x}_k - \mathbf{x}_k^{(ref)}, & \widetilde{\mathbf{u}}_k &:= \mathbf{u}_k - \mathbf{u}_k^{(ref)}, \end{aligned}$$

We note that contrarily to the first year, the above defined matrices $\mathbf{A}_k$ and $\mathbf{B}_k$ are time dependent matrices.
The optimization problem is defined on $T_{j,i}$ as follows

$$\min_{\widetilde{\mathbf{u}}} \mathcal{J}(\widetilde{\mathbf{u}}) \quad \text{where} \quad \mathcal{J}(\widetilde{\mathbf{u}}) = \frac{1}{2} \widetilde{\mathbf{x}}_{t_{j,i+1}}^\top \mathbf{Q}_{t_{j,i+1}} \widetilde{\mathbf{x}}_{t_{j,i+1}} + \frac{1}{2} \sum_{k=t_{j,i}}^{t_{j,i+1}-1} \left(\widetilde{\mathbf{x}}_k^\top \mathbf{Q}_k \widetilde{\mathbf{x}}_k + \widetilde{\mathbf{u}}_k^\top \mathbf{R}_k \widetilde{\mathbf{u}}_k \right),$$

subject to (5.6). (5.7)

Since the second goal here is to obtain control vector which transfer the state equation $\mathbf{x} = (\mathbf{x}_k)_{k\in T_{j,i}}$ from the initial state $\mathbf{x}_{t_{j,i}}$ to the imposed fixed final state $\mathbf{x}_{t_{j,i+1}} = \mathbf{x}^{(obs)}_{t_{j,i+1}}$, we can perform a translation and introduce the deviation of the state vector:

$$\begin{aligned} \bar{\mathbf{x}}_k &= \widetilde{\mathbf{x}}_k - \mathbf{x}^{(d)}_{t_{j,i+1}}, \\ \mathbf{x}^{(d)}_{t_{j,i+1}} &:= \mathbf{x}^{(obs)}_{t_{j,i+1}} - \mathbf{x}^{(ref)}_{t_{j,i+1}}, \end{aligned}$$

which gives:

$$\begin{aligned} \bar{\mathbf{x}}_{t_{j,i+1}} &= \widetilde{\mathbf{x}}_{t_{j,i+1}} - \mathbf{x}^{(d)}_{t_{j,i+1}} \\ &= (\mathbf{x}_{t_{j,i+1}} - \mathbf{x}^{(ref)}_{t_{j,i+1}}) - (\mathbf{x}^{(obs)}_{t_{j,i+1}} - \mathbf{x}^{(ref)}_{t_{j,i+1}}) \\ &= \mathbf{x}_{t_{j,i+1}} - \mathbf{x}^{(obs)}_{t_{j,i+1}} \end{aligned}$$

the state equation (5.6) becomes:

$$\begin{aligned} \bar{\mathbf{x}}_{k+1} &= \widetilde{\mathbf{A}}_k \bar{\mathbf{x}}_k + \widetilde{\mathbf{B}}_k \widetilde{\mathbf{u}}_k + \mathbf{r}_k, \\ \bar{\mathbf{x}}_{t_{j,i}} &= \widetilde{\mathbf{x}}_{t_{j,i}} - \mathbf{x}^{d}_{t_{j,i+1}}, \\ \mathbf{r}_k &= \widetilde{\mathbf{A}}_k \mathbf{x}^{d}_{t_{j,i+1}} - \mathbf{x}^{d}_{t_{j,i+1}}, \end{aligned} \tag{5.8}$$

then, we set:

$$\mathbf{z_k} = \begin{bmatrix} \bar{\mathbf{x}}_k \\ 1 \end{bmatrix}, \qquad \bar{\mathbf{A}}_\mathbf{k} = \begin{bmatrix} \widetilde{\mathbf{A}}_k & \mathbf{r}_k \\ 0 & 1 \end{bmatrix}, \qquad \bar{\mathbf{B}}_\mathbf{k} = \begin{bmatrix} \mathbf{B}_k \\ 0 \end{bmatrix}, \qquad \bar{\mathbf{Q}}_\mathbf{k} = \begin{bmatrix} \mathbf{Q}_k & 0 \\ 0 & 0 \end{bmatrix},$$

then, the state equation (5.8) becomes

$$\begin{aligned} \mathbf{z}_{k+1} &= \bar{\mathbf{A}}_k \mathbf{z}_k + \bar{\mathbf{B}}_k \widetilde{\mathbf{u}}_k, \ \forall\ k \in \widetilde{T}_{j,i} \\ \mathbf{z}_{t_{j,i}} &= \begin{bmatrix} \bar{\mathbf{x}}_{t_{j,i}} \\ 1 \end{bmatrix}. \end{aligned} \tag{5.9}$$

The optimization problem is defined on $T_{j,i}$ as follows

$$\min_{\widetilde{\mathbf{u}}} \mathcal{J}(\widetilde{\mathbf{u}}) \quad \text{where} \quad \mathcal{J}(\widetilde{\mathbf{u}}) = \frac{1}{2}\mathbf{z}^\top_{t_{j,i+1}} \bar{\mathbf{Q}}_{t_{j,i+1}} \mathbf{z}_{t_{j,i+1}} + \frac{1}{2} \sum_{k=t_{j,i}}^{t_{j,i+1}-1} \left(\mathbf{z}_k^\top \bar{\mathbf{Q}}_k \mathbf{z}_k + \widetilde{\mathbf{u}}_k^\top \mathbf{R}_k \widetilde{\mathbf{u}}_k \right),$$

$$\text{subject to (5.9).} \tag{5.10}$$

Thus, the closed loop discrete linear quadratic optimal control as outlined in Table 3.1 can be applied (paper 1 and 4 (Appendix A1, A4)) to keep the new state $\mathbf{z} = (\mathbf{z})_{k\in T_{j,i}}$ at the final time step $t_{j,i+1}$ close to 0. We point out that if we want to obtain time-varying

parameters that not need to be periodic, then the linearization scheme in the first year will be applicable for all years, i.e., $j = 2, \ldots, j_{max}$.

Here, the choice of the the matrices $\mathbf{Q}_k$ and $\mathbf{R}_k$ are given on each interval $T_{j,i}$ in section 3.6 in paper 1 (Appendix A1).

It can be seen from the discussion about the weighing matrices in section 3.1.3 that the cost function defined in the LQOC approach is heavily dependent upon the selection of these matrices. So, more precisely, we should say that the LQOC method is optimal with respect to the choice of $\mathbf{Q} = (\mathbf{Q}_k)_{k\in\widetilde{T}_{j,i}}$ and $\mathbf{R} = (\mathbf{R}_k)_{k\in\widetilde{T}_{j,i}}$. Thus, an LQOC solution which is optimal for one choice of $\mathbf{Q}$ and $\mathbf{R}$ will usually not be optimal for other choices of $\mathbf{Q}$ and $\mathbf{R}$.

For our case here, we are interested in the control complexity. As mentioned above, the cost function is defined as

$$\min_{\mathbf{u}} \left\{ \frac{1}{2}\|\mathbf{z}_{t_{j,i+1}}\|_{\mathbf{Q}_{t_{j,i+1}}} + \sum_{k=t_{j,i}}^{t_{j,i+1}-1} \|\mathbf{z}_k\|_{\mathbf{Q}_k} + \|\mathbf{u}_k - \mathbf{u}_k^{(ref)}\|_{\mathbf{R}_k} \right\},$$

where the norm $\|.\|_{\mathbf{Q}}$ is defined as $\|\mathbf{x}\|_{\mathbf{Q}} = \frac{1}{2}\mathbf{x}^\top\mathbf{Q}\mathbf{x}$.

Our main objective is to enforce the periodicity of the parameters. For this reason, the minimization of the expression $\|\mathbf{u}_k - \mathbf{u}_k^{(ref)}\|_{\mathbf{R}_k} = \|\mathbf{u}_k - \mathbf{u}_{k-T}\|_{\mathbf{R}_k}$ stands in the foreground. By choosing $\mathbf{R}_k \gg \mathbf{Q}_k$ for all $k \in \widetilde{T}_{j,i}$, the expression $\|\mathbf{u}_k - \mathbf{u}_{k-T}\|_{\mathbf{R}_k}$ will be weighted more heavily which leads to a solution $\mathbf{u}_k \simeq \mathbf{u}_{k-T}$. For the state vector $\mathbf{z}$, it is important that only the final values $\mathbf{z}_{t_{j,i+1}}$ will to be zero or closer to zero on each interval $T_{j,i}, j = 2, \ldots, j_{max},\ i = 0, \ldots, \tilde{n}_j$. On the other hand, the expression $\|\mathbf{u}_k - \mathbf{u}_0\|_{\mathbf{R}_k}$ in the first year needs not necessarily to be overweighted. However, it is important to keep the parameters in the admissible bounds and in the vicinity of the initial guess ($\mathbf{u}_0$). To examine the effect of the weighing matrices $\mathbf{R}_k$ on the behavior of the parameters in the first year, we have additionally performed sensitivity experiments with different entries of the weighing matrices $\mathbf{R}_k$ for all $k \leqslant T$.

Finally, we point out that for our NPZD model the output matrices $\mathbf{C}_k$ are identity matrices. At the end of the optimization with the closed loop linear quadratic optimal control (LQOC) method, we obtain a periodic parameter vector $\mathbf{u} = (\mathbf{u}_k)_{k\in[N-1]}$, i.e, $\mathbf{u}_k \simeq \mathbf{u}_{k-T}$ for all $k \in [N-1]$, and a model output vector $\mathbf{x} = (\mathbf{x}_k)_{k\in[M]}$.

In order to compare the model output values $\mathbf{x} := \left(x^{(N)}, x^{(P)}, x^{(Z)}, x^{(D)}\right)^\top$ to the given measurement data $\mathbf{x}^{(obs)} := \left(x^{(N,obs)}, x^{(P,obs)}, x^{(Z,obs)}, x^{(D,obs)}\right)^\top$, the actual model output $\mathbf{x}$ is transformed to aggregated values denoted by $\bar{\mathbf{x}} := \left(\bar{x}^{(N)}, \bar{x}^{(P)}, \bar{x}^{(Z)}, \bar{x}^{(D)}\right)^\top$, which are commensurable with the given measurements data (see, section 2.1, Paper 1 (Appendix *A*.1)).

We demonstrate that the LQOC method can be applied to the considered parameter op-

timization for a non-linear NPZD model using a linearization technique around reference trajectories of model variables and parameters (Papers 1 (Appendix A.1)). The obtained linearized model gives a very good model-data fit with almost perfect annually periodic parameters (Figure 2 and Figure 6 in Paper 1 (Appendix A.1)). Even with the available small number of observational data typical to oceanographic time series sites, the quality of the fit is very high. Specifically, it is much better than the one previously obtained by optimization of the non-linear model with fixed model parameters (Optimization with a Sequential Quadratic Programming (SQP), Figure 2 in Papers 1 (Appendix A.1)). Even substantial concentration changes that occur between some neighboring observational data points (e.g., for $\bar{x}^{(N)}$, in 1994, 1995 or 1997, Figure 2 in Paper 1 (Appendix A.1)) can be captured by the optimized trajectory.

Furthermore, to assess the goodness of the periodic parameters $(\mathbf{u}_k^*)_{k\in[N-1]}$ obtained by applying the LQOC method, a validation experiment will be performed. We run the original non-linear model (5.1) using these parameters without further optimization. The use of periodic parameters in comparison to constant parameters results in a significantly better model-data fit. The results for $\bar{x}^{(P)}$ and $\bar{x}^{(D)}$ are almost perfect, whereas for the other two tracers they are slightly worse (Figure 8 in Paper 1 (Appendix A.1)). The quality of the obtained periodic parameters depends on the length of the time intervals $T_{j,i}$ on which the linearization is applied. If no data are available as reference $\mathbf{x}_k^{(ref)}$, these intervals have to be enlarged, which presumably will reduce the quality of the optimized parameters. This in turn will influence the quality of the validation. Moreover, to allow for a quantitative comparison between our results and those obtained with constant parameters by Rückelt et al. (2010), we give the corresponding values of the original cost function (Section 2.2, Eq. 4 and Table 3 in Paper 1 (Appendix A.1)).

With regard to the application of the LQOC method on the NPZD model, two important points should be mentioned:

- Suppose, we have many measurement data per year. Then, we obtain a series $(T_{j,i})_{\substack{i=0,\ldots,\widetilde{n}_j,\\ j=1,\ldots,j_{max}}}$ of very small intervals between subsequent measurement data. This leads to better results, i.e., the obtained linearized model gives even higher model-data fit. The same will also hold for the original nonlinear model using the obtained periodic parameters.

- Suppose, we would not restrict ourselves to periodic parameters but use general time-dependent parameters. Then the linearization of the NPZD model on each interval $T_{j,i}$, $i = 0, \ldots, \widetilde{n}_j, j = 1, \ldots, j_{max}$ will be done about the operating points $\mathbf{x}_{j,i+1}^{(obs)}$, $i = 0, \ldots, \widetilde{n}_j$, $j = 1, \ldots, j_{max}$. Furthermore, throughout the application of the closed loop discrete-time linear quadratic optimal control, the controller leads the system from any given initial state to a fixed final state denoted by $\mathbf{x}_{j,i+1}^{(obs)}$,

$i = 0, \ldots, \widetilde{n}_j, j = 1, \ldots, j_{max}$. Thus, the model-data-fit would be closer to perfect for both the obtained linearized model and the original nonlinear model. The disadvantage of this application lies in the fact that the validation experiment will be available only for the years, in which we have applied the optimization method, i.e., we run the original nonlinear model using the obtained parameter set $(\mathbf{u}_k^*)_{k\in[M-1]}$. It is impossible to run them for an indefinite year. On the contrary, with periodic parameters $(\mathbf{u}_k^*)_{k\in[N-1]}$, one can do the validation experiment for all years.

Extended Kalman Filter

In this section, we investigate the application of the extended Kalman filter (EKF) to achieve a computationally efficient state estimation of the NPZD model. Again, in order to initially verify the approach, we first apply the EKF with model-generated measurement data $\mathbf{y}_k = (y_k^{(N)}, y_k^{(P)}, y_k^{(Z)}, y_k^{(D)})^\top$. The main goal here is to compare the estimated state $\mathbf{x}^a := (\mathbf{x}_k^a)_{k\in[1,M]}$ that is obtained by applying the EKF with periodic parameters which are obtained by using the LQOC method with the estimated state $\widetilde{\mathbf{x}}^a := (\widetilde{\mathbf{x}}_k^a)_{k\in[1,M]}$ that is obtained by applying the EKF with constant parameters which are obtained by using the SQP method. Our approach to apply the EKF to the NPZD model is as follows. We start with the discretized scheme of the NPZD model

$$\begin{aligned}
\mathbf{x}_{k+1} &= F(\mathbf{x}_k, \mathbf{u}_k) + \mathbf{q}_k, \forall k \in [M-1],\\
\mathbf{x}_1 &= \mathbf{x}_1^*, \text{ the given initial value},\\
\mathbf{y}_k &= \mathbf{C}\mathbf{x}_k + \boldsymbol{\epsilon}_k, \forall k \in [M-1],
\end{aligned}$$

where

$$\begin{aligned}
F(\mathbf{x}_k, \mathbf{u}_k) &:= [\mathbf{I}_n - \Delta t \widetilde{H}_k^{\text{diff}}]^{-1}[\mathbf{I}_n + \Delta t \widetilde{H}^{\text{sink}}]\mathcal{L}_k \circ \mathcal{L}_k \circ \mathcal{L}_k \circ \mathcal{L}_k(\mathbf{x}_k, \mathbf{u}_k),\\
\mathbf{C} &:= \begin{bmatrix} \mathbf{I}_m & 0 & 0 & 0 \\ 0 & 1.59.\mathbf{I}_m & 0 & 0 \\ 0 & 0 & \mathbf{I}_m & 0 \\ 0 & \mathbf{I}_m & \mathbf{I}_m & \mathbf{I}_m \end{bmatrix},\\
\mathbf{q}_k &\simeq \mathcal{N}(0, \mathbf{Q}_k),\\
\epsilon_k &\simeq \mathcal{N}(0, \mathbf{R}_k).
\end{aligned}$$

Remark 3. *The main objective here is to examine how the state estimation is influenced by the parameters used in the EKF approach. To satisfy this purpose, two types of assimilation experiments with model-generated data are conducted.*

We first apply the EKF with periodic parameters $\mathbf{u} = (\mathbf{u}_k)_{k\in[1,M-1]}$ *which are obtained by using the LQOC method:*

$$\begin{aligned} \mathbf{x}_{k+1} &= F(\mathbf{x}_k, \mathbf{u}_k) + \mathbf{q}_k, \forall k \in [M-1], \\ \mathbf{x}_1 &= \mathbf{x}_1^*, \text{ the given initial value}, \\ \mathbf{y}_k &= \mathbf{C}\mathbf{x}_k + \boldsymbol{\epsilon}_k, \forall k \in [M-1]. \end{aligned} \tag{5.11}$$

On the other hand, we apply the EKF with constant parameters $\widetilde{\mathbf{u}}^*$ *which are obtained by using the SQP method:*

$$\begin{aligned} \mathbf{x}_{k+1} &= F(\mathbf{x}_k, \widetilde{\mathbf{u}}^*) + \mathbf{q}_k, \forall k \in [M-1], \\ \mathbf{x}_1 &= \mathbf{x}_1^*, \text{ the given initial value}, \\ \mathbf{y}_k &= \mathbf{C}\mathbf{x}_k + \boldsymbol{\epsilon}_k, \forall k \in [M-1]. \end{aligned} \tag{5.12}$$

We point out that the matrix $\mathbf{C}$ *does not imply that all states are available. But in our case, we only want to examine how quickly estimated states converge to the true state* $\mathbf{x}$*. Regarding this matter, we compare both estimated states* $\mathbf{x}^a$ *(obtained by model (5.11)) and* $\widetilde{\mathbf{x}}^a$ *(obtained by model (5.12)) under the same precondition (the same process noise vector* $\mathbf{q}$ *and Measurement noise vector* $\boldsymbol{\epsilon}$*). For this purpose and for simplicity, the matrix* $\mathbf{C}$ *is chosen such that all states are available. This section is a motivation for the application of the EKF on the NPZD model with real data.*

For our test with the model-generated measurement data $\mathbf{y}_k$, the matrix $\mathbf{C}$ produced by:

$$\begin{aligned} y_k^{(N)} &:= x_k^{(N)}, \\ y_k^{(P)} &:= 1.59.x_k^{(P)}, \\ y_k^{(Z)} &:= x_k^{(Z)}, \\ y_k^{(D)} &:= x_k^{(P)} + x_k^{(Z)} + x_k^{(D)}. \end{aligned}$$

As mentioned above, we test the extended Kalman filter approach by using synthetic data (model-generated measurement data). The model noise covariance matrices $\mathbf{Q}_k$ and the measurement noise covariance matrices $\mathbf{R}_k$ are calculated by using the standard deviation (Table 2 in Paper 2 (Appendix *A*.2)).
First, we assume that the optimal periodic parameters $\mathbf{u}^* = (\mathbf{u}_k^*)_{k\in[N-1]}$ obtained by applying the LQOC and the optimal constant parameters $\widetilde{\mathbf{u}}^*$ obtained by applying the SQP method are available.

We outline the EKF equations for both cases:

- compute the next predicted state (the a priori state)
  - for the estimation state with optimal periodic parameters

$$\begin{aligned}\mathbf{x}_{k+1}^{f} &= F(\mathbf{x}_{k}^{a}, \mathbf{u}_{k}^{*}), \quad k \in [M-1] \\ \mathbf{x}^{a} &= E[\mathbf{x}_1]\end{aligned}$$

  - for the estimation state with optimal constant parameters

$$\begin{aligned}\widetilde{\mathbf{x}}_{k+1}^{f} &= F(\widetilde{\mathbf{x}}_{k}^{a}, \widetilde{\mathbf{u}}^{*}), \quad k \in [M-1] \\ \widetilde{\mathbf{x}}^{a} &= E[\mathbf{x}_1]\end{aligned}$$

- compute the next predicted error covariance
  - for the estimation state with optimal periodic parameters

$$\begin{aligned}\mathbf{P}_{k+1}^{f} &= \mathbf{A}_k \mathbf{P}_{k}^{a} \mathbf{A}_{k}^{\top} + \mathbf{Q}_k, \quad k \in [M-1] \\ \mathbf{A}_k &:= \mathcal{D}_x F(\mathbf{x}_{k}^{a}, \mathbf{u}_{k}^{*}), \quad k \in [M-1]\end{aligned}$$

  - for the estimation state with optimal constant parameters

$$\begin{aligned}\widetilde{\mathbf{P}}_{k+1}^{f} &= \widetilde{\mathbf{A}}_k \widetilde{\mathbf{P}}_{k}^{a} \widetilde{\mathbf{A}}_{k}^{\top} + \mathbf{Q}_k, \quad k \in [M-1] \\ \widetilde{\mathbf{A}}_k &= \mathcal{D}_x F(\widetilde{\mathbf{x}}_{k}^{a}, \widetilde{\mathbf{u}}^{*})\end{aligned}$$

- obtain measurements $\mathbf{y}_{k+1}$
- calculate the Kalman gain
  - for the estimation state with optimal periodic parameters

$$\mathbf{G}_{k+1} = \mathbf{P}_{k+1}^{f} \mathbf{C} \left(\mathbf{C} \mathbf{P}_{k+1}^{f} \mathbf{C}^{\top} + \mathbf{R}_{k+1} \right)^{-1}, \quad k \in [M-1]$$

  - for the estimation state with optimal constant parameters

$$\widetilde{\mathbf{G}}_{k+1} = \widetilde{\mathbf{P}}_{k+1}^{f} \mathbf{C} \left(\mathbf{C} \widetilde{\mathbf{P}}_{k+1}^{f} \mathbf{C}_{k+1}^{\top} + \mathbf{R}_{k+1} \right)^{-1}, \quad k \in [M-1]$$

- update the a posteriori state
  - for the estimation state with optimal periodic parameters

$$\mathbf{x}_{k+1}^{a} = \mathbf{x}_{k+1}^{f} + \mathbf{G}_{k+1} \left(\mathbf{y}_{k+1} - \mathbf{C} \mathbf{x}_{k+1}^{f} \right), \quad k \in [M-1]$$

– for the estimation state with optimal constant parameters

$$\widetilde{\mathbf{x}}^a_{k+1} = \widetilde{\mathbf{x}}^f_{k+1} + \widetilde{\mathbf{G}}_{k+1}\left(\mathbf{y}_{k+1} - \mathbf{C}\widetilde{\mathbf{x}}^f_{k+1}\right), \quad k \in [M-1]$$

In order to compare the assimilation with optimal periodic parameters to the assimilation with optimal constant parameters, we perform two different data assimilation experiments. We calculate the model and measurement noise covariance matrices and, additionally, we investigate the impact of noise in the data used for the assimilation of the system. For this purpose, we conduct two types of assimilation experiments. First, we assume that the entries of the measurement covariance matrix have very small values compared to the model covariance matrix. In a second experiment, a low model noise compared to the measurement noise is investigated.
For all experiments mentioned above, we demonstrate that the obtained estimated model output is closer to the measurements if periodic parameters instead of constant parameters are used in the assimilation scheme. Furthermore, we assess the data-fit quality of the estimated model output by calculating statistical metrics of the model/data (Paper 2 (Appendix *A*.2)).

Open Loop Discrete Linear Quadratic Optimal Control

In this section, the Discrete Open Loop Optimal Control (DOLOC) will be discussed (the method is outlined in Paper 3 (Appendix A.3)). We investigate the applicability of this approach to analyze the impact of the linearization scheme on the model-data fit of the nonlinear NPZD model. The idea of this method is to first obtain a linear equation system as (5.2). To achieve this, we introduce a linearization about a given reference trajectories of the discretized scheme of the NPZD model (5.1). On one hand, the reference trajectory for the state variable will be based on available real measurement data. On the other hand, it will be based on synthetic data, which is substituted by model results, that were produced with a reference parameter set ($\mathbf{u}_0$) (model-generated measurements data). Then, we apply the DOLOC method for the two linearization schemas, this yields us two periodic parameter sequences $(\mathbf{u}_k)_{k\in[N-1]}$ and $(\bar{\mathbf{u}}_k)_{k\in[N-1]}$. Then, a validation experiment employing the two optimized periodic parameter sequence in the original non-linear NPZD model will be introduced.
For the first case, we use the same strategy as for the closed loop method. For the second case, the model-generated measurement data is given for all $k \in [M]$ (five years). The following strategy will be used:

- For the first year ($j = 1$)

– The reference trajectories for the state and the control vector are defined as

$$\begin{aligned}\mathbf{u}^{(ref)} &:= \mathbf{u}_0,\\ \mathbf{x}_k^{(ref)} &:= \mathbf{x}_k^{synt}, \forall\, k \in [N].\end{aligned}$$

– The linearized state equation reads

$$\begin{aligned}\widetilde{\mathbf{x}}_{k+1} &= \widetilde{\mathbf{A}}_k\widetilde{\mathbf{x}}_k + \widetilde{\mathbf{B}}_k\widetilde{\mathbf{u}}_k, \quad \forall\, k \in [N-1],\\ \widetilde{\mathbf{x}}_1 &= \bar{\mathbf{x}}_1 - \mathbf{x}_1^{(ref)},\end{aligned}$$

where

$$\begin{aligned}\widetilde{\mathbf{A}}_k &:= [\mathbf{I}_n - \Delta t\widetilde{H}_k^{\text{diff}}]^{-1}[\mathbf{I}_n + \Delta t\widetilde{H}^{\text{sink}}]\mathbf{A}_k, \qquad \mathbf{A}_k := \mathcal{D}_x G(\mathbf{x}_k^{(ref)}, \mathbf{u}_0),\\ \widetilde{\mathbf{B}}_k &:= [\mathbf{I}_n - \Delta t\widetilde{H}_k^{\text{diff}}]^{-1}[\mathbf{I}_n + \Delta t\widetilde{H}^{\text{sink}}]\mathbf{B}_k, \qquad \mathbf{B}_k := \mathcal{D}_u G(\mathbf{x}_k^{(ref)}, \mathbf{u}_0),\\ \widetilde{\mathbf{x}}_k &:= \bar{\mathbf{x}}_k - \mathbf{x}_k^{(ref)}, \qquad\qquad\qquad\qquad \widetilde{\mathbf{u}}_k := \bar{\mathbf{u}}_k - \mathbf{u}_0.\end{aligned}$$

– Then, we apply the DOLOC method (Paper 3 (Appendix *A*.3)) to determine the model output vector $\bar{\mathbf{x}} := (\bar{\mathbf{x}}_k)_{k\in[N]}$ and model parameter vector $\bar{\mathbf{u}} := (\bar{\mathbf{u}}_k)_{k\in[N-1]}$.

- For all further years ($j = 2, \ldots, j_{max}$)

  – The reference trajectories for the state vector and the control vector are defined as

$$\begin{aligned}\mathbf{u}_k^{(ref)} &:= \bar{\mathbf{u}}_{k-N}, \quad \forall\, k \in \{(j-1)N+1, \ldots, jN-1\},\\ \mathbf{x}_k^{(ref)} &:= \bar{\mathbf{x}}_{k-N}, \quad \forall\, k \in \{(j-1)N+1, \ldots, jN\}.\end{aligned}$$

  – The linearized state equation reads

$$\begin{aligned}\widetilde{\mathbf{x}}_{k+1} &= \widetilde{\mathbf{A}}_k\widetilde{\mathbf{x}}_k + \widetilde{\mathbf{B}}_k\widetilde{\mathbf{u}}_k, \quad \forall\, k\{(j-1)N, \ldots, jN-1\},\\ \widetilde{\mathbf{x}}_{(j-1)N} &= \bar{\mathbf{x}}_{(j-1)N} - \mathbf{x}_{(j-1)N+1}^{(ref)}, \text{the given initial state},\end{aligned}$$

  where

$$\begin{aligned}\widetilde{\mathbf{A}}_k &:= [\mathbf{I}_n - \Delta t\widetilde{H}_k^{\text{diff}}]^{-1}[\mathbf{I}_n + \Delta t\widetilde{H}^{\text{sink}}]\mathbf{A}_k, \qquad \mathbf{A}_k := \mathcal{D}_x\mathbf{h}(\mathbf{x}_k^{(ref)}, \mathbf{u}_k^{(ref)}),\\ \widetilde{\mathbf{B}}_k &:= [\mathbf{I}_n - \Delta t\widetilde{H}_k^{\text{diff}}]^{-1}[\mathbf{I}_n + \Delta t\widetilde{H}^{\text{sink}}]\mathbf{B}_k, \qquad \mathbf{B}_k := \mathcal{D}_u\mathbf{h}(\mathbf{x}_k^{(ref)}, \mathbf{u}_k^{(ref)}),\\ \widetilde{\mathbf{x}}_k &:= \bar{\mathbf{x}}_k - \mathbf{x}_k^{(ref)}, \qquad\qquad\qquad\qquad \widetilde{\mathbf{u}}_k := \bar{\mathbf{u}}_k - \mathbf{u}_k^{(ref)}.\end{aligned}$$

– Then, we apply the DOLOC method to determine the model output vector $\bar{\mathbf{x}} := (\bar{\mathbf{x}}_k)_{k\in\{N+1,\dots,M\}}$ and the parameter vector $\bar{\mathbf{u}} := (\bar{\mathbf{u}}_k)_{k\in\{N+1,\dots,M-1\}}$.

We point out that the main goal of this work (DOLOC, Paper 3 Appendix *A*.3) is to analyze the impact of the linearization scheme on the model-data-fit of the original nonlinear NPZD model. For this reason, we compute two periodic control sequences for both above defined linearization schemes, namely one sequence $(\mathbf{u}_k)_{k\in[N-1]}$ for the linearization about real measurements data and another sequence $(\bar{\mathbf{u}}_k)_{k\in[1,N-1]}$ for the linearization about synthetic data (model-generated measurements data).
As a validation experiment we run the original non-linear model using the obtained periodic parameters $(\mathbf{u}_k)_{k\in[N-1]}$ as well as $(\bar{\mathbf{u}}_k)_{k\in[N-1]}$ without further optimization.
We demonstrate that the use of periodic parameters obtained via linearization around measurement data results in a significantly better model-data fit than the use of periodic parameters obtained via linearization around synthetic data (Figure 5 in Paper 3 (Appendix A.3)). One can say that the use of measurement data in the linearization scheme makes sense, since the obtained periodic parameters have an impact not only on the linearized model, but also on the original nonlinear NPZD model. Moreover, though the periodic parameters obtained by using the synthetic data in the linearization scheme provides not very acceptable results, if we run the original nonlinear model using these parameters, but we can introduce periodic parameter optimization with variable coefficients and optimizing them may well be a starting point for further model development and improvement.

Summary and Outlook

The proposed methodologies in the framework of optimal control theory using Discrete Linear Quadratic Optimal Control with both closed loop and open loop and Kalman filter, turned out to have great potential for an enhancement and improvement of a climate model.

The here proposed work is devoted to the optimal control problem for a non-linear system. It is based on the results obtained for a typical marine ecosystem model, namely a one dimensional non-linear model of the NPZD type introduced by Oschlies and Garçon (1999). The primary question of this work was to study the impact of the time dependent parameters on the model-data fit. To achieve this, two parameter optimization methods, discrete linear quadratic optimal control with both closed loop (LQOC) and open loop (DOLOC), and a state estimation method (EKF), for specifying the influence of the periodic parameters have been considered. More precisely, the quality of the model fit to measurement data was not optimal and it was difficult to identify the parameters by optimization of the non-linear model with fixed model parameters. This reflect the aim to obtain a model that is applicable for arbitrary time intervals. This happens by the application of the linear quadratic optimal control (LQOC) method on the non-linear NPZD model.

In the first step, in order to apply the (LQOC) method, the linearization of the marine ecosystem model was essential. For this purpose, a reference trajectory of the model variables and the parameters was performed. The reference trajectory for the model variables was based on the available measurement data. The linearized model obtained in this gave a very good model-data fit with almost perfect annually periodic parameters. The obtained periodic parameters were used to improve the original non-linear model. Furthermore, the extended model was able to reproduce and predict the real data much better than the non-linear model with optimized constant parameters. Regarding the results obtained by the application of the (LQOC) method on the NPZD model, a better understanding of model deficiency should be contributed and eventually help to improve marine ecosystem models. In the second step, to verify the impact of the periodic parameters on the model-data fit, an extended Kalman filter method was used. The proposed method provided very reasonable results with the periodic parameters compared to those with fixed parameters.

In the third step, an application of open loop discrete linear optimal control (DOLOC) was used. The aim was to investigate the impact of the linearization scheme on the model-data fit of the original nonlinear NPZD model. For this purpose, a given synthetic data instead measurement data was used in the linearization scheme. The results of the model-data fit remained still better than the one previously obtained by optimization of the non-linear model with fixed model parameters. In contrast to the results obtained by using the measurement data in the linearization scheme, the extended model was not able to reproduce the real data in a better way. As a consequence the linearization scheme has an impact not only on the linearized model, but also on the original nonlinear model. This happens at the quality of the obtained parameters.

It can be concluded that the application of the proposed methodologies on different marine ecosystem model for constant-periodic parameters comparison studies will be useful to demonstrate the capabilities of the introduced approaches. On the other hand, further analysis of the temporal deviations of individual parameters about the annual mean may help making inferences about processes that the model cannot describe well when constant parameters are used.

APPENDIX

Biogeosciences, 10, 1–14, 2013
www.biogeosciences.net/10/1/2013/
doi:10.5194/bg-10-1-2013

Biogeosciences Open Access

Reducing the model-data misfit in a marine ecosystem model using periodic parameters and linear quadratic optimal control

M. El Jarbi[1], J. Rückelt[1], T. Slawig[1], and A. Oschlies[2]

[1]Institute for Computer Science, Cluster The Future Ocean, Christian-Albrechts Universität zu Kiel, 24098 Kiel, Germany
[2]Helmholtz Centre for Ocean Research Kiel (GEOMAR), 24148 Kiel, Germany

Correspondence to: M. El Jarbi (mej@informatik.uni-kiel.de)

Received: 12 July 2012 – Published in Biogeosciences Discuss.: 2 August 2012
Revised: 31 January 2013 – Accepted: 1 February 2013 – Published:

Abstract. This paper presents the application of the Linear Quadratic Optimal Control (LQOC) method to a parameter optimization problem for a one-dimensional marine ecosystem model of NPZD (N for dissolved inorganic nitrogen, P for phytoplankton, Z for zooplankton and D for detritus) type. This ecosystem model, developed by Oschlies and Garcon, simulates the distribution of nitrogen, phytoplankton, zooplankton and detritus in a water column and is driven by ocean circulation data. The LQOC method is used to introduce annually periodic model parameters in a linearized version of the model. We show that the obtained version of the model gives a significant reduction of the model-data misfit, compared to the one obtained for the original model with optimized constant parameters. The found inner-annual variability of the optimized parameters provides hints for improvement of the original model. We use the obtained optimal periodic parameters also in validation and prediction experiments with the original non-linear version of the model. In both cases, the results are significantly better than those obtained with optimized constant parameters.

1 Introduction

In this paper we present an application of the LQOC (Linear Quadratic Optimal Control) method on a parameter optimization in a marine ecosystem model. This method (see for example Kwakernaak and Sivan, 1972; Lewis and Syrmos, 1995) is a mathematical technique to compute time dependent parameters (in some applications also called controls) in linear dynamical systems. The key goal of the method is to minimize a given quadratic cost function subject to a linear system. For the cost function, a model-data fit in least-squares formulation can be used, and thus the method is applicable to parameter optimization or model calibration problems. The optimal time-dependent parameters are obtained via an algorithm that basically uses the system matrices of the underlying linear model. When applying the method to a non-linear dynamical system (as most marine ecosystem models), the linearization of the system is essential. For this purpose, a reference trajectory of model variables and parameters is needed, which can be based on observational data and parameter guesses. By an appropriate choice of the parameter trajectory, periodic parameters can be obtained. These can then be used to improve the original non-linear model.

Marine ecosystem models describe biogeochemical processes in the ocean and are used, e.g., for calculating the effect of marine photosynthesis on the global carbon cycle. Typically, such kind of models have several parameters, for example, growth and mortality rates for the different types of plankton taken into account. Since most of these parameters are not known exactly and are difficult to measure, parameter identification or estimation is an important tool to calibrate a model. Parameter identification or estimation is usually done by performing a parameter optimization in order to minimize the misfit between model output and given data, commonly represented by a least-squares type cost functional. Additionally, uncertainty estimates corresponding to data errors may be computed. A parameter optimization may improve a model's quality also to another extent: If a model still shows deficiencies after the parameters have been optimized, reasons other than inappropriate parameter values are likely to be responsible for remaining poor model behavior, see for

example Fasham and Evans (1995), Hurtt and Armstromg (1996), Fennel et al. (2001), Prunet et al. (1996).

The computational effort to perform such kind of optimization runs for the coupled system of ocean circulation and marine biogeochemistry that describes a marine ecosystem is quite high, especially in three space dimensions. Thus, several simplifications may be used: One of them is to compute the marine biogeochemistry in a so-called offline mode, i.e., to solve the transport equations for the tracers with precomputed ocean circulation fields (velocity, temperature, salinity) as forcing or input. Another approach is to use one-dimensional models, which simulate a single water column only. This simplification is motivated by the fact that most of the ecosystem processes (as for example growth and dying) are happening locally in space and that the main spatial interactions are vertical mixing and sinking of organic matter. Moreover, it has been shown that parameters obtained in a one-dimensional optimization can also be beneficial when used in three-dimensional computations, see Oschlies and Schartau (2005).

The motivation for this paper is based on the results obtained for a typical marine ecosystem model, namely an NPZD model (N for dissolved inorganic nitrogen, P for phytoplankton, Z for zooplankton and D for detritus) introduced in Oschlies and Garçon (1999). As was reported in several publications with different optimization algorithms, the quality of the model fit to observations was not optimal, and in some cases it was difficult to identify the parameters uniquely, see for example Ward (2009), Ward et al. (2010), Rückelt et al. (2010b). In most cases (and in all these studies), the parameters of the marine ecosystem models are assumed to be temporally constant. This reflects the aim to obtain a model that is applicable for arbitrary time intervals. In contrast, in our work we allow the parameters to vary temporally over the year while remaining periodic over all years of the considered time interval.

Our main research question is if such kind of relaxation is able to significantly improve the model-to-data fit. Eknes and Evensen (2002) and Schartau et al. (2001) have examined the possibility of using a sequential data assimilation method for state estimation in a biological model. On the other hand, there are several papers on parameter estimation only, see Schartau et al. (2001), Fasham and Evans (1995), Hurtt and Armstromg (1996), Fennel et al. (2001), Prunet et al. (1996), Matear (1995), Spitz et al. (1998). Work by Losa et al. (2003) combined state and parameter estimation using a sequential weak constraint parameter estimation in an ecosystem model. An example for time-dependent parameters is introduced in the work by Mattern (2012), where a statistical emulator technique to estimate time-dependent values for two parameters of a 3-dimensional biological ocean model is used. The author demonstrated that emulator techniques are valuable tools for data assimilation and for analyzing and improving biological ocean models. He also used temporally changing parameters, but without imposing annual periodicity.

We use the annual periodicity constraint on the parameters in order to allow for some temporal flexibility of the parameters but at the same time to retain the temporal universality of the optimized model, e.g., for application to time periods outside the range of observations. The LQOC used here does not require a prescribed periodic parameterization of the parameters, it will automatically generate an optimal periodic function for each parameter. Moreover, it allows to balance the two aims of a good model–data fit on one hand and parameter periodicity on the other by introducing weighting matrices.

We verify our approach in validation and prediction experiments employing the optimized periodic parameters in the original non-linear model.

The structure of the paper is as follows: in Sect. 2 we briefly describe the model, the data and the cost function which we use for optimization. In Sect. 3 we briefly describe the LQOC method and its application on the NPZD model. In Sect. 4 we present our results obtained by the LQOC method with respect to the quality of the model–data misfit and the periodicity of the parameters. We furthermore show results for validation and prediction with the original non-linear model using the optimized periodic parameters. Section 5 ends the paper with some conclusions.

2 Model equation and optimization problem

The model used here, as example, is a one-dimensional marine ecosystem model presented in Oschlies and Garçon (1999). It is of NPZD type, i.e., it simulates the interaction of dissolved inorganic nitrogen (N), phytoplankton (P), zooplankton (Z) and detritus (D), whose concentrations (in $\mathrm{mmol\,N\,m^{-3}}$) are denoted by the model variables $(y^l)_{l=\mathrm{N,\,P,\,Z,\,D}} =: \boldsymbol{y}$. These four variables are functions $y^l : [0, t_\mathrm{e}] \times [-H, 0] \to \mathbb{R}$ of space and time, with H denoting the depth of the water column and t_e the total integration time.

The model is then given as the following system of partial differential equations:

$$\frac{\partial y^l}{\partial t} = -\omega^l \frac{\partial y^l}{\partial z} + \frac{\partial}{\partial z}\left(\kappa \frac{\partial y^l}{\partial z}\right) + q^l(\boldsymbol{y}, \boldsymbol{u}), l = \mathrm{N, P, Z, D}, \quad (1)$$

here z denotes the vertical spatial coordinate. The q^l are the biogeochemical coupling terms which depend on space and time via light intensity and also on temperature, and on most of the parameters summarized in the vector $\boldsymbol{u}$.

In this spatially one-dimensional setting, the only physical process taken into account is vertical diffusion, which appears as a space and time-dependent mixing coefficient κ, taken (as well as temperature) from the Ocean Circulation and Climate Advanced Model OCCAM (see Sinha and Yool, 2006) in hourly profiles. The equation for detritus also contains a sinking term with constant speed $\omega^\mathrm{D} > 0$, which is also optimized as u_{12}, whereas $\omega^\mathrm{N} = \omega^\mathrm{P} = \omega^\mathrm{Z} = 0$ in

Eq. (1). In total, we have $p = 12$ parameters $\boldsymbol{u} = (u_1, \ldots, u_p)$ to be optimized.

The biogeochemical coupling (or source-minus-sink) terms are taken from Oschlies and Garçon (1999) and read

$$\begin{aligned} q^{\mathrm{N}}(\boldsymbol{y},\boldsymbol{u}) &= -\bar{J}(y^{\mathrm{N}})y^{\mathrm{P}} + u_4 y^{\mathrm{Z}} + u_{10} y^{\mathrm{D}}, \\ q^{\mathrm{P}}(\boldsymbol{y},\boldsymbol{u}) &= \bar{J}(y^{\mathrm{N}})y^{\mathrm{P}} - u_8 y^{\mathrm{P}} - G(u_6,u_7)y^{\mathrm{Z}}, \\ q^{\mathrm{Z}}(\boldsymbol{y},\boldsymbol{u}) &= u_1 G(u_6,u_7)y^{\mathrm{Z}} - u_4 y^{\mathrm{Z}} - u_9 y^{\mathrm{Z}^2}, \\ q^{\mathrm{D}}(\boldsymbol{y},\boldsymbol{u}) &= (1-u_1)G(u_6,u_7)y^{\mathrm{Z}} + u_9 y^{\mathrm{Z}^2} + u_8 y^{\mathrm{P}} - u_{10} y^{\mathrm{D}}. \end{aligned} \tag{2}$$

Here $\bar{J}$ is the daily averaged phytoplankton growth rate as a function of depth z and time t, and G is the grazing function:

$$\begin{aligned} \bar{J}(y^{\mathrm{N}}) &= \min\left(\bar{J}(z,t), u_2 c^T \tfrac{y^{\mathrm{N}}}{u_{12}+y^{\mathrm{N}}}\right), \\ G(u_6,u_7) &= \tfrac{u_7 u_6 y^{\mathrm{P}^2}}{u_7 + u_6 y^{\mathrm{P}^2}}. \end{aligned}$$

The circulation data (taken from an ocean model) are the turbulent mixing coefficient $\kappa = \kappa(z,t)$ and the temperature $T = T(z,t)$, which is used in the non-linear term c^T where $c = 1.066$ is kept constant. Table 1 lists the model parameters with their original symbols as in Oschlies and Garçon (1999). For more details see also Schartau and Oschlies (2003a).

2.1 Observational data and corresponding model output

The observational data used here, denoted by $\boldsymbol{y}^{\mathrm{obs}}$, is taken from the Bermuda Atlantic Time-series Study (called BATS) as a part of the US Joint Global Ocean Flux Study, see Michaels and Knap (1996).

The BATS data are provided by the Bermuda Biological Station for Research (BBSR) situated in the Atlantic Ocean, 700 miles from the East Coast of the US at coordinates 31° N 64° W (see http://bats.bios.edu/).

In this work, each observational data has to be compared to an equivalent value generated by the model. For this purpose, the model output is interpolated in time and space to match the observational data. In addition, some transformations have to be done: modeled zooplankton has to be integrated in space, and chlorophyll *a* values are calculated by multiplying the nitrogen-based concentration of the modeled phytoplankton by a factor of 1.59 mg Chl/(mmol N), which corresponds to a chlorophyll to carbon mass ratio of 1 : 50 and a C : N mole ratio of 106 : 16. For more details see Ward (2009).

Summarizing, there are five types of observational data $\boldsymbol{y}^{\mathrm{obs}} := (y^{l,\mathrm{obs}})_{l=\mathrm{N,\,P,\,Z,\,D,\,PP}}$, which correspond to aggregated values $\bar{\boldsymbol{y}} := (\bar{y}^{l})_{l=\mathrm{N,\,P,\,Z,\,D,\,PP}}$ of the model output. The used data and their corresponding model variables are

1. Dissolved inorganic nitrogen $y^{\mathrm{N,\,obs}}$ (mmol m^{-3}) corresponding to model variable $y^{\mathrm{N}} =: \bar{y}^{\mathrm{N}}$.
2. Chlorophyll *a* $y^{\mathrm{P,\,obs}}$ (mg m^{-3}) corresponding to the scaled model variable $y^{\mathrm{P}}/1.59 =: \bar{y}^{\mathrm{P}}$.
   Here using a constant conversion factor of 1.59 mg (Chl *a*)/(mmol N).
3. Vertically integrated mesozooplankton biomass $y^{\mathrm{Z,\,obs}}$ (mmol m^{-2}) corresponding to

$$\int \frac{y^{\mathrm{Z}} - 0.096504}{1.2344}\,\mathrm{d}z =: \bar{y}^{Z}. \tag{3}$$

   Here, an additional assumption about the relation of mesozooplankton biomass $y^{\mathrm{Z,\,meso}}$ to total zooplankton biomass $\bar{y}^{Z}$ according to the formula

$$y^{\mathrm{Z}} = 1.2344 \cdot y^{\mathrm{Z,\,meso}} + 0.096504.$$

4. Particulate organic nitrogen $y^{\mathrm{D,\,obs}}$ (mmol N m^{-3}) corresponding to $y^{\mathrm{P}} + y^{\mathrm{Z}} + y^{\mathrm{D}} =: \bar{y}^{\mathrm{D}}$.
5. Carbon fixation or primary production (PP) as carbon uptake $y^{\mathrm{PP,\,obs}}$ in mmol C m^{-3} d^{-1}. As modeled primary production, the temporal mean of the model output y^{P} multiplied by the phytoplankton growth rate $\bar{J}(y^{\mathrm{N}})y^{\mathrm{P}}$.

2.2 The optimization problem

The aim of the optimization is to fit the model output $\bar{\boldsymbol{y}}$ that was aggregated, in the above mentioned way, to the given observational data $\boldsymbol{y}^{\mathrm{obs}}$ over a chosen time interval of $j_{\max}$ years. We denote by $N_{l,j}$ the number of observational data for $y^{l,\mathrm{obs}}$ for each observed quantity $l = \mathrm{N, P, Z, D, PP}$ in year $j = 1, \ldots, j_{\max}$. These numbers may be different for each l and j. The i-th observational in year j of $y^{l,\mathrm{obs}}$ is denoted by $y^{l,\mathrm{obs}}_{j,i}$, and the corresponding aggregated model output value by $(\bar{y}^{l}_{j,i})$. We now firstly compute the averaged annual misfit per model output/tracer, weighted using the inverse of the standard deviations taken from Schartau and Oschlies (2003a) and summarized in the vector

$$\sigma = (\sigma_l)_{l=\mathrm{N,\,P,\,Z,\,D,\,PP}} = (0.1, 0.01, 0.01, 0.0357, 0.025),$$

and by the number $N_{l,j}$ of observational per tracer and year:

$$F_{l,j} := \sum_{i=1}^{N_{l,j}} \frac{(\bar{y}^{l}_{j,i} - y^{l,\mathrm{obs}}_{j,i})^2}{\sigma_l^2 N_{l,j}},\ l = \mathrm{N, P, Z, D, PP},\ j = 1, \ldots, j_{\max}.$$

If there are no observational data for a state variable/tracer in a year (i.e., $N_{l,j} = 0$), the sum is set to zero. The overall cost function is then calculated as

$$F = \frac{1}{N_{\mathrm{total}}} \sum_{j=1}^{j_{\max}} \sum_{l=N}^{\mathrm{PP}} F_{l,j}, \tag{4}$$

where N_{total} is the total number of non-zero terms $F_{l,j}$ actually occurring in the sum. In the usual case we have $N_{\mathrm{total}} = 5 j_{\max}$. If ever $N_{l,j} = 0$ and thus $F_{l,j} = 0$ for a year and tracer, N_{total} is decreased accordingly.

Table 1. Parameters of the ecosystem model to be optimized with the LQOC method. Here $\boldsymbol{u}_0 = (u_{0,i})_{i=1,...,12}$ is the vector of parameters taken from Oschlies and Garçon (1999), $\min(u_i)$ and $\max(u_i)$ their respective upper and lower bounds used in Schartau and Oschlies (2003a).

Parameter	u_i	$u_{0,i}$	Units	$\min(u_i)$	$\max(u_i)$
Assimilation efficiency of zooplankton	γ_1	0.75		0.3	0.93
Growth rate parameter	a	0.6	day^{-1}	0.2	1.46
Initial slop of P-I Curve	α	0.025	$\mathrm{m}^2\,\mathrm{W}^{-2}\,\mathrm{d}^{-1}$	0.001	0.256
Zooplankton excretion	γ_2	0.03	day^{-1}	0.01	0.955
Light attenuation by phytoplankton	k_c	0.03	$\mathrm{m}^{-1}(\mathrm{mmol\,m}^{-3})^{-1}$	0.01	0.073
Pry capture efficiency	ϵ	1	$(\mathrm{mmol\,m}^{-3})^{-2}\,\mathrm{d}^{-1}$	0.025	1.6
Maximum grazing rate	g	2	d^{-1}	0.04	2.56
Specific mortality rate	μ_p	0.03	day^{-1}	0.01	0.635
Zooplankton quadratic mortality	μ_z	0.2	$(\mathrm{mmol\,m}^{-3})^{-1}\,\mathrm{d}^{-1}$	0.01	0.955
Remineralization rate parameter of detritus	μ_D	0.05	day^{-1}	0.02	0.146
Sinking velocity of detritus	w_s	5	$\mathrm{m\,day}^{-1}$	1	128
Half-saturation constant for N uptake rate	K_N	0.5	$\mathrm{mmol\,m}^{-3}$	0.1	0.730

3 Application of linear quadratic optimal control to the NPZD model

In this section we apply the LQOC method to the discretized version of the NPZD model. The LQOC method is widely used in engineering applications and well studied from the mathematical side, see e.g., Anderson and Moore (1971), Casti (1987), Lunze (1997), Sima (1996). Non-linear problems can be treated by linearization, see Clemens (1993).We present the details of the linearization and enforcement of the periodicity of the parameters.

3.1 Discretization scheme

We here give a brief description of the temporal and spatial discretization of the model equations described in Eq. (1). The vertical grid consists of 32 layers with thickness increasing with depth. In Rückelt et al. (2010a) it has already been demonstrated that, at least from the point of view of the optimization results, the vertical model grid can be reduced to this number instead of the originally employed 66. It has been demonstrated that optimization of the model yield practically identical results w.r.t. parameter match and quality of the optimal solution. Anyhow, the method used here can as well be applied for the original 66 layers.

The model is discretized in time using an operator splitting method: given a time-step size Δt (one hour in the model), the discretized scheme reads

$$[\mathbf{I} - \Delta t \mathbf{L}_k^{\mathrm{diff}}]\, \boldsymbol{y}_{k+1} = [\mathbf{I} + \Delta t \mathbf{L}_k^{\mathrm{sink}}] \mathcal{B}_k^q \circ \mathcal{B}_k^q \circ \mathcal{B}_k^q \circ \mathcal{B}_k^q (\boldsymbol{y}_k, \boldsymbol{u}_k), \quad k = 1, \ldots, M-1. \tag{5}$$

Here $\boldsymbol{y}_k = (y_k^\mathrm{N}, y_k^\mathrm{P}, y_k^\mathrm{Z}, y_k^\mathrm{D})$ is the vector of all four tracers and $\boldsymbol{u}_k$ the parameter vector (which is here already assumed to be time-varying), both at the current time step k. The total number of time steps is M. The matrices $\mathbf{L}_k^{\mathrm{diff}}$, $\mathbf{L}_k^{\mathrm{sink}}$ are 4×4 block-diagonal and represent the discretization of diffusion (discretized by second order central differences) and sinking (discretized by an upstream scheme), respectively, and $\mathbf{I}$ is the identity matrix.

The interpretation of the scheme (Eq. 5) is the following: In every time step $k \to k+1$, at first the non-linear coupling terms $\boldsymbol{q}_k = (q_k^\mathrm{N}, q_k^\mathrm{P}, q_k^\mathrm{Z}, q_k^\mathrm{D})$ are computed at every spatial grid point and integrated by four explicit Euler steps with step size $\frac{\Delta t}{4}$, each of which is described by the operator

$$\mathcal{B}_k^q(\boldsymbol{y}_k, \boldsymbol{u}_k) := \left[\mathbf{I} + \frac{\Delta t}{4} q_k(\boldsymbol{y}_k, \boldsymbol{u}_k)\right]. \tag{6}$$

Then, an explicit Euler step with full step-size Δt is formed for the sinking term, represented by the matrix $[\mathbf{I} + \Delta t \mathbf{L}_k^{\mathrm{sink}}]$. This matrix does only depend on the time step k if the sinking velocity w_s is to be optimized. Finally, an implicit Euler step is applied for the diffusion operator, discretized with second order central differences. Due to $\kappa = \kappa(z,t)$ the resulting matrix $[\mathbf{I} - \Delta t \mathbf{L}_k^{\mathrm{diff}}]$ depends on the current time step k.

The discrete system can now be formally written as

$$\begin{aligned} \boldsymbol{y}_{k+1} &= [\mathbf{I} - \Delta t \mathbf{L}_k^{\mathrm{diff}}]^{-1} [\mathbf{I} + \Delta t \mathbf{L}_k^{\mathrm{sink}}] \mathcal{B}_k^q \circ \mathcal{B}_k^q \circ \mathcal{B}_k^q \circ \mathcal{B}_k^q (\boldsymbol{y}_k, \boldsymbol{u}_k), \\ &=: f(\boldsymbol{y}_k, \boldsymbol{u}_k), \quad k = 1, ..., M-1, \end{aligned} \tag{7}$$

where f is a non-linear function.

3.2 Reference tracer trajectory

In order to apply the LQOC method to the discretized non-linear system (Eq. 7), we perform a linearization around reference trajectories of state $\boldsymbol{y}^{\mathrm{ref}}$ and control $\boldsymbol{u}^{\mathrm{ref}}$. The latter is described in Sect. 3.5. The relation between model variables and observational data described in Sect. 2.1 can be used to define the reference trajectory $\boldsymbol{y}^{\mathrm{ref}}$ as follows

1. $y^{\mathrm{N,\,ref}} := y^{\mathrm{N,\,obs}}$.
2. $y^{\mathrm{P,\,ref}} := y^{\mathrm{P,\,obs}} \cdot 1.59$.
3. $y^{\mathrm{Z,\,ref}}$ is taken as constant over the whole water column such that the integral equals the value of the

observational data $y^{\mathrm{Z,\,obs}}$ (which is a mean value). Here the formula (Eq. 3) is used.

4. $y^{\mathrm{D,\,ref}} := y^{\mathrm{D,\,obs}} - y^{\mathrm{Z,\,ref}} - y^{\mathrm{P,\,obs}}$.

Because the data for the different tracers are not given for the same instances of time, we only use those instances where data for all four tracers are available. Only for those instances reference values for all tracers can be computed by the above transformations. To describe this procedure, we define for every year $j = 1, \ldots, j_{\max}$:

- $N_{l,j}$: number of data for $y^{l,\mathrm{obs}}$, $l = \mathrm{N, P, Z, D}$.
- $y^{l,\mathrm{obs}}_{j,i}$: the i-th observational data, $i = 1, \ldots, N_{l,j}$.
- $t^{l}_{j,i}$: instance of time of $y^{l,\mathrm{obs}}_{j,i}$, $i = 1, \ldots, N_{l,j}$, rounded to an integer number.
- I_j: set of instances where data for all tracers are available:

$$I_j := \{t_{j,i}\}_{i=1,\ldots,N_j} := \bigcap_l \{t^l_{j,i}\}_{i=1,\ldots,N_{l,j}},$$

- N_j: number of elements in this intersection.

Because we have no reference value $\boldsymbol{y}^{\mathrm{ref}}$ at the end of each year, we use linear interpolation between the data $\boldsymbol{y}^{\mathrm{obs}}_{j,N_j}$ and $\boldsymbol{y}^{\mathrm{obs}}_{j+1,1}$ to generate such value, denoted by $\boldsymbol{y}^{\mathrm{ref}}_{j,N_j+1}$.

Since there are no data for every vertical layer, we additionally interpolate the data linearly in space to obtain a reference trajectory in every grid point.

3.3 Linearization

We apply the linearization on each time interval $[t_{j,i}, t_{j,i+1}]$ separately. For this purpose, we split the interval into sections of the length Δt (here $\Delta t = 1$ h), as shown in Fig. 1.

The discrete time steps τ_k in this interval are

$$\tau_{t_{j,i}} = t_{j,i},$$
$$\tau_{k+1} = \tau_k + \Delta t, \quad k = t_{j,i}, \ldots, t_{j,i+1}.$$

They correspond to the steps used in the temporal discretization, see Sect. 3.

Now we linearize the model around the data $\boldsymbol{y}^{\mathrm{ref}}_{j,i+1}$ and the parameter vector $\boldsymbol{u}^{\mathrm{ref}}_k$ (described below in Sect. 3.5). For this purpose, we introduce

$$\mathbf{A}_k := \frac{\partial f}{\partial \boldsymbol{y}}(\boldsymbol{y}^{\mathrm{ref}}_{j,i+1}, \boldsymbol{u}^{\mathrm{ref}}_k),$$
$$\mathbf{B}_k := \frac{\partial f}{\partial \boldsymbol{u}}(\boldsymbol{y}^{\mathrm{ref}}_{j,i+1}, \boldsymbol{u}^{\mathrm{ref}}_k),$$
$$b_k := f(\boldsymbol{y}^{\mathrm{ref}}_{j,i+1}, \boldsymbol{u}^{\mathrm{ref}}_k) - \boldsymbol{y}^{\mathrm{ref}}_{j,i+1},$$
$$\boldsymbol{x}_k := \boldsymbol{y}_k - \boldsymbol{y}^{\mathrm{ref}}_{j,i+1},$$
$$\boldsymbol{v}_k := \boldsymbol{u}_k - \boldsymbol{u}^{\mathrm{ref}}_k.$$

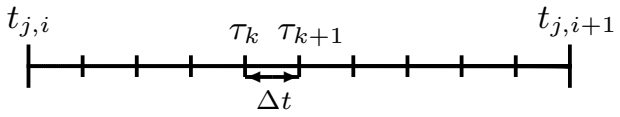

Fig. 1. Example for an interval on which the linearization is applied.

Here

- $\boldsymbol{x}_k \in \mathbb{R}^m$ is the deviation of the model output (i.e., all tracers over the whole water column) from the reference trajectory,
- $\boldsymbol{v}_k \in \mathbb{R}^p$ is the deviation of the actual parameters from the reference parameter trajectory.

The dimension m of $\boldsymbol{x}_k$ is determined by the number of tracers (in our case 4) and the numbers of grid cells in the water column (in our case 32), which results in $m = 4 \cdot 32$. The dimension p of $\boldsymbol{v}_k$ is determined by the number of model parameters, here $p = 12$.

The matrices $\mathbf{A}_k \in \mathbb{R}^{m\times m}$ and $\mathbf{B}_k \in \mathbb{R}^{m\times p}$ are called system matrix and input matrix, respectively. For this example, they were generated by Algorithmic or Automatic Differentiation (AD), see Griewank (2000). Here we used the software TAF (Transformations of Algorithms in Fortran), see Giering and Kaminski (1998).

Summarizing, the state equation reads

$$\boldsymbol{x}_{k+1} = \mathbf{A}_k \boldsymbol{x}_k + \mathbf{B}_k \boldsymbol{v}_k + b_k, \quad k = t_{j,i}, t_{j,i}+1, \ldots, t_{j,i+1}. \quad (8)$$

This is the typical form of a discrete linear system with state variable $\boldsymbol{x}_k$ and parameter (or control) $\boldsymbol{v}_k$.

3.4 Application of the LQOC theory

The theory of linear quadratic optimal control gives a formula for the optimal parameter trajectory $\boldsymbol{v}$ that minimizes the cost function

$$J(\boldsymbol{v}) = \frac{1}{2} \sum_{k=t_{j,i}}^{t_{j,i+1}} \boldsymbol{x}_k^\top \mathbf{Q}_k \boldsymbol{x}_k + \boldsymbol{v}_k^\top \mathbf{R}_k \boldsymbol{v}_k \quad (9)$$

under the constraint Eq. (8). Here for every k

- $\mathbf{Q}_k \in \mathbb{R}^{m\times m}$ is a positive semi-definite diagonal weighting matrix for the state vector,
- $\mathbf{R}_k \in \mathbb{R}^{p\times p}$ is a positive definite diagonal weighting matrix for the parameter vector.

The matrices $\mathbf{Q}_k$ and $\mathbf{R}_k$ are usually chosen to be diagonal. They reflect the relative importance of keeping tracer variables and parameters, respectively, close to their reference trajectories. In our case, this translates to quality of the model-to-data fit and periodicity of the parameters, see

the next subsection. Selecting large elements of either matrix will emphasize the corresponding effect.

At end of the optimization on all intervals $[t_{j,i}, t_{j,i+1}]$, $j = 1, \ldots, j_{\max}$, $i = 1, \ldots, N_j$, we obtain the optimal state variable and the optimal periodic parameters $(\boldsymbol{y}_k^*, \boldsymbol{u}_k^*)$, for $k = 1, \ldots, M-1$. The realization of the LQOC method is presented in algorithm 1.

3.5 Choice of the reference parameter trajectory

A main objective of this work is to enforce periodicity of the parameters. To obtain annually periodic parameters, we denote the length of a time period – which in our case is one year – measured in time steps by $T = t_{1,N_1+1}$. We now choose the reference trajectory for the parameter to be

$$\boldsymbol{u}_k^{\text{ref}} := \begin{cases} \boldsymbol{u}_0, & k \leq T \\ \boldsymbol{u}_{k-T}, & k > T. \end{cases} \tag{10}$$

Here $\boldsymbol{u}_0 \in \mathbb{R}^p$ is an initial guess, in our case we took the values from Oschlies and Garçon (1999), compare Table 1. These values are used in the first year ($k \leq T$) only. As a result, in the first year the choice of the cost function (Eq. 9) will force periodicity to the constant reference parameters. This effect can be reduced by choosing appropriate small values in the matrices $\mathbf{R}_k$ in the first year. In the following years, the difference of the current parameter $\boldsymbol{u}_k$ to its counterpart from the year before is minimized. This enforces periodicity. Thus the crucial point in adjusting the matrices $\mathbf{R}_k$ throughout an optimization run is to allow both:

- for sufficiently large deviation from the constant reference parameters in the first year, to enable their temporal variation,
- and for smaller deviation and thus more or less strict periodicity in the following years.

3.6 Particular choice of $\mathbf{Q}_k, \mathbf{R}_k$

In our example, the weighting matrices $\mathbf{Q}_k$ are taken as constant for all k, namely

$$\mathbf{Q}_k = \mathbf{Q} = \text{diag}(\frac{1}{\sigma_l^2})_{l=\text{N, P, Z, D, PP}}, \quad k = 1, \ldots, M,$$

where σ_l are the standard deviations taken from the original cost function (Eq. 4). The matrices $\mathbf{R}_k$ are taken as

$$\mathbf{R}_k = \text{diag}(r_n^k)_{n=1,\ldots,p}, \quad r_n^k > 0.$$

These values are chosen differently in the first year (on one hand) and in all subsequent years (on the other hand). In all years except the first one (i.e., $k \geq T$), the $\mathbf{R}_k$ are used to enforce periodicity of the parameters. The bigger the r_n^k for these years are, the better periodicity of the parameters is expected. Following this idea, the optimal choice for the $\mathbf{R}_k$ in the first year would be just zero matrices. But, by this choice, the requirements for the LQOC method and algorithm 1 – where the $\mathbf{R}_k$ have to be positive definite – are not satisfied. As a consequence, it is desirable to chose the r_n^k for the first year as small as possible.

On the other hand, the choice of the r_n^k in the first year can be used to keep the parameters in the admissible bounds: Since they can be forced to keep in the vicinity of the initial guess in the first year and to stay close due to the periodicity enforcement in the following years, by a careful setting of the r_n^k in the first year both aims (periodicity and boundedness) can be balanced. This effect is not guaranteed by the LQOC method, but turned out to be realizable in our case, see the next section.

Summarizing, for our computations we chose for $n = 1, \ldots, p$, the values

$$r_n^k = \begin{cases} \frac{1}{|(u_{0,n})|^2}, & k \leq T \\ \frac{1}{|(u_{k-T,n})|^2}, & k \geq T+1, \end{cases} \tag{11}$$

where $\boldsymbol{u}_0$ is as listed in Table 1.

4 Optimization results

In this section we present the results of the parameter optimization runs performed with the LQOC method. We show both the obtained fit of the linearized model output (with optimal parameters) to the data and the annual periodicity of the obtained parameters. Note that we only compare values of the original cost function F, the function J actually minimized in the LQOC setting is just a tool of the method.

4.1 Fit of linear model output to observational data

This section shows a comparison between the optimized model output, obtained by the LQOC method with periodic parameters, and the observational data. As a reference we also compare the results to those obtained by a direct optimization of the original non-linear model using constant parameters with a Sequential Quadratic Programming (SQP) method that takes into account parameter bounds. This method was used in Rückelt et al. (2010b).

Figure 2 shows the model results, obtained by the LQOC method with periodic parameters, for aggregated model output $\bar{\boldsymbol{y}}$ and the observational data $\boldsymbol{y}^{\text{obs}}$ for the years 1994 to 1998 for the uppermost layer at depths $z \approx 5\,\text{m}$. Shown are results for a part of the whole time interval at some distinct depth layers only. The total number of depth layers considered in the optimization process is 32 and the total number of time steps is 43 800. In contrast to the results obtained for constant model parameters with the original non-linear model, the LQOC method with periodic parameters gives a nearly perfect fit of the data. Even substantial concentration changes that occur between some neighboring observational data points (e.g., for $y^{\text{N, mod}}$, in 1994, 1995 or 1997) can be captured by the optimized trajectory. We performed the

Algorithm 1. Algorithm of the LQOC method.

for $j = 1, \ldots, j_{\max}$ **do**
for $i = 1, \ldots, N_j$ **do**

(a) Given the equation system as
$\boldsymbol{x}_{k+1} = \mathbf{A}_k \boldsymbol{x}_k + \mathbf{B}_k \boldsymbol{v}_k + b_k, \;\; k = t_{j,i}, t_{j,i}+1, \ldots, t_{j,i+1},$
and the cost function as
$J(\boldsymbol{v}) = \frac{1}{2} \sum_{k=t_{j,i}}^{t_{j,i+1}} \boldsymbol{x}_k^\top \mathbf{Q}_k \boldsymbol{x}_k + \boldsymbol{v}_k^\top \mathbf{R}_k \boldsymbol{v}_k.$

1. Solve the first matrix difference Riccati equation
$\mathbf{P}_k = \mathbf{Q}_k + \mathbf{A}_k^\top \mathbf{P}_{k+1} \mathbf{A}_k - \mathbf{A}_k^\top \mathbf{P}_{k+1} \mathbf{B}_k (\mathbf{R}_k + \mathbf{B}_k^\top \mathbf{P}_{k+1} \mathbf{B}_k)^{-1} \mathbf{A}_k \mathbf{B}_k^\top \mathbf{A}_k, \;\; k = t_{j,i+1}-1, \ldots, t_{j,i}$
with final condition $\mathbf{P}_{t_{j,i+1}} = \mathbf{Q}_{t_{j,i+1}}$.

2. Solve the second matrix difference Riccati equation
$\boldsymbol{h}_k = \mathbf{A}_k^\top (\mathbf{P}_{k+1} \boldsymbol{b}_k + \boldsymbol{h}_{k+1}) \mathbf{A}_k^\top \mathbf{P}_{k+1} \mathbf{B}_k (\mathbf{R}_k; + \mathbf{B}_k^\top \mathbf{P}_{k+1} \mathbf{B}_k)^{-1} \mathbf{B}_k^\top (\mathbf{P}_{k+1} \boldsymbol{b}_k + \boldsymbol{h}_{k+1}), \;\; k = t_{j,i+1}-1, \ldots, t_{j,i}$
with final condition $\boldsymbol{h}_{t_{j,i+1}} = 0$.

3. Solve the two auxiliary matrix difference equations
$\mathbf{K}_k = -(\mathbf{R}_k + \mathbf{B}_k^\top \mathbf{P}_{k+1} \mathbf{B}_k)^{-1} \mathbf{B}_k^\top \mathbf{P}_{k+1} \mathbf{A}_k, \;\; k = t_{j,i}, \ldots, t_{j,i+1}-1.$
$\mathbf{S}_k = -(\mathbf{R}_k + \mathbf{B}_k^\top \mathbf{P}_{k+1} \mathbf{B}_k)^{-1} \mathbf{B}_k^\top (\mathbf{P}_{k+1} \boldsymbol{b}_k + \boldsymbol{h}_{k+1}), \;\; k = t_{j,i}, \ldots, t_{j,i+1}-1.$

4. Compute the optimal state $\boldsymbol{y}_k^*$ from
$\boldsymbol{y}_{k+1}^* := \boldsymbol{x}_{k+1}^* + \boldsymbol{y}_{j,i+1}^{\mathrm{ref}}$
$= \boldsymbol{y}_{j,i+1}^{\mathrm{ref}} + (\mathbf{A}_k + \mathbf{B}_k K_k)(\boldsymbol{y}_k^* - \boldsymbol{y}_{j,i+1}^{\mathrm{ref}}) + \mathbf{B}_k \mathbf{S}_k, \;\; k = t_{j,i}, \ldots, t_{j,i+1}-1.$

5. Obtain the optimal parameters vector $\boldsymbol{u}_k^*$ from
$\boldsymbol{u}_k^* := \boldsymbol{v}_k + \boldsymbol{u}_k^{\mathrm{ref}}$
$= \boldsymbol{u}_k^{\mathrm{ref}} + \mathbf{K}_k (\boldsymbol{y}_k^* - \boldsymbol{y}_{j,i+1}^{\mathrm{ref}}) + \mathbf{S}_k, \;\; k = t_{j,i}, \ldots, t_{j,i+1}-1.$

end
end

optimization for the years 1994 to 1998, in contrast to the years 1991 to 1996 that were used in Rückelt et al. (2010b), since no zooplankton data are available at BATS for the years 1991 to 1993. This would be disadvantageous for the linearization procedure in the LQOC method.

In Rückelt et al. (2010b), a minimum value of the cost function (Eq. 4) of $F \approx 70$ was obtained for optimized constant parameters for the time 1991 to 1996. For the time 1994 to 1998, the value obtained by the SQP method and constant parameters is very similar. Also the quality of the fit – depicted in Fig. 2 – is comparable. The better fit obtained by the LQOC method also results in a significantly lower value ($F \approx 1.35$) of the original cost function (Eq. 4). Figure 3 shows the mismatch between model output and the reference data – which are interpolated values of the sparse observational data – for all points in time and space.

Figure 3 also shows – except for dissolved inorganic nitrogen $\bar{y}^{\mathrm{N}}$ – a better fit at the surface than in deeper layer. The possible reason for this is the lack of observational data on the lower layers, which requires interpolation over relatively large space intervals. Thus, the interpolation error there is bigger than in upper layers where the database is denser. This, naturally, affects the quality of the reference trajectory, and thus also of the linearized model and the obtained optimal parameters.

Figure 4 shows the LQOC results with periodic parameters and the observational data $\boldsymbol{y}^{\mathrm{obs}}$ for the years 1994 to 1998 for the lower layer at depths $z \approx 184.32$ m. Here the LQOC method with the periodic parameters provides a nearly perfect fit, in contrast to the one obtained with constant parameters.

4.2 Sensitivity with respect to the weighting matrices $\mathbf{R}_k$

To examine the effect of the weighting matrices $\mathbf{R}_k$ in the first year, on the behavior of the parameters and the cost function F, we have additionally performed sensitivity experiments with different entries r_i^k of the weighting matrices $\mathbf{R}_k$ for $k \leq T$. We present two additional experiments for $n = 1, \ldots, p$ with

$$r_n^k = \begin{cases} \frac{1}{|\min(\boldsymbol{u}_n)|^2}, & k \leq T \\ \frac{1}{|\max(\boldsymbol{u}_n)|^2}, & k \geq T. \end{cases}$$

The values of $\min(\boldsymbol{u}_n)$ and $\max(\boldsymbol{u}_n)$ are listed in Table 1. The corresponding values of the r_n^k for these two choices and the r_n^k from Eq. (11) (here called reference simulation) are shown

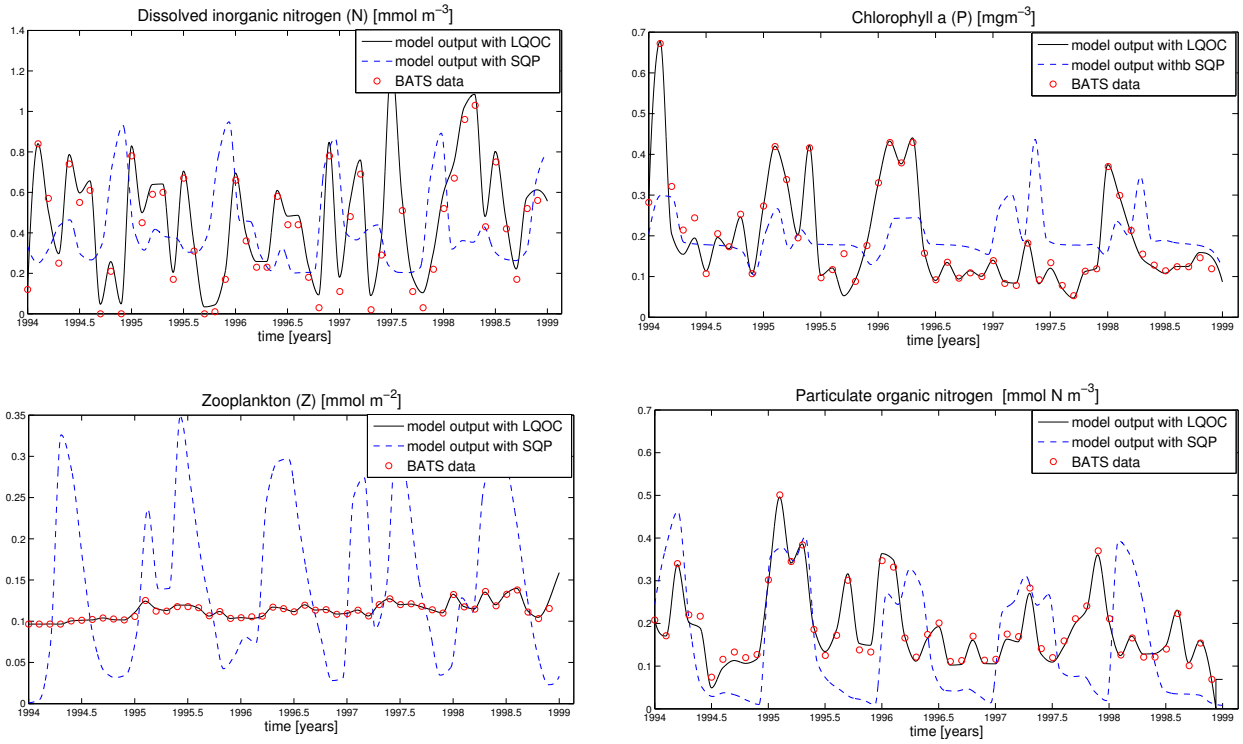

Fig. 2. Observational data $\boldsymbol{y}^{l,\mathrm{obs}}, l = \mathrm{N, P, Z, D}$, and aggregated model trajectories $\bar{\boldsymbol{y}}^{l}, l = \mathrm{N, P, Z, D}$, optimized with periodic parameters obtained by the LQOC method and with a sequential quadratic programming (SQP)method. Values are shown for the upper layer at depth $z \approx 5\,\mathrm{m}$ and years 1994–1998.

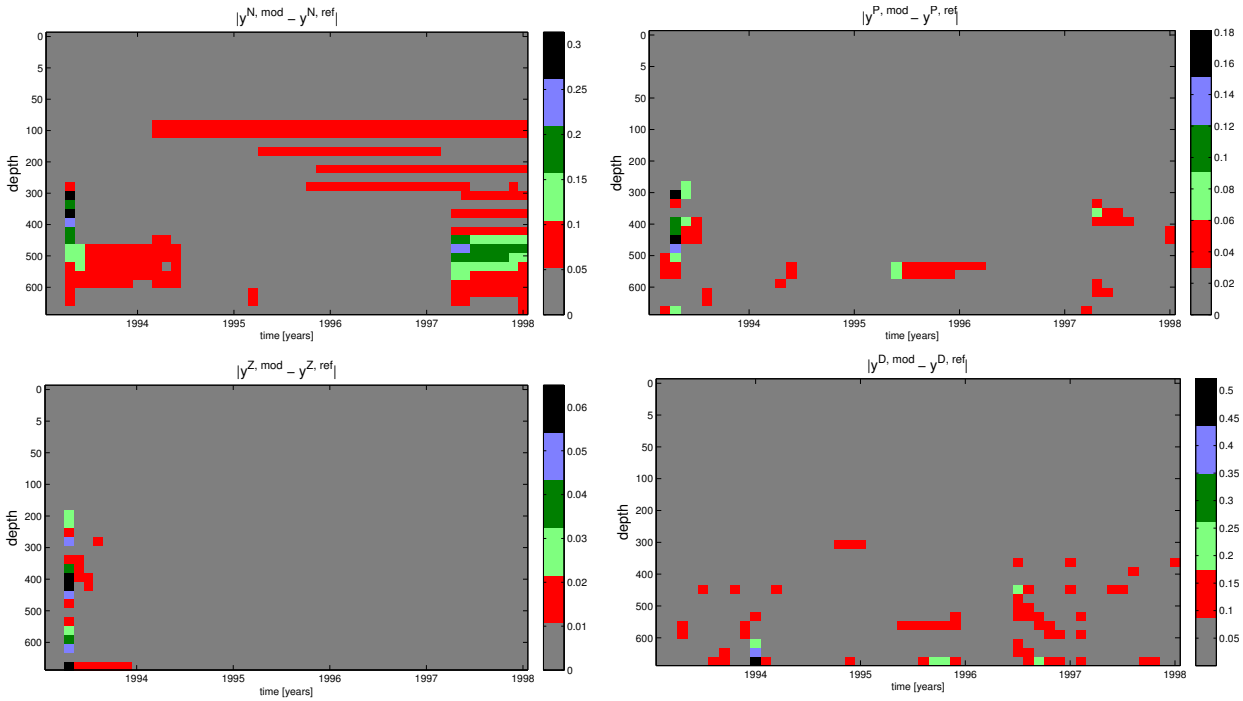

Fig. 3. Model-to-data misfit for four tracers with respect to space and time obtained by the LQOC method.

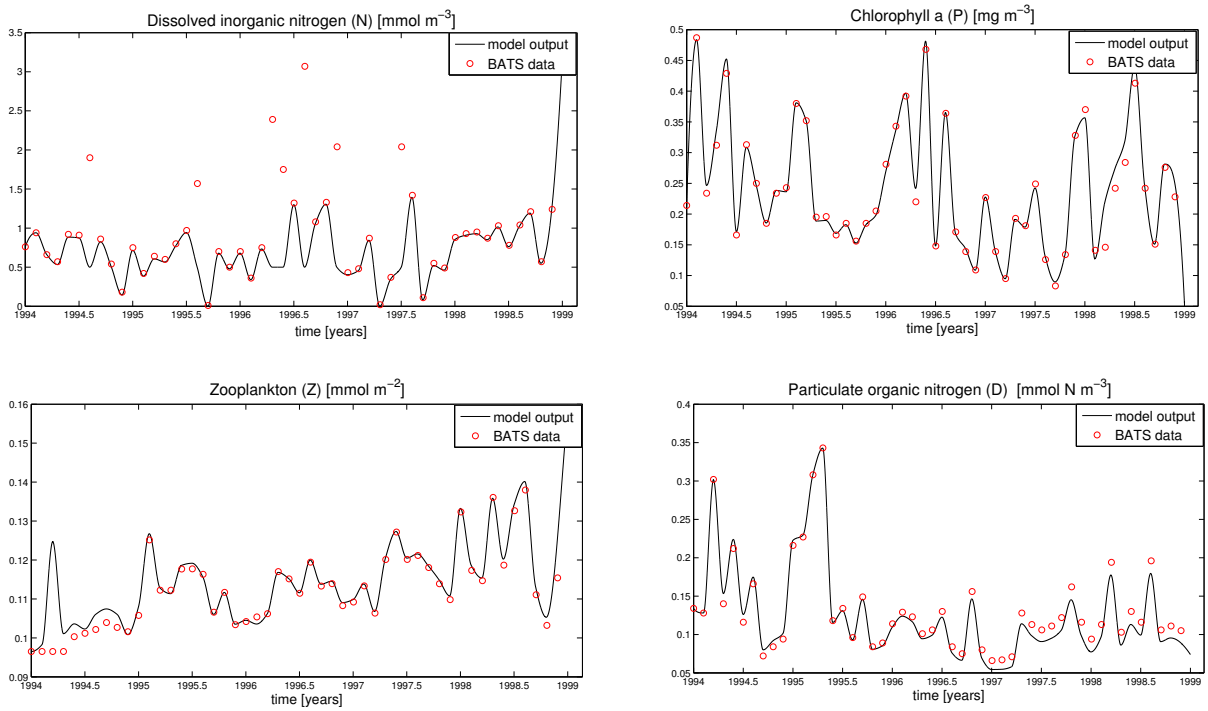

Fig. 4. Observational data $\boldsymbol{y}^{l,\mathrm{obs}}, l = \mathrm{N, P, Z, D}$, and aggregated model trajectories $\bar{\boldsymbol{y}}^{l}, l = \mathrm{N, P, Z, D}$, optimized with *periodic parameters obtained by the LQOC method*. Values are shown for the lower layer at depths $z \approx 184.32$ m.

in Table 2. The trajectories of the tracers $\boldsymbol{y}$, the parameters $\boldsymbol{u}$, and the value of the cost function F, depend heavily on the choice of the corresponding entries r_n^k in the matrix R_k. Figure 5 shows the trajectories for three tracers and different r_n^k. All experiments show only minor differences from the reference simulation with the r_n^k from Eq. (11). The results show that a decrease in the entry r_n^k can lead to a small decrease in the cost function. The sensitivities of the parameters with respect to the choice of r_n^k can be seen in Fig. 6. It is obvious that for smaller values of r_n^k the variability of the parameters is getting larger.

4.3 Periodicity of the parameters

In this section we show that the above model-to-data fit can be achieved with parameters that are almost annually periodic. Enforcement of periodicity was achieved by an appropriate adjustment of the matrices $\mathbf{R}_k$ in the cost function (Eq. 9) used in the LQOC framework, see Sect. 3. It was also possible to keep the parameters in their desired bounds (see Table 1), although the LQOC method does not to impose these bounds explicitly.

Figures 6 illustrates the temporal behavior of the parameters that were optimized with the LQOC method. Depicted are only the ten that show a temporal variation. Two parameters remain constant in time. These figures show different trajectories for each parameter for two years with the different choices of the r_n^k, compare Table 2. As mentioned above,

Table 2. Values of r_i^n for the reference simulation (second column) and the two additional sensitivity experiments.

i	$r_i^n = \frac{1}{\lvert(u_{0,i})\rvert^2}$	$r_i^n = \frac{1}{\lvert\min(u_i)\rvert^2}$	$r_i^n = \frac{1}{\lvert\max(u_i)\rvert^2}$
1	1.77	11	1.15
2	2.77	25	0.469
3	1600	10^4	15.25
4	1111	10^4	1.09
5	1111	10^4	187
6	1	1600	0.39
7	0.25	625	0.152
8	1111	10^4	42.48
9	25	10^4	1.09
10	400	2500	46
11	0.04	1	6.101^{-5}
12	4	100	1.876
cost F see Eq. (4)	1.35	1.9	0.95

it is obvious that for a smaller r_n^k, the amplitude of the parameters increases, but it always remains almost periodic. Since the periodicity of the parameters is nearly perfect, then it is enough to plot for 2 yr.

The parameters controlling growth of phytoplankton, namely the maximum growth rate a and the initial slope of the P-I curve α, show in Fig. 6 both maximum values in early summer and in winter, with a clear minimum value

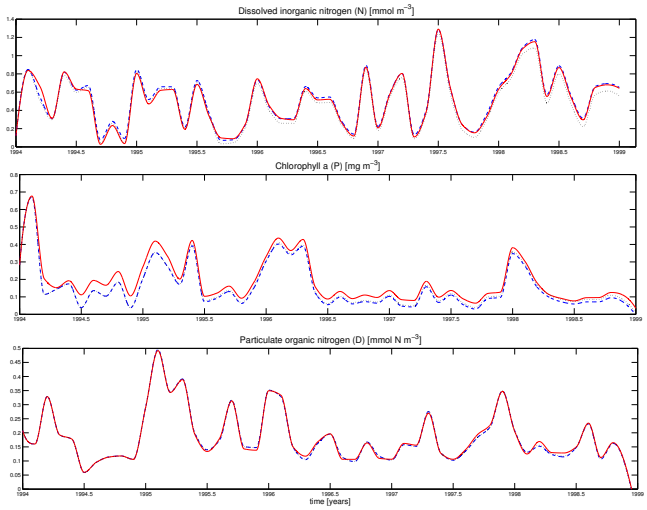

Fig. 5. Model output trajectories with different r_n^k, the reference simulation (dashed), with larger r_n^k (solid) and with smaller r_n^k (dotted) for the upper layer at depth $z \approx 5$ m and years 1994–1998.

in spring during the peak of the annual chlorophyll signal. This is consistent with earlier assimilation studies that, for assumed constant parameters, tended to overestimate plankton production at BATS during the bloom end of winter and, at the same time, tended to underestimate production in oligotrophic summer conditions and in early winter, see Schartau et al. (2001). Such a trend to relatively high values of α has also been found in earlier studies that optimized parameter values by data assimilation, see Fasham and Evans (1995), Schartau et al. (2001). Earlier studies assuming time-independent parameter values have attributed relatively high values of α to the absence of a dial cycle in the turbulent mixing, which might allow for substantial phytoplankton growth even in winter during reduced daytime mixing, see Schartau and Oschlies (2003a). This is consistent with the findings of the current study, that also suggest high values of α during the period of deep mixing in winter. In addition, our optimized model predicts even higher values of the initial slope parameters α for late spring and early summer, where the mixed layer is usually shallow and growth is limited by nutrients rather than light in the surface mixed layer. A large value of α can, however, help to establish a subsurface chlorophyll maximum in better agreement with the observations. This was also noted by Schartau and Oschlies (2003b). Our results reported here indicate that high values of α may, at BATS, be more important for the establishment of the deep chlorophyll in late spring than for the maintenance of phytoplankton production during periods of deep mixing in winter. Maintenance of high primary production during summer has been difficult to achieve by earlier models run at BATS (Schartau et al., 2001). As nutrient supply to the surface waters is low during the stratified season, models with fixed carbon-to-nutrient stoichiometry and constant model parameters do not seem to be able to reach observed levels of primary production in the surface layer, see Schartau and Oschlies (2003b). In the current study, the carbon-to-nutrient factor used to convert simulated (nitrogen-based) primary production to observed (carbon-based) primary production is constant as well. However, the seasonally varying parameters can contribute to maintain high levels of primary production during summer in the absence of substantial inputs of new nutrients. This is realized by enhanced recycling of biomass, evident by high maximum grazing rates, high assimilation efficiencies, high prey capture efficiencies and high zooplankton excretion in late spring and early summer. Similarly, remineralization of detritus is highest in late spring as well. These high rates all contribute to fast recycling of nutrients in the surface ocean, which helps to maintain observed high rates of primary production and thereby reduces the model–data misfit function. The relative deviations of the calculated parameters are shown in Fig. 7.

4.4 Validation of the non-linear model with periodic parameters

In this section, the periodic parameters obtained by the LQOC method are used in a validation experiment using the original non-linear NPZD model. We run the original non-linear model using these parameters without further optimization for the years 1994 to 1998 and analyze the corresponding model–data misfit.

Figure 8 shows a comparison of the model output using optimal periodic parameters and optimal constant parameters (obtained by the SQP method), as well as the observational data in the uppermost layer. The use of periodic parameters in comparison to constant parameters results in a significantly better model–data fit. The results for y^{P} and y^{D} are almost perfect, whereas for the other two tracers they are slightly worse. The results look similar for all layers.

In order to allow for a quantitative comparison between our results and those obtained with constant parameters by Rückelt et al. (2010b), we give the corresponding values of the original cost function (Eq. 4) in Table 3. The better fit with periodic parameters also results in a significantly reduced value $F \approx 15.05$ of the cost function (Eq. 4). We are not able to obtain the same value of the cost function as with the linearized model, see Sect. 4.1, which is reasonable since there we have used the observational data for the reference trajectory.

The quality of the obtained periodic parameters depends on the length of the time intervals $[t_{j,i}, t_{j,i+1}]$ on which the linearization (with a constant reference value for the model output) is applied. If no data are available as reference $\boldsymbol{y}_k^{\mathrm{ref}}$, these intervals have to be enlarged, which presumably will reduce the quality of the optimized parameters. This in turn will influence the quality of the validation.

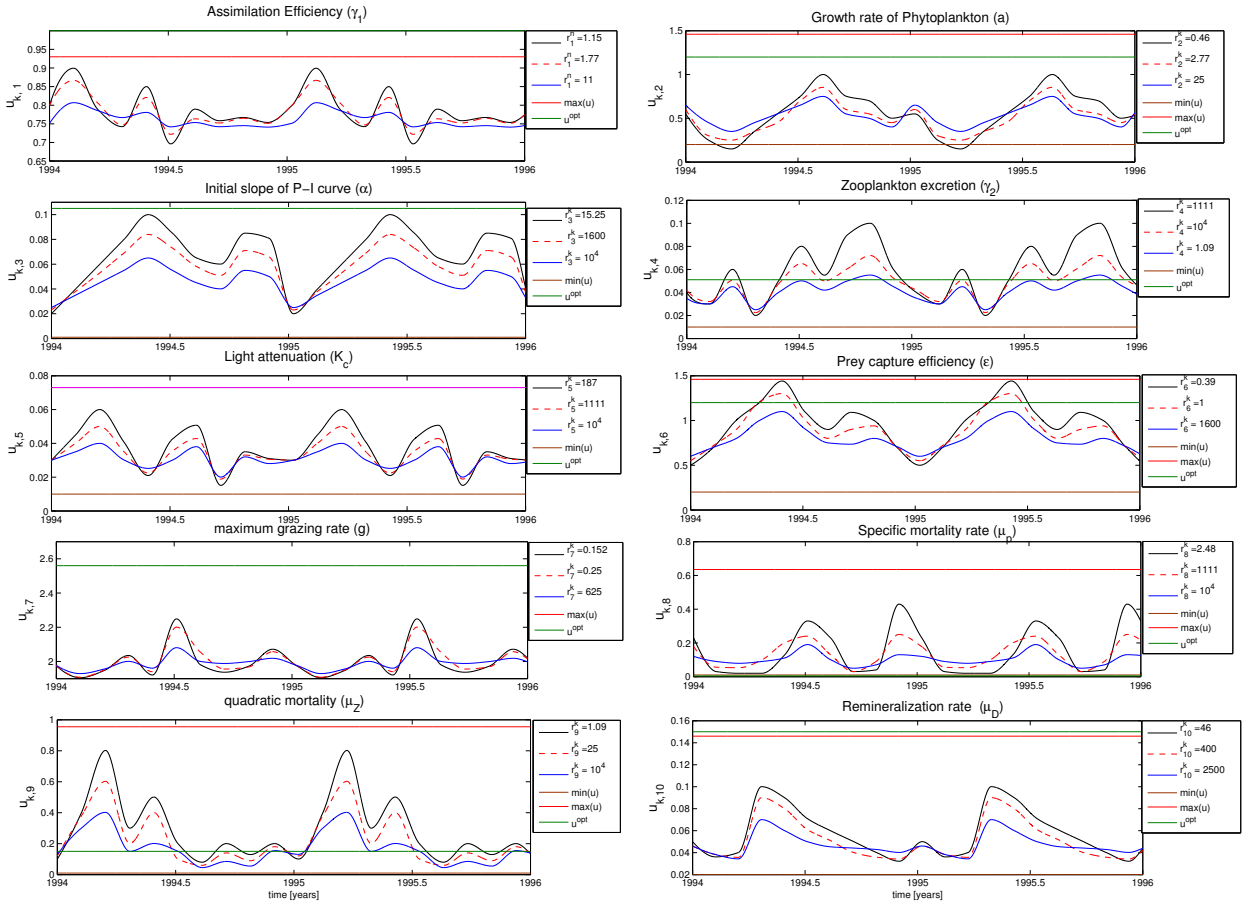

Fig. 6. Periodicity of optimal parameters $(u_{k,n})_{n=1,\ldots,10}$ obtained by the LQOC method, $\min(u), \max(u)$ are, respectively, the upper and lower bounds listed in Table 1, u^{opt} is the optimal parameter obtained by Rückelt et al. (2010b). We point out that $\min(u)$ and $\max(u)$ are not shown in all plots. Because the values are very low or high.

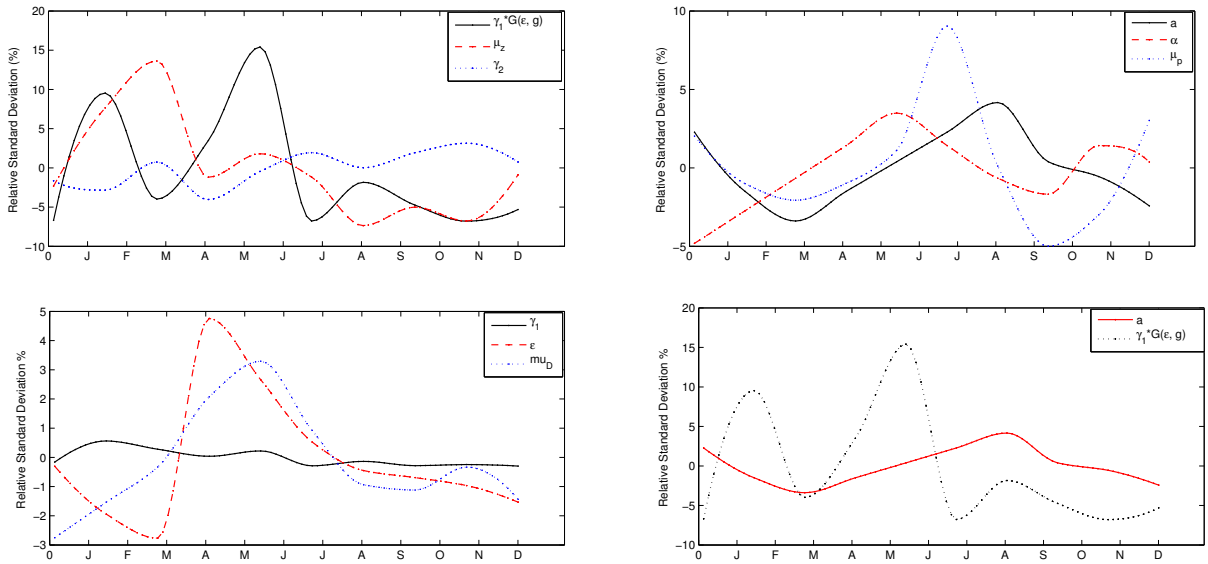

Fig. 7. Relative temporal variations of some of the model parameters in a typical year. Since the periodicity of the parameters is nearly perfect, no difference between the five years is visible.

Table 3. Values of the cost function for each year: for the optimization (with constant and periodic parameters), the validation presented in Sect. 4.4, and the prediction presented in Sect. 4.5.

Experiment	Model	Parameters	1994	1995	1996	1997	1998	Total cost F
Optimization (SQP)	non-linear	constant	71.91	68.50	64.14	65.39	80.06	70
Optimization (LQOC)	linear	periodic	2.09	1.18	1.94	0.53	0.98	1.35
Validation	non-linear	periodic	9.77	9.82	15.37	24.66	15.62	15.05
Prediction	non-linear	periodic	–	–	16.7	20.8	30.15	22.55

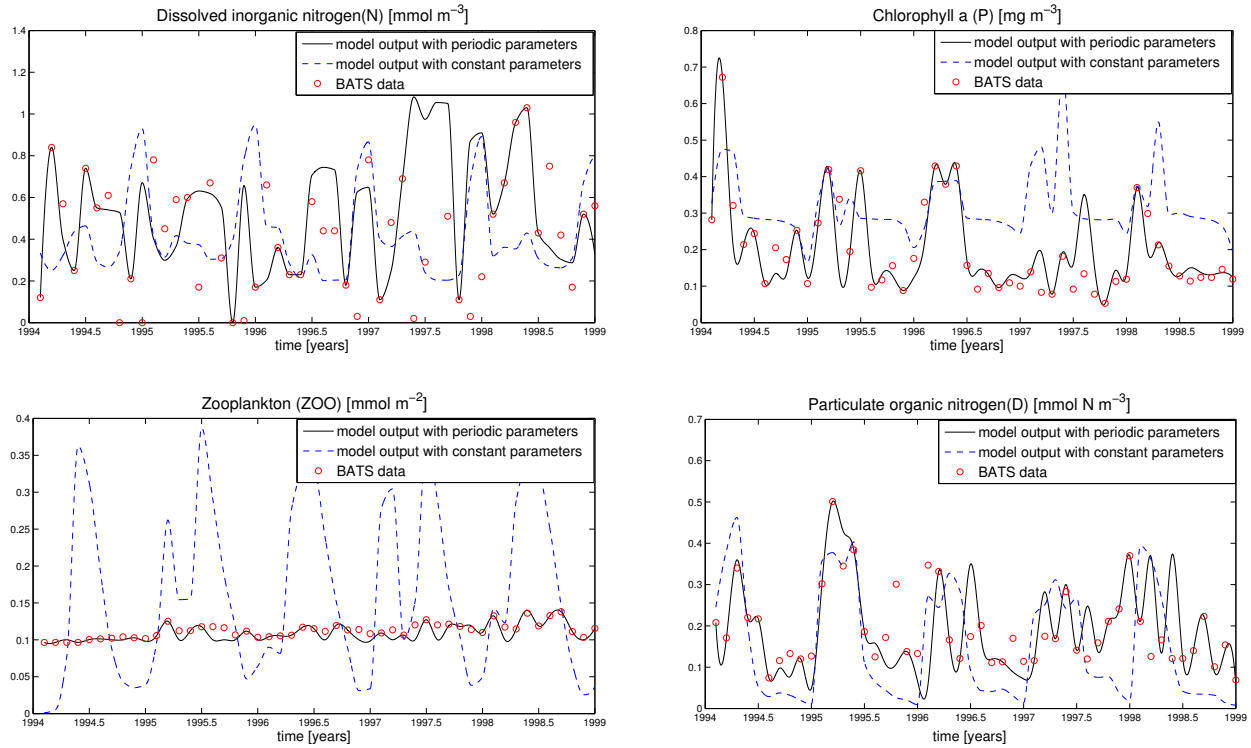

Fig. 8. Observational BATS data $\boldsymbol{y}^{l,\mathrm{obs}}, l = \mathrm{N, P, Z, D}$, and aggregated model trajectories $\bar{\boldsymbol{y}}^{l}, l = \mathrm{N, P, Z, D}$, obtained by using the optimal periodic parameters in the non-linear model, and the optimal trajectories for the constant parameters with a sequential quadratic programming (SQP) method at depth $z \approx 5\,\mathrm{m}$ for the years 1994–1998.

4.5 Prediction experiment

In this section we present a prediction experiment with the optimal periodic parameters in the original non-linear NPZD model. We now use only a part (two years, 1994 and 1995) of the time interval to determine optimal periodic parameters using the LQOC method. Then we use these parameters on the remaining part (three years, 1996 to 1998) of the time interval. In these three years, the periodic parameters obtained during the first two years are applied without further optimization.

Figure 9 shows a comparison between the predicted model output and the observational data for the years 1996 to 1998 in the uppermost layer. The fit is quite good. The qualitative behavior of the tracers at different times and spatial layers is similar. Table 3 shows the resulting values of the cost function.

The fit of the predicted output is slightly worse than for the output in the validation experiment described in Sect. 4.4, but still much better than the results obtained with the optimized constant parameters.

5 Conclusions

In this paper, we use the method of linear quadratic optimal control (LQOC) to determine optimal periodic parameters in a one-dimensional marine ecosystem model. We demonstrate that the LQOC method can be applied on the considered parameter optimization problem for a non-linear NPZD type model using a linearization technique around reference

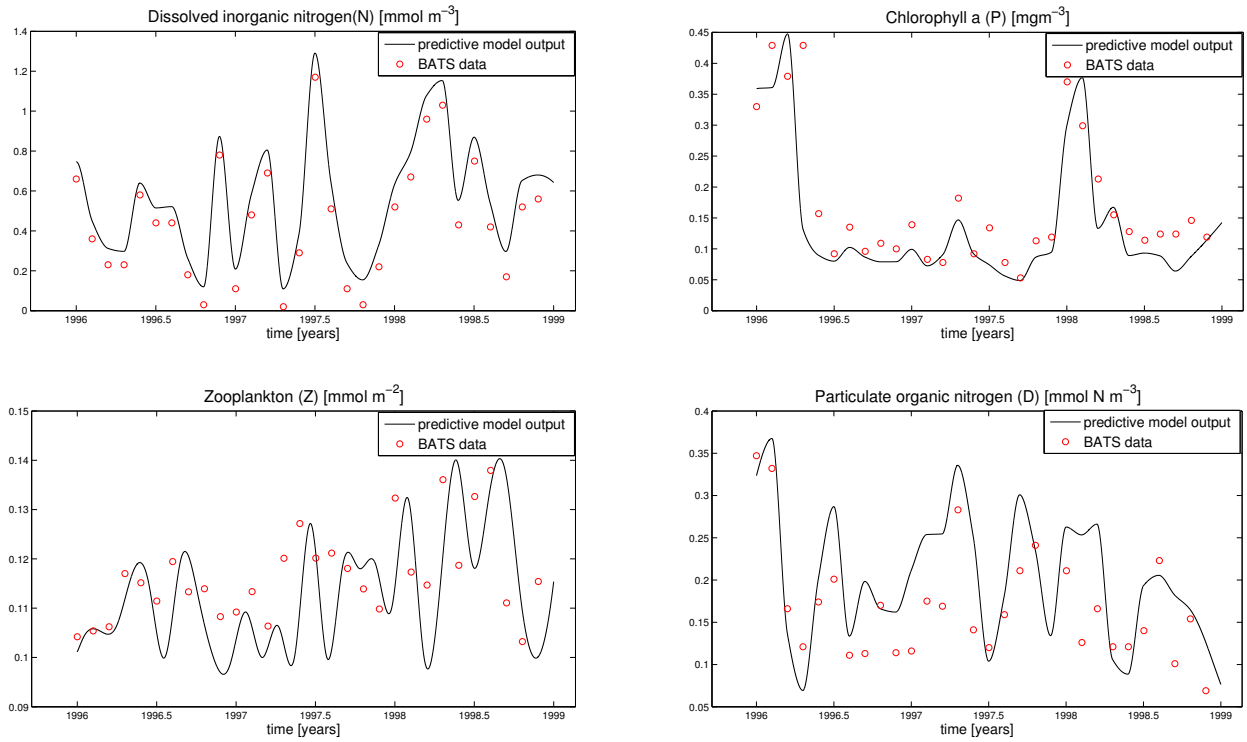

Fig. 9. Observational BATS data $\boldsymbol{y}^{l,\mathrm{obs}}, l = \mathrm{N, P, Z, D}$, and aggregated model trajectories $\bar{\boldsymbol{y}}^{l}, l = \mathrm{N, P, Z, D}$, obtained by using the optimal periodic parameters in the non-linear model as a prediction at depth $z \approx 5$ m for the years 1996–1998.

trajectories of model variables (biogeochemical tracers) and parameters, where the system matrices were obtained by automatic differentiation.

We show how a reference tracer trajectory can be built from sparse data, and how an appropriate choice of reference parameter trajectory can be used to obtain annual periodic parameters that additionally stay in prescribed bounds.

The linearized model obtained in this way gives a very good model–data fit with almost perfect annually periodic parameters. Even with the available small number of observational data typical to oceanographic time series sites, the quality of the fit is very high. Specifically, it is much better than the one previously obtained by optimization of the non-linear model with fixed model parameters.

The obtained periodic parameters are used in the original non-linear model. Using them, the model is able to reproduce and predict the real data much better than the non-linear model with optimized constant parameters.

The method allows to further analyze temporal deviations of individual parameters about the annual mean. This may help in making inferences about processes that the model cannot describe well when constant parameters are used. This latter analysis should contribute to a better understanding of model deficiencies and, eventually, help to improve marine ecosystem models.

Acknowledgements. The authors would like to thank the reviewers and the editor for many helpful comments and suggestions. This research was supported by the DFG Cluster Future Ocean.

Edited by: K. Fennel

References

Anderson, B. D. O. and Moore, J. B.: Linear Optimal Control, Prentice-Hall, Englewood Cliffs, NJ, 1971.

Casti, J. L.: Linear Dynamic Systems, Academic Press, 1987.

Clemens, D.: optimal non-linear Control for Power Systems, IEEE Conference on Control Application, 241–245, 1993.

Eknes, M. and Evensen, G.: An ensemble Kalman filter with a 1-d marine ecosystem model., J. Mar. Syst., 36, 75–100, 2002.

Fasham, M. and Evans, G.: The use of optimization techniques to model marine ecosystem dynamics at the JGOFS station at 47° N 20° W. Philos. T. Roy. Soc. B, 348, 203–210, 1995.

Fennel, K., Losch, M., Schröter, J., and Wenzel, M.: Testing a marine ecosystem model: sensitivity analysis and parameter optimization, J. Mar. Syst., 28, 45–63, doi:10.1016/S0924-7963(00)00083-X, 2001.

Giering, R., Kaminski, A: Recipes for adjoint code construction, ACM T. Math. Software, 24, 437–474, 1998.

Griewank, A.: Evaluating derivatives principles and techniques of algorithmic differentiation, Frontiers in Appl. Math., vol. 19, SIAM, Philadelphia, PA 2000.

Hurtt, G. and Armstromg, R.: A pelagic ecosystem model calibrated with BATS data, Deep-Sea Res., 43, 653–683, 1996.

Kwakernaak, H. and Sivan, R. : Linear Optimal Control Systems, Wiley-Interscience, New York, London, Sydney, 1972.

Lewis, F. L. and Syrmos, V. L. : Optimal Control (2nd Edn.), John Wiley & Sons, Inc., New York, 1995.

Losa, S. N., Kivman, G. A., Schroeter, J., and Wenzel, M.: Sequential Weak constraint parameter estimation in an ecosystem model, J. Mar. Syst., 43, 31–49, 2003.

Lunze, J.: Regelungstechnik 2, Springer-Verlag, Berlin Edn., 1997 (in German).

Matear, R. J.: Parameter optimization and analysis of ecosystem models using simulated annealing: a case study at Station P, J. Mar. Res., 53, 571–607, 1995.

Mattern, J.: Estimating time-dependent parameters for a biological ocean model using an emulator approach, J. Mar. Syst., 96-97, 32–47, 2012.

Michaels, A. F. and Knap, A. H.: Overview of the U.S. JGOFS Bermuda Atlantic Time-series Study and Hydrostation S program, Deep-Sea Res. Pt. II, 43, 157–198, 1996.

Oschlies, A.: Feedbacks of biotically induced radiative heating on upper-ocean heat budget, circulation, and biological production in a coupled ecosystem-circulation model, J. Geophys. Res., 109, C12031, doi:10.1029/2004JC002430, 2004.

Oschlies, A. and Garçon, V.: An eddy-permitting coupled physical-biological model of the North Atlantic, 1. Sensitivity to advection numerics and mixed layer physics, Global Biogeochem. Cy., 13, 135–160, 1999.

Oschlies, A. and Schartau, M.: Basin-scale performance of a locally optimized marine ecosystem model, J. Mar. Res. 63, 335–358, 2005.

Prunet, P., Minster, J. F., and Ruiz-Pino, D.: Assimilation of surface data in a one-dimensional physical-biogeochemical model of the surface ocean: 1. Method and preliminary results, Global Biogeochem. Cy., 10, 111–138, 1996.

Rückelt, J., Oschlies, A., and Slawig, T.: Optimization of Parameters and Initial Values in a Marine NPZD-Type Ecosystem Model, Technical Report 1013, CAU Kiel, Institut für Informatik, 2010a.

Rückelt, J., Sauerland, V., Slawig, T., Srivastav, A., Ward, B., and Patvardhan, C.: Parameter Optimization and Uncertainty Analysis in a Model of Oceanic CO_2-Uptake using a Hybrid Algorithm and Algorithmic Differentiation, Nonlinear Anal.-Real., 10, 3993–4009, 2010b.

Rugh, W. J.: Linear System Theory, 2nd Edn., Prentice-Hall, Upper Saddle River, New Jersey 07458, 1996.

Schartau, M. and Oschlies, A.: Simultaneous data-based optimization of a 1d-ecosystem model at three locations in the north Atlantic: Part I – method and parameter estimates, J. Mar. Res., 61, 765–793, 2003a.

Schartau, M. and Oschlies, A.: Simultaneous data-based optimization of a 1D-ecosystem model at three locations in the North Atlantic: Part II – Standing stocks and nitrogen fluxes, J. Mar. Res., 61, 795–821, 2003b.

Schartau, M., Oschlies, A., and Willebrand, J.: Parameter estimates of a zero-dimensional ecosystem model applying the adjoint method, Deep Sea Res. Pt. II, 48, 1769–1800, 2001.

Sinha, B. and Yool, A.: Extension of the OCCAM 1 general circulation model to include the biogeochemical cycles of carbon and oxygen, Part I: Technical description. Research and Consultancy Report No. 5, National Oceanography Centre, Southampton, 2006.

Sima, V.: Algorithms for Linear-Quadratic Optimization, in: Pure and Applied Mathematics, Marcel Dekker Inc., New York, NY, vol. 200, 1996.

Spitz, Y., Moisan, J., Abbott, M., and Richman, J.: Data assimilation and a pelagic ecosystem model: parameterization using time series observations, J. Mar. Syst., 16, 51–68, 1998.

Ward, B.: Marine Ecosystem Model Analysis Using Data Assimilation, Ph.D. thesis, available at: http://ocean.mit.edu/~benw/Thesis.pdf (last access: 1 August 2012), 2009.

Ward, B., Anderson, M., Friedrichs, T., and Oschlies, A.: Parameter optimisation techniques and the problem of underdetermination in marine biogeochemical models, J. Mar. Syst. Con. Lett., 81, 34–43, 2010.

Estimating Marine Ecosystem Model Using Kalman Filter with Periodic Parameters

Mustapha El Jarbi[a], Thomas Slawig[1]

[a]*Institute for Computer Science, Cluster The Future Ocean, Christian-Albrechts Universität zu Kiel, 24098 Kiel, Germany*

Abstract

The Purpose of this paper is to provide a comprehensive presentation and interpretation of the Extended Kalman Filter (EKF) and its numerical implementation. The extended Kalman filter is an approximate filter for non-linear systems, based on first-order linearization. Its use for the state estimation problem for linear systems. The EKF is essentially a predictor-corrector algorithm that is optimal in the sense of minimizing the trace of the covariance matrix of the errors. We examine the extended Kalman filter in data assimilation for a one-dimensional ecosystem model of NPZD (N for dissolved inorganic nitrogen, P for phytoplankton, Z for zooplankton and D for detritus) type. The ecosystem model has been developed by Oschlies and Garcon. It simulates the distribution of nitrogen, phytoplankton, zooplankton and detritus in a water column and is driven by ocean circulation data.

The main goal here is to compare the estimated state that obtained by an EKF with time-dependent parameters to the one obtained with constant parameters. For each case, three statistical metrics are computed and analyzed. We show that the EKF provide a significantly better results with time-dependent parameters compared to the one with constant parameters.

Keywords: Biogeochemical Models, NPZD Model, Parameter Optimization, Linear Quadratic Optimal Control, Periodic Parameters.

1. Introduction

An estimation or prediction on the state of a system is a critical problem in many areas, particularly in the fields of meteorology, oceanography and telecommunication. In meteorology and oceanography, one has different kinds of measurements: Radio-surveys, meteorological station, oceanic buoys, etc. These measurements are generally incomplete, intermittent

and not identically distributed, whereas for most applications, it is useful to have data on regular grids in space and time. These data can be used to initialize the forecasting models.

Data assimilation technique have been used in several studies, on one hand, for estimating poorly known parameters in marine ecosystem models by essentially trying to minimize the misfit between model simulations and observed data [6, 7, 11, 18, 23, 29, 32]. On the other hand, data assimilation can be further used for the model's state estimation [2, 4, 5, 17, 29]. Thus, one consider the problem of estimating the model state over some time period by simultaneously extracting a maximum amount of information out of a dynamical model and a set of measurements. Data assimilation systems of coupled physical-biogeochemical models provide a new perspective regarding the forecasting of ecosystems.

The Kalman filter is a statistical data assimilation scheme which provides the best estimate, in the sense last-squares of a linear system using only observations available up to the analysis time. It is a set of of mathematical equations that combine information from a model output and measurements to produce a better estimation of the dynamical system. Essentially, it implements a predictor-corrector type estimator that is optimal in the sense, that it minimizes the estimated error covariance under some hypotheses. The state and the covariance matrix of forecast errors are predicted (using the model) and, if measurement data is available, a correction step is performed (see [35]). The extended Kalman Filter (EKF) used in this paper, implements a Kalman filter for a system dynamics that results from the linearization of the original non-linear model around previous state estimates.

In this paper a four-component one-dimensional ecosystem model, namely an NPZD model (N for dissolved inorganic nitrogen, P for phytoplankton, Z for zooplankton and D for detritus), introduced in [21], is used in data assimilation experiments. The main objective of this paper is to compare state estimation using constant parameters with state estimation using time-dependent parameters. In order to achieve this, two groups of data assimilation experiments are carried out. Firstly, the importance of noise in the data and in the model on the state assimilation is examined. Secondly, to verify our approach and assess its data-fit quality, statistical model/data comparison is introduced. The structure of the paper is as follows: In Section 2, we briefly describe both, the general structure of the marine ecosystem model and the "synthetic" measurement data that we consider for the data assimilation. The equations of the Kalman filter method used for the state assimilation are described in Section

3, highlighting the extensions of the classical filter. In Section 4, the different assimilation experiments and the Kalman filter strategy are described. The importance of noise in the assimilation data is documented. In Section 5, formal quantitative metrics of model skill that measure agreement between the estimated output and the used measurement are proposed. Finally, we discuss our results and summarize our main findings.

2. Materials and Methods

2.1. The Model

The model under consideration is a coupled system of four tracers, namely dissolved inorganic nitrogen (N), phytoplankton (P), zooplankton (Z) and detritus (D), thus also called NPZD model, in the following summarized in the state vector $\mathbf{x} = (x^i)_{i=N,P,Z,D}$ and described by the following coupled PDE system

$$\begin{aligned} \frac{\partial x^i}{\partial t} &= -\omega^i \frac{\partial x^i}{\partial z} + \frac{\partial}{\partial z}\left(\kappa_\rho \frac{\partial x^i}{\partial z}\right) + S^i(\mathbf{x}, \mathbf{u}), \\ i &= N, P, Z, D. \end{aligned} \tag{1}$$

with $x^i \in (-H, 0) \times (0, T)$ and additional appropriate initial values. Here $x^i(t, z)$ denotes the concentration of tracer i at time t and the vertical spatial location z, H the depth of the water column and T the time horizon. The terms S^i are the biogeochemical coupling (or source-minus-sink) terms for the four tracers and $\mathbf{u} = (u_1, u_2, \ldots, u_n)$ is the vector of unknown physical and biological parameters - with $n = 12$ in this model- and that are subject to optimization. We briefly present the coupling terms [more details can be found in [21]]:

$$\begin{aligned} \mathbf{S}^N(\mathbf{x}, \mathbf{u}) &= -\min\left(\mu(x^P), u_2 c^\theta \tfrac{x^N}{u_{11}+x^N}\right) x^P + u_{10} x^D + u_4 x^Z, \\ \mathbf{S}^P(\mathbf{x}, \mathbf{u}) &= \min\left(\mu(x^P), u_2 c^\theta \tfrac{x^N}{u_{11}+x^N}\right) x^P - \tfrac{u_6 u_7 x^{P^2}}{u_7+u_6 x^{P^2}} x^Z - u_8 x^P, \\ \mathbf{S}^Z(\mathbf{x}, \mathbf{u}) &= u_1 \tfrac{u_6 u_7 x^{P^2}}{u_7+u_6 x^{P^2}} x^Z - u_4 x^Z - u_9 x^{Z^2}, \\ \mathbf{S}^D(\mathbf{x}, \mathbf{u}) &= (1-u_1) \tfrac{u_6 u_7 x^{P^2}}{u_7+u_6 x^{P^2}} x^Z + u_9 x^{Z^2} + u_8 x^P - u_9 x^D. \end{aligned} \tag{2}$$

The function μ describes the dependency of photosynthesis on the amount of light at depth z. It depends on the value of phytoplankton x^P by a non-local (integral) relation over the water column. Here two additional parameters u_3 and u_5 are involved. The circulation data (taken from an ocean model) are the turbulent mixing coefficient $\kappa_\rho = \kappa_\rho(t, z)$ and the temperature

$\theta = \theta(t, z)$, which is used in the non-linear term c^θ where $c = 1.066$ is kept constant. Table 1 lists the model parameters with their original symbols as in [21] and the optimal constant parameter values obtained by using the SQP method in [25].

Table 1: Optimal constant parameters u_i^* of the NPZD model obtained by using the SQP method in [25]. We give their original symbols u_i as in[21] and units.

parameter	u_i	u_i^*	units
Assimilation efficiency of zooplankton	β	1.0	1
Phytoplankton growth rate parameter	μ_{m}	0.946	day^{-1}
Slope of photosynthesis vs light intensity	α	0.105	$\mathrm{m}^2\ \mathrm{W}^{-2}\ \mathrm{d}^{-1}$
Zooplankton loss rate	$\phi_{\mathrm{m}}^{\mathrm{Z}}$	0.051	day^{-1}
Light attenuation by phytoplankton	k	0.073	$\mathrm{m}^2(\mathrm{mmol\ N})^{-1}$
Grazing encounter rate	ϵ	4	$\mathrm{m}^6(\mathrm{mmol\ N})^{-2}\ \mathrm{d}^{-1}$
Maximum grazing rate	g	4	d^{-1}
Phytoplankton linear mortality	ϕ_m^{P}	0.004	day^{-1}
Zooplankton quadratic mortality	ϕ_{Z}^*	0.04	$\mathrm{m}^3(\mathrm{mmol\ N})^{-1}\ \mathrm{d}^{-1}$
Detritus remineralization rate	μ_{m}	0.15	day^{-1}
Half saturation for NO3 uptake	K_{N}	0.1	mmol $N\ \mathrm{m}^{-3}$
Sinking velocity of detritus	w_{s}	105	$\mathrm{m\,day}^{-1}$

2.2. Synthetic Data

To reduce the number of uncertainties when dealing with real measurement data, it is essential to initially prove feasibility of the proposed estimation approach by considering a "Twin-experiment" mode in a first step.

A twin experiment is just a notation for data assimilation experiments where the data are simulated using the model rather than using real data. The only reason for using simulated data is to examine the properties of the assimilation methodology. The motivation is that unless the method works fine in the twin experiment, there is no point using it with real data. The model output is considered as a reference providing synthetic data that can be used to access the performance of the Kalman filter implemented in the model. The synthetic data

(or observations) $\mathbf{y}^d$ are substituted by model results, that were produced with a reference parameter set. We assume that the entire state vector $\mathbf{y}^d$ is given for all time steps during an annual cycle.

3. The Kalman Filter

The Kalman filter was introduced By Rudolf Emil Kalman, see [13]. The Kalman filter is a recursive procedure. In each calculation step it delivers an estimate of the current state of the system based on an erroneous measurement of the system state and the previous state. The current state of the process to be estimated is indicated by a state vector $\mathbf{x}_{k+1}$. The previous state is indicated by $\mathbf{x}_k$. A matrix $\mathbf{A}_k$ that converts the previous state to the current state is needed. Furthermore, the system can be influenced from the outside. This effect is referred with the variable control input $\mathbf{u}_k$ and the matrix $\mathbf{B}_k$. Table 2 lists all the symbols used in the Kalman filter description. Formally, Consider a linear stochastic difference equation, which

Table 2: List of symbols used in the Kalman filter description.

Variables	Description
$\mathbf{x}_k$	$n \times 1$ - System state vector at time k
$\mathbf{x}_k^f$	$n \times 1$- A priori estimate state at time k
$\mathbf{x}_k^a$	$n \times 1$ - A posteriori estimate state at time k
$\mathbf{u}_k$	$m \times 1$ - Input/control vector
q_k	$n \times 1$ - Process noise vector
$\mathbf{y}_k$	$p \times 1$ - Measurement vector
ϵ_k	$p \times 1$ - Measurement noise vector
$\mathbf{A}_k$	$n \times n$ - State transition matrix
$\mathbf{B}_k$	$n \times m$ - Input/control matrix
$\mathbf{H}_k$	$p \times n$ - Measurement matrix
$\mathbf{Q}_k$	$n \times n$ - Model noise covariance matrix
$\mathbf{R}_k$	$p \times p$ - Measurement noise covariance matrix

is written in a state space form (see e.g. [1, 9, 33, 35, 36]),

$$\mathbf{x}_{k+1} = \mathbf{A}_k \mathbf{x}_k + \mathbf{B}_k \mathbf{u}_{k-1} + q_k, \quad k = 1, \ldots, M-1, \tag{3a}$$

$$\mathbf{x}_1 \quad \text{is the given initial state} \tag{3b}$$

with a measurement $\mathbf{y}_k \in \mathbb{R}^m$, given as

$$\mathbf{y}_k \quad = \quad \mathbf{H}_k \mathbf{x}_k + \epsilon_k, \quad k = 1, \ldots, M-1. \tag{4}$$

The random variables q_k and ϵ_k represent the process and the measurement noise, respectively. They are assumed to be independent, normally distributed with zero mean, and with covariance as specified in covariance matrices $\mathbf{Q}_k$ for the stochastic model term q_k and $\mathbf{R}_k$ for the observation noise term ϵ_k, respectively.

The Kalman filter algorithm has two main steps: the forecast step (prediction) using the model difference equations which are responsible for projecting forward (in time) the current state and error covariance estimates to obtain the a priori estimates for the next time step, and the data assimilation step (correction) using the measurement update equations which are responsible for incorporating a new measurement into the a priori estimate to obtain an improved a posteriori estimate. Hence the Kalman filter has a "predictor-corrector" structure.

Model Forecast Step (Prediction)

The prediction is the first step of the Kalman filter. The predicted state or better the a priori state is calculated by neglecting the dynamic noise (process noise) and solving the difference equation

$$\mathbf{x}^f_{k+1} = \mathbf{A}_k \mathbf{x}^a_k + \mathbf{B}_k \mathbf{u}_k, \tag{5a}$$

$$\mathbf{x}^a_1 = \mathcal{E}[\mathbf{x}_a], \tag{5b}$$

where $\mathbf{x}_1$ is the given initial state and $\mathcal{E}[.]$ means the expected value. The forecast error covariance is given by

$$\mathbf{P}^f_{k+1} = \mathbf{A}_k \mathbf{P}^a_k \mathbf{A}^\top_k + \mathbf{Q}_k, \tag{6a}$$

$$\mathbf{P}^a_1 \quad \text{is the given initial error covariance.} \tag{6b}$$

Data Assimilation Step

The model and data are blended to obtain an improved estimate. We begin with the goal of finding an equation that computes an a posteriori state estimate $\mathbf{x}_k^a$ as a linear combination of an a priori estimate $\mathbf{x}_k^f$ and a weighted difference between an actual measurement $\mathbf{y}_k$ and a measurement prediction $\mathbf{H}_k\mathbf{x}_k^f$:

$$\mathbf{x}_{k+1}^a = \mathbf{x}_{k+1}^f + \mathbf{G}_{k+1}\left(\mathbf{y}_{k+1} - \mathbf{H}_{k+1}\mathbf{x}_{k+1}^f\right). \tag{7}$$

In equation (7) , G_{k+1} is a $n \times m$ matrix called the Kalman Gain and the difference $\mathbf{y}_{k+1} - \mathbf{H}_{k+1}\mathbf{x}_{k+1}^f$ is called the measurement innovation, or the residual. This residual reflects the discrepancy between the predicted measurement $\mathbf{H}_{k+1}\mathbf{x}_{k+1}^f$ and the actual measurement $\mathbf{y}_{k+1}$. The Kalman gain matrix $\mathbf{G}_{k+1}$ is calculated such that the a posteriori error covariance is minimized (Kalman 1960). It is given by

$$\mathbf{G}_{k+1} = \mathbf{P}_{k+1}^f\mathbf{H}_{k+1}\left(\mathbf{H}_{k+1}\mathbf{P}_{k+1}^f\mathbf{C}_{k+1}^\top + \mathbf{R}_{k+1}\right)^{-1}, \tag{8}$$

And the a posteriori error covariance $\mathbf{P}_{k+1}^a$ is calculated as follows:

$$\mathbf{P}_{k+1}^a = \left(\mathbf{I}_n - \mathbf{G}_{k+1}\mathbf{H}_{k+1}\right)\mathbf{P}_{k+1}^f, \tag{9}$$

where $\mathbf{I}_n$ denotes the identity matrix.

3.1. the Extended Kalman Filter

The Extended kalman Filter (EKF) deals with the non-linear process model and non-linear measurement model.

the non-linear process model is described as

$$\mathbf{x}_{k+1} = f(\mathbf{x}_k, \mathbf{u}_k) + q_k, \quad k = 1, \ldots, M-1, \tag{10a}$$

$$\mathbf{x}_1 \quad \text{is the given initial state} \tag{10b}$$

and the measurement model is given by

$$\mathbf{y}_k = h(\mathbf{x}_k) + \epsilon_k, \quad k = 1, \ldots M-1. \tag{11}$$

Model Forecast Step (Prediction)

Using process model:

$$\mathbf{x}^f_{k+1} = f(\mathbf{x}^a_k, \mathbf{u}_k), \tag{12a}$$

$$\mathbf{P}^f_{k+1} = \mathbf{A}_{k+1}\mathbf{P}^a_{k+1}\mathbf{A}^\top_{k+1} + \mathbf{Q}_k, \tag{12b}$$

where $\mathbf{A}_{k+1} = \mathcal{D}_x f(\mathbf{x}^f_{k+1}, \mathbf{u}_{k+1})$, $\mathcal{D}_x f$ is the Jacobian of function f with respect to $\mathbf{x}$ evaluated at $\mathbf{x}^f_{k+1}$

Data Assimilation Step

Using the measurement:

$$\mathbf{x}^a_{k+1} = \mathbf{x}^f_{k+1} + \mathbf{G}_{k+1}\left(\mathbf{y}_{k+1} - h(\mathbf{x}^f_{k+1})\right), \tag{13a}$$

$$\mathbf{G}_{k+1} = \mathbf{P}^f_{k+1}\mathbf{H}_{k+1}\left(\mathbf{H}_{k+1}\mathbf{P}^f_{k+1}\mathbf{C}^\top_{k+1} + \mathbf{R}_{k+1}\right)^{-1}, \tag{13b}$$

$$\mathbf{P}^a_{k+1} = (\mathbf{I}_n - \mathbf{G}_{k+1}\mathbf{H}_{k+1})\,\mathbf{P}^f_{k+1}, \tag{13c}$$

where $\mathbf{H}_{k+1} = \mathcal{D}h(\mathbf{x}^a_{k+1})$, $\mathcal{D}h$ is the Jacobian of function h with respect to $\mathbf{x}$ evaluated at $\mathbf{x}^a_{k+1}$

4. Assimilation Experiments

4.1. Kalman Filter Protocol

In an attempt to explore the assimilation performance of the ecosystem model, the process and measurement noise covariance matrices $\mathbf{Q}_k$ and $\mathbf{R}_k$, respectively, and the initial error covariance matrix $\mathbf{P}^a_1$ are necessary. We initialize $\mathbf{P}^a_1$ by assigning very small initial variances on the diagonal, see Table 3.

The measurement noise covariance matrix $\mathbf{R}_k$ specified in equation (8) and the process noise covariance matrix $\mathbf{Q}_k$ specified in equation (6a) are assumed to be homogenous and uncorrelated in space, and parameterized accordingly as diagonal matrix of the form $\sigma^2_d\mathbf{I_n}$ and $\sigma^2_a\mathbf{I_n}$ where σ^2_d and σ^2_a are the Measurement error variance and process error variance (the standard deviation), respectively (see Table 3). The two matrices assumed to be constant and are defined as follows

$$\mathbf{R}_k = \mathbf{R} = diag(\sigma^2_d)_{d=N,P,Z,D} \quad \mathbf{Q}_k = \mathbf{Q} = diag(\sigma^2_a)_{a=N,P,Z,D} \tag{14}$$

Table 3: The variances used in the assimilation experiments.

Description	N	P	Z	D
Model error variance				
(mmol N m^{-3})^2	$1.12 \cdot 10^{-3}$	$2.18 \cdot 10^{-3}$	$6.69 \cdot 10^{-4}$	$1.76 \cdot 10^{-3}$
Measurement error variance				
(mmol N m^{-3})^2	$5.42 \cdot 10^{-2}$	$2.85 \cdot 10^{-4}$	$4.5 \cdot 10^{-5}$	$4.48 \cdot 10^{-4}$
Initial error covariance				
(mmol N m^{-3})^2	$1 \cdot 10^{-2}$	$1 \cdot 10^{-4}$	$1 \cdot 10^{-4}$	$1 \cdot 10^{-4}$

A main objective of the this work is to investigate the effect of the parameters which have been used in the EKF approach, on the model-data misfit. To satisfy this purpose, two types of assimilation experiments are conducted:

- EKF method with periodic parameters,
- EKF method with constant parameters.

The periodic parameters used here are obtained by using the linear quadratic optimal control method. This method was used in [3]. On the other side, the constant parameters used here were obtained by using a sequential quadratic programming (SQP) method. This method was used in [25].

4.2. Discussion of the Covariance Matrices

In this section we examine some special cases of the process noise covariance matrix $\mathbf{Q}$ and the measurement noise covariance matrix $\mathbf{R}$. From Equation 8, $\mathbf{G}_k$ is decreases with $\mathbf{R}$ and increases with $\mathbf{Q}$. Thus the convergence properties are dependent on the relative magnitudes of the process and measurement noise. Moreover, the estimated output $\mathbf{H}_k\mathbf{x}_k^a$ tend to follow the measurement value quite closely. Indeed since $\mathbf{G}_{k+1}$ is a weighting function acting on the measurement it is clear that this effect is more prominent when $\mathbf{G}_k$ is high.

Furthermore, we discuss the two cases $\sigma_a > \sigma_d$ and $\sigma_a < \sigma_d$.

- $\sigma_a > \sigma_d$: If the intensity of the measurement noise is smaller than the intensity of the process noise, then the estimator interprets a large deviation from the model output $\mathbf{y}_k$

to the estimated output $\mathbf{H}_k\mathbf{x}^a$ as an indication that the estimate state is bad and needs to be corrected. Since $\mathbf{R}^{-1}$ has large entries we obtain large Kalman gain matrices $\mathbf{G}_k$. Thus, the difference between the model output and the estimated output is forced to get small since this is not caused by measurement errors.

- $\sigma_a < \sigma_d$: If the measurement noise is larger than the process noise, then the entries in $\mathbf{R}$ are large too and the optimal estimator is much more conservative in reacting to deviations of the estimated output $\mathbf{H}_k\mathbf{x}^a$ to the measured output $\mathbf{y}_k$. This leads to smaller Kalman gain matrices $\mathbf{G}_k$. With a small Kalman gain matrix $\mathbf{G}_k$ the difference between the model output and the estimated output will not be penalized as hard as it is done for a large Kalman gain matrix $\mathbf{G}_k$, since these deviations are mostly caused by larger measurement errors.

To confirm the above discussion, we perform two experiments which assess the effect that changes in the values of the noise sources have on the overall performance of a extended Kalman filter approach. Two types of assimilation experiments are conducted:

- assuming that the elements of the measurement error matrix have very small values compared to the model error,
- perturbing the assimilated measurements in order to take into account the presence of noise in the data.

4.3. Implementation

4.3.1. Discretization scheme of NPZD Model

The continuous model (1) is discretized and solved using an operator splitting method, which is explain in this section. Let a time $\tau > 0$ be given. Then, at first the non-linear coupling operators $\mathbf{S}_k = (S_k^N, S_k^P, S_k^Z, S_k^D)$ [cf,. (2)] are computed at every spatial grid point and integrated by four explicit Euler steps with step size $\frac{\Delta t}{4}$, each of which is described by the operator

$$\mathbf{T}_k(\mathbf{x}_k, \mathbf{u}_k) := \left[\mathbf{x}_k + \frac{\Delta t}{4} S_k(\mathbf{x}_k, \mathbf{u}_k)\right]. \tag{15}$$

Then, an explicit Euler step with full step-size Δt is formed for the sinking term which is spatially discretized by upstream scheme. This step is summarized in a matrix, denoted

by $\mathbf{L}^{\text{sink}}$ which only depends on the time step k if the sinking velocity w_s is time-dependent. Finally, an implicit Euler step for the diffusion operator, discretized with second order central differences is applied. Due to $\kappa_\rho = \kappa_\rho(z,t)$ the resulting matrix denoted by $\mathbf{L}_k^{\text{diff}}$ depends on k. Thus, the operator splitting method can be summarized by the following operator equation:

$$\begin{aligned} \mathbf{x}_{k+1} &= (\mathbf{L}_k^{\text{diff}})^{-1}\mathbf{L}^{\text{sink}}\mathbf{T}_k \circ \mathbf{T}_k \circ \mathbf{T}_k \circ \mathbf{T}_k(\mathbf{x}_k, \mathbf{u}_k), \\ k &= 1, \ldots, M-1. \end{aligned} \tag{16}$$

5. Statistical Metrics of Model/Data

We calculate three statistical metrics that are used to quantify model-data misfit: model bias (bias), root mean squared error (RMSE) and model efficiency (ME).

The model bias measures the mean deviation between model-output $\mathbf{y}^a$ (results, estimated) and the measurements $\mathbf{y}^d$:

$$b_k = \frac{1}{n}\sum_{j=1}^{n}\left(\mathbf{y}_{j,k}^a - \mathbf{y}_{j,k}^d\right), \tag{17}$$

where M represents the number of model/data pairs and j and k are the spatial and temporal indices, respectively. The bias b_k is negative if the model underestimates the measurements, while a positive bias reflects an overestimation of measurements by the model. The main purpose of bias is to indicate a persistent error in magnitude of the modeled variable.

The root-mean-square error (RMSE) is a frequently used measure of the differences between values predicted by a model (an estimator) and the values actually observed. The RMSE is defined as the square root of the mean square error

$$\text{RM}_k = \sqrt{\frac{1}{n}\sum_{j=1}^{n}\left(\mathbf{y}_{j,k}^a - \mathbf{y}_{j,k}^d\right)^2}. \tag{18}$$

The smaller the absolute values of RMSE, the better the model/data fit.

The model efficiency (ME) measures the deviations between model and measurements relative to the variability in the measurements

$$\text{ME}_k = 1 - \frac{\sum_{j=1}^{n}\left(\mathbf{y}_{j,k}^a - \mathbf{y}_{j,k}^d\right)^2}{\sum_{j=1}^{n}\left(\mathbf{y}_{j,k}^d - \sum_{j=1}^{n}\mathbf{y}_{j,k}^d\right)^2} \tag{19}$$

ME is always less than or equal to one, i.e., $ME_k = 1$ indicates a perfect match between model and measurements, $ME_k > 0$ indicates that the model is a better prediction than the measurement climatology, while $ME < 0$ implies that the observant observational climatology is a better predictor than the model.

6. Results and Discussion

In order to discuss the comparison between the assimilation with periodic and constant parameters, different data assimilation experiments are performed. The aim here is to (1) assimilate with the given measurement noise and model noise errors (see Table 3), (2) obtain high values for the entries of the model error matrix and low values for the entries of the measurement error matrix (see Table 4). A comparison between assimilation with periodic and constant parameters will be performed for both experimental settings.

6.1. First Data Assimilation Experiment: Using Calculated Noise Matrices

In this Section we highlight the role of the parameters used for the assimilation experiments with the extended Kalman filter. We use fix ratios of the process noise covariance matrices and measurement noise covariance matrices, respectively (see Table 2).

The assimilation will be done with both periodic parameters and constant parameters. As mentioned in Section 4.1, the periodic parameters are taken from [3] and the constant parameters are taken from [25].

We only present the results obtained by the EKF. Figure 1 illustrates the results by using both periodic parameters and constant parameters. For both cases, we compare the estimated output data and the synthetic data (twin data) of dissolved inorganic nitrogen (N), phytoplankton (P), zooplankton (Z) and detritus (D), for the years 1994 to 1998 in the uppermost layer at depth $z \simeq 5$m. The total number of depth layers considered in the assimilation is $n = 32$ and the total number of time steps is $M = 43800$. For all four tracers, the green line corresponds to the estimated output with constant parameters, the red line is the estimated output with periodic parameters and the black line presents the synthetic data. We can see that, for all four tracers, the estimated output with periodic parameters is often smaller than the estimated output with constant parameters. It is indeed recognizable, that the estimated

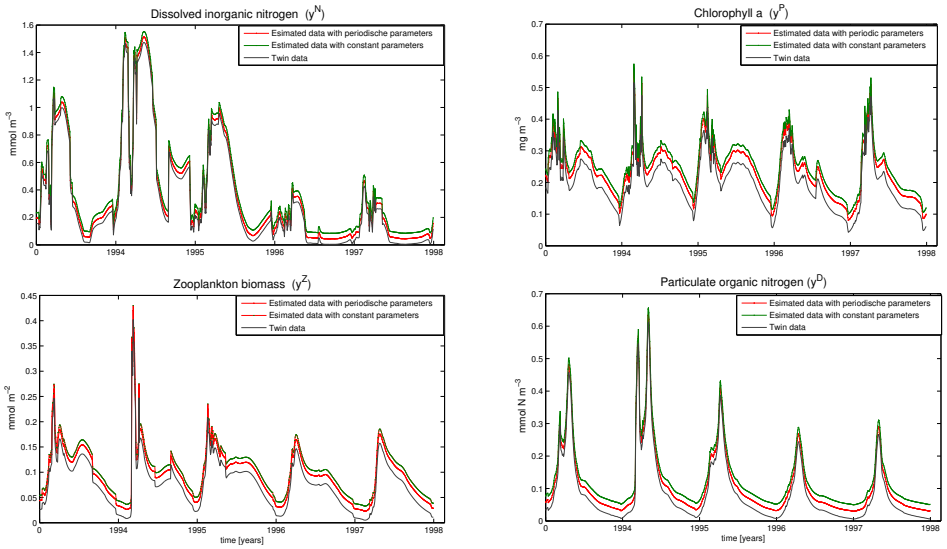

Figure 1: Output $\mathbf{y}^a$ for N, P, Z, D, estimated with periodic parameters (red line) and with constant parameters with (green line), and Synthetic data $\mathbf{y}^d$ (black line). Each plot is given for the upper layer at depth $z \approx 5m$ and years 1994-1998.

output with periodic parameters is similar to that with constant parameters, but for all four tracers the deviation from the synthetic data to the estimated output with periodic parameters is smaller than the deviation to the estimated output with constant parameters.

We point out that the result of this test with the given error variances in Table 3 doesn't clearly implicate that the solution with periodic parameters follows the synthetic data much better than the solution with constant parameters. But this becomes clear in the following Section, if we make the intensity of the measurement noise smaller than the intensity of the model noise and vice versa. It becomes clearer, if we regard the mean deviation between the estimated output with periodic parameters, the estimated output with constant parameters, and the synthetic data.

6.2. Second Data Assimilation Experiment: Using Noise Matrices with High/Low Values

This Section presents the ratios between the process and measurement noise covariance matrix Q and R, respectively and its effect on the overall performance of the EKF approach

Table 4: The variances used in the assimilation experiments.

Description	N	P	Z	D
Model error variance				
(mmol N m^{-3})^2	$1.12 \cdot 10^{-1}$	$2.18 \cdot 10^{-1}$	$6.69 \cdot 10^{-2}$	$1.76 \cdot 10^{-1}$
Measurement error variance				
(mmol N m^{-3})^2	$5.42 \cdot 10^{-2}$	$2.85 \cdot 10^{-4}$	$4.5 \cdot 10^{-5}$	$4.48 \cdot 10^{-4}$

both with optimal periodic parameters as well as with optimal constant parameters. We refer to the experiments as:

(A) Experiment being characterized by a high model error compared to the measurement error (Fig. 2).

(B) Experiment being characterized by a low model error compared to the measurement error (Fig. 3).

As it was mentioned in Section 4.2 the Kalman gain matrix $\mathbf{G}_k$ depends on the choice of the intensity matrices R and Q. So we want to analyze them for different choices of the error noise. Table 4 shows the chosen values for R and Q.

Figure 2 presents the results of the first experiment (A) by showing the estimated output with periodic parameters (red line), the estimated output with constant parameters (green line) and the synthetic data (black line). We can see that the solution here is better than the solution presented above. Figure 2 shows that the estimated output with periodic parameters is smaller than that with constant parameters. For all four tracers, we observe that the results with periodic parameters are nearly the same. But the estimated output with constant parameters is also much better compared to those obtained in Subsection 6.1. One can see that the deviation from the synthetic data is smaller.

Figure 3 shows the results of the second experiment (B). In this Figure, it is quite obvious that, for all four tracers, the deviations between the estimated output and the synthetic data will be too high. We can see that with both, periodic parameters and constant parameters, the EKF method presented here tends to provide poor estimates for all four tracers, especially

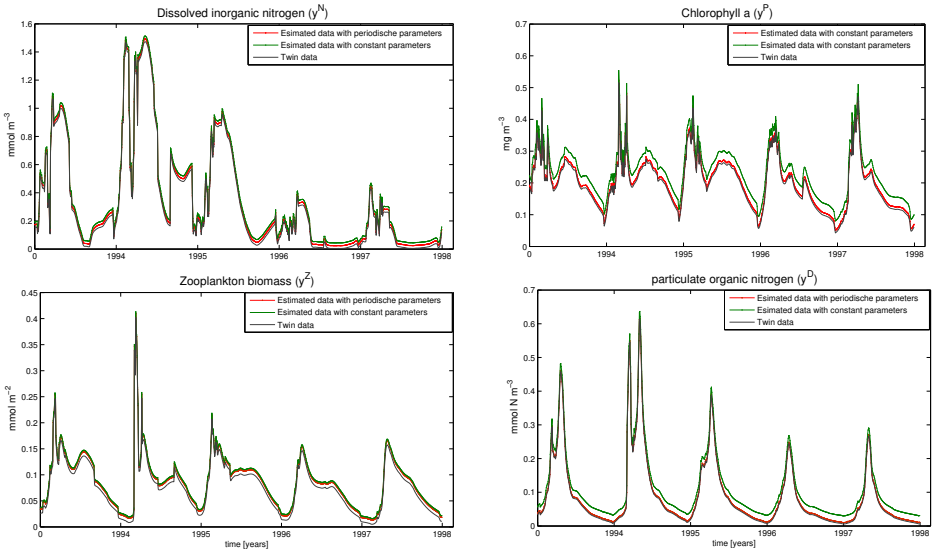

Figure 2: Output $\mathbf{y}^a$ for N, P, Z, D at high and low ratios of Q and R, estimated with periodic parameters (red line) and with constant parameters (green line), and Synthetic data $\mathbf{y}^d$ (black line). Each plot is given for the upper layer at depth $z \approx 5m$ and years 1994-1998.

for zooplankton and detritus. As a summary we can say, that if we choose different values for σ_d and σ_a, the Kalman gain matrix changes depending on the difference of both standard deviations. If we have small measurement errors, the EKF method tries to improve the difference between the estimated output and the synthetic data much more, which leads to larger deviations from the reference since it has to react to larger model noise.

6.3. Statistical Model/Data Comparison

In order to assess the fit of the estimated data to the synthetic data (twin data), model bias, the RMSE and the ME [cf., (17), (18), (19)] were calculated for dissolved inorganic nitrogen (N), phytoplankton (P), zooplankton (Z) and detritus (D) with both periodic parameters and constant parameters. We point out that for the synthetic data, the estimated state is closer to the data, yielding smaller RMSE and larger ME values. Figures 4 to 7 show the results of model bias, RMSE and ME for all four tracers and for both experiments (periodic parameters and constant parameters). All values concerning the seasonal mean of the estimated and

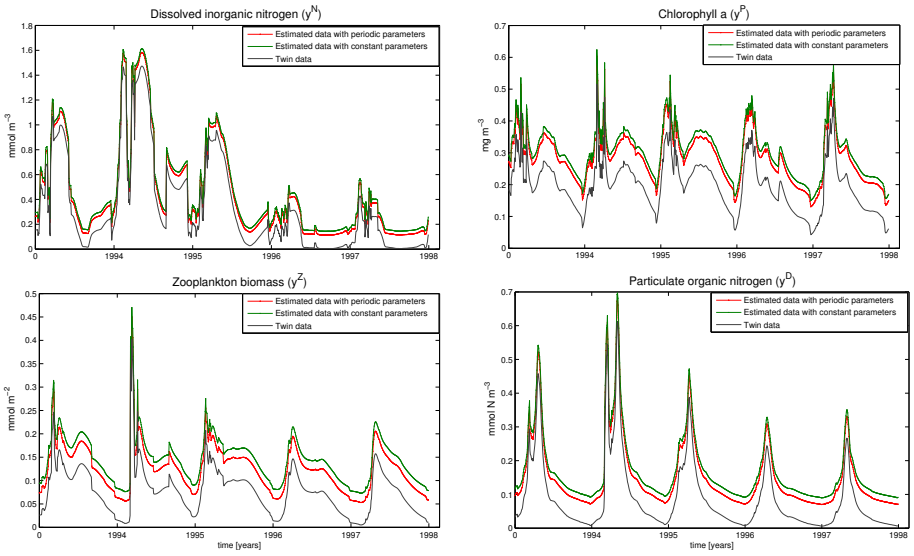

Figure 3: Estimated output $\mathbf{y}^a$ for N, P, Z, D at low and high ratios of Q and R, estimated with periodic parameters (red line) and with constant parameters (green line), and Synthetic data $\mathbf{y}^d$ (black line). Each plot is given for the upper layer at depth $z \approx 5m$ and years 1994-1998.

synthetic variables of the four tracers are shown in Table 5 for the assimilation with periodic parameters (first experiment) and in Table 6 for the constant parameters (second experiment), respectively. It becomes clear that the assimilation with periodic parameters provides fairly good estimates of all four tracers compared to the assimilation with constant parameters.

The bias (17) describes the systematic errors. It has the same unit as the dependent variable. According to formula (17), a positive bias error indicates a predisposition of the model output (estimated data) to the synthetic data. Conversely, a negative bias error implies a tendency of the model to synthetic data. The bias values fluctuate for all tracers except for particulate organic nitrogen (D) between positive and negative values (Fig. 4 to 7). But as shown in Tables 5 and 6, for both experiments the bias is close to 0 as expected. While for the first experiment, the bias of all tracers is located between 0.045 and 0.067 (Table 5), the corresponding ranges for the second experiment are 0.07 to 0.1.

The RMSE (18) error measures the typical model output (estimated data) magnitude in units of the synthetic data. By squaring the difference term, it tends to give more weight to

Table 5: Bias, RMSE and ME for assimilation with periodic parameters.

	N ($mmolm^{-3}$)	P (mgm^{-3})	Z ($mmolm^{-2}$)	D ($mmolNm^{-3}$)
Bias	0.045	0.055	0.046	0.067
RMSE	0.18	0.22	0.23	0.24
ME	0.91	0.97	0.89	0.87

Table 6: Bias, RMSE and ME for assimilation with constant parameters.

	N *mmol N*	P mgm^{-3}	Z *mmol* m^{-2}	D *mmol N* m^{-3}
Bias	0.09	0.07	0.08	0.09
RMSE	0.25	0.30	0.32	0.35
ME	0.77	0.87	0.76	0.71

large discrepancies between estimated fields and synthetic data.

It has the same unit as the dependent variable. It can take only values $\geqslant 0$. For all tracers, the RMSE is $\leqslant 0.25$ for the first experiment (Table 5), while it is $\leqslant 0.35$ for the second experiment (Table 6).

The ME (19) evaluates the predictive skill of the model relative to the predictive skill of a climatology; positive values of ME indicate that the model represents an improvement over climatology, while negative values indicate that climatology is a better predictor of the observation. Figures 4 to 7 show that ME is positive for all tracers and for both experiments. The ME for the first experiment (Table 5) is relatively large compared to the second experiment (Table 6). The values range from 0.87 to 0.91 for the first experiment and from 0.71 to 0.87 for the second experiment. ME for the dissolved inorganic nitrogen (N) and chlorophyll a (P) has values near one, indicating that the model predicts observations (here synthetic data) much better than climatology (Table 5).

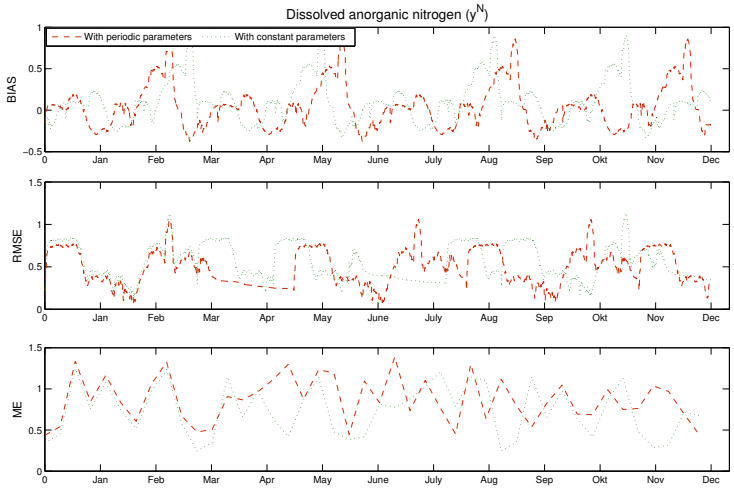

Figure 4: Model bias, root mean square error (RMSE) and model efficiency (ME) between estimated model-output $\mathbf{y}^a$ and the measurements $\mathbf{y}^d$ (synthetic data) for dissolved inorganic nitrogen (N), estimated with periodic parameters (red line) and with constant parameters (green line). Runs from January to December of 1994.

7. Conclusion

An extended Kalman filter has been used with a simple four-component marine ecosystem model which is a one-dimensional NPZD model developed by Oschlies and Garcon. The main objective of this paper was to compare the performance of the Kalman filter for time-dependent parameters and constant parameters.

First, two assimilation experiments were described. One where the measurement error and the model error were parameterized as diagonal matrices with the standard deviations around mean distribution as their entries. And a second where the importance of the noise in the data and in the model on the assimilation results were presented. Both experiments show that the estimated output for all four tracers is much better with time-dependent parameters as with constant parameters.

Additionally, to quantify model-data misfit, three statistics (Bias, RMSE and ME) were calculated. For all four tracers, the Bias and RMSE for the estimation with periodic parameters are less than those obtained with constant parameters. Time-series of all three statistics were frequently useful as well. We demonstrated, that using time-dependent parameters in-

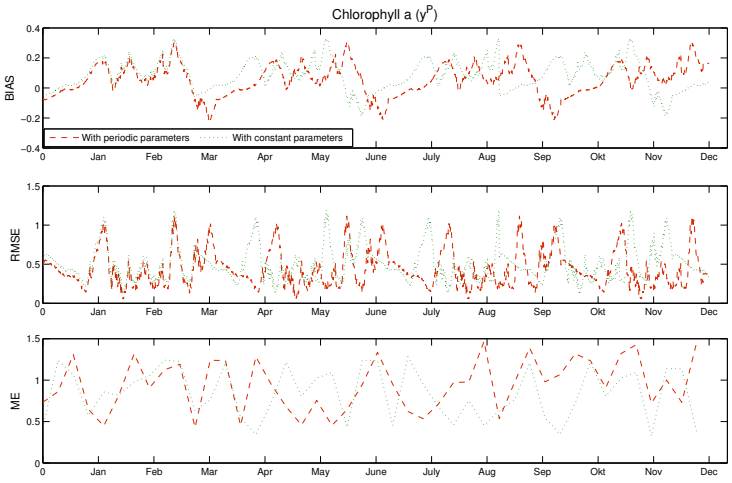

Figure 5: Model bias, root mean square error (RMSE) and model efficiency (ME) between estimated model-output $\mathbf{y}^a$ and the measurements $\mathbf{y}^d$ (synthetic data) for phytoplankton (P), estimated with periodic parameters (red line) and with constant parameters (green line). Runs from January to December of 1994.

stead of constant parameters results in better state estimation and is quite suitable for the considered problem.

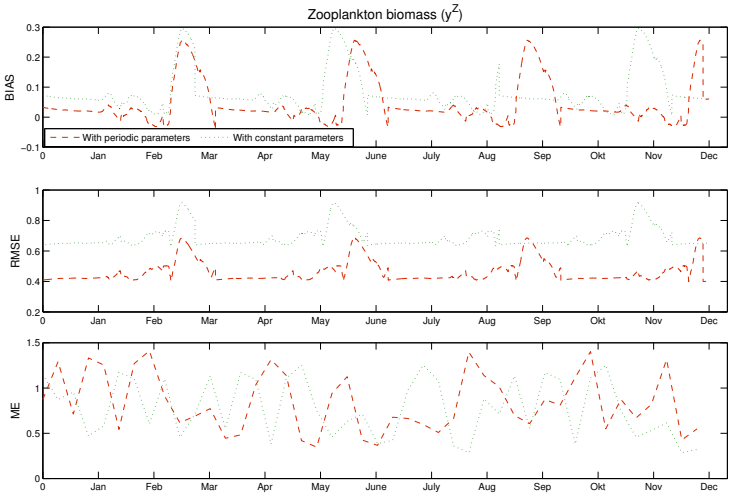

Figure 6: Model bias, root mean square error (RMSE) and model efficiency (ME) between estimated model-output $\mathbf{y}^a$ and the measurements $\mathbf{y}^d$ (synthetic data) for zooplankton (Z), estimated with periodic parameters (red line) and with constant parameters (green line)runs from January to December of 1994.

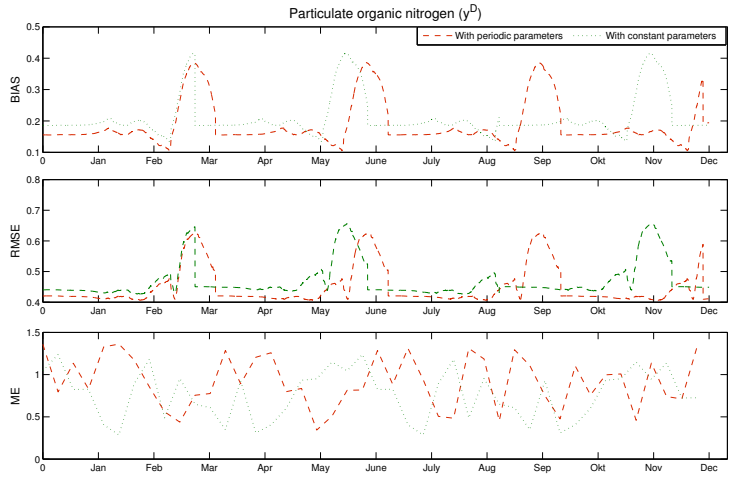

Figure 7: Model bias, root mean square error (RMSE) and model efficiency (ME) between estimated model-output $\mathbf{y}^a$ and the measurements $\mathbf{y}^d$ (synthetic data) for detritus (D), estimated with periodic parameters (red line) and with constant parameters (green line). Runs from January to December of 1994.

References

[1] Balakrishnan. A. V.: Kalman filtering theory, Springer london, 1987

[2] Carmillet, V., Brankart, J.-M., Brasseur, P., Drange, H., Evensen, G.,: A singular evolutive extended Kalman filter to assimilate ocean color data in a coupled physicalbiochemical model of the North Atlantic. Ocean Model. 3, 167–192, 2001.

[3] El Jarbi M., Rückelt J., Slawig T., Oschlies A.: Reducing the Model-Data Misfit in a Marine Ecosystem Model Using Periodic Parameters and Linear Quadratic Optimal Control, Biogeosciences 10:1169-1182, doi:10.5194/bg-10-1169-2013.

[4] Eknes, M. and Evensen, G.: An ensemble Kalman filter with a 1-d marine ecosystem model., J. Mar. Syst. 36, 75–100, 2002.

[5] Evans, G.T., Parslow, J.S.: A model of annual plankton cycles. Biol. Oceanogr. 3, 327–347, 1985.

[6] Fasham, M. and Evans, G.: The use of optimization techniques to model marine ecosystem dynamics at the JGOFS station at 47 °N 20 °W. Philos. Trans. R. Soc. Lond., B 348, Philos. Trans. R. Soc. Lond., B 348, 203–210, 1995.

[7] Fennel, K., Losch, M., Schröter, J., and Wenzel, M.: Testing a marine ecosystem model: sensitivity analysis and parameter optimization, J. Mar. Syst., 28, 45–63, doi:10.1016/S0924-7963(00)00083-X, 2001.

[8] Giering, R., Kaminski, A: Recipes for adjoint code construction ACM Transactions on Mathematical Software, 24 (4) (1998), pp. 437–474

[9] Grewal,M. S., Andrews, A. P.: kalman Filtering Theory and practice Using matlab, Thrid Edition, Wiley, 2011.

[10] Griewank, A.: Evaluating derivatives principles and techniques of algorithmic differentiation Frontiers in Appl. Math., vol. 19SIAM, Philadelphia, PA (2000)

[11] Harmon, R. and Challenor, P.: A markov chain monte carlo method for estimation assimilation into models, ., Ecological modelling., 101, 41–59, 1996.

[12] Hurtt, G. and Armstromg, R.: A pelagic ecosystem model calibrated with BATS data., Deep-Sea Res., 43, 653–683, 1996.

[13] Kalman,. R.: A new Approach to linear Filtering and Prediction Problem. Transactionsof the ASME-Jornal of Basic Engineering 82, 35–45, 1960.

[14] Kwakernaak, H. and Sivan, R. : Linear Optimal Control Systems. Wiley- Interscience. New York - London - Sydney, 1972.

[15] Lewis, F. L. and Syrmos, V. L. : Optimal Control (2nd Ed.). John Wiley & Sons, Inc. New York, 1995.

[16] Losa, S. N., Kivman, G. A., Schroeter, J., and Wenzel, M.: Sequential Weak constraint parameter estimation in an ecosystem model, J. Mar. Syst., 43, 31–49, 2003.

[17] Natvik, L.-J., Eknes, M., Evensen, G.,: A weak constraint inverse for a zero-dimensional four component marine ecosystem model. J. Mar. Syst. 28 (1–2), 19–44, 2001.

[18] Matear, R. J.: Parameter optimization and analysis of ecosystem models using simulated annealing: a case study at Station P, J. Mar. Res., 53, 571–607, 1995.

[19] Mattern, J.: Estimating time-dependent parameters for a biological ocean model using an emulator approach, J. Mar. Syst., 96–97, 32–47, 2012.

[20] Oschlies, A.: Feedbacks of biotically induced radiative heating on upper-ocean heat budget, circulation, and biological production in a coupled ecosystem-circulation model, J. Geophys. Res., 109, C12031, doi:10.1029/2004JC002430, 2004.

[21] Oschlies, A. and Garçon, V.: An eddy-permitting coupled physical-biological model of the North Atlantic 1. Sensitivity to advection numerics and mixed layer physics, Global Biogeochem. Cy., 13, 135–160, 1999.

[22] Oschlies, A. and Schartau, M.: Basin-scale performance of a locally optimized marine ecosystem model, J. Mar. Res. 63, 335–358, 2005.

[23] Prunet, P., Minster, J. F., and Ruiz-Pino, D.: Assimilation of surface data in a one-dimensional physical-biogeochemical model of the surface ocean: 1. Method and preliminary results, Global Biogeochem. Cy., 10, 111–138, 1996.

[24] Rückelt, J., Oschlies, A., Slawig, T.: Optimization of Parameters and Initial Values in a Marine NPZD-Type Ecosystem Model, Technical Report 1013, CAU Kiel, Institut für Informatik, 2010.

[25] Rückelt, J., Sauerland, V., Slawig, T., Srivastav, A., Ward, B., and Patvardhan, C.: Parameter Optimization and Uncertainty Analysis in a Model of Oceanic CO_2-Uptake using a Hybrid Algorithm and Algorithmic Differentiation, non-linear Analysis, 10, 3993–4009, 2010.

[26] Rugh, W. J.: Linear System Theory, 2nd Edn., Prentice-Hall, Upper Saddle River, New Jersey 07458, 1996.

[27] Schartau, M. and Oschlies, A.: Simultaneous data-based optimization of a 1d-ecosystem model at three locations in the north Atlantic: Part I – method and parameter estimates, J. Mar. Res., 61, 765–793, 2003.

[28] Schartau, M. and Oschlies, A.: Simultaneous data-based optimization of a 1D-ecosystem model at three locations in the North Atlantic: Part II – Standing stocks and nitrogen fluxes, J. Mar. Res., 61, 795–821, 2003.

[29] Schartau, M., Oschlies, A., and Willebrand, J.: Parameter estimates of a zero-dimensional ecosystem model applying the adjoint method, Deep Sea Res. Pt. II, 48, 1769–1800, 2001.

[30] Sinha, B., and Yool, A.: Extension of the OCCAM 1 general circulation model to include the biogeochemical cycles of carbon and oxygen, Part I: Technical description. Research and Consultancy Report No. 5, National Oceanography Centre, Southampton, 2006.

[31] Sima, V.: Algorithms for Linear-Quadratic Optimization, Pure and Applied Mathematics, Marcel Dekker, Inc., New York, NY, vol. 200, 1996.

[32] Spitz, Y., Moisan, J., Abbott, M., and Richman, J.: Data assimilation and a pelagic ecosystem model: parameterization using time series obervations, J. Mar. Syst., 16, 51–68, 1998.

[33] Sorenson H. W. : Kalman Filtering: Theory and Application, EEE Press, 1960.

[34] Ward, B., Anderson, M., Friedrichs, T., and Oschlies, A.: Parameter optimisation techniques and the problem of underdetermination in marine biogeochemical models, J. Mar. Syst. Con. Lett., 81, 34–43, 2010.

[35] Welch, G. and Bishop, G.: An Introduction to the Kalman Filter. SIGGRAPH 2001 - Course 8, ACM, New York, 2001.

[36] Zarchan, P., Musoff, H,.: Fundamental of kalman Filtering: APractical Approach (2nd edition)(Progress in Asrtonautics and Aeronautics). American institute of Aeronautics, 765 pp,2000.

[37] Sauerland, V.: Algorithm Engineering for some Complex Practice Problems: Exact Algorithms, Heuristics and Evolutionary Algorithms. PhD thesis, Christian-Albrechts-Universität Kiel, Technische Fakultät, 2012.

Extension of a Marine Ecosystem Model using Discrete Open Loop Optimal Control

M. El Jarbi* and T. Slawig
Department of Computer Science, Algorithmic Optimal Control – CO_2 Uptake of the Ocean,
Excellence Cluster The Future Ocean,
Christian-Albrechts-Platz 4,
24118 Kiel, Germany
E-mail: mej@informatik.uni-kiel.de
E-mail: ts@informatik.uni-kiel.de
*Corresponding author

Abstract: The objective of this paper is to apply an optimization method for an enhancement of a climate model, namely a one dimensional non-linear marine ecosystem model of NPZD (N for dissolved inorganic nitrogen, P for phytoplankton, Z for zooplankton and D for detritus) type. The main goal of this work is to obtain periodic parameters and to investigate the impact of the linearization on the model output. For this purpose, two experiments are carried out. The first experiment deals with linearization about synthetic data. In the second experiment we linearize about reference trajectory based on measurement data. In both cases we use the obtained optimal periodic parameters also in a validation experiment with the original non-linear version of the model. The quality of the model-data fit of the original non-linear NPZD model using periodic parameters obtained with synthetic data is poor compared to the data fit quality obtained with measurement data.

Keywords: Biogeochemical Model, NPZD Model, Parameter Optimization, Open Loop Optimal Control, Periodic Parameters.

Reference to this paper should be made as follows: El Jarbi, M. and Slawig, T. (2014) 'Extension of a Marine Ecosystem Model using Discrete Open Loop Optimal Control', *Int. J. Mathematical Modeling and Numerical Optimisation*, Vol. x, No. x, pp.xxx–xxx.

Biographical notes: M. El Jarbi is currently a Ph.D. student in the research group *Algorithmic Optimal Control - CO_2 Uptake of the Ocean* at the Christian-Albrechts-Universität zu Kiel in the Institute for Computer Science. His research interest lie in the field of parameter optimization in climate models, Linear Optimal Control for nonlinear optimization.

T. Slawig is professor at the Christian-Albrechts-Universität zu Kiel in the Institute for Computer Science. He is leader of the research group *Algorithmic Optimal Control - CO_2 Uptake of the Ocean* in the Cluster *Future Ocean*. His research interest lie in the field of optimal control for partial differential equations, optimization and algorithmic differentiation.

1 Introduction

The one-dimensional marine ecosystem model under consideration simulates the interaction of dissolved inorganic nitrogen, phytoplankton, zooplankton and detritus (dead material), thus is of so-called NPZD type (Oschlies and Garcon, 1999), whose concentrations (in mmol N m^{-3}) are denoted by the model variables $(x^{(l)})_{l=N,P,Z,D} =: \mathbf{x}$.
The model is given by the following system of partial differential equations:

$$\frac{\partial x^{(l)}}{\partial t} = -\omega^{(l)} \frac{\partial x^{(l)}}{\partial z} + \frac{\partial}{\partial z}\left(\nu_\rho \frac{\partial x^{(l)}}{\partial z}\right) + S^{(l)}(\mathbf{x}, \mathbf{u}), \quad l = N, P, Z, D, \tag{1}$$

with $x^{(l)} : [0, T] \times [-H, 0] \longrightarrow \mathbb{R}$, where T is the time horizon and H the maximum depth (the height of the water column). The variable z denotes the only remaining, vertical spatial coordinate. The $S^{(l)}$ are biogeochemical coupling terms for the four tracer and $\mathbf{u} = (u_1, \ldots, u_p)$ is the vector of unknown physical and biological parameters, with $p = 12$ for this specific model. The equation for detritus also contains a sinking term with total speed $\omega^{(D)} = \omega_s > 0$ which is also optimized as u_{12}, whereas $\omega^{(N)} = \omega^{(P)} = \omega^{(Z)} = 0$ in (1).

A open loop optimal control problem is defined as

$$\min_{\mathbf{u}} \mathcal{J}(\mathbf{u}) \quad \text{subject to} \quad (1), \tag{2}$$

where $\mathcal{J}$ is a cost functional which will be introduced later.

The main objective of this paper is first to obtain periodic parameters by applying open loop discrete linear optimal control DOLOC using linearization of the model and to investigate the impact of the linearization scheme on the fit of model-data fit by using the obtained periodic parameters in the original non-linear NPZD model. In order to achieve this, two groups of parameter optimization experiments are carried out. First, a linearization about synthetic data for the state is performed. Second, a linearization based on available measurement data is introduced. In order to verify our approach and assess the goodness of the obtained periodic parameters for both experiments, an additional validation experiment is carried out, too. We demonstrate that by introduction of time varying parameters, we have enhanced the original non-linear NPZD model. Using measurement data in the linearization scheme it delivers very good results and it still provides reasonable results if synthetic data is used instead.

The work presented in this paper is motivated by results obtained for a typical marine ecosystem model, namely the NPZD model introduced in (Oschlies and Garcon, 1999; Schartau and Oschlies, 2003a). As reported in several publications regarding different optimization algorithms, the quality of the model-to-data fit was not optimal, and in some cases it was difficult to identify the parameters uniquely, see for example (Fasham and Evans, 1995; Losa et al., 2003; Matear,

1995; Prunet et al., 1996; Ward et al., 2010; Rückelt et al., 2010). In most cases (and in all these studies), the parameters of the marine ecosystem models are assumed to be temporally constant. This reflects the aim to obtain a model that is applicable for arbitrary time intervals. In contrast, in our work we allow the parameters to vary temporally over the year while remaining periodic over all years of the considered time interval.

To obtain our model, we discretize and linearize the non-linear state (1) about a reference trajectory and apply a Discrete Open Loop Optimal Control DOLOC problem. An Open Loop discrete linear optimal control, also called a non-feedback controller, is a type of controller that computes its input (control, parameter vector) into a system using only the current state and its model of the system. A characteristic of the open loop controller is that it does not use feedback to determine if its output has achieved the desired goal of the input (control). This means that the system does not observe the output of the process it controls. Consequently, a true open loop system can not correct any error it makes. We allow the parameters to be time-dependent, apply a well-established method for optimal control, and additionally impose the constraint of annual periodicity.

The structure of our paper is as follows: In Section 2 we briefly describe the model and the cost function to be optimized. In Section 2.4 we briefly describe the DOLOC method. Its application to the NPZD model and the reference trajectory are presented in Section 3. In Section 4 we present our results obtained by the DOLOC method with respect to the quality of the model-data misfit and the periodicity of the parameters. We furthermore show results for validation with the original non-linear model using the optimized periodic parameters. Section 5 ends the paper with some conclusions.

2 One-Dimensional NPZD-Model

In this section we briefly describe the NPZD model in the continuous form, see (1), as well as in the discrete form that we use to apply the DOLOC approach. The considered model (1) is a one-dimensional marine ecosystem model driven by pre-computed ocean circulation data (Oschlies and Garcon, 1999). It simulates the interaction of dissolved inorganic nitrogen (N), phytoplankton (P), zooplankton (Z) and detritus (D).

2.1 Model Equations

The model is given as a system of partial differential equations (1). The biogeochemical coupling (or source-minus-sink) terms are taken from (Oschlies and Garcon, 1999) (with model parameters stated in Table 1) and read:

$$\begin{aligned}
S^{(N)}(\mathbf{x},\mathbf{u}) &= -\bar{J}(x^{(N)},z,t)x^{(P)} + u_4 x^{(Z)} + u_{10}x^{(D)},\\
S^{(P)}(\mathbf{x},\mathbf{u}) &= \bar{J}(x^{(N)},z,t)x^{(P)} - u_8 x^{(P)} - G(u_6,u_7)x^{(Z)},\\
S^{(Z)}(\mathbf{x},\mathbf{u}) &= u_1 G(u_6,u_7)x^{(Z)} - u_4 x^{(Z)} - u_9 {x^{(Z)}}^2,\\
S^{(D)}(\mathbf{x},\mathbf{u}) &= (1-u_1)G(u_6,u_7)x^{(Z)} + u_9 {x^{(Z)}}^2, + u_8 x^{(P)} - u_{10}x^{(D)}.
\end{aligned} \tag{3}$$

Here, $\bar{J}$ is the daily averaged phytoplankton growth rate as a function of depth z and time t, and G is the grazing function:

$$\bar{J}(x^{(N)}, z, t) = \min\left(\bar{J}(z,t), u_2 c^T \frac{x^{(N)}}{u_{12} + x^{(N)}}\right), \quad G(u_6, u_7) = \frac{u_7 u_6 {x^{(P)}}^2}{u_7 + u_6 {x^{(P)}}^2}.$$

The zooplankton grazing function G describes the transfer from phytoplankton to zooplankton and detritus. The circulation data are the turbulent mixing coefficient $\kappa = \kappa(z,t)$ and the temperature $T = T(z,t)$ which is used in the non-linear term c^T where $c = 1.066$ is a constant. In total, there are twelve model parameters subject to optimization, all of them being summarized in Table 1. For more details on the model and the involved parameters we refer the reader to (Oschlies and Garcon, 1999; Schartau and Oschlies, 2003a) for a more thorough description.

Table 1 Parameters of the ecosystem model to be optimized with the DOLOC method. Here $\mathbf{u}_0 = (u_{0,i})_{i=1,\ldots,12}$ is the vector of parameters taken from (Oschlies and Garcon, 1999)

parameter	u_i	$u_{0,i}$	units
Assimilation efficiency of zooplankton	γ_1	0.75	
Growth rate parameter	a	0.6	day^{-1}
Initial slop of P-I Curve	α	0.025	$\mathrm{m}^2\ \mathrm{W}^{-2}\ \mathrm{d}^{-1}$
Zooplankton excretion	γ_2	0.03	day^{-1}
Light attenuation by phytoplankton	k_c	0.03	$\mathrm{m}^{-1}(\mathrm{mmol\ m}^{-3})^{-1}$
Prey capture efficiency	ϵ	1	$(\mathrm{mmol\ m}^{-3})^{-2}\,\mathrm{d}^{-1}$
Maximum grazing rate	g	2	d^{-1}
Specific mortality rate	μ_p	0.03	day^{-1}
Zooplankton quadratic mortality	μ_z	0.2	$(\mathrm{mmol\ m}^{-3})^{-1}\ \mathrm{d}^{-1}$
Remineralization rate parameter of detritus	μ_D	0.05	day^{-1}
Sinking velocity of detritus	w_s	5	$\mathrm{m\ day}^{-1}$
Half-saturation constant for N uptake rate	K_N	0.5	$\mathrm{mmol\ m}^{-3}$

Carbon Primary Production

In addition to the tracers N, P, Z and D, the so-called carbon fixation or carbon primary production measured as carbon uptake (denoted as PP in the following) is additionally taken into account in the optimization process for this model (Schartau and Oschlies, 2003a; Rückelt et al., 2010). For a given depth z and time t, it can be formulated as

$$y^{(\mathrm{PP})} := \bar{J}(x^{(N)}, z, t) \cdot x^{(P)} \cdot \mathcal{R}, \tag{4}$$

where $\mathcal{R}$ denotes the Redfield ratio, see, e.g., (Redfield et al., 1963). It depends non-linearly on the states $x^{(N)}$ and $x^{(P)}$, i.e., the tracers dissolved inorganic nitrogen (N) and phytoplankton (P). The relation between carbon (C), nitrogen

(N) and phosphorus (P) in marine phytoplankton is given as $C : N : P = 106 : 16 : 1$. Thus, N can be used as a model state from which the potential uptake of CO_2 can be estimated (assuming that there is no limit on phosphorus P and carbon dioxide CO_2 in the water). The state PP is calculated internally in the model simulation and provided as an additional state $y^{(\mathrm{PP})}$ of the full model output $\mathbf{y}$.

Measurement Data and Model Output

The measurement data used here, denoted by $\mathbf{y}^{(\mathrm{mes})} := (y^{(l,\mathrm{mes})})_{l=N,P,Z,D,\mathrm{PP}}$, are taken from the Bermuda Atlantic Time-series Study (called BATS) as a part of the US Joint Global Ocean Flux Study, see (Michaels and Knap, 1996). The BATS data are provided by the Bermuda Biological Station for Research (BBSR) situated in the Atlantic Ocean 700 miles from the East Coast of the U.S. at coordinates 31N 64W (see `http://www.bbsr.edu/users/ctd/`). In this work each measurement value has to be compared to a corresponding value generated by the model $\mathbf{y} := (y^{(l)})_{l=N,P,Z,D,\mathrm{PP}}$. For this purpose, some transformations have to be done as follows

1. A linear transformation to chlorophyll a (denoted as CHL) as a function of phytoplankton $x^{(P)}$, using a constant conversion factor.

2. A linear transformation to particulate organic nitrogen (denoted as PON), calculated as the sum of phytoplankton $x^{(P)}$, zooplankton $x^{(Z)}$ and detritus $x^{(D)}$.

3. For zooplankton, a vertically averaged concentration in the water column down to the given depth of the measurement point (which is approximately 200 meters) is calculated.

4. Vertically integrated mesozooplankton biomass $y^{(Z,\mathrm{mes})}$ in (mmol m^{-2}) corresponding to

$$\int \frac{x^{(Z)} - 0.096504}{1.2344}\, dz =: y^{(Z)} \tag{5}$$

   Here, an additional assumption about the relation of mesozooplankton biomass $y^{(Z,meso)}$ to total zooplankton biomass $y^{(Z)}$ according to the formula

$$y^{(Z)} = 1.2344 \cdot y^{(Z,meso)} + 0.096504$$

   is incorporated.

5. A 24-hourly temporal mean of the modeled carbon primary production CUP is calculated to make it commensurable with observations from 24-hourly incubation measurements.

2.2 Optimization Problem

In this work, we consider five types of measurement data $\mathbf{y}^{(\text{mes})} := (y^{(l,\text{mes})})_{l=N,P,Z,D,\text{PP}}$, which correspond to aggregated values $\mathbf{y} := (y^{(l)})_{l=N,P,Z,D,\text{PP}}$ of the model output.

The aim of the optimization is to fit the model output $\mathbf{y}$ to the given measurement data $\mathbf{y}^{(\text{mes})}$ over a chosen time interval of j_{max} years.

We denote by $N_{l,j}$ the number of measurement data for $y^{(l,\text{mes})}$ for each observed quantity $l = N, P, Z, D, \text{PP}$ and each year $j = 1, \ldots, j_{max}$.

These numbers may be different for each l and j.

The i-th measurement in year j of $y^{(l,\text{mes})}$ is denoted by $y_{i,j}^{(l,\text{mes})}$, and the corresponding aggregated model output value by $y_{i,j}^{(l)}$.

We now firstly compute the averaged annual misfit per model output/tracer, each weighted with the inverse of its standard deviation taken from (Schartau and Oschlies, 2003a) and summarized in the vector

$$\sigma = (\sigma_l)_{l=N,P,Z,D,\text{PP}} = (0.1,\ 0.01,\ 0.01,\ 0.0357,\ 0.025),$$

and with the inverse of the number $N_{l,j}$ of measurements per tracer and year:

$$\mathcal{F}_{l,j} := \sum_{i=1}^{N_{l,j}} \frac{(y_{i,j}^{(l)} - y_{i,j}^{(l,\text{mes})})^2}{\sigma_l^2 N_{l,j}},\ l = N, P, Z, D, \text{PP}, j = 1, \ldots, j_{max}.$$

If there are no measurement data for a state variable/tracer in a year (i.e., $N_{l,j} = 0$), the sum is set to zero.

The overall cost function is then calculated as

$$\mathcal{F} = \frac{1}{N_{total}} \sum_{j=1}^{j_{max}} \sum_{l=N}^{\text{PP}} \mathcal{F}_{l,j}, \tag{6}$$

where N_{total} is the total numbers of non-zero terms $\mathcal{F}_{l,j}$ actually occurring in the sum.

In the usual case we have $N_{total} = 5 j_{max}$.

Whenever $N_{i,j} = 0$ (and thus $\mathcal{F}_{l,j} = 0$) for a year and tracer, N_{total} is decreased accordingly.

2.3 Discretization Scheme

The continuous model (1) is discretized and solved using an operator splitting method, which for a given time step Δt reads

$$\begin{aligned}[\mathbf{I} - \Delta t \mathbf{H}_k^{\text{diff}}]\, \mathbf{x}_{k+1} =& [\mathbf{I} + \Delta t \mathbf{H}^{\text{sink}}] \mathcal{L}_k \circ \mathcal{L}_k \circ \mathcal{L}_k \circ \mathcal{L}_k(\mathbf{x}_k, \mathbf{u}_k), \\ & k = 1, \ldots, M-1. \end{aligned} \tag{7}$$

Here $\mathbf{x}_k = (x_k^{(N)}, x_k^{(P)}, x_k^{(Z)}, x_k^{(D)})$ is the vector of all four tracers and $\mathbf{u}_k$ the parameter vector (which is already assumed to be time-varying, here), both at the current time step k.

The total number of time steps is M.

The matrices $\mathbf{H}_k^{\text{diff}}$, $\mathbf{H}^{\text{sink}}$ are 4×4 block-diagonal and represent the discretization of diffusion (discretized by second order central differences) and sinking (discretized by an upstream scheme), respectively, $\mathbf{I}$ is the identity matrix and $\mathcal{L}_k$ is a nonlinear operator which will be introduced below.

The interpretation of the scheme (7) is the following: In every time step $k \to k+1$, at first the non-linear coupling terms $\mathbf{S}_k = (S_k^{(N)}, S_k^{(P)}, S_k^{(Z)}, S_k^{(D)})$ are computed at every spatial grid point and integrated by four explicit Euler steps with stepsize $\frac{\Delta t}{4}$, each of which is described by the operator

$$\mathcal{L}_k(\mathbf{x}_k, \mathbf{u}_k) := \left[I + \frac{\Delta t}{4} \mathbf{S}_k(\mathbf{x}_k, \mathbf{u}_k) \right]. \tag{8}$$

Then, an explicit Euler step with full step-size Δt is performed for the sinking term, represented by the matrix $[\mathbf{I} + \Delta t \mathbf{H}^{\text{sink}}]$.

Finally, an implicit Euler step is applied for the diffusion operator, discretized with second order central differences.

Due to $\kappa = \kappa(z,t)$ the resulting matrix $[\mathbf{I} - \Delta t \mathbf{H}_k^{\text{diff}}]$ depends on the current time step k.

The discrete system can now be formally written as

$$\begin{aligned} \mathbf{x}_{k+1} &= [\mathbf{I} - \Delta t \mathbf{H}_k^{\text{diff}}]^{-1} [\mathbf{I} + \Delta t \mathbf{H}_k^{\text{sink}}] \mathcal{L}_k \circ \mathcal{L}_k \circ \mathcal{L}_k \circ \mathcal{L}_k(\mathbf{x}_k, \mathbf{u}_k) \\ &=: f(\mathbf{x}_k, \mathbf{u}_k), \quad k = 1, \ldots, M-1, \end{aligned} \tag{9}$$

where f is a non-linear function.

2.4 Discrete Open Loop Optimal Control

In this section we briefly describe the usage of the Discrete Open Loop Optimal Control DOLOC method. It is a mathematical technique to compute optimal controls in linear dynamical systems. The general aim of the DOLOC method is to influence the state of a system by using controls to obtain a desired or optimal state related to a cost functional. Discrete Open Loop Optimal Control is a non-feedback system in which the control input to the system is determined using only the current state of the system and a model of the system. There is no feedback to determine if the system is achieving the desired output based on the reference input or set point. In contrast to a closed loop control system, DOLOC does not observe itself to correct itself. DOLOC is thus more prone to errors and cannot compensate for disturbances to the system.

Usually, also the control variables or parameters are time-dependent.

The method is widely used in engineering applications and well-studied from the mathematical point of view, see e.g. (Anderson and Moore, 1971; Casti, 1987; Ghosh, 2004; Kwakernaak and Sivan, 1972); Lewis and Syrmos, 1995; Lunze, 1997; Nagrath, 2006; Rothwell and Cloud, 2002; Rugh, 1996; Shinners, 1998; Sima, 1996). Extensions to non-linear problems are possible, in the first place by linearizing the dynamical system of equations (Clemens, 1993). In this section we provide a brief but self contained of the discrete linear open loop optimal

control. We consider a discrete-time linear system described by the state space representation:

$$\left.\begin{aligned} \mathbf{x}_{k+1} &= A_k\mathbf{x}_k + B_k u_k, \quad k = 1,\dots,M-1 \\ \mathbf{x}_1 &= \mathbf{x}_1^*. \end{aligned}\right\} \tag{10}$$

Where $\mathbf{x}_1^*$ ia a given initial vector in $\mathbb{R}^n$, $\mathbf{x}_k \in \mathbb{R}^n$ is the state vector, $\mathbf{u}_k \in \mathbb{R}^m$ is the control vector, $A_k \in \mathbb{R}^{n\times n}$ is the transition matrix, $B_k \in \mathbb{R}^{n\times m}$ is the control input matrix. The idea of the open loop optimal control method is to minimize the following cost function

$$\mathcal{J}(u) = \frac{1}{2}x_M^\top Q_M x_M + \frac{1}{2}\sum_{k=1}^{M-1} x_k^\top Q_k x_k + u_k^\top R_k u_k, \tag{11}$$

subject to the constraints (10. Here for every k, $Q_k \in \mathbb{R}^{n\times n}$ is a positive semi-definite diagonal weighting matrix for the state vector and $R_k \in \mathbb{R}^{m\times m}$ is a positive definite diagonal weighting matrix for the control vector. The matrices are Q_k and R_k are usually chosen to be diagonal. We will use the notations

$$\begin{aligned} \mathbf{x} &= (\mathbf{x}_k)_{k=1,\dots,M} \in \mathbb{R}^{M\times n} \cong \mathbb{R}^{Mn}, \\ \mathbf{u} &= (\mathbf{u}_k)_{k=1,\dots,M-1} \in \mathbb{R}^{(M-1)\times m} \cong \mathbb{R}^{(M-1)m}, \end{aligned}$$

for the discrete trajectory of state, the control and the measurement vector, respectively.

We will in the following find a sequence of control, $\mathbf{u}_1^*,\dots,\mathbf{u}_{M-1}^*$, that minimizes the cost function (11) for a given $\mathbf{x}_1^*$.
We can recursively use the first equation in (10) as:

$$\begin{aligned} \text{for k =2,} \quad \mathbf{x}_2 &= A_1\mathbf{x}_1^* + B_1\mathbf{u}_1, \\ \text{for k =3,} \quad \mathbf{x}_3 &= A_2A_1\mathbf{x}_1^* + (B_2\mathbf{u}_2) + A_2B_1\mathbf{u}_1) \\ \text{for k =4,} \quad \mathbf{x}_4 &= A_3A_2A_1\mathbf{x}_1^* + (B_3\mathbf{u}_3 + A_3B_2\mathbf{u}_2 + A_2B_2\mathbf{u}_2) \\ &\dots \\ \text{for k=M-1,} \quad \mathbf{x}_M &= A_{M-1}A_{M-2}A_{M-3}\dots A_1\mathbf{x}_1^* + (B_{M-1}\mathbf{u}_{M-1} + \dots + A_{M-1}A_{M-2}A_{M-3}\dots A_2B_1\mathbf{u}_1). \end{aligned}$$

Thus, this system can be written in matrix form as follows:

$$\underbrace{\begin{bmatrix}\mathbf{x}_1\\ \vdots \\ \mathbf{x}_M\end{bmatrix}}_{\mathcal{X}} = \underbrace{\begin{bmatrix} I_{n\times n} \\ A_1 \\ \vdots \\ A_{M-1}A_{M-2}\cdots A_1\end{bmatrix}}_{\mathcal{L}^x}\mathbf{x}_1^* + \underbrace{\begin{bmatrix} 0 & 0 & 0\cdots & 0 \\ B_1 & 0 & 0\cdots & 0 \\ A_2B_1 & B_2 & 0\cdots & 0 \\ \vdots & \vdots & \vdots\ \vdots & \vdots \\ A_{M-1}\cdots B_1 & A_{M-2}\cdots B_1 & & B_{M-1}\end{bmatrix}}_{\mathcal{L}^u}\underbrace{\begin{bmatrix}\mathbf{u}_1\\ \vdots \\ \mathbf{u}_{M-1}\end{bmatrix}}_{\mathcal{U}}$$

The above can be expressed as a system equation

$$\mathcal{X} = \mathcal{L}^x\mathbf{x}_1^* + \mathcal{L}^u\mathcal{U} \tag{12}$$

where $\mathcal{X} = (\mathbf{x}_1, \ldots, \mathbf{x}_M)^\top \in \mathbb{R}^{Mn}$, $\mathcal{U} = (\mathbf{u}_1, \ldots, \mathbf{u}_{M-1})^\top \in \mathbb{R}^{(M-1)m}$, $\mathcal{L}^x \in \mathbb{R}^{Mn\times n}, \mathcal{L}^u \in \mathbb{R}^{Mn\times(M-1)m}$ and $I_{n\times n}$ is the identity matrix in $\mathbb{R}^{n\times n}$.

Using this relation, the quadratic time-dependant cost function (11) becomes:

$$\begin{aligned}\mathcal{J}(\mathcal{U}) &= \mathcal{X}^T Q\mathcal{X} + \mathcal{U}^T R\mathcal{U} \\ &= \begin{bmatrix}\mathbf{x}_1^* \\ \mathcal{U}\end{bmatrix}^T \begin{bmatrix}(\mathcal{L}^x)^T Q\mathcal{L}^x & (\mathcal{L}^x)^T Q\mathcal{L}^u \\ (\mathcal{L}^u)^T Q\mathcal{L}^x & R + (\mathcal{L}^u)^T Q\mathcal{L}^u\end{bmatrix} \begin{bmatrix}\mathbf{x}_1^* \\ \mathcal{U}\end{bmatrix}\end{aligned}$$

Where Q and R are block diagonal matrices and defined as follows

$$\begin{aligned}Q &= [Q_1, \ldots, Q_M] \in \mathbb{R}^{Mn\times Mn}, \\ R &= [R_1, \ldots, R_{M-1}] \in \mathbb{R}^{(M-1)m\times(M-1)m}.\end{aligned}$$

The derivative of $\mathcal{J}$ with respect to $\mathcal{U}$ in order to find the minimum gives:

$$\frac{\partial \mathcal{J}}{\partial \mathcal{U}} = \left[R + (\mathcal{L}^u)^\top Q\mathcal{L}^u\right]\mathcal{U} + (\mathcal{L}^u)^\top Q\mathcal{L}^x\mathbf{x}_1^*$$

and equating it to zero, we find

$$\mathcal{U}^* = -\left[R + (\mathcal{L}^u)^\top Q\mathcal{L}^u\right]^{-1}(\mathcal{L}^u)^\top Q\mathcal{L}^u\mathbf{x}_1^* \tag{13}$$

Now the state equation can be written as

$$\mathcal{X}^* = \left[\mathcal{L}^x - \left[R + (\mathcal{L}^u)^T Q\mathcal{L}^u\right]^{-1}(\mathcal{L}^u)^\top Q\mathcal{L}^u\right]\mathbf{x}_1^* \tag{14}$$

and for any initial value $\mathbf{x}_1^*$ the optimal cost is

$$\mathcal{J}^* = (\mathbf{x}_1^*)^\top \left[(\mathcal{L}^x)^\top Q\mathcal{L}^x - (\mathcal{L}^x)^\top Q\mathcal{L}^u\left[R + (\mathcal{L}^u)^T Q\mathcal{L}^u\right]^{-1}(\mathcal{L}^u)^\top Q\mathcal{L}^x\right]\mathbf{x}_1^*. \tag{15}$$

3 Implementation

The DOLOC approach is based on a linearization of (9) to obtain a linear time-varying problem. The linearization is performed about reference trajectories $(\mathbf{x}^{(r)}, \mathbf{u}^{(r)})$. In order to discuss the impact of the linearization on the model output, two different kinds of linearization are performed. The aim here is to 1.) linearize about synthetic data, 2.) linearize about reference trajectory based on the available measurement data. Moreover, a comparison between both experiments and an optimization with constant parameters will be done.

Reference Parameter Trajectory

A main objective of this work is to enforce periodicity of the parameters/controls. For this purpose, let us assume that the length of a time period – measured in time steps – is $T > 0$ and that $M \bmod T = 0$. We now chose the reference trajectory for the control $\mathbf{u}^{(r)} = (\mathbf{u}_k^{(r)})_{k=1,\ldots,M-1} \in \mathbb{R}^{(M-1)p}$ to be

$$\mathbf{u}_k^{(r)} := \begin{cases} \mathbf{u}_0, & \text{if } k \leq T \\ \mathbf{u}_{k-T}, & \text{if } k > T. \end{cases} \tag{16}$$

Therein, $\mathbf{u}_0$ is the parameter vector determined by optimization in (Oschlies and Garcon, 1999). This vector was used as an initial guess, here. We enforce periodicity of $\mathbf{u}_k = \mathbf{u}_k^{(r)} + \mathbf{v}_k = \mathbf{u}_{k-T} + \mathbf{v}_k$ for $k \geq T + 1$.

Reference State Trajectory

For the reference state trajectory to the first experiment, we use synthetic data. They are substituted by model results, that were produced with a reference parameter set. We assume that the entire state vector $\mathbf{x}^{(r)}$ is given for all time steps during an annual cycle. The motivation here is that unless the method works fine with the synthetic data, there is no point using it with real data. The model output is considered as a reference providing synthetic data $\mathbf{y}^{(\text{synt})}$ that can be used to access the performance of the DOLOC method implemented in the model. For the second experiments, we use actually available measurement data $\mathbf{y}^{(\text{mes})}$. The reference trajectory for the state will be given as:

for the first experiment:

$$\mathbf{x}_k^{(r)} := \begin{cases} \mathbf{x}_k^{(\text{synt})}, & \text{if } k \leq T \\ \mathbf{x}_{k-T}, & \text{if } k > T. \end{cases} \tag{17}$$

For the second experiment, the reference trajectory $\mathbf{x}_k^{(r)}$will be based on the available measurement data. We use the same strategy described in (El Jarbi et al., 2013)

Weighting Matrices Q and R

In our example, the weighting matrices $\mathbf{Q}_k$ are taken as constant for all k, namely

$$\mathbf{Q}_k = \mathbf{Q} \;=\; \text{diag}(\frac{1}{\sigma_l^2})_{l=N,P,Z,D,PP}, \quad k = 1, \ldots, M,$$

where the σ_l are the standard deviations of the synthetic data around its mean distribution. The matrices $\mathbf{R}_k$ are taken as

$$\mathbf{R}_k = \text{diag}(r_n^{(k)})_{n=1,\ldots,p}, \quad r_n^{(k)} > 0.$$

We choose different values in the first year and in all subsequent years, respectively. In all years except for the first one (i.e. $k \geq T$), the $\mathbf{R}_k$ are used to enforce periodicity of the parameters. The bigger the $r_n^{(k)}$ for these years are, the better is the expected periodicity of the parameters. Following this idea, the optimal choice for the $\mathbf{R}_k$ in the first year would be just zero matrices.

But by this choice the requirements for the DOLOC method – where the $\mathbf{R}_k$ have to be positive definite – are not satisfied.

As a consequence, it is desirable to choose the $r_n^{(k)}$ for the first year as small as possible.

On the other hand, the choice of the $r_n^{(k)}$ in the first year can be used to keep the parameters in the admissible bounds. Since they can be kept in vicinity of the initial guess in the first year and forced to stay close to it due to the periodicity enforcement in the following years, by a careful setting of the $r_n^{(k)}$ in the first year both aims (periodicity and boundedness) can be balanced. This effect is not guaranteed by the DOLOC method, but turns out to be realizable in our case, as we will see in the next section.

Summarizing, for our computations we chose for $n = 1, \ldots, p$ the values

$$r_n^{(k)} = \begin{cases} \dfrac{1}{|(u_{0,n})|^2}, & k \leq T \\ \dfrac{1}{|(u_{k-T,n})|^2}, & k \geq T+1, \end{cases} \tag{18}$$

where $\mathbf{u}_0$ is as listed in Table 1.

4 Optimization Results

In this section we present the results of the parameter optimization runs performed with the DOLOC method. We present the fit of the annual periodicity of the obtained parameters for the two experiments . Additionally, we show how the obtained periodic parameters of the linearized model validate with the original non-linear model.

4.1 First Parameter Optimization Experiment: Linearization About the Synthetic Data

In this subsection we examine the optimized model output obtained by the DOLOC method with periodic parameters and synthetic data. Figure 1 shows the model results obtained by the DOLOC method with periodic parameters for aggregated model output $\mathbf{y}$ and synthetic data $\mathbf{y}^{(\mathrm{synt})}$ for the years 1994 to 1998 for the uppermost layer at depths $z \approx 5m$. The presented results concern a part of the whole time interval at some distinct depth layer, only. The total number of depth layers considered in the optimization process is 32 and the total number of time steps is $43,800$. We can see, that the model output for all four tracers follows the synthetic data in a better way. Moreover, the difference between both plots is scarily recognizable.

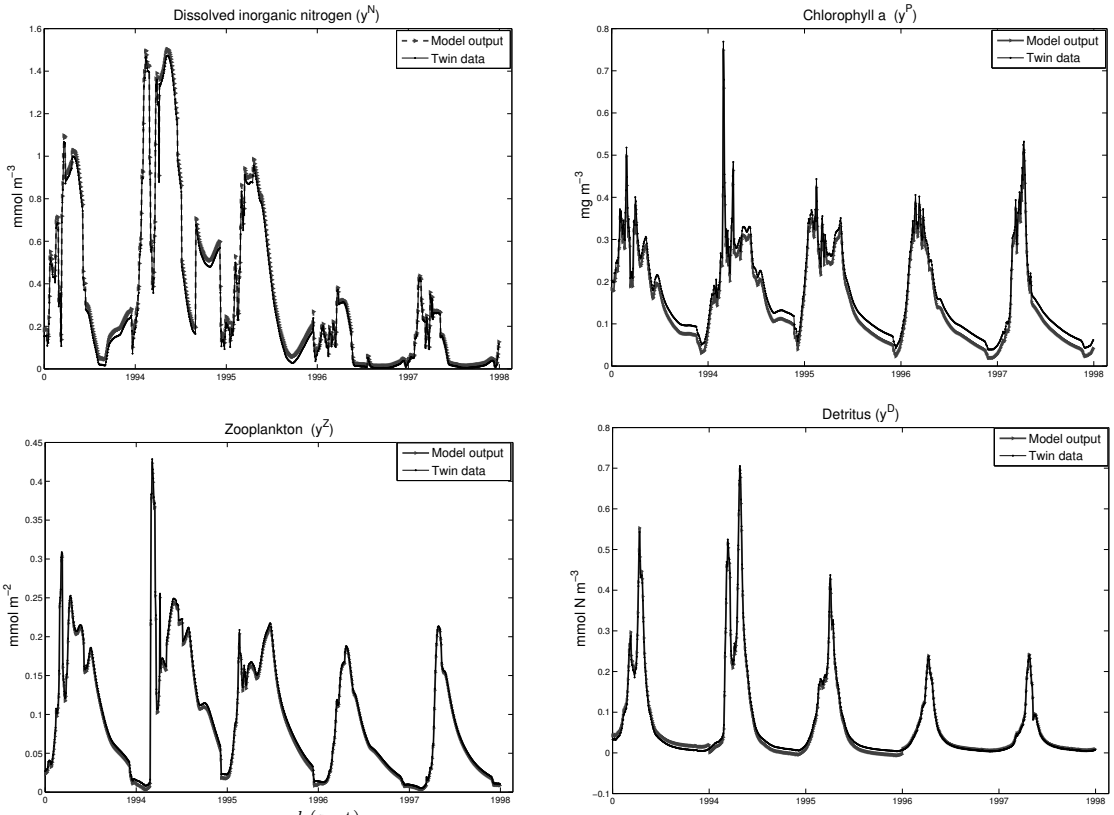

Figure 1 Synthetic data $\mathbf{y}^{l,(\mathrm{synt})}, l = N, P, Z, D$ and aggregated model trajectories $\mathbf{y}^{(l)}, l = N, P, Z, D$, optimized with periodic parameters obtained by the DOLOC method. Values are shown for the upper layer at depth $z \approx 5m$ and years 1994-1998.

Figures 2 illustrates the temporal behavior of the parameters that were optimized with the DOLOC method. Depicted are only those ten parameters that show a temporal variation. Two parameters remain constant in time. These figures show different trajectories for each parameter for two years with the different choices of the r_n^k (compare Table 1). As mentioned before, it is obvious that for a smaller r_n^k, the amplitude of the parameters increases, but it always remains almost periodic. Since the periodicity of the parameters is nearly perfect, it is enough to show the plot for 2 years.

The parameters controlling the growth of phytoplankton, namely the maximum growth rate a and the initial slope of the P-I curve α shown in Figure 2 both take their maximum values in early summer and in winter and have a clear minimum value in spring during the peak of the annual chlorophyll signal. This is consistent with earlier assimilation studies that, for assumed constant parameters, tended to overestimate plankton production at BATS during the bloom end of winter and, at the same time, tended to underestimate production in oligotrophic summer conditions and in early winter, see (Schartau et al., 2001). Such a trend to relatively high values of α has also been found in earlier studies that optimized

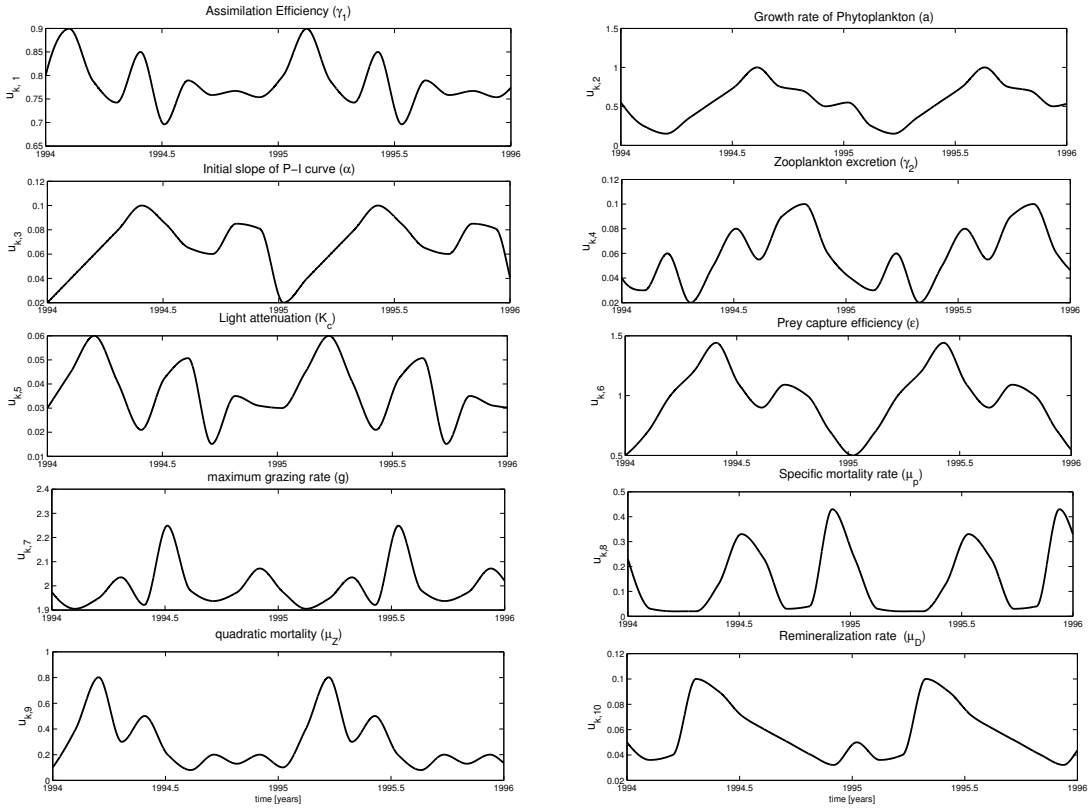

Figure 2 Periodicity of optimal parameters $(u_{k,n})_{n=1,\dots,10}$ obtained by the DOLOC method using the synthetic data in the linearization scheme.

parameter values by data assimilation, see (Fasham and Evans, 1995; Schartau et al., 2001). Earlier studies assuming time-independent parameter values have attributed relatively high values of α to the absence of a dial cycle in the turbulent mixing, which might allow for substantial phytoplankton growth even in winter during reduced daytime mixing, see (Schartau and Oschlies, 2003a). This is consistent with the findings of the current study, that also suggests high values of α during the period of deep mixing in winter.

In addition, our optimized model predicts even higher values of the initial slope parameters α for late spring and early summer, where the mixed layer is usually shallow and growth is limited by nutrients rather than light in the surface mixed layer. A large value of α can, however, help to establish a subsurface chlorophyll maximum in better agreement with the observations. Our results reported here indicate that, at BATS, high values of α may be more important for the establishment of deep chlorophyll in late spring than for the maintenance of phytoplankton production during periods of deep mixing in winter. Maintenance of high primary production during summer has been difficult to achieve by earlier models run at BATS (Schartau et al., 2001). As nutrient supply to the surface waters is low during the stratified season, models with fixed carbon-to-nutrient

stoichiometry and constant model parameters do not seem to be able to reach observed levels of primary production in the surface layer, see (Schartau and Oschlies, 2003b).

In the current study, the carbon-to-nutrient factor used to convert simulated (nitrogen-based) primary production into observed (carbon-based) primary production is constant as well. However, the seasonally varying parameters can contribute to maintain high levels of primary production during summer in the absence of substantial inputs of new nutrients. This is realized by enhanced recycling of biomass, evident by high maximum grazing rates, high assimilation efficiencies, high prey capture efficiencies and high zooplankton excretion in late spring and early summer. Similarly, remineralization of detritus is highest in late spring as well. These high rates all contribute to fast recycling of nutrients in the ocean surface, which helps to maintain observed high rates of primary production and thereby reduces the model-data misfit function.

4.2 Second Parameter Optimization Experiment: Linearization About the Measurement Data

As s second case, this Section presents a comparison between the optimized model output obtained by the (DOLOC) with periodic parameters and the measurement data.

Figure 3 shows the model results obtained by the DOLOC method with periodic parameters for aggregated model output $\mathbf{y}$ and the measurement data $\mathbf{y}^{(\mathrm{mes})}$ for the years 1994 to 1998 for the uppermost layer at depths $z \approx 5m$. The DOLOC method with periodic parameters gives a nearly perfect fit of the data. It is recognizable, that the model output for all four tracers almost exactly hits the measurement data. We point out that it is not an accident that the results are very nice with both synthetic data and measurement data. The aim of the method is to minimize the error $e_k = \mathbf{y}_k - \mathbf{y}_k^{(r)}$, where $\mathbf{y}$ denotes the model output and $\mathbf{y}_k^{(r)}$ is the available reference trajectory (e.g., the measurement and the synthetic data). For this reason, if we use reference trajectory for the linearization about the state, we will reach a nearly perfect fit of the data. Moreover, the error defined above also depends on the choice of Q and R. If we choose a larger R, the control (e.g., $\mathbf{u}_k - \mathbf{u}_k^{(r)}$) is forced to get smaller and so the state (e.g., here, the error) tends to zero more slowly. If we take a smaller R, larger values for the control are allowed which leads to a faster decay to zero of the state.

Figure 4 illustrates the temporal behavior of the parameters that were optimized with the DOLOC method. This figure shows different trajectories for each parameter for two years. One can see that the above model-to-data fit can be achieved with parameters that are almost annually periodic. In comparison to Figure 2, which is obtained using the linearization about the synthetic data, we observe that the deviation to the reference parameters (see Table 1) is smaller when using the measurement data in the linearization scheme. What that means and what effect it has to the model output in relation to the measurement data if the original non-linear NPZD model is used will be studied in the next section.

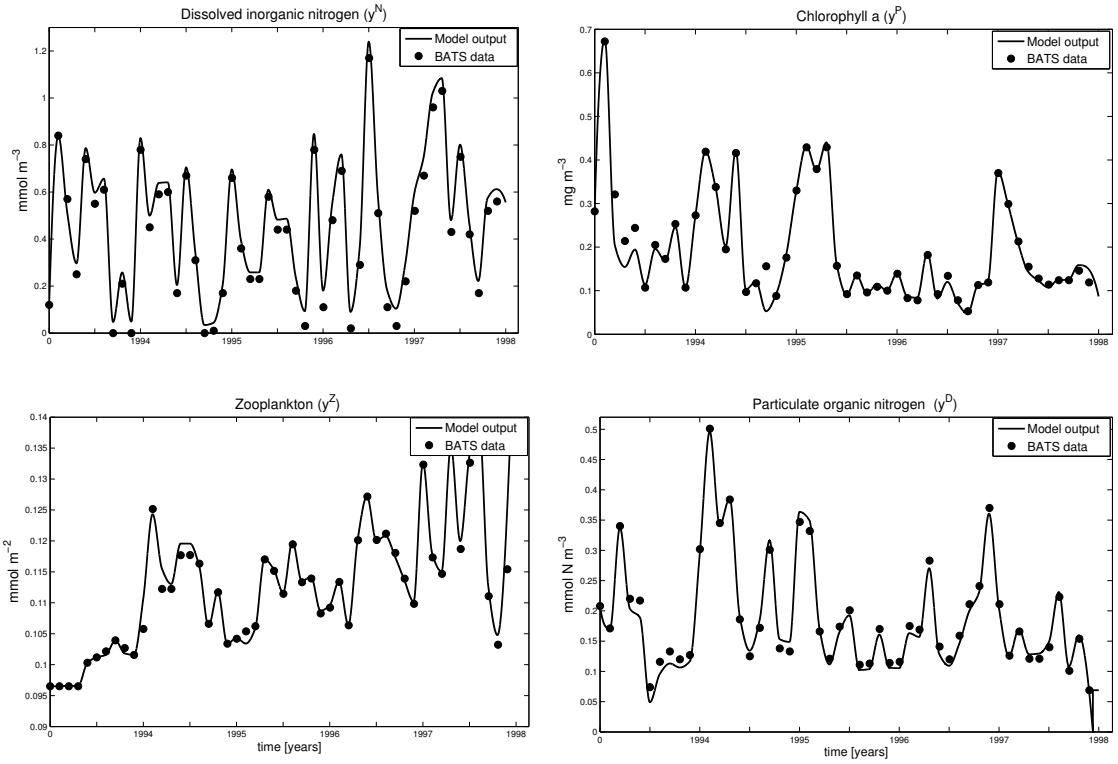

Figure 3 Observational BATS data $\mathbf{y}^{(l,\mathrm{mes})}, l = N, P, Z, D$ and aggregated model trajectories $\mathbf{y}^{(l)}, l = N, P, Z, D$, optimized with periodic parameters obtained by the DOLOC method. Values are shown for the upper layer at depth $z \approx 5m$ and years 1994-1998.

4.3 Validation of the Non-Linear Model with Periodic Parameters

In this section, we examine the importance of the linearization scheme for the parameter optimization using the DOLOC method. The periodic parameters obtained by the DOLOC method are validated by an experiment using the original non-linear NPZD model. We run the original non-linear model with the parameters obtained by using the linearization about synthetic data, as well as with the parameters obtained by using the linearization about measurement data. We do both runs for the years 1994 to 1998 without further parameter optimization and analyze the corresponding model-data misfit.

Figure 5 shows a comparison of the model output using the obtained optimal periodic parameters by the first and second experiment, respectively, along with the measurement data in the uppermost layer. The use of periodic parameters obtained by the linearization about the measurement data in comparison to those obtained by the linearization about the synthetic data results in a significantly better model-data fit. The results for $y^{(P)}$ and $y^{(D)}$ are almost perfect, whereas

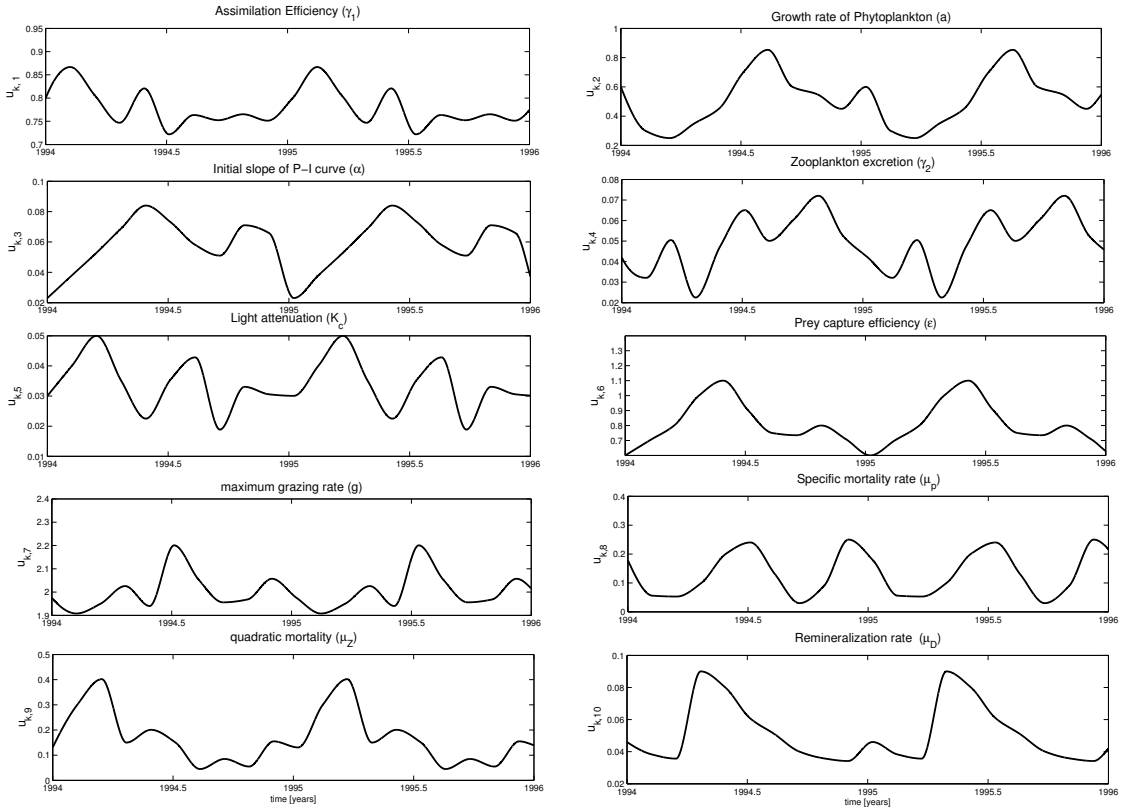

Figure 4 Periodicity of optimal parameters $(u_{k,n})_{n=1,\ldots,10}$ obtained by the DOLOC method using the measurement data in the linearization scheme.

for the other two tracers they are slightly worse. The results look similar for all layers.

We point out that the quality of the obtained periodic parameters depends on the selection of the reference trajectory of the state. The periodic parameters obtained by using the measurement data in the linearization scheme are not so large and they need not react in such a way as for the other linearization scheme, in which the periodic parameters react more to deviations. Figure 6 shows the absolute deviation to the reference parameters (see, Table 1) for both linearization schemes. The periodic parameters obtained by using the measurement data interpret a small deviation from the measurement data to the model output of the non-linear NPZD model. Thus the difference $(\mathbf{y} - \mathbf{y}^{(\mathrm{mes})})$ is forced to get small since larger parameter values would not improve the results in a justifiable way. Figure 6 confirms the better solution behavior of the second experimental setting.

Summarizing the results, one can say that relatively large parameters do not yield a better validation. It seems that a linearization about measurement data is much more meaningful than a linearization about synthetic data.

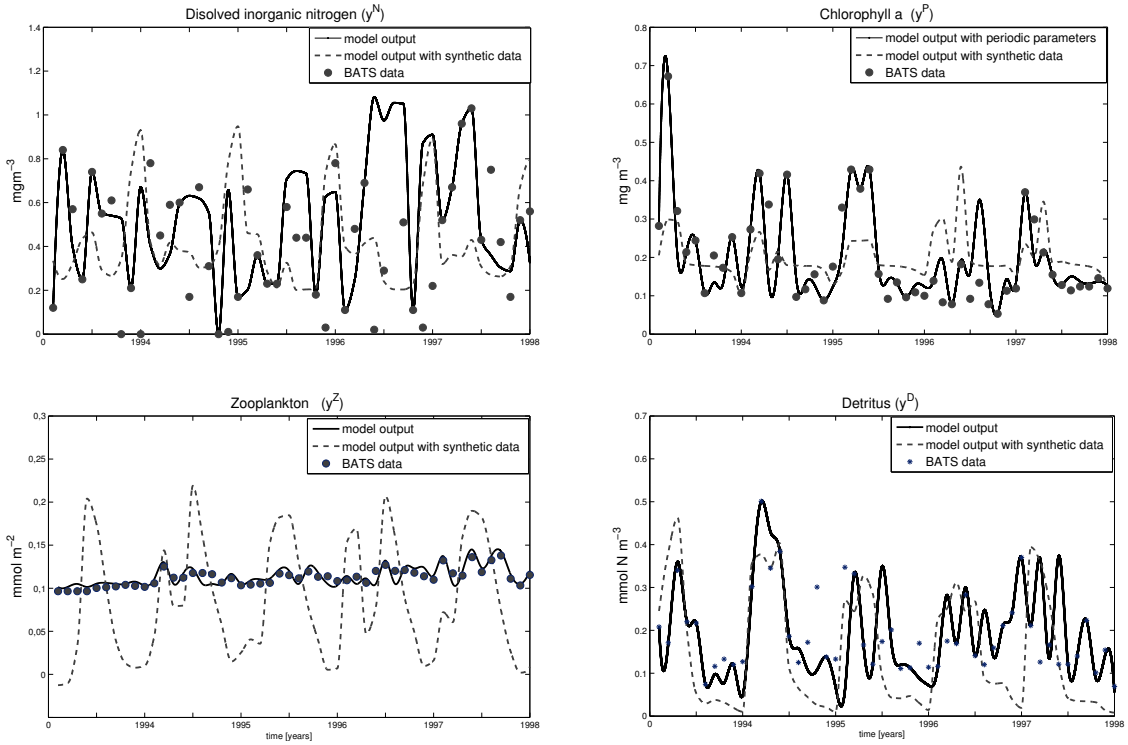

Figure 5 Observational BATS data $\mathbf{y}^{(l,\mathrm{mes})}, l = N, P, Z, D$ and aggregated model trajectories $\mathbf{y}^{(l)}, l = N, P, Z, D$ obtained by incorporating optimal periodic parameters from the DOLOC experiments into the original non-linear model. The results are given for depth $z \approx 5m$ and for the years 1994 - 1998. One result is obtained by taking the optimal periodic parameters that were derived with DOLOC using synthetic data in the linearization scheme. The other result is obtained by taking the optimal periodic parameters that were derived with DOLOC using measurement data in the linearization scheme. In both cases the optimization with DOLOC was initialized with constant parameters obtained by a Sequential Quadratic Programming (SQP) method.

5 Conclusion

In this paper, we used the method of Discrete Open Loop Optimal Control DOLOC to determine optimal periodic parameters in a one-dimensional marine ecosystem model for two optimization experiments.

We demonstrated that the DOLOC method can be applied on the considered parameter optimization problem for a non-linear NPZD type ecosystem model using a linearization technique about reference trajectories of model variables (biogeochemical tracers and synthetic data) and parameters, where the system matrices were obtained by automatic differentiation.

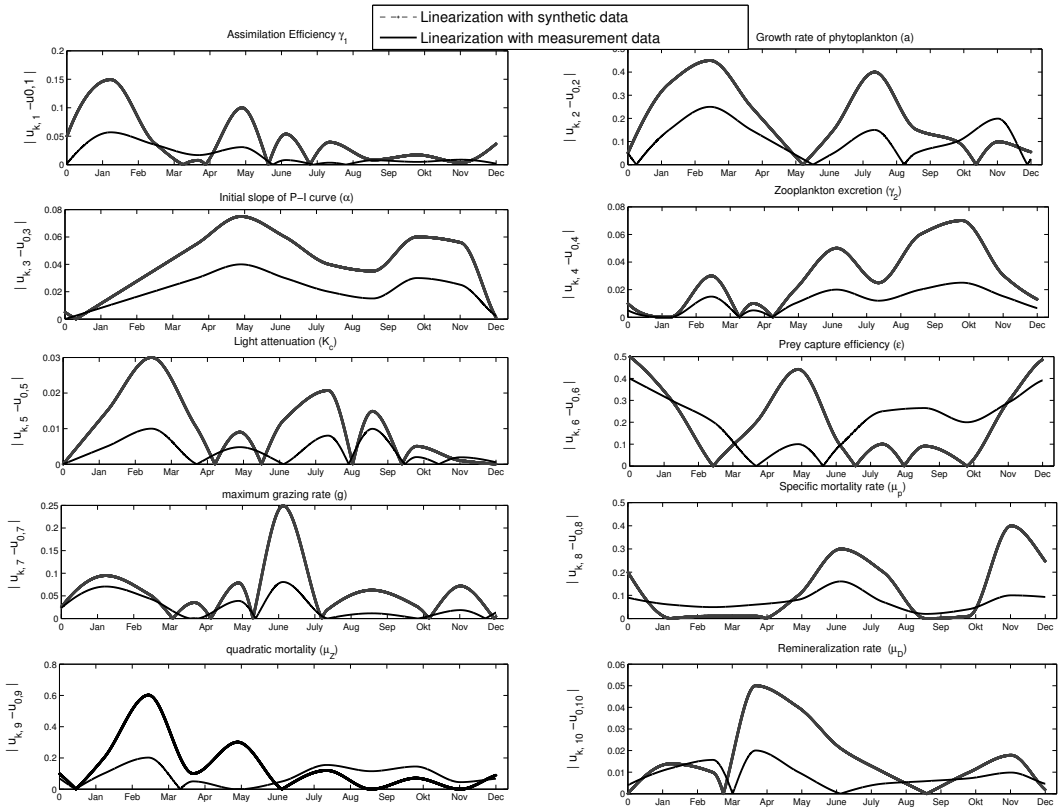

Figure 6 Periodicity of optimal parameters $(u_{k,n})_{n=1,\ldots,10}$ obtained by the DOLOC method.

We have shown how the fit of the model output to measurement data can be affected by selecting the reference tracer trajectory, and how an appropriate choice of reference parameter trajectory can be used to obtain annual periodicity.

We have shown that the linearized model obtained by using measurement data gives a very good model-to-data fit with almost perfect annually periodic parameters. Even if we use synthetic data in the linearization scheme, the quality of the fit is also reasonable. Especially, it is much better than the one previously obtained by optimization of the non-linear model with time constant parameters.

We see that the use of measurement data for the reference trajectory in the linearization scheme makes sense, since the obtained periodic parameters have an impact not only on the linearized model, but also on the original non-linear NPZD model. So a suitable periodic parameter set can lead to very good results.

For both linearization schemes the method allows to further analyze temporal deviations of individual parameters about the annual mean. This may help making inferences about processes that the model cannot describe well when constant parameters are used. The latter analysis should contribute to a better

understanding of model deficiencies and, eventually, help to improve marine ecosystem models.

Moreover, the periodic parameters obtained by using the synthetic data in the linearization scheme may be used in the original non-linear model. Introducing periodic parameterizations with variable coefficients and optimizing them may as well be a starting point for further model development and improvement.

6 Acknowledgments

The authors would like to thank the reviewers and the editor for many fruitful comments. The authors would particularly like to thank Andreas Oschlies, IFM Geomar.

References and Notes

Anderson, B. D. O. and Moore, J. B. (1971), 'Linear Optimal Control', Prentice-Hall, Englewood Cliffs, NJ.

Casti, J. L. (1987), 'Linear Dynamic Systems', Academic Press.

Clemens, D. (1993), 'optimal Nonlinear Control for Power Systems', *IEEE Conference on Control Application*, pp. 241–245.

El Jarbi, M., Rückelt, J., Slawig, T. and Oschlies, A. (2013), 'Reducing the Model-Data Misfit in a Marine Ecosystem Model Using Periodic Parameters and Linear Quadratic Optimal Control', *Biogeosciences*, vol. 10, No. 2, pp. 1169-1182.

Fasham, M., Evans, G. (1995), 'The use of optimization techniques to model marine ecosystem dynamics at the JGOFS station at 47 °N 20 °W', *Phil. Trans. R. Soc. London, Series B*, vol. 348, No. 1324, pp. 203–210.

Ghosh, A. (2004), 'Control systems: Theory and Apllications', *Pearson Education India*.

Kwakernaak, H. and Sivan, R.(1972), 'Linear Optimal Control Systems. Wiley-Interscience', *New York*.

Lewis, F.L., Syrmos, V.L. (1995), 'Optimal Control', *(2nd Ed.). John Wiley & Sons, Inc. New York*.

Losa, S.N., Kivman, G. A., Schroeter, J. and Wenzel, M. (2003), 'Sequential Weak constraint parameter estimation in an ecosystem model', *Journal of Marine Systems*, vol. 43, No. 12, pp. 31–49.

Lunze, J. (1997), 'Regelungstechnik 2', *Springer-Verlag*, Berlin, (in German).

Matear, R.J. (1995), 'Parameter optimization and analysis of ecosystem models using simulated annealing: a case study at Station P' *Journal of Marine Research*, vol. 53, No. 4, pp. 571–607.

Michaels and Knap. (1996), 'The BATS data are provided by the Bermuda Biological Station for Research (BBSR)'. *Research vol. 43, Nos. 2 and 3.* http://www.bbsr.edu/users/ctd/, accessed on 28.09. 2014.

Nagrath, I. J. (2006), 'Control systems Engineering', *New age international*, india.

Oschlies, A. and Garcon, V. (1999), 'An eddy-permitting coupled physical-biological model of the north atlantic.1. sensitivity to advection numerics and mixed layer physics' *Global Biogeochem. Cy.* vol. 13, No. 1, pp. 35–160.

Prunet, P., Minster, J.F., and Ruiz-Pino, D.(1996), 'Assimilation of surface data in a one-dimensional physical-biogeochemical model of the surface ocean: 1. Method and preliminary results', *Global Biogeochemical Cycles*, vol. 10, No. 1, pp. 111–138.

Redfield, A. Ketchum,B. and Richard,F. (1963), 'The influence of organisms on the composition of sea water', *in: M. Hill (Ed.)*, The Sea, Wiley, New York, pp. 26–77.

Rothwell, E. J. and Cloud, M. J. (2002), 'Optimal Control Systems', *Desineni Subbaram Naidu.*

Rückelt, J., Sauerland, V., Slawig, T., Srivastav, A., Ward, B.and Patvardhan, C.(2010), 'Parameter Optimization and Uncertainty Analysis in a Model of Oceanic CO_2-Uptake using a Hybrid Algorithm and Algorithmic Differentiation', *non-linear Analysis*, vol. 11, No. 5, pp. 3993–4009.

Rugh, W. J.(1996), 'Linear System Theory', *2nd Edn., Prentice-Hall, Upper Saddle River*, New Jersey 07458.

Schartau, M. and Oschlies, A.(2003a), 'Simultaneous data-based optimization of a 1d-ecosystem model at three locations in the north Atlantic: Part I–method and parameter estimates', *Journal of Marine Research*, vol. 61, No. 6, pp. 765–793.

Schartau, M. and Oschlies, A.(2003b), 'Simultaneous data-based optimization of a 1D-ecosystem model at three locations in the North Atlantic: Part II – Standing stocks and nitrogen fluxes' *Journal of Marine Research*, vol. 61, No.6, pp. 795–821.

Schartau, M., Oschlies, A. and Willebrand, J.(2001), 'Parameter estimates of a zero-dimensional ecosystem model applying the adjoint method' *Deep Sea Research. Pt. II*, vol. 48, No. 8-9, pp. 1769–1800.

Shinners, M. S. (1998), 'Modern control system theory and design', *Second Edition*, John Wiley, New York.

Sima, V.(1996), 'Algorithms for Linear-Quadratic Optimization' *Pure and Applied Mathematics*, Marcel Dekker, Inc., New York, NY.

Ward, B., Anderson, M., Friedrichs, T., and Oschlies, A.(2010), 'Parameter optimisation techniques and the problem of underdetermination in marine biogeochemical models' *Journal of Marine Systems*, vol. 81, No. 1-2, pp. 34–43.

Introducing Periodic Parameters in a Marine Ecosystem Model using Discrete Linear Quadratic Control

Mustapha El Jarbi, Thomas Slawig, and Andreas Oschlies

Institute for Computer Science, Christian- Albrechts Universitaet zu Kiel,
24098 Kiel, Germany
GEOMAR, Düsternbrooker Weg 20, 24105 Kiel
{mej,ts}@informatik.uni-kiel.de
{aoschlies}@ifm-geomar.de

Abstract. This paper presents the application of the *Discrete Linear Quadratic Control (DLQC)* method for a parameter optimization problem in a marine ecosystem model. The ecosystem model simulates the distribution of nitrogen, phytoplankton, zooplankton and detritus in a water column with temperature and turbulent diffusivity profiles taken from a three-dimensional ocean circulation model. We present the linearization method which is based on the available observations. The linearization is necessary to apply the DLQC method on the nonlinear system of state equations. We show the form of the linearized time-variant problems and the resulting two algebraic Riccati Equations. By using the DLQC method, we are able to introduce temporally varying periodic model parameters and to significantly improve – compared to the use of constant parameters – the fit of the model output to given observational data.

Keywords: Optimal Control, Non-linear Systems, Parameter Optimization, Biogeochemical Modelling, Discrete Linear Quadratic Regulator Problem, Periodic Parameter, Discrete Riccati Equation

1 Introduction

We consider nonlinear partial differential diffusion-advection systems of the form

$$\frac{\partial x^i}{\partial t} = -w^i \frac{\partial x^i}{\partial z} + \frac{\partial}{\partial z}\left(\nu_\rho \frac{\partial x^i}{\partial z}\right) + q^i(\mathbf{x}, \mathbf{u}), \quad i = 1, 2, 3, 4 \tag{1}$$

$x^i : [0, T] \times [-H, 0] \longrightarrow \mathbb{R}$.
Here z denotes the vertical spatial coordinate, H the depth in the water column, q^i represents the biogeochemical coupling terms for the four species and $\mathbf{u} = (u_1, \ldots, u_p)$ is the vector of unknown physical and biological parameters. The circulation data are the turbulent mixing coefficient $\nu_\rho = \nu_\rho(z, t)$ and the temperature $\Theta = \Theta(z, t)$, which goes into the non-linear coupling terms q^i, see

(3). The vertical sinking velocity w^i is a parameter of the biological model that is nonzero only for x^4, i.e. $w^1 = w^2 = w^3 = 0$, $w^4 = ws > 0$.
The state of the system is denoted by $\mathbf{x} = (x^1, x^2, x^3, x^4)^\top$ and the control by $\mathbf{u}$. A control problem is defined as

$$\min_{\mathbf{u}} \mathcal{F}(\mathbf{x}, \mathbf{u}) \quad subject \quad to \quad (1), \tag{2}$$

where $\mathcal{F}$ is a cost functional which will be introduced later.
Our main goals are:

- to minimize a least-squares type cost functional,
- to allow the parameters to vary temporally over the year while remaining periodic over all years of the considered time interval.

The work presented in this paper is motivated by results obtained for a typical marine ecosystem model, namely the NPZD model introduced in [1], [2]. As was reported in several publications with different optimization algorithms, the quality of the model-to-dat fit was not optimal, and in some cases it was difficult to identify the parameters uniquely, see for example [3],[5],[4]. In most cases, the parameters of the marine ecosystem models are assumed to be temporally constant. This reflects the aim to obtain a model that is applicable for arbitrary time intervals. To solve this problems, we discretize and linearize the nonlinear state (1) around a reference trajectories and we interpret it as a Discrete Linear Quadratic Control (DLQC) problem. Therein, we allow the parameters to be time-dependent, apply a well-established method for optimal control, and additionally impose the constraint of annual periodicity. This avoids the process of parametrization in the sense that we do not have to know or assume how the above mentioned periodic functions look like. In contrast, the method itself will generate an optimal periodic function for each parameter. Moreover, it allows to balance the two aims that we have: By introducing weight matrices we can choose if it is more important to obtain a very good fit or nearly perfect periodicity. The method requires a reference trajectory and a reference control, i.e., the vector of model parameters. The former can be taken from the measurement data, and for the latter we use an initial guess for the parameters which can be the output of an optimization with constant parameters. The outline of this paper is as follows. In the next section we briefly described the model Equation and optimization problem (2), the DLQC problem formulation in section 3. A application of the DLQC method on the NPZD model is presented in section 4.3. Afterwards, we present our results with respect to the quality of the fit and the periodicity of the parameters and end the paper with some conclusions.

2 Model Equations and Optimization Problem

In this section we give the formulations of the NPZD model and of the corresponding parameter optimization problem and we formulate the optimization problem for the discrete model.

2.1 Model Equations

This section describes the ecosystem model. The considered system (1) is a spatially one-dimensional marine biogechemical model, that simulates the interaction of dissolved inorganic nitrogen N, phytoplankton P, zooplankton Z and detritus D. It was developed with the aim of simultaneously reproducing observations at three North Atlantic locations by the optimization of free parameters within credible limits, see [4]. The model uses the ocean circulation and temperature field in an off-line modus, i.e. these are used only as forcing, but no feedback on them is modeled. The model simulates one water column at a given horizontal position, which is motivated by the fact that there have been special time series studies at fixed locations, one of which was used here. In the model, the concentrations (in mmol N m^{-3}) of dissolved inorganic nitrogen N, phytoplankton P, zooplankton Z, and detritus D, denoted by $\mathbf{x} = (x^i)_{i=1,\dots,4} = (N, P, Z, D)$ are described by the PDE system (1).
The biogeochemical source-minus-sink terms $\mathbf{q} = (q^i)_{i=1,\dots,4}$ are explicit by given in [1]:

$$\left.\begin{aligned} q^1(\mathbf{x},\mathbf{u}) &= -\bar{J}(z,t,N)P + \gamma_2 Z + \mu_D D, \\ q^2(\mathbf{x},\mathbf{u}) &= \bar{J}(z,t,N)P - \mu_X P - G(P)Z, \\ q^3(\mathbf{x},\mathbf{u}) &= \gamma_1 G(P)Z - \gamma_2 Z - \mu_Z Z^2, \\ q^4(\mathbf{x},\mathbf{u}) &= (1-\gamma_1)G(P)Z - \mu_Z Z^2 + \mu_X P - \mu_D D - w_s \tfrac{\partial D}{\partial z} \end{aligned}\right\} \tag{3}$$

where $\bar{J}$ is the daily averaged phytoplankton growth rate as a function of depth z and time t, and G is the grazing function (see below). The remaining parameter in the above equations are defined in [1],

$$G(\epsilon, g) = \frac{g\epsilon P^2}{g + \epsilon P^2} \qquad \bar{J}(z,t,N) = \min\left(L(z,t), J_{max}\frac{N}{K_1 + N}\right), \tag{4}$$

where L denotes the purely light-limited growth rate, and J_{max} is the light-saturated growth. For more details of $\bar{J}$, L and the parameters see [1], [4].

2.2 The Optimization Problem

The aim of the optimization is to fit the aggregated model output $\mathbf{y} = C\mathbf{x}$ (C is called the output matrix) to the given observational data $\mathbf{y}^{obs}$. There are five types of measurement data $\mathbf{y}^{obs} = (y_m^{obs})_{m=1,\dots,5}$, which correspond to aggregated values $\mathbf{y} := (y_m)_{m=1,\dots,5}$ of the model output see also [3]. Thus the cost function can be written as:

$$\mathcal{F}(\mathbf{x},\mathbf{u}) := \|C\mathbf{x} - \mathbf{y}^{obs}\|_{2,\sigma}, \tag{5}$$

where $\|\|_{2,\sigma}$ is a Euclidean norm weighted using the vector

$$\sigma = (\sigma_l)_{l=1,\dots,5} = (0.1, 0.01, 0.01, 0.0357, 0.025)$$

of uncertainties corresponding to the five types of measurement data.

3 DLQC Problem Formulation

We use a discrete *linear time-varying (LTV) system*, i.e. we assume that the dynamical system is already discretized in time, namely at discrete times $t_k, k = 1, \ldots, M$. In the context of the DLQC, one usually considers a discrete-time system of the form:

$$\begin{aligned} \mathbf{x}_{k+1} &= A_k \mathbf{x}_k + B_k \mathbf{u}_k, \quad k = 1, 2, ..., M-1 \\ & x_1 \text{ (the given initial value)}, \end{aligned} \tag{6}$$

where in every time step k

- $\mathbf{x}_k = \mathbf{x}(t_k) \in \mathbb{R}^n$ is called the state vector (here the model output),
- $\mathbf{u}_k = \mathbf{u}(t_k) \in \mathbb{R}^p$ is the control (here the model parameter) vector, with the parameter vector from the model (3).
- The matrix $A_k \in \mathbb{R}^{n \times n}$ and $B_k \in \mathbb{R}^{n \times p}$ are called the system matrix and the input matrix, respectively.

We will use the notations

$$\begin{aligned} \mathbf{x} &= (\mathbf{x}_k)_{k=1,\ldots,M} \in \mathbb{R}^{M \times n} \cong \mathbb{R}^{Mn}, \\ \mathbf{u} &= (\mathbf{u}_k)_{k=1,\ldots,M-1} \in \mathbb{R}^{(M-1) \times p} \cong \mathbb{R}^{(M-1)p} \end{aligned}$$

for the whole discrete trajectories of state and control vector, respectively. The quadratic cost function of this optimal control problem is defined by:

$$\mathcal{J}(\mathbf{u}) = \frac{1}{2} \mathbf{x}_M^\top Q_M \mathbf{x}_M + \frac{1}{2} \sum_{k=1}^{M-1} \mathbf{x}_k^\top Q_k \mathbf{x}_k + \mathbf{u}_k^\top R_k \mathbf{u}_k, \tag{7}$$

where in every time step k

- Q_k is a positive semidefinite diagonal weighting matrix for the state vector for every model time step $k = 1, \ldots, M$,
- R_k is a positive definite diagonal weighting matrix for the control vector for every model time step $k = 1, \ldots, M-1$.

For the solution of a discrete linear quadratic optimal control problem with LTV systems, there exists the following theorem, see [6].

Theorem 1 *If the $Q_k, k = 1, \ldots, M$, are positive semi-definite and the $R_k, k = 1, \ldots, M-1$, are positive definite, then there exists a unique solution of the DLQC (6), (7). The optimal control is given by the* feedback law

$$\begin{aligned} \mathbf{u}_k &= -K_k \mathbf{x}_k, \quad k = 1, \ldots, M-1. \\ K_k &:= (R_k + B_k^\top \mathbf{X}_{k+1} B_k)^{-1} B_k^\top \mathbf{X}_{k+1} A_k, \qquad k = 1, \ldots, M-1 \\ \mathbf{x}_{k+1} &= (A_k - B_k K_k) \mathbf{x}_k, \qquad k = 1, \ldots, M-1. \end{aligned}$$

where the $(\mathbf{X}_k)_{k=1,\ldots,M-1}$, is the unique symmetric solution of the Discrete Riccati Equation (DRE).

$$\left.\begin{aligned} \mathbf{X}_k = Q_k + A_k^\top \mathbf{X}_{k+1} A_k - A_k^\top \mathbf{X}_{k+1} B_k (R_k + B_k^\top \mathbf{X}_{k+1} B_k)^{-1} B_k^\top \mathbf{X}_{k+1} A_k, \\ k = 1, \ldots, M-1. \end{aligned}\right\} \tag{8}$$

4 Application of DLQC to the NPZD Model

In this section we apply the LQOC method to the discretized version of the NPZD model. We present the details of discretization, linearization and the enforcement of the periodicity of the parameters (controls).

4.1 Discretization Scheme

We use a discrete linear quadratic control (DLQC). For this purpose we present the original discretization scheme of the model.
The NPZD model is forced by output from the OCCAM global circulation model, namely the hourly vertical profiles of temperature t and vertical diffusivity ν_ρ. The vertical grid consists of 32 layers with thickness increasing with depth. The time integration of the system (1) is performed by an operator splitting method:

– At first, the nonlinear coupling operators $\mathbf{q}_k = (q_k^1, q_k^2, q_k^3, q_k^4)^\top_{k=1,\dots,M-1}$ are computed at every spatial grid point and integrated by four explicit Euler steps, each of which is described by the operator:

$$B_k(\mathbf{x}_k, \mathbf{u}_k) := (\mathbf{x}_k + \frac{\tau}{4}\mathbf{q}_k(\mathbf{x}_k, \mathbf{u}_k)). \tag{9}$$

This gives an intermediate iterate

$$\hat{\mathbf{x}}_k := B_k \circ B_k \circ B_k \circ B_k(\mathbf{x}_k, \mathbf{u}_k).$$

– Then, an explicit Euler step with full step-size τ is performed for the sinking term, which is spatially discretized by an upstream scheme. This step is summarized in a matrix S. Since the sinking velocity is temporally constant, this matrix does not depend on the time step k. Thus, at the end of this step, an intermediate tracer vector $\tilde{\mathbf{x}}_k$ is computed as

$$\tilde{\mathbf{x}}_k := S\hat{\mathbf{x}}_k, \tag{10}$$

where $S = (I_k + \tau A^{adv})$.

– Finally, an implicit Euler step is applied for the diffusion operator discretized with second order central differences. The resulting matrix D_k for the diffusion depends on k since the diffusion coefficient depends on time. The matrix is tridiagonal, and the system is solved directly for $\mathbf{x}_{k+1}$

$$\tilde{D}_k\mathbf{x}_{k+1} = \tilde{\mathbf{x}}_k, \tag{11}$$

where $\tilde{D}_k = (I_k - \tau D_k)\mathbf{x}_{k+1}$.
Summarizing, the discrete system can be written as

$$\begin{aligned}\mathbf{x}_{k+1} &= \tilde{D}_k^{-1} S B_k \circ B_k \circ B_k \circ B_k(\mathbf{x}_k, \mathbf{u}_k) \\ &= \tilde{D}_k^{-1} S G(\mathbf{x}_k, \mathbf{u}_k), \qquad k = 1, ..., M-1,\end{aligned} \tag{12}$$

The function G is nonlinear and represents the discretized source minus sink terms.

4.2 Linearization of the Model

The LDQC approach is based on a linearization of (12) to obtain a linear time-varying problem. The linearization is performed around *reference trajectories* $(\mathbf{x}_k^r, \mathbf{u}_k^r)_{k=1,\dots,M-1}$. For the reference state trajectory we take available the observational data, is taken from the Bermura Atlantic Time-series Study (BATS) see also [7], the choice of the reference control trajectory is described in below. The linearized state equation now reads

$$\tilde{\mathbf{x}}_{k+1} = A_k \tilde{\mathbf{x}}_k + B_k \mathbf{v}_k + r_k, \qquad k = 1, \dots, M-1, \tag{13}$$

where

$$\begin{aligned}
A_k &= \tilde{D}_k^{-1} S \frac{\partial G}{\partial x}(\mathbf{x}_k^r, \mathbf{u}_k^r), \quad A_k \in \mathbb{R}^{n\times n} \\
B_k &= \tilde{D}_k^{-1} S \frac{\partial G}{\partial u}(\mathbf{x}_k^r, \mathbf{u}_k^r) \quad B_k \in \mathbb{R}^{n\times p}, \\
r_k &= \tilde{D}_k^{-1} S G(\mathbf{x}_k^r, \mathbf{u}_k^r) - \mathbf{x}_{k+1}^r, \quad r_k \in \mathbb{R}^n \\
\tilde{\mathbf{x}}_k &= \mathbf{x}_k - \mathbf{x}_k^r, \quad \mathbf{v}_k \;=\; \mathbf{u}_k - \mathbf{u}_k^r, \quad \tilde{\mathbf{x}}_k \in \mathbb{R}^n, \quad \mathbf{v}_k \in \mathbb{R}^p.
\end{aligned}$$

Now we write the linearized problem in the form of a (LDQC) problem, therefore we set:

$$\hat{\mathbf{x}}_k := \begin{pmatrix} \tilde{\mathbf{x}}_k \\ 1 \end{pmatrix}, \quad \hat{A}_k = \begin{pmatrix} A_k & r_k \\ 0 & 1 \end{pmatrix}, \quad \hat{B}_k = \begin{pmatrix} B_k \\ 0 \end{pmatrix}, \quad \hat{Q}_k = \begin{pmatrix} Q_k & 0 \\ 0 & 0 \end{pmatrix}$$

where $\hat{\mathbf{x}}_k \in \mathbb{R}^{n+1}$, $\hat{A}_k \in \mathbb{R}^{(n+1)\times(n+1)}$, $\hat{B}_k \in \mathbb{R}^{(n+1)\times p}$, $\hat{Q}_k \in \mathbb{R}^{(n+1)\times(n+1)}$. The linearized state equation (13) can be written in a form similar to (6), namely as:

$$\hat{\mathbf{x}}_{k+1} = \hat{A}_k \hat{\mathbf{x}} + \hat{B}_k \mathbf{v}_k \quad k = 1, ..., M-1. \tag{14}$$

Enforcing Periodicity of the Parameters. A main objective of this work is to enforce periodicity of the parameters/controls. For this purpose, let us assume that the length of a time period – measured in time steps – is $T > 0$ and that $M \bmod T = 0$. We now chose the reference trajectory for the control $\mathbf{u}^r = (\mathbf{u}_k^r)_{k=1,\dots,M-1} \in \mathbb{R}^{(M-1)p}$ to be

$$\mathbf{u}_k^r := \begin{cases} \mathbf{u}_0, & \text{if } k \le T \\ \mathbf{u}_{k-T}, & \text{if } k > T. \end{cases} \tag{15}$$

Where $\mathbf{u}_0$ is the parameter vector determined by optimization in [1], that was used as an initial guess here. we will enforce periodicity of $\mathbf{u}_k = \mathbf{u}_k^r + \mathbf{v}_k = \mathbf{u}_{k-T} + \mathbf{v}_k$ for $k \ge T+1$.

4.3 Application to NPZD Model

From Theorem 1 in section 3, the optimal control is given by

$$\mathbf{v}_k = -(R_k + \hat{B}_k^\top \hat{\mathbf{X}}_{k+1} \hat{B}_k)^{-1} \hat{B}_k^\top \hat{\mathbf{X}}_{k+1} \hat{A}_k \hat{\mathbf{x}}_k, \quad k = 1, \dots, M-1.$$

According to (15), we find

$$\mathbf{u}_k = \begin{cases} \mathbf{u}_0 - (R + \hat{B}_k^\top \hat{\mathbf{X}}_{k+1} \hat{B}_k)^{-1} \hat{B}_k^\top \hat{\mathbf{X}}_{k+1} \hat{A}_k \hat{\mathbf{x}}_k, \text{ if } k \le T, \\ \mathbf{u}_{k-T} - (R_k + \tilde{B}_k^\top \hat{\mathbf{X}}_{k+1} \hat{B}_k)^{-1} \hat{B}_k^\top \hat{\mathbf{X}}_{k+1} \hat{A}_k \hat{\mathbf{x}}_k, \text{ if } k > T. \end{cases}$$

Here the $\hat{\mathbf{X}}_k$ can be computed backwards in discrete time, starting from

$$\hat{\mathbf{X}}_M = \hat{Q}_M, \tag{16}$$

as the unique symmetric solutions of the Discrete Riccati equations (8). We set

$$\hat{\mathbf{X}}_k = \begin{bmatrix} \mathbf{X}_k & h_k \\ h_k^\top & \alpha_k \end{bmatrix} \tag{17}$$

with $h_k \in \mathbb{R}^n$ and $\alpha_k \in \mathbb{R}$ for $k = 1, \dots, M-1$. we easily get

$$\mathbf{u}_k = \begin{cases} \mathbf{u}_0 + K_k \mathbf{z}_k + S_k, \text{ if } k \le T, \\ \mathbf{u}_{k-T} + K_k \mathbf{z}_k + S_k, \text{ if } k > T, \end{cases}$$

where K_k and S_k are given by

$$K_k = -(R_k + B_k^\top \mathbf{X}_{k+1} B_k)^{-1} B_k^\top \mathbf{X}_{k+1} A_k, \quad k = M-1, \dots, 1$$
$$S_k = -(R_k + B_k^\top \mathbf{X}_{k+1} B_k)^{-1} B_k^\top (\mathbf{X}_{k+1} r_k + h_{k+1}), \quad k = M-1, \dots, 1.$$

Now, the system (16), (17) to compute the $\mathbf{X}_k$ can be separated into

$$\mathbf{X}_M = Q_M,$$
$$\mathbf{X}_k = Q_k + A_k^\top \mathbf{X}_k A_k - A_k^\top \mathbf{X}_{k+1} B_k (R_k + B_k^\top \mathbf{X}_{k+1} B_k)^{-1} B_k^\top \mathbf{X}_{k+1} A_k, \quad k = M-1, \dots, 1.$$

To evaluate the $\mathbf{X}_k$ and an additional difference equation for the h_k, namely

$$h_M = 0,$$
$$h_k = A_k^\top (\mathbf{X}_{k+1} r_k + h_{k+1}) - A_k^\top \mathbf{X}_{k+1} B_k (R_k + B_k^\top \mathbf{X}_{k+1} B_k)^{-1} B_k^\top (\mathbf{X}_{k+1} r_k + h_{k+1}),$$
$$k = M-1, \dots, 1.$$

For the application on the NPZD Model, Q_k is to be constant for all k, this can be written as following

$$Q_k = \operatorname{diag}(\frac{1}{\sigma_l^2})_{l=1,\dots,5}, \quad k = 1, \dots, M-1,$$

and the matrix R_k can be written as

$$R_k = diag \begin{cases} \frac{1}{|(\mathbf{u}_0)_i|^2}, & i = 1, \dots, p, k = 1, \dots, T \\ \frac{1}{|(\mathbf{u}_{k-T,i}|^2}, & i = 1, \dots, p, k = T+1, \dots, M-1 \end{cases}$$

5 Optimization Results

5.1 Fit of Model Output to Observational Data

This section shows a comparison between the optimized model output obtained by the DLQC method with periodic parameters and the observational data. As a reference we also compare the results to those obtained by a direct optimization of the nonlinear model using *constant parameters* with a *Sequential Quadratic Programming (SQP)* method that takes into account parameter bounds. This method was used in [4]. We performed the optimization for the years 1994 to 1998, in contrast to the years 1991 to 1996 that were used in [4]. The reason for this is that no zooplankton data are available at BATS for the years 1991 to 1993, which would be disadvantageous for the linearization procedure in the DLQC method. In [4] a minimum value of the cost function (5) of $\mathcal{F} \approx 70$ was obtained for optimized constant parameters for the five year time interval $[1991, 1996]$. For the time interval $[1994, 1998]$ a comptation with the method used in [4] gave a very similar value. In contrast to these and other (as in [3]) earlier results obtained for constant model parameters, the DLQC method gives a nearly perfect fit of the data. Figure 1 shows the model results $\mathbf{y}$ obtained with the DLQC method together with the observational data $\mathbf{y}^{obs}$ for the years 1994 to 1998. The model-data fit for $\mathbf{y}_2 = P$ (chlorophyll a) is nearly perfect. Even substantial concentration changes that occur between some neighboring measurement points (e.g. for $\mathbf{y}_4 = P + Z + D$ (particulate organic nitrogen), in 1994, 1995 or 1997) can be captured by the optimized trajectory. There are only some parts of the time interval where the trajectories are slightly farther away from the data, for example in 1996 for zooplankton and in the last two years of the simulated time interval for PON.

5.2 Periodicity of the Parameters

we show here that the above model-to-data fit can be achieved by almost annually periodic parameters. This was possible due to an appropriate adjustment of the matrices Q_k and $R_k, K = 1, \ldots, M-1$, in the cost function (7) used in the DLQC framework, see sectionl 4.3. Thus both the annual periodicity of the parameters. Due to the choice of the reference values for the parameters in the first year, we could also keep the parameters in their desired bounds, although these bounds need not to be imposed explicity. Figures 2 illustrate the temporal behavior of the selected four parameters that were optimized with the DLQC method. In these figure, the temporal changes of the parameters are plotted against the *actual* times of the linearization points which are determined by the available measurements. Obviously, the DLQC method then leads to perfectly periodic parameters.

6 Conclusion

In this paper, we successfully applied the method linear quadratic optimal control to the optimization of an one-dimensional marine ecosystem model. The model

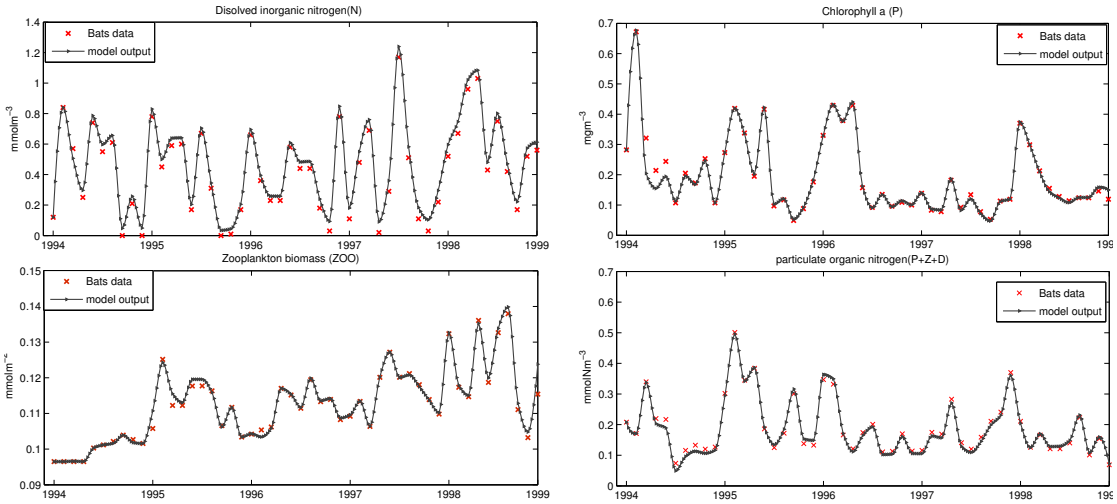

Fig. 1: Observational data $\mathbf{y}_i^{obs}, i = 1,..,4$ and aggregated model trajectories $\mathbf{y}_i, i = 1,..,4$, optimized with periodic parameters obtained by the DLQC method. Values are shown for the upper layer (depth less than 5 meters) and years 1994-1998.

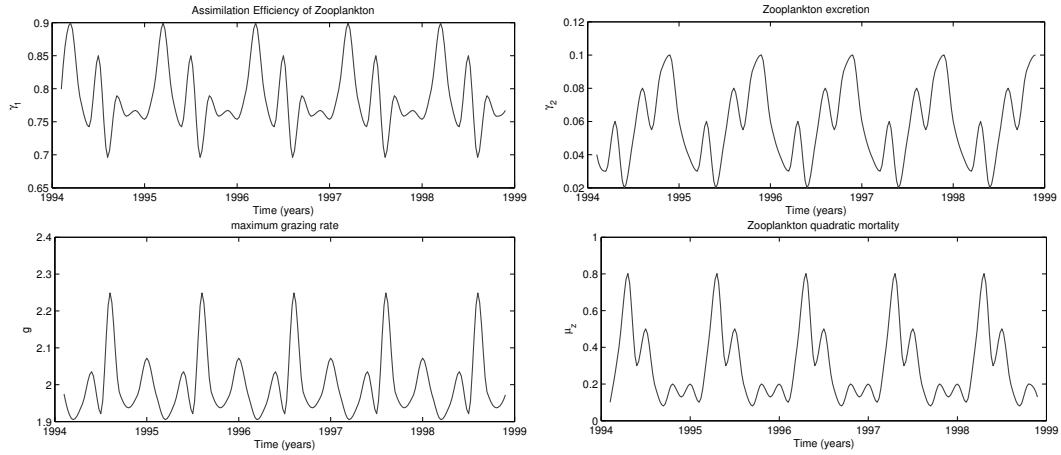

Fig. 2: Periodicity of the selected optimal parameters $u_{n,1} = \gamma_1, u_{n,4} = \gamma_2, u_{n,6} = g, u_{n,8} = \mu_z$, obtained by the DLQC method.

has to be linearized to fit in the LQOC frame work. The method permits perfect periodic evolution of model parameters and additionally notably improves the fit of the data in comparison with the solution with fixed model parameters. We demonstrated that the LQOC optimization is suitable for the considered prob-

lem and furthermore have shown that this method provides a very reasonable solution. Even with the available small number of observational data, which is typical to oceanographic time series sites, its quality is very high. Temporal deviations of individual parameters about the annual mean can be analyzed further to help making inferences about processes that the model cannot describe well when constant parameters are used. This analysis should contribute to a better understanding of model deficiencies and may improve marine ecosystem models. A next step could be to use only a part of the time horizon to estimate the periodic parameters and verifying the model and the parameters on the remaining part of the data.

Acknowledgements

The authors would like to thank Johannes Rückelt, Institute of Computer Science, Christian-Albrechts-Universität zu Kiel, for a direct optimization of the nonlinear model using constant parameters with a Sequential Quadratic Programming (SQP) method over the years 1994 to 1998.

References

1. Oschlies, A., Garon, V.: An eddy-permitting coupled physical-biological model of the North Atlantic 1. Sensitivity to advection numerics and mixed layer physics, Global Biogeochemical Cycles , vol. 13, pp. 135–160, (1999)
2. Schartau, M., Oschlies, A.: Simultaneous data-based optimization of a 1d-ecosystem model at three locations in the north Atlantic: Part I - method and parameter estimates, Journal of Marine Research vol. 61, pp. 765–793, (2003)
3. Ward, B.: Marine Ecosystem Model Analysis Using Data Assimilation, http://web.mit.edu/benw/www/Thesis.pdf, (2009)
4. Rückelt, J., Sauerland, V., Slawig, T., Srivastav, A., Ward, B., Patvardhan, C.: Parameter Optimization and Uncertainty Analysis in a Model of Oceanic CO_2-Uptake using a Hybrid Algorithm and Algorithmic Differentiation, Nonlinear Analysis B Real World Applications, vol. 10, pp. 3993–4009, (2010)
5. Ward, B.A., Anderson, M.A.M., Friedrichs, T.R., Oschlies, A.: Parameter optimisation techniques and the problem of underdetermination in marine biogeochemical models, Journal of Marine Systems and Control Letters, vol. 81, pp. 34–43, (2010)
6. Rugh, W. J.: Linear System Theory, Second Edition, Prentice-Hall, Upper Saddle River, New Jersey 07458, (1996)
7. Bermuda Atlantic Time-Series Study, `http://www.bios.edu/research/bats.html`

Bibliography

F. Amato, M. Ariola and C. Cosentino. Finite-time stability of linear time-varying systems: Analysis and controller design. IEEE Transactions on Automatic Control, vol. 55, no. 4, pp.1003–1008, 2010.

F. Amato, M. Ariola, and C. Cosentino. Finite time control via output feedback: A general approach. Proc. of the IEEE Conference on Decision and Control, Honolulu, Dec. 2003.

F. Amato, M. Ariola and C. Cosentino. Robust finite-time stabilization via dynamic output feedback. Automatica, vol. 42, no. 2, pp. 337-342, 2006.

F. Amato, M. Ariola, C. Cosentino, C. Abdallah and P. Dorato. Necessary and sufficient conditions for finite-time stability of linear systems. In Proceedings of the American Control Conference, 4452–4456, 2003.

F. Amato, M. Carbone, M. Ariola and C. Cosentino. Finite-time stability of discrete-time systems. In Proceedings of the American Control Conference, 1440–1444, 2004.

B. D. O. Anderson and J. B. Moore. Linear Optimal Control. Prentice-Hall, Englewood Cliffs, New Jersey, 1971.

B. D. O. Anderson and J. B. Moore. Optimal Linear Quadratic Methods. Prentice-Hall, Englewood Cliffs, New Jersey, 1990.

D. E. Archer, G. Eshel, A. Winguth, W. Broecker, R. Pierrehumbert, M. Tobis, and R. Jacob. Atmospheric pCO2 sensitivity to the biological pump in the ocean. Global Biogeochemical Cycles, vol. 14, no. 4, pp. 1219–1230, 2000.

Andrès Hugo Arias and Maria clara Menendes. Marine Ecology in a Changing World. CRC Press,2013.

M. Athans. The Control Handbook, chapter Kalman Filtering, pages 589–594. CRC Press,1996.

M. Athans, P. Falb. Optimal Control. McGraw-Hill, New York, 1966.

A. V. Balakrishnan. Kalman filtering theory. Optimization Software, New York, 1987.

U. Bathmann and U. Passow. Kohlenstoffpumpen im Ozean steuern das Klima. Globale Erwärmung. Biologie in unserer Zeit, vol. 40, pp. 304–313, 2010.

L. M. Braman, P. Suarez and M. K. Van Aalst. Climate change adaptation: Integrating climate science into humanitarian work. International Review of the Red Cross, vol. 92, pp. 693–712, 2010.

V. Carmillet, J. M. Brankart, P. Brasseur, H. Drange and G. Evensen, G. A singular evolutive extended Kalman filter to assimilate ocean color data in a coupled physical-biochemical model of the North Atlantic. Ocean Modelling., vol. 3, pp. 167–192, 2001.

J. L. Casti. Linear Dynamic Systems. Academic Press, 1987.

D. E. Catlin. Estimation, Control, and the Discrete Kalman Filter. Springer Verlag, 2011.

D. Clemens. Optimal non-linear Control for Power Systems. IEEE Conference on Control Application, 241–245, 1993.

P. M. Cox, R. A. Betts, C. D. Jones, S. A. Spall and I. J. Totterdell. Acceleration of global warming due to carbon-cycle feedbacks in a coupled climate model. Nature, vol. 408, pp. 184-187, 2000.

H. W. Ducklow, D. K. Steinberg and K. O. Buesseler. Upper ocean carbon export and the biological pump. Oceanography, vol. 14, pp. 50–58, 2001.

P. Dorato, An overview of finite-time stability in current trends in nonlinear systems and control: In honor of Petar Kokotovic and Turi Nicosia. Birkhäuser, pp. 185–194, 2006.

P. Dorato. Short-time stability. Proceedings of the IRE International Convention Record Part, vol. 1, no. 4, pp. 83–87, 1961.

M. El Jarbi, J. Rückelt, T. Slawig and A. Oschlies. Reducing the Model-Data Misfit in a Marine Ecosystem Model Using Periodic Parameters and Linear Quadratic Optimal Control. Biogeosciences, vol. 10, pp. 1169 -1182, 2013.

M. Eknes and G. Evensen. An ensemble Kalman filter with a 1-d marine ecosystem model. Journal of Marine Systems, vol. 36, no. 1–2, pp. 75–100, 2002.

R. W. Eppley and B. J. Peterson. Particulate organic matter flux and planktonic new production in the deep ocean. Nature, vol. 282, pp. 677–680, 1979.

G. T. Evans and J. S. Parslow. A model of annual plankton cycles. Biology & Oceanography, vol. 3, pp. 327–347, 1985.

G. T. Evans and V. C. Garçon. One-dimensional models of water column biogeochemistry. JGOFS report 23/97. JGOFS Bergen, Norway, 1997.

M. J. R. Fasham and G. T. Evans. The use of optimization techniques to model marine ecosystem dynamics at the JGOFS station at 47 °N 20 °W. Philosophical Transactions of the Royal Society of London, vol. 348, pp. 203–210, 1995.

M. J. R. Fasham. Ocean Biogeochemistry: The Role of the Ocean Carbon Cycle in Global Change. Springer-Verlag, Berlin, 2003.

K. Fennel, M. Losch, J. Schröter and M. Wenzel. Testing a marine ecosystem model: sensitivity analysis and parameter optimization. Journal of Marine Systems , vol. 28, pp. 45–63, 2001.

W. Fennel and T. Neumann. Introduction to the Modelling of Marine Ecosystems. Elsevier, 2004.

B. Friedland. Control System Design: An Introduction to State-Space Methods. McGraw-Hill, 1986.

H. P. Geering. Regelungstechnik. 6. Aufl., Springer-Verlag, Berlin, 2003.

B. P. Gibbs. Advanced Kalman Filtering, Least-Squares and Modeling. Published by John Wiley & Sons, Hoboken, New Jersey, 2011.

R. Giering and A. Kaminski. Recipes for adjoint code construction, ACM Transactions on Mathematical Software. vol. 24, no. 4, pp. 437–474, 1998.

S. Gillijns, O. B. Mendoza, J. Chandrasekar, B. L. R. De Moor, D. S. Bernstein and A. Ridley. What is the ensemble Kalman filter and how well does it work?. In Proceedings of the american control conference, pages 4448–4453, 2006.

M. S. Grewal and A. P. Andrews. Kalman Filtering: Theory and practice Using Matlab. John Wiley & Sons, New York, 2001.

A. Griewank. Evaluating derivatives principles and techniques of algorithmic differentiation. SIAM, Philadelphia, PA, 2000.

H. Grobe. Alfred Wegener Institute for Polar and Marine Research. Bremerhaven, Germany, 2006.

W. W. Hager. Updating the Inverse Of a matrix. SIAM Review, vol. 31, no. 2, pp. 221-239, 1989.

R. Harmon and P. Challenor. A Markov chain monte Carlo method for estimation assimilation into models. Ecological Modelling, vol. 101, pp. 41–59, 1996.

G. Hurtt and and R. Armstromg. A pelagic ecosystem model calibrated with BATS data. Deep-Sea Research, vol. 43, pp. 653–683, 1996.

IPCC, 2007a. in:Core Writting Team, Pachauri, R. K., Reisinger, A. (Eds.), Climate Change 2007: Synthesis Report. Contribution of Working Groups I, II and III to the Fourth Assessment Report of the Intergovernmental Panel on Climate Change. IPCC, Geneva, Switzerland, p. 104 et seq.

R. E. Kalman. A new approach to linear filtering and prediction problem. Trans. ASME, Journal of Basic Engineering, vol. 82, pp.34–45, 1960 .

H. W. Knobloch and H. Kwakernaak. Lineare Kontrolltheorie. Springer-Verlag, Berlin, 1985.

P. Kosmol. Optimierung und Aproximation. Walter de Gruyter, Berlin, 2010.

T. Kusky. Climate change. Infobase Publishing, New York New, 2009.

H. Kwakernaak and R. Sivan. Linear Optimal Control Systems. John Wiley & Sons, New York, 1972.

W. Li. The infinity norm bound for the inverse of nonsingular diagonal dominant matrices bounds for the infinity norm of the inverse of SDD and S-SDD matrices. Applied Mathematics Letters, pp. 258–263, 2008.

J. Liebig, L. Playfair, J. Webster, Chemistry in its application to agriculture and physiology. J. Owen, 1842.

S. Levis. Modeling vegetation and land use in models of the Earth System. Wiley Interdisciplinary Reviews: Climate Change. vol. 1, pp. 840–856, 2010.

F. L. Lewis and V. L. Syrmos. Optimal Control. 2nd Ed. John Wiley & Sons, New York, 1995.

F. L. Lewis. Applied Optimal Control and Estimation: Digital Design and Implementation. Prentice-Hall, Englewood Cliffs, New Jersey, 1992.

A. Locatelli. Optimal Control: An Introduction. Birkhäuser Verlag, 2001.

S. N. Losa, G. A. Kivman, J. Schroeter and M. Wenzel. Sequential Weak constraint parameter estimation in an ecosystem model. Journal of Marine Systems, vol. 43, pp. 31–49, 2003.

J. Lunze. Regelungstechnik 2. Springer-Verlag, Berlin, 1997.

A. Quarteroni, R. Sacco and F. Saleri. Numerical Mathematics. Second Edition Springer, 2007.

R. J. Matear. Parameter optimization and analysis of ecosystem models using simulated annealing: a case study at Station P. Journal of Marine Research, vol. 53, pp. 571–607, 1995.

J. Mattern. Estimating time-dependent parameters for a biological ocean model using an emulator approach. Journal of Marine Systems, vol. 96-97, pp. 32–47, 2012.

K. McGuffie and A. Henderson-Sellers. A Climate Modelling Primer. 3rd edition, John Wiley & Sons, 2005.

A. N. Michel and S. H. Wu. Stability of discrete systems over a finite interval of time. International Journal of Control, vol. 9, no. 6, pp. 679–693, 1969.

N. Moraca. Upper bounds for the infinity norm of the inverse of SDD and S-SDD matrices. Journal of Computational and Applied Mathematics, vol. 206, pp. 666-678, 2007.

L. J. Natvik, M. Eknes and G. Evensen. A weak constraint inverse for a zero-dimensional four component marine ecosystem model. Journal of Marine Systems. vol. 28, no. 1–2, pp. 19–44, 2001.

A. Oschlies. Feedbacks of biotically induced radiative heating on upper-ocean heat budget, circulation, and biological production in a coupled ecosystem-circulation model. Journal of Geophysical Research, vol. 110, 2004.

A. Oschlies and V. Garçon. An eddy-permitting coupled physical-biological model of the North Atlantic 1. Sensitivity to advection numerics and mixed layer physics. Global Biogeochem. Cycles, vol. 13, pp. 135–160, 1999.

A. Oschlies and M. Schartau. Basin-scale performance of a locally optimized marine ecosystem model. Journal of Marine Research, vol. 63, pp. 335–358, 2005.

M. Prieß. Surrogate-Based Optimization for Marine Ecosystem Models. Ph.D. thesis, 2012.

M. Prieß, S. Koziel and T. Slawig. Surrogate-based optimization of climate model parameters using response correction. Journal of Computational Science, vol. 2, pp. 335–344, 2011.

P. Prunet, J. F. Minster and D. Ruiz-Pino. Assimilation of surface data in a one-dimensional physical-biogeochemical model of the surface ocean: 1. Method and preliminary results. Global Biogeochem. Cycles, vol. 10, pp. 111–138, 1996.

J. A. Raven and P. G. Falkowski. Oceanic sinks for atmospheric CO_2. Plant, Cell & Environment, vol. 22, pp. 741–755, 1999.

U. Riebesell, K. G. Schulz, R. G. J. Bellerby, M. Botros, P. Fritsche, M. Meyerhöfer, C. Neill, G. Nondal, A. Oschlies, J. Wohlers and E. Zöllner. Enhanced biological carbon consumption in a high CO_2 ocean. Nature, vol. 450, pp. 545–548, 2007.

W. Rickels, G. Klepper, J. Dovern, G. Betz, N. Brachatzek, S. Cacean, K. Güssow, K., J. Heintzenberg, S. Hiller, C. Hoose, T. Leisner, A. Oschlies, U. Platt, A. Proelß, O. Renn and S. M. Z. Schäfer. Gezielte Eingriffe in das Klima ? Eine Bestandsaufnahme der Debatte zu Climate Engineering. Sondierungsstudie für das Bundesministerium für Bildung und Forschung, 2011.

J. Riccati. Observations regarding differential equations of the second order. quae Lipsiae publicantur, Supplementa, vol. 8, pp. 66–73, 1724.

J. Rückelt, A. Oschlies and Slawig. Optimization of Parameters and Initial Values in a Marine NPZD-Type Ecosystem Model, Technical Report 1013, CAU Kiel, Institut für Informatik, 2010.

J. Rückelt, V. Sauerland, T. Slawig, A. Srivastav, B. Ward and C. Patvardhan, C. Parameter Optimization and Uncertainty Analysis in a Model of Oceanic CO_2-Uptake using a Hybrid Algorithm and Algorithmic Differentiation. Nonlinear Analysis B Real World Applications, vol. 10, pp. 3993–4009, 2010.

W. J. Rugh. Linear System Theory. 2nd Edn., Prentice-Hall, Englewood Cliffs, 1996.

J. L. Sarmiento and N. Gruber. Ocean Biogeochemical Dynamics. Chapter 10: Oceanic carbon cycle, atmospheric CO_2, and climate Princeton University Press, Princeton et al., 2004.

J. L. Sarmiento and N. Gruber. Ocean Biogeochemical Dynamics. Princeton University Press, Princeton et al., 2006.

M. Schartau. Data-assimilation studies of marine, nitrogen based, ecosystem models in the North Atlantic Ocean. Ph.D. thesis. Christian-Albrechts-Universität Kiel, 2001.

M. Schartau and A. Oschlies. Simultaneous data-based optimization of a 1d-ecosystem model at three locations in the north Atlantic: Part I – method and parameter estimates. Journal Of Marine Research, vol. 61, pp. 765–793, 2003a

M. Schartau and A. Oschlies. Simultaneous data-based optimization of a 1D-ecosystem model at three locations in the North Atlantic: Part II – Standing stocks and nitrogen fluxes. J. Mar. Res., vol. 61, pp. 795–821, 2003b.

M. Schartau, A. Oschlies and J. Willebrand. Parameter estimates of a zero-dimensional ecosystem model applying the adjoint method. Deep Sea Res. Pt. II, vol. 48, pp. 1769–1800, 2003b.

B. Sinha and A. Yool. Extension of the OCCAM 1 general circulation model to include the biogeochemical cycles of carbon and oxygen, Part I: Technical description. Research and Consultancy Report No. 5, National Oceanography Centre, Southampton, 2006.

V. Sima. Algorithms for Linear-Quadratic Optimization. Marcel Dekker Verlag, 1996.

Y. Spitz, J. Moisan, M. Abbott and J. Richman. Data assimilation and a pelagic ecosystem model: parameterization using time series observations. Journal of Marine Systems, vol. 16, pp. 51–68, 1998.

E. D. Sontag. Mathematical Control Theory. 2nd edition, Springer-Verlag, New York, 1998.

H. W. Sorenson. Kalman Filtering: Theory and Application. EEE Press., 1960.

J. Stoer and R. Bulirsch. Introduction to Numerical Analysis. 3rd edition, Springer-Verlag, New York, 2002.

H. Storch, S. Güss, and M. Heimann. Das Klimasystem und seine Modellierung. Eine Einführung. Springer-Verlag, Berlin, 1999.

X. Su, X. Zhi and Q. Zhang. Finite-Time Boundedness Control of Time-Varying Descriptor Systems, Mathematical Problems in Engineering, 2013.

T. Takahashi, S. C. Sutherland, C. Sweeney, A. Poisson, N. Metzl, B. Tilbrook, N. Bates, R. Wanninkhof, R. A. Feely, C. Sabine, J. Olafsson and Y. C. Nojiri. Global sea-air CO_2 flux based on climatological surface ocean pCO_2, and seasonal biological and temperature effects. Deep-Sea Res. Pt. II, vol. 49, pp. 1601-1622, 2002.

J. M. Varah, Ä lower bound for the smallest singular value of a matrix, Linear Algebra Applications, Vol. 11, pp. 3–5, 1975

B. Ward. Marine Ecosystem Model Analysis Using Data Assimilation. Ph.D. thesis, 2009.

B. Ward, M. Anderson, T. Friedrichs and A. Oschlies. Parameter optimisation techniques and the problem of underdetermination in marine biogeochemical models. J. Mar. Syst. Con. Lett., vol. 81, pp. 34–43, 2010.

G. Welch and G. Bishop. An introduction to the Kalman filter. Dept. Comp. Sci., Univ. North Carolina, 2004.

J. Zabczyk. Mathematical Control Theory: An Introduction. Birkhäuser Verlag, 1992.

P. Zarchan and H. Musoff. Fundamental of kalman Filtering: A Practical Approach 2nd edition, American institute of Aeronautics, 2000.

Erklärung

Hiermit bestätige ich,

1. dass die vorliegende Abhandlung nach Inhalt und Form meine eigene Arbeit ist,
2. dass die vorliegende Arbeit weder in gleicher noch ähnlicher Form einer anderen Prüfungsbehörde zuvor vorgelegen hat und
3. dass diese Arbeit unter Einhaltung der Regeln guter wissenschaftlicher Praxis der Deutschen Forschungsgemeinschaft entstanden ist.

Ferner erkläre ich, dass Teile dieser Arbeit bereits an anderer Stelle veröffentlicht bzw. zur Veröffentlichung eingereicht sind. Im Detail sind das

- Reducing the model-data misfit in a marine ecosystem model using periodic parameters and linear quadratic optimal control, in: Biogeosciences, 10, 1169-1182, 2013.
- Introducing Periodic Parameters in a Marine Ecosystem Model Using Discrete Linear Quadratic Control, in: System Model ling and Optimization , 481-490 (2013)
- Extension of a Marine Ecosystem Model using Discrete Open Loop Optimal Control, to appear in International Journal of Mathematical Modelling and Numerical Optimisation (2014)
- Estimating Marine Ecosystem Model Using Kalman Filter with Time-Variant Parameters

---

Mustapha El Jarbi
20. Juni 2014